# Development of Adenosine Signalling

# in the Cerebellum

## Alison Atterbury

A thesis submitted for the degree of Doctor of Philosophy

University of Warwick, Department of Biological Sciences

August 2010

**For Harry Chapman**

I will miss you always.

# Contents

# Chapter 2   Materials and Methods

# Chapter 3   The presence and distribution of $A_1R$ and $A_{2A}R$ in the rat cerebellum at different stages of development

# Chapter 4  Presynaptic pharmacology of immature parallel fibre-Purkinje cell synapses in the rat cerebellum

## Chapter 5  Adenosine signalling at immature parallel fibre-Purkinje cell synapses in the rat cerebellum

# Chapter 6  Discussion

# Tables

# Figures

# Acknowledgements

Finally, I would like to show my gratitude to the best discovery during my PhD, Francesco and my wonderful mom, dad and sister for their love, support and supply of good wine.

# Declaration

I, Alison Atterbury, hereby declare that all of the work reported in this thesis is my own unless stated otherwise in the text or figure legends. None of this work has previously been submitted for any degree at this or any other institution. All sources of information used in the preparation of this thesis are indicated by references.

# Abstract

The release and clearance of adenosine are reasonably well-documented in the mature CNS but relatively little is known about how adenosine signalling changes during postnatal development. The activation of presynaptic $A_1$ receptors ($A_1R$) at cerebellar parallel fibre terminals is known to inhibit synaptic transmission and the expression of $A_1R$ has been observed in mature rat cerebellar slices. However its distribution during development or in relation to parallel fibre–Purkinje cell (PF-PC) synapses has not previously been described. In the mature cerebellum blockade of presynaptic $A_1R$ at PF-PC synapses enhances synaptic transmission suggesting an inhibitory adenosine tone and an extracellular purine tone is detectable with microelectrode biosensors under basal conditions. The active release of adenosine can be stimulated with trains of activity in the molecular layer of mature slices although this does not appear to be a source of the basal extracellular adenosine tone.

This study used immunohistochemistry to determine the distribution of $A_1R$ at PF-PC synapses in cerebellar slices at postnatal day 3 prior to PF-PC synapse formation, postnatal days 8-14 and postnatal days 21-28. This study also used cerebellar slices from rats at postnatal days 9-14 to investigate the pharmacological profile of the immature rat PF-PC synapse with electrophysiology and microelectrode biosensors.

The immunohistochemistry suggests that $A_1R$ are widely distributed across Purkinje cell bodies and their dendrites and within the granule layer of the cerebellum and that its expression does not change during development. The same staining patterns were also observed prior to PF-PC synapse formation.

Application of adenosine resulted in a variable $A_1R$-mediated inhibition at immature PF-PC synapses. This did not appear to be gender-specific or correlated with age of rat and the synapses otherwise appeared identical in their properties. The comparison of log concentration-response curves generated for an $A_1R$ agonist suggested that some $A_1R$ may have a lower efficacy at this stage of development. Blockade of presynaptic $A_1R$ at immature PF-PC synapses suggested that an inhibitory adenosine tone is low or absent at this stage of development and is not the result of a low $A_1R$ expression or developmental differences in $A_1R$ efficacy. Inhibition of adenosine clearance via adenosine deaminase, adenosine kinase and equilibrative transporters had little effect on synaptic transmission suggesting that little adenosine is moving between the intracellular and extracellular spaces under basal conditions in immature slices. Active adenosine release measured by electrophysiology and microelectrode biosensors could be stimulated with hypoxia in immature slices but this was delayed and slower in comparison to the release observed in mature slices. Adenosine could not be actively released at immature PF-PC synapses in response to electrical stimulation in the molecular layer.

# Abbreviations

| | |
|---|---|
| [$^3$H] NECA | [3H] adenosine-5'-(N-ethylcarboxamide) |
| 5-HT | 5-hydroxytryptamine |
| 8-CPT | 8-cyclopentyltheophylline |
| $A_1R$ | adenosine $A_1$ receptor |
| $A_{2A}R$ | adenosine $A_{2A}$ receptor |
| $A_{2B}R$ | adenosine $A_{2B}$ receptor |
| $A_3R$ | adenosine $A_3$ receptor |
| AD | adenosine deaminase |
| ADO | adenosine |
| ADP | adenosine 5' diphosphate |
| AMP | adenosine 5' monophosphate |
| AMPAR | alpha-amino-3-hydroxy-5-methyl-4-isoxazolepropionic acid receptor |
| ATP | adenosine 5' triphosphate |
| aCSF | artificial cerebrospinal fluid |
| BSA | bovine serum albumin |
| cAMP | adenosine 3'5'-cyclic monophosphate |
| CART | cocaine- and amphetamine-regulated transcript |
| CB1 | endocannabinoid type 1 receptor |
| CF EPSC | climbing fibre excitatory postsynaptic current |
| CF-PC | climbing fibre-Purkinje cell |
| cGMP | guanosine 3'5'-cyclic monophosphate |
| CHA | cyclohexyladenosine |

| | |
|---|---|
| **CHO** | Chinese hamster ovary |
| **CNQX** | 6-cyano-7-nitroquinoxaline-2, 3-dione |
| **CNS** | central nervous system |
| **CNT** | concentrative nucleoside transporter |
| **CPA** | $N^6$-cyclopentyladenosine |
| **CPT** | cyclopentyltheophylline |
| **CPX** | 8-cyclopentyl-1,3-dipropylxanthine |
| **CSF** | cerebrospinal fluid |
| **DAB** | 3,3' diaminobenzidine |
| **DCN** | deep cerebellar nuclei |
| **DNA** | deoxyribonucleic acid |
| **DPCPX** | 8-cyclopentyl-1,3-dipropylxanthine |
| **EEG** | electroencephalographic |
| **EHNA** | erythro-9-(2-hydroxy-3-nonyl) adenine |
| **EMG** | electromyography |
| **E-NPPase** | ecto-nucleotide pyrophosphatase/phosphodiesterase |
| **ENT** | equilibrative nucleoside transporter |
| **E-NTPDase** | ecto-nucleoside triphosphate diphosphohydrolase |
| **EPSC** | excitatory postsynaptic current |
| **EPSP** | excitatory postsynaptic potential |
| **GABA** | gamma-aminobutyric acid |
| **GABA$_A$** | gamma-aminobutyric acid type A receptor |
| **GABA$_B$** | gamma-aminobutyric acid type B receptor |
| **GDP** | guanosine 5' diphosphate |
| **GFAP** | glial fibrillary protein |

| | |
|---|---|
| **GIRKs** | G-protein dependent inwardly rectifying $K^+$ channels |
| **GMP** | guanosine 5' monophosphate |
| **GPCR** | G-protein coupled receptor |
| **GPI** | glycosylphosphatidylinositol |
| **GTP** | guanosine 5' triphosphate |
| **$H_2O_2$** | hydrogen peroxide |
| **HPLC** | high-pressure liquid chromatography |
| **HYPO** | hypoxanthine |
| **INO** | inosine |
| **L-AP4** | L-(+)-2-amino-4-phosphonobutyric acid |
| **LTP** | long term potentiation |
| **mGluR** | metabotropic glutamate receptor |
| **$mGlu_{1\alpha}R$** | metabotropic glutamate type 1α receptor |
| **mGluR4** | metabotropic glutamate type 4 receptor |
| **MNTB** | medial nucleus of the trapezoid body |
| **NBMPR** | nitrobenzylthioinosine |
| **NBTI** | 6-[(4-nitrobenzyl)thiol]-9-β-D-ribofuranosylpurine |
| **NECA** | N-ethylcarboxamidoadenosine |
| **NGS** | normal goat serum |
| **non-REM** | non-rapid eye movement |
| **NT** | nucleoside transporter |
| **PAP** | peroxidase anti-peroxidase |
| **PET** | positron emission topography |
| **PBS** | phosphate-buffered saline |
| **PIA** | N6-(phenylisopropyl) adenosine |

| | |
|---|---|
| **PF EPSP** | parallel fibre excitatory postsynaptic potential |
| **PF-PC** | parallel fibre-Purkinje cell |
| **PKC** | protein kinase C |
| **PLC** | phospholipase C |
| **PFA** | paraformaldehyde |
| **PNP** | purine nucleoside phosphorylase |
| **PPADS** | pyridoxal phosphate-6-azophenyl-2,4-disulfonic acid |
| **PPD** | paired pulse depression |
| **PPF** | paired pulse facilitation |
| **PPR** | paired pulse ratio |
| **RNA** | ribonucleic acid |
| **SAH** | S-adenosylhomocysteine |
| **TTX** | tetrodotoxin |
| **UBC** | unipolar brush cell |
| **UDP** | uridine diphosphate |
| **UTP** | uridine triphosphate |
| **vGluT** | vesicular glutamate transporter |
| **XO** | xanthine oxidase |

# Chapter 1    Introduction

## 1.1   Purines and their receptors

### 1.1.1  Purines

The nitrogenous purine bases, adenine and guanine, and pyrimidine bases, cytosine, thymine and uracil are the building blocks of nucleic acids that form deoxyribonucleic acid (DNA) and ribonucleic acid (RNA).   Adenosine and guanosine are purine nucleosides that contain a pentose sugar in addition to their purine base.  Purine nucleotides consist of a purine base, ribose sugar and additional phosphate group(s) and include adenosine 5' triphosphate (ATP), adenosine 5' diphosphate (ADP), adenosine 5' monophosphate (AMP), guanosine 5' triphosphate (GTP), guanosine 5' diphosphate (GDP) and guanosine 5' monophosphate (GMP).

Plant and animal cells contain an abundance of the purine nucleosides and nucleotides in addition to the cyclic purine nucleotides, adenosine 3'5'- cyclic monophosphate (cAMP) and guanosine 3'5'- cyclic monophosphate (cGMP). Within the mammalian CNS extracellular purines act as important intercellular signalling molecules that exert a number of effects via cellular uptake or cell-surface purinergic receptors (Rathbone, Middlemiss et al. 1999).

## 1.1.2 Purinoceptors

The idea of neurotransmission by purines was first introduced in 1972 following previous reports of the release of a substance from inhibitory nerves within the guinea pig *taenia coli* (muscle bands of the large intestine) that was neither cholinergic nor adrenergic. Subsequent elimination of potential transmitters concluded this substance to be the purine nucleotide ATP that was possibly acting via a specific receptor (Burnstock 1972).

In 1978, Burnstock suggested that a family of purinoceptors existed that could be divided into two groups. These were classified based on agonist/antagonist potency, resultant changes in cAMP levels and induction of prostaglandin synthesis. Adenosine is the primary natural ligand at P1 purinoceptors and P2 purinoceptors recognise ATP,ADP, uridine 5' triphosphate (UTP), uridine 5' diphosphate (UDP) and UDP-glucose (Burnstock 1980). It is now understood that the family of P1 and P2 purinoceptors are present in all types of mammalian cells and are likely to be the most abundant receptor type in mammalian tissue (Abbracchio, Burnstock et al. 2009).

The P2 receptors are further divided into P2X receptors that recognise ATP and P2Y receptors that are activated by ATP, ADP, UTP, UDP or UDP-glucose. P2X receptors are ligand-gated ion channels with subunits encoded by seven genes ($P2X_{1-7}$) which assemble as either homomeric ($P2X_{1-5, 7}$) or heteromeric trimers ($P2X_{1/2, 1/4, 1/5, 2/3, 2/6, 4/6}$). All P2X channels are permeable to $Na^+$, $K^+$ and $Ca^{2+}$ cations. P2Y receptors are metabotropic G-protein coupled receptors (GPCR) composed of 8

subtypes ($P2Y_{1, 2, 4, 6, 11, 12, 13, 14}$). These can be further subdivided into a group that are primarily coupled to $G_{q/11}$ to activate phospholipase C (PLC) ($P2Y_{1, 2, 4, 6, 11}$) and a group that are coupled to $G_{i/o}$ to inhibit adenylate cyclase ($P2Y_{12, 13, 14)}$ (Abbracchio, Burnstock et al. 2009). Adenosine is the focus of this study so only P1 receptors will be discussed further.

The group of P1 adenosine receptors is divided into four subtypes known as $A_1$, $A_{2A}$, $A_{2B}$ and $A_3$. All are metabotropic G-protein coupled receptors with an intracellular C-terminal and seven highly-conserved transmembrane domains of hydrophobic amino acids that form a pocket for the binding of adenosine (figure 1.1) (Ralevic and Burnstock 1998).

In general within the CNS, the $A_1$ receptors ($A_1R$) have the highest affinity for adenosine and can couple to $G_{i1/2/3}$ and $G_o$ to inhibit adenylate cyclase or activate phospholipase C and inhibit N-type $Ca^{2+}$ channels or stimulate $K^+$ channels. Conversely, the $A_{2A}$ receptor ($A_{2A}R$) primarily stimulates adenylate cyclase via coupling to $G_s$ proteins although it is also known to couple with $G_{olf}$ proteins in the striatum and can stimulate transmitter release via activation of protein kinase C (PKC). The lower affinity $A_{2B}$ receptor ($A_{2B}R$) largely activates adenylate cyclase via $G_s$ proteins but can also stimulate PLC via $G_q$ proteins. The poorly characterised low-affinity $A_3$ receptor ($A_3R$) mediates inhibition of adenylate cyclase by coupling to $G_{i2/3}$ and possibly stimulation of PLC via $G_{q/11}$ (see figure 1.2 for summary). The development of knockout mice for $A_1R$, $A_{2A}R$ and $A_3R$ suggests that none of these receptors play a significant role in development (Dunwiddie and Masino 2001; Burnstock 2007).

Subtypes of P1 receptor were first described when binding and potency of adenosine and its analogues were examined in either cultured mouse brain cells or isolated membrane preparations from a number of different cells (van Calker, Muller et al. 1979; Londos, Cooper et al. 1980). In these independent studies only two subtypes of adenosine receptor were originally detailed based on the ability of the adenosine receptor to either inhibit or stimulate adenylate cyclase activity, via an associated G-protein, to regulate production of cAMP. The nomenclature adapted by van Calker to describe the two types of adenosine receptor ($A_1$/$A_2$) is now widely accepted in preference to the alternative study's use of $R_i$ ($A_1$), where receptor activation mediates inhibition of adenylate cyclase and $R_a$ ($A_2$), where the receptor facilitates stimulation of the enzyme. In this alternative nomenclature the 'R' is used to represent the 'ribose' component that binds to the adenosine receptor (Londos, Cooper et al. 1980). The studies describe $A_1$ ($R_i$) receptors as those where adenylate cyclase is inhibited by N6-(phenylisopropyl)adenosine (PIA) > adenosine > N-ethylcarboxamidoadenosine (NECA) and $A_2$ ($R_a$) receptors as those where adenylate cyclase activity is enhanced with the reverse potency sequence of NECA > adenosine $\geq$ PIA. Methylxanthines act as antagonists at both $A_1$ and $A_2$ receptors in the order of potency 3-isobutyl-lmethylxanthine > theophylline > caffeine.

The $A_{2A}$ and $A_{2B}$ subtypes of $A_2$ receptor were identified following observations by Daly in 1983 of a group of $A_2$ receptors within the rat striatum and nucleus accumbens with a higher affinity for adenosine than those present in other areas of the brain. A subsequent study described the high-affinity striatal $A_{2A}R$ as a receptor where binding of the $A_1$ and $A_2$ receptor-selective compound [3H]adenosine-5'-(N-ethylcarboxamide) ([$^3$H]NECA) is observed in the presence of the $A_1R$ agonist $N^6$-

4

cyclopentyladenosine (CPA) (Bruns, Lu et al. 1986). Molecular cloning confirmed the existence of two distinct $A_2$ receptor subtypes which are broadly similar with the exception of the $A_{2A}R$ having a larger intracellular C-terminal (Fredholm, Abbracchio et al. 1994).

Molecular methods were used to identify the final P1 receptor subtype, the $A_3R$. The rat striatal cDNA sequence R226 was found to be a GPCR of the P1 receptor family but without sufficient homology within the transmembrane regions to be considered as an $A_1$ or $A_2$ receptor subtype. Functional expression found that the receptor was able to bind recognised adenosine receptor agonists but with a different pharmacological profile to the $A_1R$, $A_{2A}R$ or $A_{2B}R$ although inhibition of adenylate cyclase is observed in the same way as at the $A_1R$. In contrast to the other adenosine receptor subtypes the $A_3R$ is xanthine-insensitive (Zhou, Li et al. 1992). The $A_3R$ subtype varies between species and is generally of low abundance. It is the least well characterised of the P1 family of receptors.

Several species have now been used to clone all four subtypes of P1 adenosine receptor and functional expression in mammalian cells or *Xenopus* oocytes has enabled the biochemical and pharmacological characterisation of each (Ralevic and Burnstock 1998). A number of subtype-selective agonists and antagonists have been identified with the agonists differing only slightly in structure from that of adenosine (Burnstock 2007; Abbracchio, Burnstock et al. 2009).
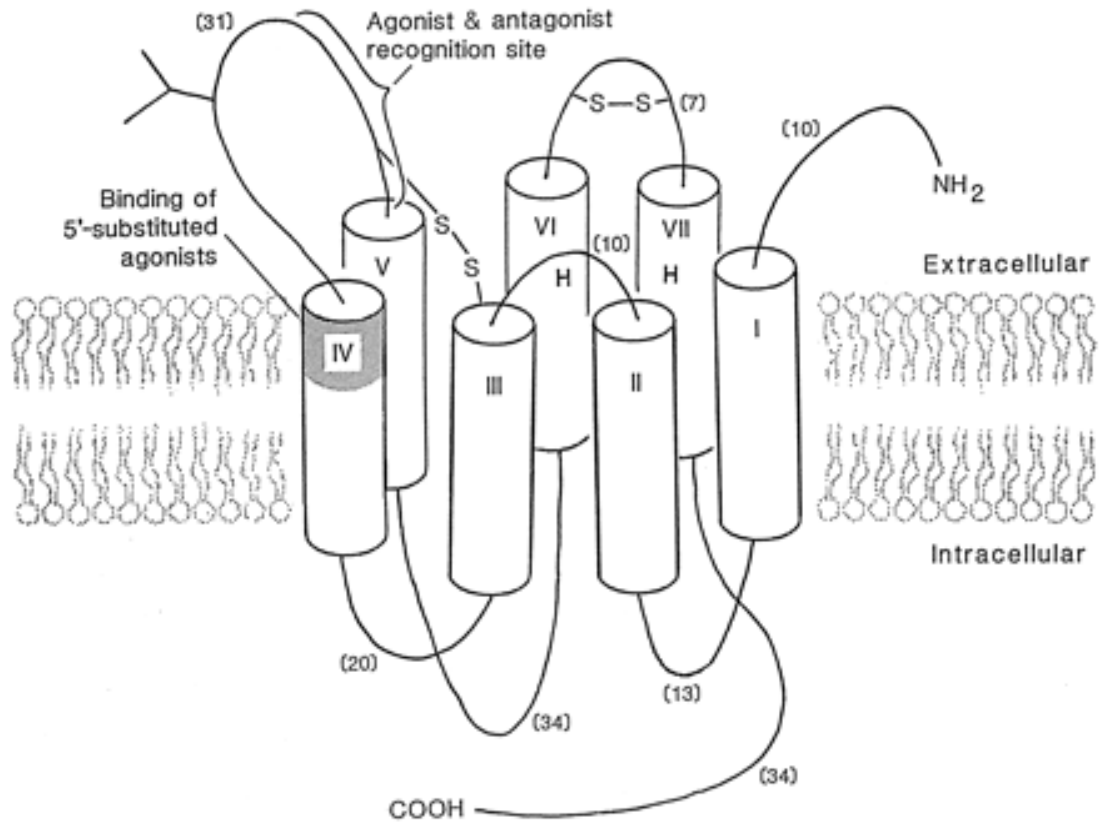
**Figure 1.1   Structure of the A$_1$ receptor (A$_1$R)**
The A$_1$R is one of four known P1 receptor subtypes. All are G-protein coupled receptors (GPCR) consisting of seven highly-conserved hydrophobic transmembrane domains (I – VII) that form a binding pocket for adenosine.  Each hydrophobic domain forms an α-helix connected by hydrophilic loops.  There is an extracellular N-terminal and intracellular C-terminal.  The number of amino acids comprising the hydrophilic loops and the N-terminal and C-terminal regions of the bovine A$_1$R are indicated in brackets (Ralevic and Burnstock 1998).

| Receptor | Adenosine affinity | G-protein | Transduction mechanisms[a] | Physiological actions in brain | Distribution in brain |
|---|---|---|---|---|---|
| **A$_1$** | ~70 nM | G$_i$ and G$_o$ | Inhibits adenylate cyclase<br><br>Activates GIRKs<br><br>Inhibits Ca$^{2+}$ channels<br><br>Activates PLC | Inhibits synaptic transmission<br><br>Hyperpolarizes neurons | Widespread[b] |
| **A$_{2A}$** | ~150 nM | G$_s$[c] | Activates adenylate cyclase<br><br>Inhibits Ca$^{2+}$ channels<br><br>Activates Ca$^{2+}$ channels (?) | Facilitates transmitter release<br><br>Inhibition of transmitter release | Primarily striatum<br><br>olfactory tubercle<br><br>nucleus accumbens[d] |
| **A$_{2B}$** | ~5100 nM | G$_s$[c] | Activates adenylate cyclase<br><br>Activates PLC | Increases in cAMP in brain slices<br><br>Modulation of Ca$^{2+}$ channel function (?) | Widespread[e] |
| **A$_3$** | ~6500 nM | G$_{i3}$, G$_q$ | Activates PLC<br><br>Inhibits adenylate cyclase<br><br>Increases intracellular Ca$^{2+}$ | Uncouples A$_1$, mGlu receptors (?) | Widespread[e] |

## Figure 1.2   Adenosine receptors in the brain

[a]GIRKs, G-protein–dependent activation of inwardly rectifying K$^+$ channels; PLC, phospholipase C.

[b]Based upon numerous ligand binding studies and in situ hybridization studies.

[c]Primary mechanism of coupling.

[d]Ligand binding and in situ hybridization generally shows high levels in these regions, very low levels elsewhere; reverse transcriptase–polymerase chain reaction (RT-PCR) shows more widespread expression.

[e]Relatively low levels, not detectable with in situ hybridization but apparent with RT-PCR

(Dunwiddie and Masino 2001)

## 1.2   Adenosine signalling in the CNS

### 1.2.1  The effects of adenosine in the CNS

Activation of high-affinity $A_1R$ at presynaptic terminals is linked to a decreased release of excitatory and inhibitory neurotransmitters via inhibition of $Ca^{2+}$ channels. Inhibition of a number of 'classical' neurotransmitters including gamma-aminobutyric acid (GABA) (Courjaret, Troger et al. 2009) and acetylcholine (De Lorenzo, Veggetti et al. 2004) have been described although the inhibition of excitatory glutamatergic transmission is the most frequently occurring. Activation of $A_1R$ in the CNS is also associated with reduced neuronal activity via hyperpolarisation of the resting membrane potential due to the G-protein dependent activation of inwardly rectifying $K^+$ channels (GIRKs) (Dunwiddie and Masino 2001; Boison 2008).

Action of the purinergic messenger adenosine at its cell surface receptors within the CNS is implicated in a diversity of physiological and pathophysiological conditions. A number of studies have demonstrated a role for adenosine in promoting sleep and reducing arousal. Measurement of extracellular adenosine concentrations in the basal forebrain and thalamus of cats, where the efferent cholinergic neurones involved in the control of electroencephalographic activation (EEG arousal) are present, showed that increases in adenosine are linked to prolonged and deeper sleep following periods of wakefulness. Microdialysis perfusion of adenosine into these brain regions also induces sleep (Porkka-Heiskanen, Strecker et al. 1997). Conversely, intravenous injections of the adenosine receptor antagonist caffeine into

males during non-rapid eye movement (non-REM sleep) promotes arousal and disturbs sleep (Lin, Uhde et al. 1997). Analysis of rat EEGs following the administration of the $A_1R$ agonist $N^6$-cyclopentyladenosine (CPA) and $A_1R$ antagonist 8-cyclopentyl-1,3-dipropylxanthine (CPX) demonstrates a role for this specific adenosine receptor subtype in sleep (Fulga and Stone 1998) although it is unlikely that the $A_1R$ is solely responsible for sleep regulation. A comparison of sleep patterns and response to sleep deprivation in $A_1R$ knockout mice and wildtype mice of the same line demonstrated no significant differences between the two groups (Stenberg, Litonius et al. 2003). This may partly be explained by a number of studies which have more recently suggested a role for the high-affinity $A_{2A}R$ in sleep (Dunwiddie and Masino 2001).

Extracellular adenosine plays a role in respiration via receptors located at carotid bodies responsible for the detection of oxygen levels in the blood. A number of studies have demonstrated an increased catecholamine discharge from the carotid sinus nerve resulting in enhanced ventilation, which is reversible with adenosine receptor antagonists like caffeine, following administration of intravenous adenosine in different species (Lahiri, Mitchell et al. 2007). The $A_{2A}R$ located on type I cells, which are the primary oxygen sensors of the carotid body, are thought to contribute to this. Calcium imaging in rat carotid bodies demonstrated replication of the increased $[Ca^{2+}]_i$ response to adenosine with the $A_{2A}R$ agonist CGS-21680 which could be blocked with the $A_{2A}R$ antagonist ZM-241385 (Xu, Xu et al. 2006).

A further physiological role for adenosine is in the regulation of locomotor activity via $A_{2A}R$ within the striatum. The $A_{2A}R$ agonist CGS-21680 reduces locomotor

activity in normal mice and has no effect on $A_{2A}R$ knockout mice, which also demonstrate a reduced exploratory behaviour. The locomotor stimulatory effects of caffeine are also absent in $A_{2A}R$ knockout mice (Ledent, Vaugeois et al. 1997). Increased locomotor activity in $A_3R$ knockout mice suggests this adenosine receptor subtype may also be involved in locomotion (Fredholm, Abbracchio et al. 1994).

A prolonged release of extracellular adenosine in response to the increased demand for energy from ATP during pathological events is a well-documented neuroprotective action that results in vasodilation and an increase in local cerebral blood flow. Increased levels of extracellular adenosine have been described during trauma, stress, pain, seizures, hypoxia and ischemia (Dunwiddie and Masino 2001; Latini and Pedata 2001). Synaptic depression of extracellular field potentials during periods of hypoxia induced in rat hippocampal slices can be blocked by the $A_1R$ antagonist 8-cyclopentyltheophylline (8-CPT) (Fowler 1989; Gribkoff and Bauman 1992). Similarly, a complete depression of synaptic potentials as a result of increased extracellular adenosine blocking glutamate release is observed during periods of induced ischemia in rat hippocampal slices. Again, the synaptic depression can be blocked by the addition of 8-CPT to the superfusate (Pedata, Latini et al. 1993). The neuroprotective effects of adenosine are mediated primarily through cellular pathways triggered by $A_1R$ activation. These mechanisms inhibit some $Ca^{2+}$ channels to reduce glutamate and other neurotransmitter release and hyperpolarise neurones to limit the entry of $Ca^{2+}$, which causes excitotoxic damage and maintain stores of ATP that are needed to actively remove intracellular $Ca^{2+}$ (Dunwiddie and Masino 2001).

A role for adenosine as an endogenous anticonvulsant has been demonstrated in a number of studies using models of epilepsy. Kainic acid-induced motor seizures in rats are suppressed by the adenosine receptor agonist N-ethylcarboxamidoadenosine (NECA) or the adenosine-uptake blocker dilazep (Zhang, Franklin et al. 1990). Conversely, in rat hippocampal slices where the CA3 region is known to be the primary generator of epileptiform activity, blockade of adenosine receptors by theophylline and caffeine induces convulsant activity and enhances kainic-acid induced burst firing (Ault, Olney et al. 1987). The adenosine system is also involved in the astrocytic proliferation observed in epilepsy. This astrogliosis increases levels of the enzyme adenosine kinase (AK) responsible for the regulation of intracellular levels of adenosine. Its upregulation reduces the local inhibitory tone of adenosine and is associated with spontaneous chronic seizures. Transgenic mice overexpressing the AK enzyme are also prone to spontaneous seizures. Therapeutic potential has been demonstrated for $A_1R$ agonists and AK inhibitors in the treatment of epilepsy. (Boison 2008).

A neuromodulatory role for adenosine has been documented in a number of neurological diseases. The action of adenosine, primarily at $A_{2A}R$, plays a role in Parkinson's disease, Alzheimer's disease, Huntington's disease and Schizophrenia (Boison 2008).

There is growing evidence that adenosine plays an important role in the processing of information by cerebellar circuits. Endogenous adenosine (Braas, Newby et al. 1986), $A_1R$ (Goodman and Snyder 1982; Rivkees, Price et al. 1995; Yoshioka, Hosoda et al. 2002) and nucleoside transporters (Anderson, Baldwin et al. 1999;

Anderson, Xiong et al. 1999) are all present within the cerebellum as are the enzymes required for purine metabolism: ecto-ATPase (Wang and Guidotti 1998), 5'-nucleotidase (Schoen, Graeber et al. 1987) and adenosine deaminase (Geiger and Nagy 1986) with activity comparable to or higher than in other brain regions (Wink, Braganhol et al. 2003). Application of adenosine can selectively produce synaptic inhibition in the cerebellum (Kocsis, Eng et al. 1984) and the tonic activation of $A_1R$, producing synaptic inhibition, provides indirect evidence for an extracellular tone of adenosine in cerebellar slices (Takahashi, Kovalchuk et al. 1995). However the physiological relevance of these studies remains unclear (Wall, Atterbury et al. 2007).

## 1.2.2  The formation and control of intracellular adenosine

Intracellular adenosine can be formed via the dephosphorylation of AMP by cytosolic 5'-nucleotidase or via the hydrolysis of S-adenosylhomocysteine (SAH) by SAH hydrolase (figure 1.3) (Boison 2006). It was first assumed that only metabolic stress and increased ATP catabolism would result in the formation of adenosine via dephosphorylation of AMP due to the $K_m$ of cytosolic 5'-nucleotidase (5 mM) being higher than the physiological intracellular concentration of AMP (0.1 -0.5 mM) (Dunwiddie and Masino 2001). However, COS-7 cells expressing cytosolic 5'-nucleotidase cloned from pigeon heart have a significantly higher concentration of adenosine than untransfected cells suggesting a basal activity of the enzyme in the absence of metabolic stress. An abundance of cytosolic 5'-nucleotidase in brain

tissue was also demonstrated using Northern blot and PCR techniques (Sala-Newby, Skladanowski et al. 1999).

Immunohistochemistry has demonstrated localisation of the SAH hydrolase enzyme in the neocortex, cerebellum, hippocampus and olfactory tubercle of the rat brain (Patel and Tudball 1986) and adenosine can be formed via the action of this enzyme in both glial and neuronal primary cell cultures from chick embryos (Ceballos, Tuttle et al. 1994). In rat hippocampal slices the potent SAH hydrolase inhibitor adenosine-2,3-dialdehyede has no effect on the outflow of adenosine as measured by HPLC under ischemic conditions or following electrical stimulation. Tissue levels of SAH are also low in these slices indicating that SAH hydrolase is unlikely to play a major role in intracellular adenosine production and that its activity will be confined to regions containing higher substrate levels (Latini, Corsi et al. 1995).

The adenosine concentration in the intracellular space is maintained at low levels by the action of adenosine kinase (AK) which phosphorylates adenosine to form AMP and adenosine deaminase (ADA) which deaminates adenosine to form inosine. The phosphorylation of adenosine by AK is the predominant metabolic pathway as this enzyme has a higher affinity for adenosine. The $K_m$ is 2 µM for AK and 17 - 45 µM for ADA in the rat whole brain. Deamination of adenosine by ADA is likely to be more important in pathological conditions when intracellular adenosine concentrations are increased (Boison 2006).

A number of studies have demonstrated that AK is the key enzyme in the regulation of adenosine metabolism. In rat hippocampal slices the inhibition of neuronal

13

activity observed with application of adenosine is replicated with perfusion of the AK inhibitor iodotubericidin but to a lesser extent or not at all with inhibition of SAH hydrolase with adenosine-2,3-dyaldehyede or ADA with erythro-9-(2-hydroxy-3-nonyl) adenine (EHNA) (Pak, Haas et al. 1994). In the rat prepiriform cortex the ability of adenosine to suppress bicuculline methiodide-induced seizures is potentiated following application of the AK inhibitor 5'-amino-5'-deoxyadenosine again suggesting an important role for this enzyme in the control of extracellular adenosine (Zhang, Franklin et al. 1993) and in rat hippocampal slices labelled with [³H]-adenine a greater proportion of [³H]-adenosine is released following inhibition of AK with iodotubericidin. In contrast blocking ADA with EHNA has no effect on the proportion of [³H]-adenosine released under normoxic conditions (Lloyd and Fredholm 1995).

Intracellular adenosine may potentially be inactivated via the reversible reaction of SAH hydrolase which requires L-homocysteine in combination with adenosine to form SAH. In rat hippocampal slices [¹⁴C] adenosine was incorporated primarily into nucleotides with only a very small amount into other metabolites or SAH. The addition of L-homocysteine increased the amount of [¹⁴C] adenosine incorporated into SAH suggesting that the reversible reaction of SAH hydrolase contributes very little to the metabolism of intracellular adenosine due to low levels of L-homocysteine in the brain limiting the pathway (Reddington and Pusch 1983).

### 1.2.3  The sources of extracellular adenosine

The extracellular concentration of adenosine in the brain varies by region but is estimated to be between 25 nM and 250 nM (Dunwiddie and Diao 1994). There are at least three mechanisms for adenosine to access the extracellular space to maintain this basal concentration which is responsible for the tonic activation of high affinity $A_1$ and $A_{2A}R$. Firstly, the extracellular ATP released from neurones (Edwards, Gibb et al. 1992; Dale 1998) or through the opening of gap junction hemichannels (Pearson, Dale et al. 2005) as a transmitter or co-transmitter can be rapidly converted to adenosine by ectonucleotidases. Alternatively, adenosine that has been formed intracellularly can be released directly into the extracellular space via facilitated diffusion transporters (Craig and White 1993; Sweeney 1996) or, as more recent studies have suggested, adenosine can be released into the extracellular space in a neuronal activity-dependent manner (Wall and Dale 2008) (see figure 1.4 for summary).

In support of extracellular ATP being the source of adenosine it has been shown that application of adenine nucleotides (cAMP, AMP, ADP and ATP) to the cell bodies of CA1 pyramidal neurones in the rat hippocampus results in the same postsynaptic activation of $A_1R$ and subsequent stimulation of $K^+$ channels to decrease excitatory transmission that is observed with direct application of adenosine. Blockade of the ectonucleotidase pathway demonstrates that the adenine nucleotides do not interact directly with the $A_1R$ but that rapid conversion of the non-cyclic adenine nucleotides to adenosine following their release into the extracellular space is essential for the transient activation of $A_1R$. The cyclic adenine nucleotide, cAMP, is more likely to

account for slow changes in extracellular adenosine concentration (Dunwiddie, Diao et al. 1997).

The ectonucleotidase enzyme families include: the plasma membrane-located E-NTPDase (ecto-nucleoside triphosphate diphosphohydrolase) family (E-NTPDase 1-6) responsible for the hydrolysis of ATP to ADP or AMP; the E-NPPase (ecto-nucleotide pyrophosphatase/phosphodiesterase) family of membrane proteins (NPP1-3) which use purine and pyrimidine nucleotides as substrates to primarily form AMP via hydrolysis although NPP2 can also produce adenosine from AMP; the alkaline phosphatases of which little evidence exists for a role in the metabolism of extracellular nucleotides and the GPI (glycosylphosphatidylinositol)-anchored ecto-5'-nucleotidase which catalyses the final step of extracellular nucleotide metabolism by dephosphorylating AMP to form adenosine (Zimmermann 2000).

Nucleoside transporters may provide a further source of extracellular adenosine. There are two structurally unrelated nucleoside transporter (NT) protein families; the equilibrative nucleoside transporter (ENT) family passively mediate the transport of nucleosides across the cell membrane in either direction to equilibrate extracellular and intracellular concentrations, and the concentrative nucleoside transporter (CNT) family are symporters that enable the active transport of nucleosides against their concentration gradient into the cell coupled with the inward movement of $Na^+$ down its electrochemical gradient as a source of energy (Cass, Young et al. 1998).

The ENT transporter family are classified according to their sensitivity to the nucleoside transport inhibitor nitrobenzylthioinosine (NBMPR). The *es* subtype of

16

ENT (ENT1) is sensitive to inhibition by NBMPR and the *is* subtype of ENT (ENT2) is insensitive to NBMPR or blocked only at high micromolar concentrations. Both ENT1 and ENT2 proteins are equally sensitive to inhibition by dipyridamole (Cass, Young et al. 1998). In-situ hybridisation and RT-PCR using the ENT1 transporter cloned from rat jejunum (rENT1) shows a wide distribution of rENT1 mRNA throughout the hippocampus, cortex, cerebellum and striatum of the rat brain with [3H] NBMPR binding sites also present largely in the cortex and striatum and to a lesser extent in the hippocampus and cerebellum (Anderson, Xiong et al. 1999). A similar study using cloned rat cDNA for ENT2 (rENT2) shows a strong antisense signal in a number of brain regions and suggests that ENT2 may be a more predominant equilibrative transporter subtype than ENT1 in the rat brain (Anderson, Baldwin et al. 1999).

Under normoxic conditions the widely distributed equilibrative transporters generally remove adenosine from the extracellular space along its concentration gradient and a number of studies demonstrate an increase in extracellular adenosine tone following their pharmacological inhibition (Latini and Pedata 2001). However, the release of preloaded L-[3H]adenosine from rat brain synaptosomal protein preparations following their suspension in buffer can be partially blocked by both NBMPR and dipyridamole indicating that some of this adenosine efflux is via equilibrative transporters and that these have the potential to provide a source of extracellular adenosine *in vivo* (Gu, Foga et al. 1995).

It is possible that the equilibrative transporters could provide a source of extracellular adenosine in pathological situations where the usually low concentration of

intracellular adenosine, maintained through activity of the AK enzyme, is increasedInhibition of AK with NH2dAD can mimic the inhibition of spinal reflex potentials observed following an acute increase in $CO_2$ (hypercapnia) in the neonatal rat isolated spinal cord. The fall in $pH_i$ inactivates the AK enzyme resulting in an increase in extracellular adenosine presumably due to release along its reversed concentration gradient via equilibrative transporters (Otsuguro, Yamaji et al. 2006). However, inhibition of equilibrative transporters in rat hippocampal slices does not prevent the release of adenosine during ischemia and microelectrode biosensor recordings instead demonstrate that release is enhanced twofold indicating that equilibrative transporters are unlikely to facilitate adenosine release during ischemia (Frenguelli, Wigmore et al. 2007).

To support the involvement of equilibrative transporters in the removal of increased intracellular adenosine resulting from the inhibition of AK to the extracellular space, application of NBTI and dipyridamole to inhibit ENT1 and ENT2 proteins results in blockade of inhibition at the PF-PC synapse caused by iodotubericidin in 50 % of cerebellar slices (Wall, Atterbury et al. 2007).

In addition to increases in intracellular adenosine caused by the inhibition of AK, the extra demand for energy during metabolic stress will increase the cytoplasmic catabolism of ATP to adenosine (figure 1.3) and this increased intracellular adenosine concentration will result in the facilitative release of adenosine along its concentration gradient to the extracellular space possibly via equilibrative transporter proteins (Latini and Pedata 2001).

The involvement of the five known CNT transporter subtypes in the regulation of extracellular adenosine levels is largely undetermined due to the lack of selective inhibitors available although it is thought that the CNT proteins may enable release of adenosine into the extracellular space in pathological conditions such as hypoxia, ischemia and seizures where neurones are no longer able to maintain physiological $Na^+$ electrochemical gradients. This potentially could result in the release of adenosine coupled to reversed $Na^+$ transport in concentrative transporters (Dunwiddie and Masino 2001; Latini and Pedata 2001).

Finally, it has been more recently recognised that adenosine can be released under normal conditions in an activity-dependent manner. High frequency stimulation of Schaffer-collateral axons in organotypic hippocampal slice cultures results in the short-term depression of excitatory postsynaptic currents (ESPCs) recorded in CA1 cells which can be attenuated with application of the $A_1R$ antagonist DPCPX. The short-term depression is not affected by inhibition of 5'-ectonucleotidase with $\alpha,\beta$ methylene-ADP or ENT protein inhibition with dipyridamole suggesting that the adenosine released is not a result of extracellular ATP breakdown or facilitative transport from the cytoplasm (Brager and Thompson 2003). Similarly, trains of stimuli applied to the Calyx of Held which is a giant nerve terminal in the mammalian auditory brainstem results in synaptic depression which can be reduced with the $A_1R$ antagonist DPCPX and which is not affected by application of the ectonucleotidase inhibitor ARL 67156 to prevent the breakdown of ATP to ADP thereby suggesting direct release of adenosine (Wong, Billups et al. 2006). Application of a physiological electrical stimulus to the molecular layer of rat cerebellar slices results in an inhibition of excitatory postsynaptic potentials (EPSPs)

that can be blocked with $A_1R$ antagonists. A slow rising current can also be detected on an adenosine microelectrode biosensor placed on the surface of the molecular layer, but not on an ATP biosensor signal, that is not affected by the ENT protein inhibitors NBTI or dipyridamole. This suggests either direct release of adenosine or a rapid metabolism of ATP although the adenosine signal is not affected by blockade of ATP metabolism with Evans Blue, ARL67156 or $\alpha,\beta$ methylene-ADP (Wall and Dale 2007).

Release of adenosine into the extracellular space under normal conditions that is not the result of released ATP breakdown may be achieved via the exocytosis of a neurotransmitter that acts on a neuron or astrocyte to enable adenosine release. This mechanism is difficult to prove due to the large number of antagonists that would need to be tested in order to block the unknown 'interposed' neurotransmitter release. Alternatively adenosine may directly be released by exocytosis from synaptic vesicles which will be unlikely if, as many studies suggest, AK is actively maintaining a low intracellular adenosine concentration (Wall and Dale 2008).

## 1.2.4 The removal of adenosine from the extracellular space

Extracellular adenosine is primarily inactivated by its movement across neuronal or glial cell membranes into the cytoplasm by facilitated diffusion using ENT1 or ENT2 proteins or active transport using CNT proteins (Dunwiddie and Masino 2001; Latini and Pedata 2001). Application of NBTI via microdialysis to block ENT1 proteins *in vivo* results in a 2.4 fold increase in interstitial adenosine levels in the pig cortex

under normal conditions (Gidday, Kim et al. 1996). The effect of equilibrative transporter protein inhibition is variable at the parallel fibre-Purkinje cell (PF-PC) synapse in the rat cerebellum (Wall, Atterbury et al. 2007).

The enzyme ADA is responsible for the deamination of adenosine to inosine in the extracellular as well as the intracellular space. Inosine is inactive at $A_{2A}R$ and $A_{2B}R$ but a weak agonist with a low efficacy at $A_1R$ and $A_3R$ in CHO cells expressing human adenosine receptors. Although inosine cannot be considered a natural ligand at adenosine receptors it may activate $A_1R$ and $A_3R$ under some circumstances (Fredholm, Irenius et al. 2001).

It has previously been discussed how the intracellular enzyme AK is more important in the regulation of adenosine metabolism than ADA under normal conditions. EctoADA is structurally and functionally identical to cytosolic ADA and is known to be anchored to the cell surface by CD26 and $A_1R$ enabling extra-enzymatic co-stimulatory functions (Franco, Casado et al. 1997). EctoADA is likely to play an important role in the removal of adenosine from the extracellular space in pathological conditions where the increased intracellular adenosine concentration results in transporter proteins no longer being able to remove extracellular adenosine (Dunwiddie and Masino 2001).

## 1.2.5 The development of adenosine signalling in the CNS

Although the release, clearance and effects of adenosine are reasonably well-documented within the mature CNS relatively little is known about how adenosine signalling changes during postnatal development. Adenosine binding to presynaptic $A_1R$ inhibits EPSCs at the glutamatergic synapse between the calyx of Held in the auditory brainstem and a postsynaptic principal cell in the medial nucleus of the trapezoid body (MNTB) of rats at postnatal days 5-7. A developmental decline in the adenosine-induced presynaptic inhibition occurs during the second postnatal week in parallel with a significant reduction in $A_1R$ immunoreactivity at the calyx of Held synapse (Kimura, Saitoh et al. 2003). Conversely, presynaptic inhibition of EPSPs following application of adenosine to CA1 hippocampal neurones does not change in slices from rats aged between postnatal day 5 and postnatal day 120. However, the increase in inhibition observed by blocking adenosine uptake with NBTI is less obvious in younger animals suggesting that a developmental increase in extracellular adenosine tone occurs although $A_1R$ properties are maintained (Psarropoulou, Kostopoulos et al. 1990).

Hippocampal CA3 neurones act as a pacemaker of epileptiform activity possibly as a result of the intrinsic recurrent excitatory circuits in this area (MacVicar and Dudek 1980). Adenosine is a less potent anti-epileptic at immature hippocampal CA3 neurones as inhibition of stimulus-induced postsynaptic potentials via activation of $A_1R$ with the agonist N6-(phenylisopropyl) adenosine (PIA) is significantly less than in the adult hippocampus. It is also likely that endogenous adenosine produces an anti-epileptic tone in adult but not immature animals as the $A_1R$ antagonist 8-

cyclopentyl-1,3-dipropylxanthine (DCPCX) induces proconvulsant spontaneous bursts more frequently at adult hippocampal CA3 neurones (Descombes, Avoli et al. 1998).

In another study application of adenosine results in a similar inhibition of transmitter release at CA3-CA1 neurones in both juvenile (postnatal day 15-21) and mature (postnatal day 28-35) rat hippocampal slices.  The inhibition results in an increase in paired pulse facilitation (PPF) of EPSPs in mature but not juvenile slices suggesting that the presynaptic ability of adenosine to affect transmitter release increases during development.  Application of adenosine increases the PPF in juvenile slices pre-treated with $Ca^{2+}$ to increase transmitter release suggesting that the increase in probability of release known to occur during maturation is responsible for the developmental differences in the affect of adenosine on PPF (Dumas and Foster 1998).  However,  a study using rat hippocampal slices and the $A_1R$ antagonist DPCPX demonstrates that the deterioration in long-term potentiation (LTP) from young adulthood to middle age in particular groups of synapses is likely to be due age-related changes in $A_1R$ or the processes that they trigger (Rex, Kramar et al. 2005)

The role of AK, the key enzyme in the regulation of adenosine metabolism, is likely to change during postnatal development.  During early postnatal development of the mouse hippocampus AK immunoreactivity is most prominent in neurones with a gradual transition of expression to newly-formed GFAP-positive astrocytes until around postnatal day 14 with neuronal expression being maintained in only a few areas.  Staining of myelin shows the switch in expression correlates with the onset of

neuronal myelination suggesting that neuronal expression of AK may prevent myelination during early postnatal development. The increased effect of $A_1R$ antagonists on EPSPs during hippocampal development suggests that the astrocytic expression of AK in mature slices allows regulation of adenosine concentration in the mature hippocampus according to metabolic needs and synaptic activity thus maintaining a greater tonic inhibition via $A_1R$ and the previously described decreased excitability and susceptibility to seizures (Studer, Fedele et al. 2006).
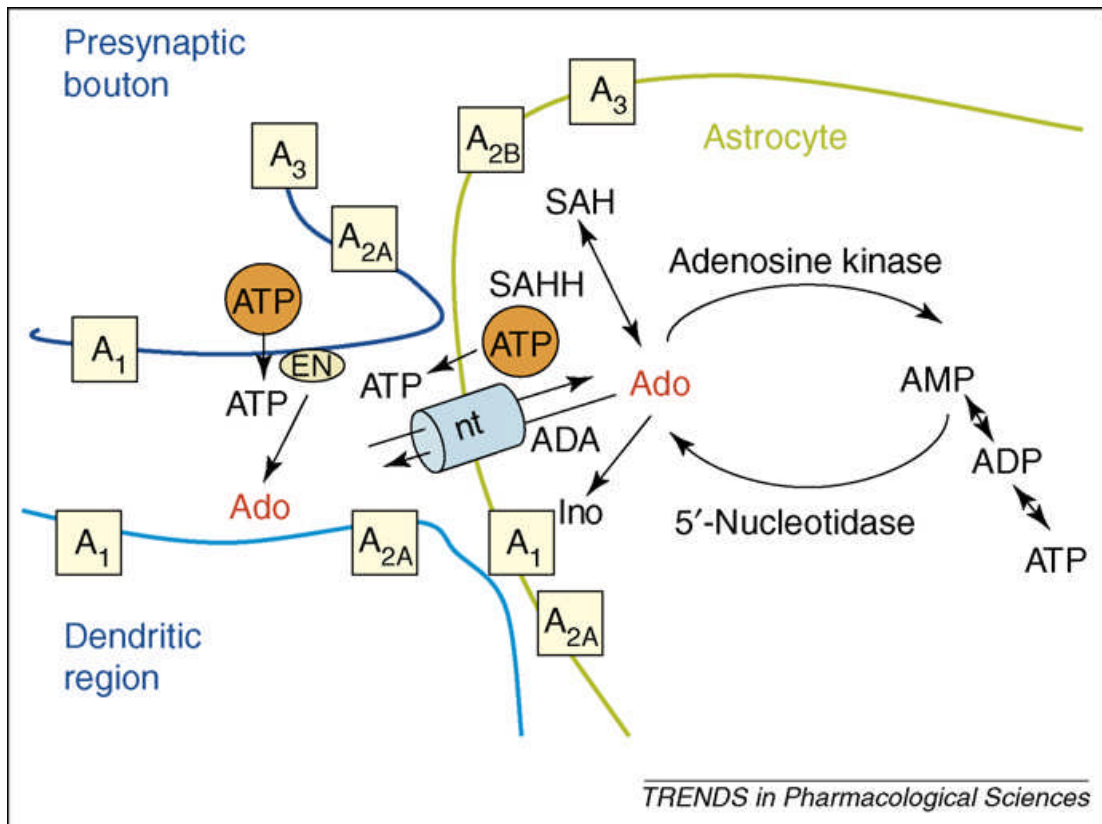
**Figure 1.3   The formation and control of intracellular adenosine**

Intracellular adenosine can be formed via the dephosphorylation of AMP by cytosolic 5'-nucleotidase or to a lesser extent via the hydrolysis of S-adenosylhomocysteine (SAH) by SAH hydrolase (SAHH).   Under normoxic conditions a low intracellular concentration of adenosine is maintained predominantly by the enzyme adenosine kinase (AK) which phosphorylates adenosine to form AMP.   Intracellular adenosine can also be deaminated by the lower-affinity enzyme adenosine deaminase (ADA) to from inosine (Ino).   During metabolic stress the increased production of adenosine via cytoplasmic ATP catabolism will result in an increased ADA activity and the removal of adenosine from the intracellular space along its reversed concentration gradient via nucleoside transporter (nt) proteins in the cell membrane.   Cleavage of released ATP by ectonucleotidases (EN) contributes to the extracelluar formation of adenosine (Boison 2006).
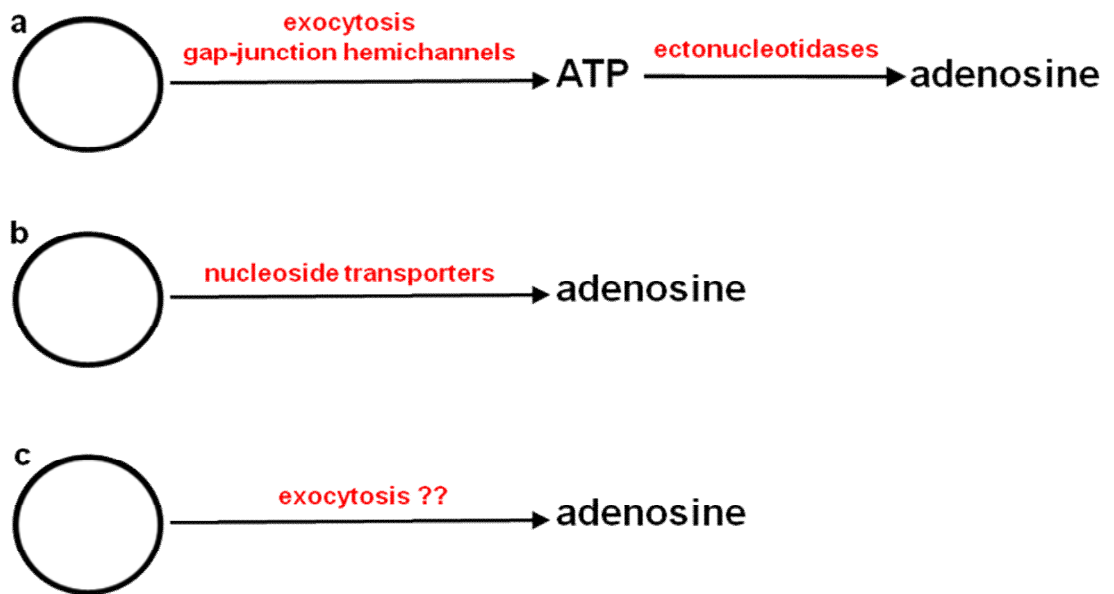
**Figure 1.4   Possible sources of extracellular adenosine**

There are at least three mechanisms for adenosine to access the extracellular space. This could be **(a)** via the metabolism of extracellular ATP released by exocytosis or through gap junction hemichannels.   Alternatively, **(b)** adenosine that has been formed intracellularly can be released into the extracellular space via equilibrative or concentrative nucleoside transporters or **(c)** possibly by via neuronal activity-dependent exocytosis.

## 1.3   The mammalian cerebellum

### 1.3.1   The roles of the cerebellum

A number of lesion and neural recording studies provide evidence for at least three ways in which the cerebellum is involved in the motor control of balance and locomotion. Firstly, although the spinal cord and brainstem are responsible for the basic generation of locomotor co-ordination (Morton and Bastian 2004), the cerebellum contributes to the timing and rate of muscle activity during locomotion. Cerebellar lesions in cats trained to walk on a motorised treadmill result in walking and balance difficulties demonstrated by abnormal timings in limb movements and decreased stride lengths (Yu and Eidelberg 1983) and in extracellular microelectrode recording studies discharges of simple spikes from Purkinje cells in the anterior lobe of the cerebellum in cats are recorded in time with stepping during steady walking on a moving belt (Edgley and Lidierth 1988).

Secondly the cerebellum contributes to the control of balance during locomotion. Postural ataxia frequently described as a 'drunken gait' with swaying and falling during locomotion is observed in patients with lesions of the anterior lobe of the cerebellum, cerebellar hemisphere and vestibulo-cerebellum (Mauritz, Dichgans et al. 1979). The cerebellar control of balance and gait are likely to be coupled and separate from the cerebellar control of limb movement as cerebellar lesion patients with impaired balance that perform poorly in a weight-shifting task are more likely to demonstrate cerebellar gait ataxia or walking incoordination than those with only a leg-placement deficit (Morton and Bastian 2003). Finally the cerebellum is likely to

use motor learning to allow adaptations to the locomotor pattern. Patients with cerebellar lesions and minimal ataxia are able to adapt sway and stride length to repeated and predictable changes in treadmill speed during ongoing locomotion but analysis of stepping patterns and electromyography (EMG) measurements of antagonistic pairs of leg muscles highlight inconsistencies in both strategy and the activation pattern of muscles when compared to control subjects (Rand, Wunderlich et al. 1998).

In addition to the well-documented contribution to motor function and motor learning the cerebellum has more recently been linked to non-motor cognitive processes although evidence is often not convincing largely due to the motor control required for cognitive tasks. Retrograde transneuronal transport of herpes simplex virus type 1 from an area of the primate prefrontal cortex known to be involved in spatial working memory labels neurones in the dentate nucleus of the cerebellum. These neurones are not labelled from motor areas of the cerebral cortex thus providing anatomical evidence of a cognitive role for the cerebellum (Middleton and Strick 1994). A number of human functional neuroimaging studies also indicate an involvement of the cerebellum in higher order cognitive functions (Timmann and Daum 2007). In further human studies a 'cerebellar cognitive affective syndrome' defined by a number of cognitive disturbances including loss of verbal fluency, memory and reasoning impairments and attention deficiency has been described in patients with diseases restricted to the cerebellum (Schmahmann and Sherman 1998).

## 1.3.2 The anatomy of the cerebellum

The cerebellum is attached to the brainstem beneath the occipital lobes of the cerebral hemispheres. The mammalian cerebellum can be divided longitudinally into a vermis in the midline region either side of which is a hemisphere with a flocculus and paraflocculus structure extending outwards from its lower lateral edge (figure 1.5a). The outer surface of the cerebellum is repeatedly folded dividing the vermis into ten lobules (I-X) separated by deep fissures along its anterior-posterior axis. These lobules are most easily observed in saggital sections of the cerebellar vermis and are divided into three lobes: the anterior lobe (I–V), the posterior lobe (VI–IX) and the flocculonodular lobe (X) (figure 1.5b). The hemispheres, flocculus and paraflocculus have their own distinct foliation patterns (Hawkes 2005; Sillitoe and Joyner 2007).

The entire cerebellum can be divided into three distinct cellular layers: the outer molecular layer, the Purkinje cell body monolayer and the inner granule layer that covers a white matter core containing the afferent and efferent axons of the cerebellum. The three pairs of deep cerebellar nuclei (DCN) which act as targets for the efferent projections underlie the cerebellar cortex (figure 1.6).

The mossy fibres are the larger of two major glutamatergic afferent pathways into the cerebellum. The ascending spinal, reticular and vestibular mossy fibres and descending pontocerebellar mossy fibres enter as bundles through either the superior, middle or inferior cerebellar peduncles. The climbing fibres from nuclei of the inferior olive located within the medulla oblongata of the brainstem enter through the

inferior cerebellar peduncle and are the second major afferent pathway into the cerebellum. Both mossy fibres and climbing fibres also send collateral projections to innervate neurones in the DCN. A third diffuse group of minor afferent projections from the locus coeruleus, pedunculopontine nucleus and raphe nucleus form noradrenergic, cholinergic and serotonergic synapses within the cerebellum. The Purkinje cell axons are the only efferent pathway from the cerebellum to the neurones of the DCN which interact with other areas of the CNS (Hawkes 2005; Sillitoe and Joyner 2007).

### 1.3.3  The cells and circuitry of the cerebellum

The inner granule layer is densely packed with the small somata of glutamatergic granule cells which are the most abundant neuronal cells in the brain. Granule cell dendrites within this layer form synaptic glomeruli with inhibitory Golgi cell axons and excitatory mossy fibre terminals. Granule cell axons extend upwards into the molecular layer forming ascending synapses with the proximal dendrites of Purkinje cells before branching medio-laterally at right angles to Purkinje cell dendrites as long parallel fibres (preserved in transverse sections) that form synapses with the larger diameter distal regions of the Purkinje cell dendritic tree (figure 1.7). Approximately 20 % of these Purkinje cell interactions are with ascending axons and the remainder with parallel fibres (Gundappa-Sulur, De Schutter et al. 1999).

A single mossy fibre interacts with 20-30 granule cells and each parallel fibre forms synapses with around half of the Purkinje cells it traverses resulting in each Purkinje

cell having around 150,000 - 175,000 parallel fibre synapses. The activation of approximately 50 granule cells is required to release sufficient glutamate from parallel fibres to generate a sodium-dependent action potential in a Purkinje cell (Barbour 1993) through the activation of its alpha-amino-3-hydroxy-5-methyl-4-isoxazolepropionic acid receptors (AMPAR).

The somata of two inhibitory interneurones are also located within the granule layer. The previously mentioned GABAergic Golgi cell interneurone axons extend from somata within the granule layer to form part of the synaptic glomeruli and their dendrites extend to the molecular layer to receive excitatory glutamatergic input from parallel fibres allowing feedback inhibition to granule cells (figure 1.7). The Lugaro cells are the second inhibitory interneurones with somata within the granule layer. These are positioned just below the Purkinje cell layer although little is understood about their function (Hawkes 2005; Sillitoe and Joyner 2007). An excitatory interneurone has more recently been described within the granule layer. Glutamatergic unipolar brush cells (UBCs) have a single dendrite that terminates in a brush-like tip of dendrioles which receives excitatory input from afferent mossy fibres. The dendrioles form dendro-dendritic excitatory synapses with granule cell dendrites to enable amplification of the mossy fibre signal (figure 1.7) (Mugnaini, Dino et al. 1997).

The Purkinje layer is predominantly a monolayer of large Purkinje cell bodies. Purkinje cell axons extend out through the granule layer and white matter to form GABAergic synapses with DCN to facilitate the sole output of the cerebellar cortex. Some axonal projections also synapse with interneurones in the granule layer to

provide feedback inhibition (figure 1.7). The extensively branched dendritic trees of Purkinje cells extend throughout the molecular layer flattened in the plane perpendicular to the fissures and parallel fibres and are therefore maintained in saggital sections (figure 1.5a) (Hawkes 2005; Sillitoe and Joyner 2007). The somata of candelabrum cell interneurones with dendrites extending into the molecular layer and the upper granule layer (Laine and Axelrad 1994) and Bergmann glia astrocytes with processes that extend into the molecular layer are also interspersed between the much larger and more numerous Purkinje cell bodies (figure 1.7).

The outer molecular layer is largely composed of overlapping Purkinje cell dendritic trees receiving glutamatergic inputs from parallel fibres and climbing fibres (figure 1.7). In contrast to the mossy fibre input each Purkinje cell is innervated by only one climbing fibre (in mature animals) which passes through the granule layer, branches after passing the Purkinje cell soma and wraps around the large proximal dendrites of its target cell to form several hundred synapses. The release of glutamate from a climbing fibre through stimulation of the inferior olive activates Purkinje cell AMPAR to generate a large excitatory postsynaptic potential in the Purkinje cell dendrite which results in an all-or-nothing sodium-dependent action potential in the Purkinje cell soma (Eccles, Llinas et al. 1966).

The molecular layer also contains two further inhibitory interneurones: stellate cells and basket cells. The dendrites of basket cells receive glutamatergic input from parallel fibres within the molecular layer. Their axons form inhibitory GABAergic synapses with Purkinje cell bodies with each soma enveloped by the axons of multiple basket cells. The small stellate cells are located in the outer third of the

molecular layer with dendrites that receive excitatory inputs from parallel fibres. Their axons form inhibitory synapses with Purkinje cell dendrites thus working with basket cells to provide feed-forward inhibition (figure 1.7) (Hawkes 2005; Sillitoe and Joyner 2007).

In summary, the climbing fibres and mossy fibres provide two excitatory inputs to the cerebellum that converge on the Purkinje cells which also interact with inhibitory interneurones. Purkinje cells integrate the information and provide the sole output of the cerebellum by forming inhibitory GABAergic synapses with three pairs of DCN.

### 1.3.4 Postnatal development of the cerebellum

Around the time of birth granule cell precursors that form an external granule layer over the entire surface of the cerebellum proliferate then remain at the top of the external granule layer for up to 48 hours following the final mitosis. During this period each granule cell develops uneven bipolar horizontal processes before migrating tangentially across the external granule layer along the longer process (figure 1.8). At the boundary of the external granule layer and molecular layer the granule cells form descending processes to allow radial migration through the molecular layer in association with Bergmann glia processes. (Komuro and Yacubova 2003). The bipolar granule cell axons remain as bundles of parallel fibres at the top of the molecular layer allowing the formation of glutamatergic synapses with distal Purkinje cell dendrites from around postnatal day 5 in the rat cerebellum (Altman 1972).

Following a brief stationary period in the Purkinje layer the granule cells continue to migrate independently of Bergmann glia processes into the internal granule layer (figure 1.8). Migration of a granule cell from the top of the external granule layer through the molecular and Purkinje layers to its final position in the internal granule layer takes around two days with the external granule layer ceasing to exist in the mouse by the end of the third postnatal week (Komuro and Yacubova 2003).

During the same postnatal period the Purkinje layer transforms from a multi-layered structure to a monolayer of Purkinje cell bodies and the dendritic trees of Purkinje cells branch extensively into the molecular layer. In addition the two major glutamatergic inputs to the cerebellum are formed: the climbing fibres that synapse with the large proximal Purkinje cell dendrites and the mossy fibres that form synaptic glomeruli with granule cell axons and Golgi cell dendrites. (Goldowitz and Hamre 1998).

In the adult cerebellum only one climbing fibre stimulates each Purkinje cell. However in the early postnatal cerebellum Purkinje cells are innervated by multiple climbing fibres. This was first reported when it was noted that two types of all-or-none response are apparent in half of electrophysiological recordings from rat cerebellar Purkinje cells at postnatal day 8 or 9 and that these are absent if climbing fibres are destroyed with 3-acetyl pyridine. Whole cell patch clamp recordings in cerebellar slices from mice frequently record five discrete climbing fibre excitatory postsynaptic currents (CF EPSCs) at postnatal day 4 but during the next few postnatal days functional differentiation of the climbing fibres occurs so that one strong CF EPSC and possibly several weaker CF EPSCs are measurable at postnatal day 10 suggesting that one climbing fibre is selectively strengthened during this

period of postnatal development (Hashimoto and Kano 2003).  A 'late phase' of climbing fibre elimination that is dependent on PF-PC synapse formation occurs during the second and third postnatal weeks until each Purkinje cell is innervated by one climbing fibre at around postnatal day 20 in mice (Hashimoto, Yoshida et al. 2009).
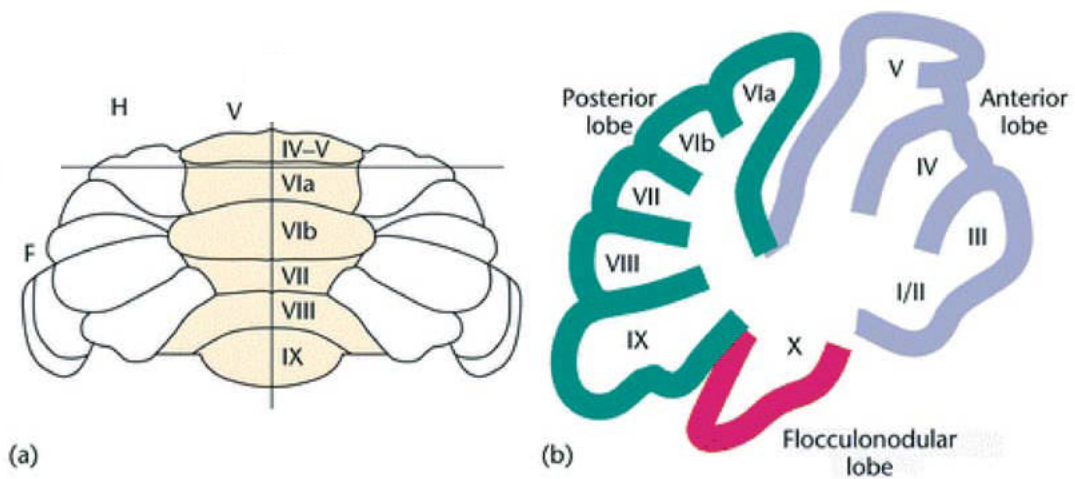
**Figure 1.5   The anatomy of the mammalian cerebellum**

The mammalian cerebellum **(a)** consists of a vermis (V) in the midline region either side of which is a hemisphere (H) with a flocculus (F) and paraflocculus structure at its lower lateral edge.  Folding of the outer surface of the cerebellum divides the vermis into ten lobules (I-X) separated by deep fissures **(b)** which are most easily observed in saggital sections (vertical line in **(a)**).  The lobules form three lobes:  the anterior lobe (I–V), the posterior lobe (VI–IX) and the flocculonodular lobe (X) (Hawkes 2005).
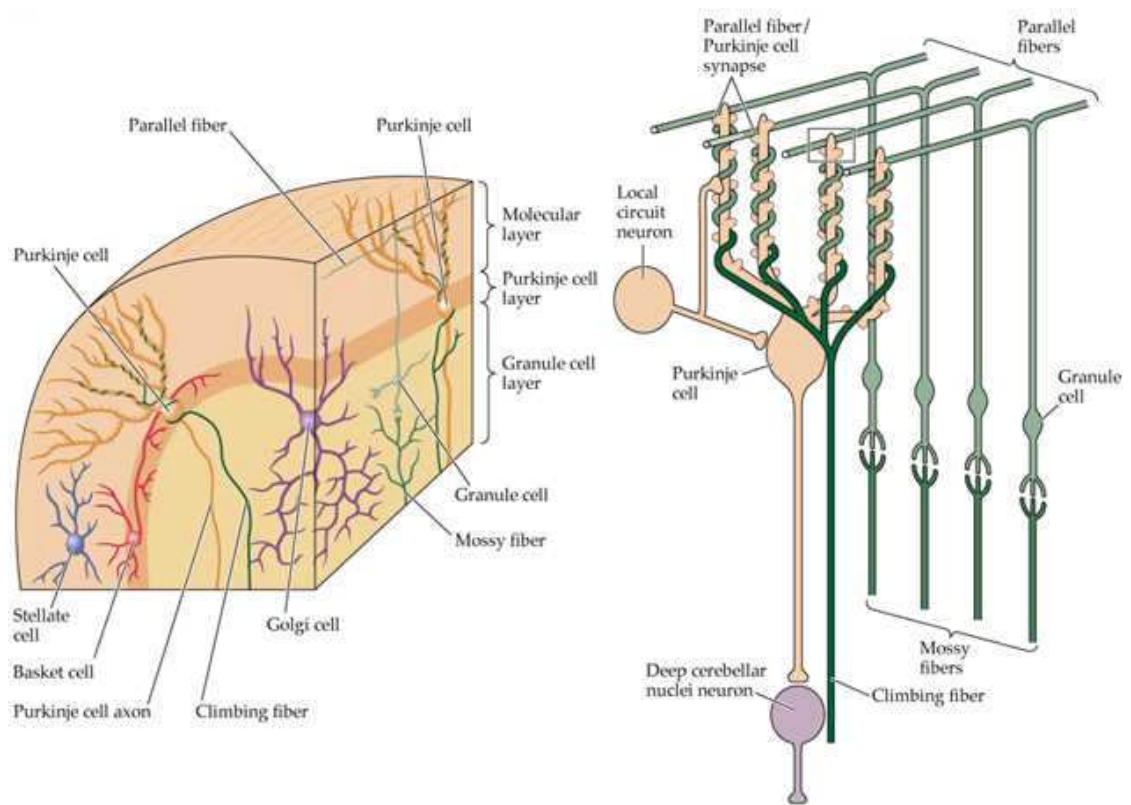
**Figure 1.6   The trilaminar organisation of the cerebellum**

The entire cerebellum can be divided into three distinct cellular layers: the outer molecular layer, the Purkinje layer and the inner granule cell layer that covers a white matter core containing the afferent and efferent axons of the cerebellum.  The deep cerebellar nuclei which act as targets for the efferent projections underlie the cerebellar cortex  (FitzGerald 2002).
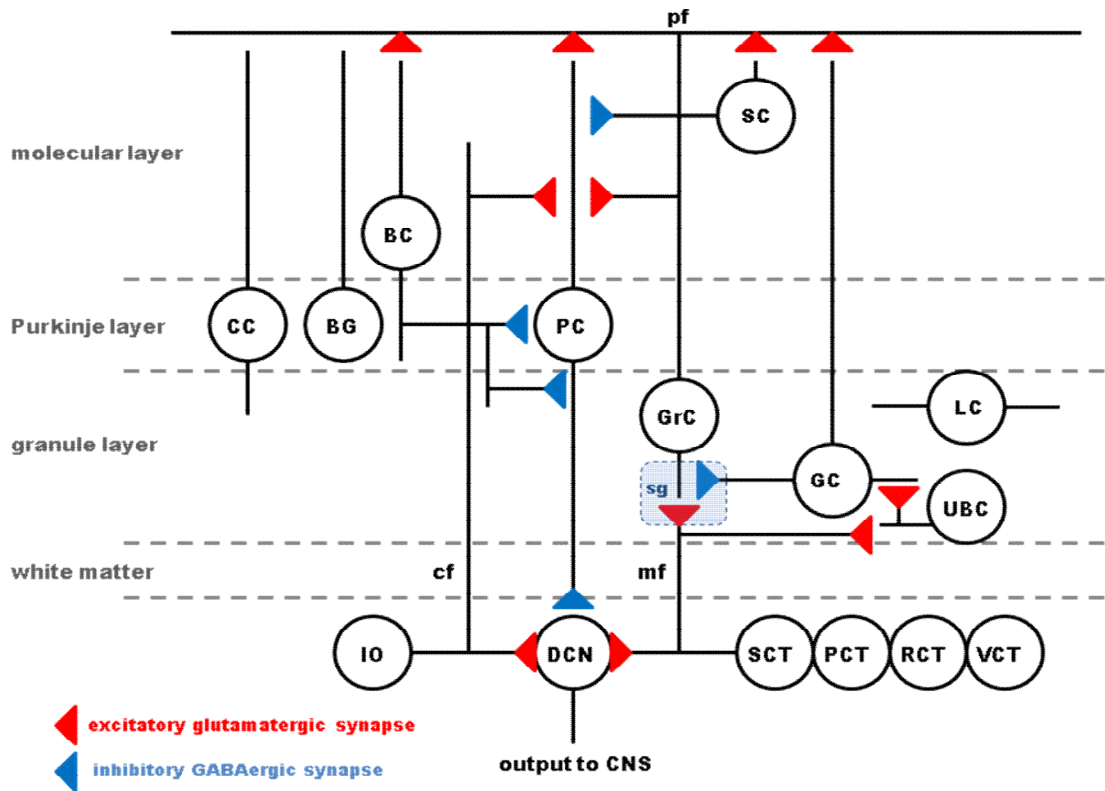
**Figure 1.7   The cells and circuitry of the cerebellum**

Key: climbing fibre (cf), mossy fibre (mf), parallel fibre (pf), synaptic glomeruli (sg), inferior olive (IO), deep cerebellar nuclei (DCN), spinocerebellar tract (SCT), pontocerebellar tract (PCT), reticulocerebellar tract (RCT), vestibulocerebellar tract (VCT), unipolar brush cell (UBC), Golgi cell (GC), Lugaro cell (LC), granule cell (GrC), Purkinje cell (PC), Bergmann glia (BG), candelabrum cell (CC), basket cell (BC), stellate cell (SC).
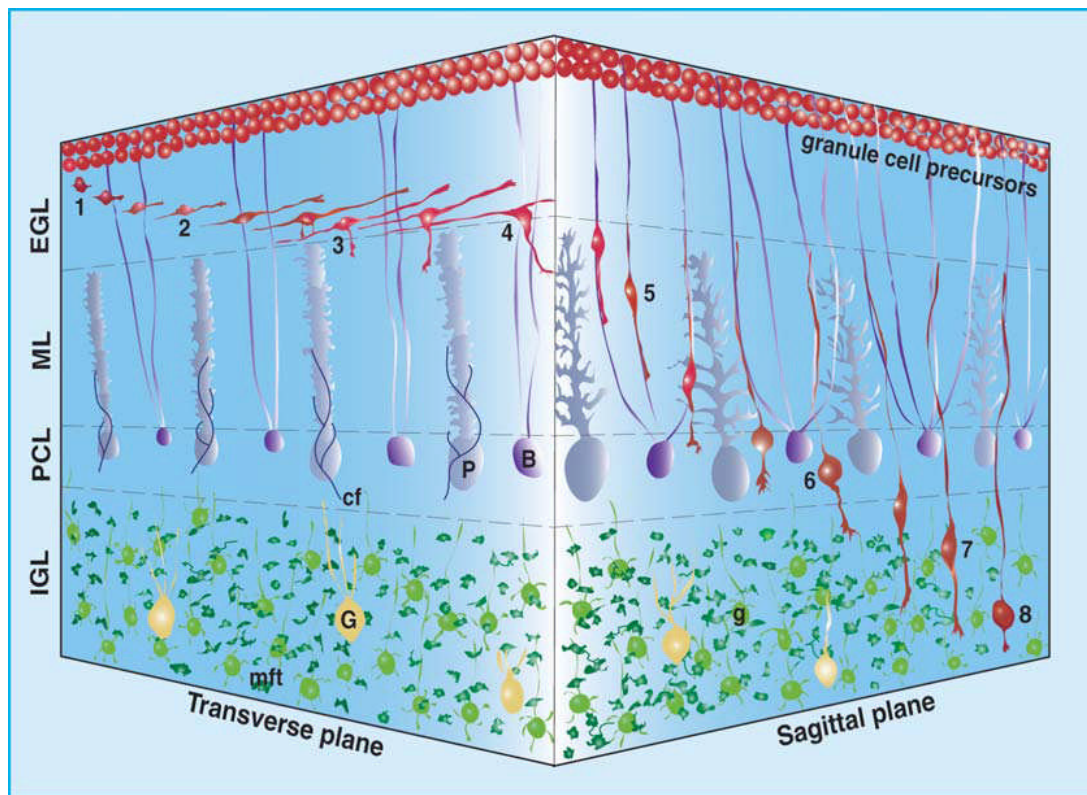
**Figure 1.8 The postnatal migration of granule cells in the cerebellum from the external granule layer to internal granule layer**

1. Extension of uneven bipolar horizontal processes near the top of the external granule layer (EGL).
2. Tangential migration in the middle of the EGL along the longer process.
3. Development of vertical process near the border between the EGL and the molecular layer (ML).
4. Initiation of radial migration at the EGL-ML border.
5. Bergmann glia-associated radial migration in the ML.
6. Stationary state in the Purkinje cell layer (PCL).
7. Glia-independent radial migration in the internal graule layer (IGL).
8. Completion of migration in the middle or the bottom of the IGL.
   (Komuro and Yacubova 2003)

## 1.4    Adenosine in the cerebellum

### 1.4.1  Adenosine receptors in the cerebellum

Early autoradiographic studies indicate that adenosine receptors are highly localised in some areas of the brain.  Incubation of rat brain sections with the radiolabelled $A_1R$ agonist [$^3$H] cyclohexyladenosine produces $A_1R$ labelling throughout the brain particularly in the cerebellum where dense staining is observed in the molecular layer, moderate staining in the granule layer and very light staining in the white matter.  In brain sections from reeler mice with distorted cerebella the [$^3$H] cyclohexyladenosine labelling is distorted in a pattern corresponding to the parallel fibres of the granule cells providing evidence for the specific localisation of $A_1R$ to these axons within the molecular layer (Goodman and Snyder 1982).

Immunohistochemical detection of $A_1R$ using polyclonal antisera against identical peptides from the rat and human $A_1R$ provides the resolution to individual processes and cell bodies within the cerebellum not attained with autoradiography.  The $A_1R$ staining intensity within the molecular layer is not as intense with this detection method as that seen with autoradiography which may be due to the protocol causing degeneration of the many small unmyelinated axons and dendrites, or $A_1R$ present on them, in this area of the brain.  Immunohistochemical staining reveals moderate labelling of granule cells in the granule layer and heavy labelling of basket cells that often envelop the lightly-labelled Purkinje cells in the molecular layer of the cerebellum suggesting the possibility that $A_1R$ may modulate interactions between these two cell types (Rivkees, Price et al. 1995).

Double immunolabelling shows co-localisation of the $A_1R$ and $P2Y_1$ receptor in the Purkinje cell and molecular cell layers of the rat cerebellum. Co-immunoprecipitation of the the $A_1R$ with the $P2Y_1$ receptor using an $A_1R$ antibody confirms that the receptors interact as hetero-oligomers and are present in the absence of any receptor activation by exogenous agonists so may be functionally significant (Yoshioka, Hosoda et al. 2002).

Immunoprecipitation of rat cerebellum synaptosomes reveals areas where metabotropic glutamate type $1\alpha$ receptors ($mGlu_{1\alpha}R$) and $A_1R$ do not co-distribute and areas where the two receptors interact to form heteromers dependent on the $mGlu_{1\alpha}R$ C-terminal tail. At the level of calcium mobilisation in response to application of adenosine and glutamate agonists this interaction shows a synergistic effect and therefore functional significance in transfected HEK293 cells (Ciruela, Casado et al. 1995).

A number of studies describe $A_{2A}R$ expression in dopamine-innervated areas of the rat brain but have provided little evidence for the presence of $A_{2A}R$ outside of the striatum. A subpopulation of Purkinje cells within the rat cerebellum show a low expression of $A_{2A}R$ when incubated with a $^{35}S$-labelled cRNA probe for the $A_{2A}R$ (Svenningsson, Le Moine et al. 1997). Immunohistochemistry using a high affinity monoclonal antibody specific to the $A_{2A}R$ shows a light labelling of scattered Purkinje cells in the rat cerebellum correlating with low $A_{2A}R$ mRNA levels whilst also confirming localisation of $A_{2A}R$ mainly to areas of the brain receiving dopaminergic projections (Rosin, Robeva et al. 1998). Positron emission tomography (PET) scans using the $A_{2A}R$ antagonist $[^{11}C]TMSX$ demonstrate that

$A_{2A}R$ are enriched in the human striatum and are widespread in other areas of the human brain with moderate levels of $A_{2A}R$ binding in the cerebellum (Mishina, Ishiwata et al. 2007).

Minimal support exists for the presence of $A_{2B}R$ within the cerebellum although a functional role has been suggested. Adenosine can synergistically potentiate the rapid $[Ca^{2+}]_i$ transient increase evoked by the action of ATP at P2Y receptors in the majority of cerebellar astrocytes. This effect is mimicked by the $A_1R$ and $A_{2A/B}R$ agonist NECA but not prevented by DPCPX, an antagonist at $A_1R$ and $A_{2A}R$. A similar number of the cerebellar astrocytes positively stain for $A_{2B}R$ antibody (Jimenez, Castro et al. 1999). Application of ADA to eliminate endogenous adenosine activity in cultured cerebellar granule cells either increases or decreases $[Ca^{2+}]_i$ depending on the cell state suggesting a role for multiple adenosine receptors in the same cell type. The effects of various agonists and antagonists at adenosine receptors and the identification of adenosine receptor subtype cDNA in the cerebellar granule cells indicates the possible involvement of $A_1R$, $A_{2B}R$ and possibly $A_3R$ in calcium modulation (Vacas, Fernandez et al. 2003).

Few studies have demonstrated the presence or role for $A_3R$ in the cerebellum. The radioligand $[^{125}I]$ AB-MECA binds specifically to $A_1R$ and $A_3R$ in mouse brain membrane preparations and the majority of binding is displaced by the $A_1R$ antagonist CPX leaving low levels of residual binding representing $A_3R$. In the mouse brain the highest levels of residual radioligand binding are localised in the cerebellum and correspond with $A_3R$ mRNA detection although these levels are very low (Jacobson, Nikodijevic et al. 1993). Application of X-gal to cerebellar slices of

transgenic mice containing a construct with a promoter region of the $A_3R$ gene coupled to the β-galactosidase reporter gene reveals β-galactosidase activity in the cerebellum in one of four transgenic lines (Yaar, Lamperti et al. 2002).

## 1.4.2 Adenosine signalling and the control of basal levels in the cerebellum

High levels of endogenous adenosine demonstrated by intense adenosine immunoreactivity in the soma and dendrites of rat cerebellar Purkinje cells (Braas, Newby et al. 1986) in addition to the previously described high concentration of $A_1R$ in the cerebellum (Goodman and Snyder 1982; Rivkees, Price et al. 1995; Yoshioka, Hosoda et al. 2002) suggest that this area of the brain is likely to be an important site of adenosine action. In addition the nucleoside transporters ENT1 and ENT2 are expressed in the cerebellum (Anderson, Baldwin et al. 1999; Anderson, Xiong et al. 1999) and the cerebellum contains the enzymes involved in adenosine metabolism.

The soma and dendrites of rat cerebellar Purkinje cells show immunoreactivity for ecto-ATPase with weaker staining present in the granule layer of the cerebellum (Wang and Guidotti 1998). The enzyme 5'-nucleotidase is present on glial plasma membranes in the molecular, Purkinje and granule layers of the cerebellum (Schoen, Graeber et al. 1987) and ADA activity can be detected in the cerebellum using high-pressure liquid chromatography (HPLC) to detect the formation of inosine and hypoxanthine in homogenates of rat brain (Geiger and Nagy 1986). A later study using a similar enzyme assay and synaptic membranes from porcine brain shows the

activity of ADA in the cerebellum to be similar to that of the hippocampus and medulla oblongata but lower than that of the cortex (Kukulski, Sevigny et al. 2004).

In electrophysiological studies it has been established that application of adenosine to rat cerebellar slices can selectively block PF EPSPs in the cerebellum (Kocsis, Eng et al. 1984). Application of the $A_1R$ antagonist 8-CPT to mature rat cerebellar slices potentiates EPSCs providing indirect evidence that PF-PC synaptic transmission is tonically inhibited by activation of $A_1R$ (Takahashi, Kovalchuk et al. 1995). This continual activation of $A_1R$ is most likely to be due to endogenous adenosine as application of adenosine to rat cerebellar slices reduces PF EPSP amplitude. The use of microelectrode biosensors to directly measure a basal extracellular concentration of adenosine in rat cerebellar slices detects a purine tone of the adenosine metabolites inosine and hypoxanthine but does not reliably detect adenosine. This is most likely to be due to a heterogeneous distribution of inosine and hypoxanthine in the extracellular space resulting in technical difficulties when calculating adenosine concentration from biosensor signals rather than low levels of adenosine (Wall, Atterbury et al. 2007).

The possible sources of extracellular adenosine in the CNS have previously been discussed. Within the cerebellum the direct release of adenosine has been recorded (Wall and Dale 2007) and some studies have described ATP as a potential source of extracellular adenosine. Inhibition of PF EPSPs occurs following application of ATP to rat cerebellar slices which can be inhibited by blockade of $A_1R$ with 8-CPT suggesting that the exogenous ATP is metabolised to adenosine (Wall, Atterbury et al. 2007). The mean frequency of spontaneous postsynaptic currents (sPSCs) in

Purkinje neurones, as a result of ATP acting at P2 receptors, increases in rat cerebellar slices following application of the ecto-ATPase inhibitor ARL67156 from the second postnatal week onwards. This suggests the tonic release of ATP and therefore provides indirect evidence for a source of the basal extracellular adenosine tone in the cerebellum (Casel, Brockhaus et al. 2005). Calcium signals in Bergmann glia triggered by brief bursts of parallel fibre activity in rat cerebellar slices can be blocked with application of the P2 receptor antagonist pyridoxal phosphate-6-azophenyl-2,4-disulfonic acid (PPADS) suggestive of the release of ATP from parallel fibres providing another possible source of extracellular adenosine (Beierlein and Regehr 2006). However, direct measurement of ATP in cerebellar slices with microelectrode biosensors does not reveal an ATP signal although this may be due to a rapid breakdown of ATP (Wall, Atterbury et al. 2007).

It has previously been discussed how nucleoside transporters contribute to the removal of adenosine from the extracellular space in the CNS. In the cerebellum inhibition of ENT1 and ENT2 proteins with NBTI and dipyridamole decreases PF EPSP amplitude in some slices which is reversible following blockade of $A_1R$ with 8-CPT and has little or no effect on PF EPSP amplitude in other slices suggesting that these transporters contribute to the control of extracellular adenosine concentration at only a subset of PF-PC synapses and that other NBTI/dipyridamole-insensitive transporters are responsible for the removal of adenosine from the extracellular space or that the ENT2 protein which is only weakly blocked by NBTI/dipyridamole is more prevalent at some synapses than ENT1 (Wall, Atterbury et al. 2007).

In comparison to other areas of the brain (Zhang, Franklin et al. 1993; Pak, Haas et al. 1994; Lloyd and Fredholm 1995) AK appears to be the major determining factor in the control of extracellular adenosine concentration in the cerebellum. In rat cerebellar slices inhibition of AK with iodotubericidin increases the adenosine concentration sufficiently to decrease PF EPSP amplitude by ~50 % and this increase in purine concentration can be simultaneously measured on microelectrode biosensors. In contrast synaptic transmission is reduced by only ~10 % when ADA is inhibited with EHNA suggesting that AK is more important in regulating the adenosine concentration (Wall, Atterbury et al. 2007).

Studies measuring developmental changes in the distribution of $A_1R$ or basal adenosine tone and its regulation have not been described in the juvenile rat cerebellum.

## 1.5 Additional pharmacology of the cerebellar parallel fibre-Purkinje cell synapse

Activation of four presynaptic receptor types is known to decrease the probability of vesicle release at the PF-PC synapse. In addition to the previously described action of adenosine at $A_1R$, activation of gamma-aminobutyric acid type B (GABA$_B$) receptors, endocannabinoid type 1 (CB1) receptors and metabotropic glutamate type 4 receptors (mGluR4) can also inhibit transmission at this synapse.

A role for GABA$_B$ receptors at the PF-PC synapse was suggested following binding study observations of a high density of these receptors in the molecular layer of the cerebellum. Inhibition of Purkinje cell synaptic potentials generated by parallel fibre stimulation in rat cerebellar slices is observed with the GABA$_B$ agonist baclofen and reversed with GABA$_B$ antagonists acting at presynaptic receptors (Batchelor and Garthwaite 1992). The involvement of CB1 receptors at the PF-PC synapse was implicated when it was observed that the presynaptic inhibition of parallel fibre-evoked EPSCs in Purkinje cells with the endocannabinoid receptor agonist WIN 55212-2 is blocked with application of the CB1 receptor antagonist SR 141716 in rat cerebellar slices (Takahashi and Linden 2000).

The mGluR4 receptor is unlike the other three receptors in that it is unique to the PF-PC synapse of the cerebellum. Its action at this synapse was identified when it was observed that the inhibition of synaptic transmission in Purkinje cells following application of L-(+)-2-amino-4-phosphonobutyric acid (L-AP4) to the cerebellar slices of wildtype mice does not occur in slices from mGluR4 knockout mice. A

presynaptic autoreceptor function at the PF-PC synapse was suggested whereby synaptically released glutamate activates presynaptic mGluR4 to inhibit further glutamate release and maintain presynaptic glutamate stores during elevated levels of synaptic activity (Pekhletski, Gerlai et al. 1996). Although inhibition of EPSPs is also observed at the PF-PC synapse in rat cerebellar slices following application of L-AP4 (Neale, Garthwaite et al. 2001), conditions inducing activation of mGluR4 *in vivo* have not yet been described. Immunogold labelling of rat cerebellar slices confirms the presynaptic localisation of mGluR4 in clusters at PF terminals forming synapses with PC dendrites although not all synapses are labelled with the antisera suggesting that not all would be regulated by an autoreceptor function (Mateos, Azkue et al. 1998).

## 1.6  Aims

- To determine the presence and distribution of the $A_1R$ and $A_{2A}R$ at the PF-PC synapse at different stages of development in the rat cerebellum using immunohistochemistry.

- To examine the presynaptic pharmacology of immature PF-PC synapses in the rat cerebellum using electrophysiology.

- To calculate the basal adenosine concentration and establish the importance of nucleoside transporter proteins and metabolic enzymes in controlling adenosine in the extracellular space at immature parallel fibre-Purkinje cell synapses in the rat cerebellum using microelectrode biosensor measurements and electrophysiology.

# Chapter 2    Materials and Methods

## 2.1    Immunohistochemistry

### 2.1.1  Solutions for immunohistochemistry

The solution (pH 7.4) for cerebellar dissection contained (mM) NaCl 127, $KH_2PO_4$ 1.2, KCl 1.9, $NaHCO_3$ 26, glucose 10, $CaCl_2$ 0.5 and $MgCl_2$ 7.

The phosphate-buffered saline (PBS) for washing slices (media prep, University of Warwick) contained (g/l) NaCl 8, KCl 0.2, $Na_2HPO_2$ 1.15 and $KH_2PO_4$ 0.2.

The solution for fixing cerebellar blocks (PFA, pH 7.4) contained 4 % paraformaldehyde in PBS.

The immuno PBS for diluting antibodies contained 0.4 % Triton X100 and 1 % BSA in PBS.

The alternative immuno PBS for diluting antibodies contained 5 % BSA in PBS.

## 2.1.2 Antibodies for immunohistochemistry

All of the antibodies were frozen in aliquots, thawed and diluted in immuno PBS for immuohistochemistry.  The primary antibodies used were:

- chicken anti-glial fibrillary protein (GFAP) (Millipore, AB5541)

- monoclonal mouse anti-calbindin D-28K (Sigma, C9848)

- rabbit anti-adenosine $A_1R$ (Calbiochem, 119117)

- rabbit anti-adenosine $A_{2A}R$ (Fisher Scientific, AFPA1042)

- rabbit anti-mGluR4 (Invitrogen, 513100)

- rabbit anti-vGluT1 (Invitrogen, 482400)

All of the secondary antibodies used as probes against the primary antibodies were Alexa Fluor® IgG antibodies (Invitrogen). The antibodies used were:

- goat anti-mouse 405 nm for calbindin D-28K

- goat anti-rabbit 488 nm for $A_1R$, $A_{2A}R$, mGluR4 and vGluT1

- goat anti-rabbit 546 nm for $A_1R$ in sequential staining protocol

- goat anti-chicken 594 nm for GFAP

- goat anti-rabbit 633nm for GFP-labelled CHO cells transfected with $A_1R$

## 2.1.3 Preparation of cerebellar slices for immunohistochemistry

In accordance with the Animals (Scientific Procedures) Act (1986) male Wistar rats at postnatal days 2-3 (P2-3), 8-14 (P8-14) or 21-28 (P21-28) were killed by cervical dislocation and decapitated.  The cerebellum was rapidly removed whilst washing with ice-cold dissection aCSF bubbled with 95 % $O_2$ and 5 % $CO_2$ and fixed in ice-

cold 4 % PFA at 4 ℃ overnight. The cerebellum was rinsed 3 times with PBS then transferred to PBS and stored at 4 ℃ until required. A Microm HM 650V microslicer was used to cut 40-125 µm transverse or parasagittal slices which were placed into separate wells of a 24-well plate each containing 1 ml PBS.

In one instance, the cerebellum was rapidly removed with ice-cold dissection aCSF bubbled with 95 % $O_2$ and 5 % $CO_2$, then parasaggital slices of cerebellar vermis (250 µm) were cut on a Microm HM 650V microslicer in ice-cold dissection aCSF. The slices were transferred to individual wells of a 24-well plate each containing 300 µl 4 % PFA and left to fix for 20 minutes at room temperature. The slices were rinsed 3 times for 5 minutes with PBS and stored in 1 ml PBS until required.

## 2.1.4  Single immunoflourescence

The PBS was removed from each well and non-specific binding sites were blocked with 500 µl 10 % normal goat serum diluted in immuno PBS for 1 hour at room temperature with agitation. The slices were washed 5 times for 5 minutes with agitation in PBS then incubated in 200 µl monoclonal mouse anti-calbindin D-28K antibody (1:1000) diluted in immuno PBS for 1 hour at room temperature with agitation then overnight at 4 ℃. Primary antibody dilutions were stored at 4 ℃ and re-used up to 3 times with no loss of activity. The slices were washed 5 times for 5 minutes with agitation in PBS then double-labelled with 300 µl Alexa Fluor® IgG 405 nm secondary antibody (1:500) diluted in immuno PBS for 4 hours at room temperature with agitation. The secondary antibody was discarded and the slices

washed 5 times for 5 minutes with agitation in PBS. The slices were mounted on glass slides using a drop of VectaShield mounting medium (Vector Laboratories), covered with glass coverslips, sealed and stored in the dark at 4 ℃.

## 2.1.5  Double immunofluorescence

The protocol used was the same as for single immunofluorescence. Double immunofluorescence was used for combinations of monoclonal mouse anti-calbindin D-28K antibody (1:1000) with either rabbit anti-adenosine $A_1R$ (1:100), rabbit anti-adenosine $A_{2A}R$ (1:100), rabbit anti-mGluR4 (1:100) or rabbit anti-vGluT1 (1:100) antibodies diluted in immuno PBS. The slices were double-labelled with combinations of Alexa Fluor® IgG secondary antibodies (1:500) diluted in immuno PBS. The secondary antibodies used were 405 nm against mouse for calbindin D-28K and 488 nm against rabbit for $A_1R$, $A_{2A}R$, mGluR4 and vGluT1.

An alternative method was also used (personal correspondence, Frenguelli lab) to ensure that the same antibody staining patterns were observed. The cerebellar block was fixed in PFA and the slices transferred to individual wells of a 24-well plate in the usual way. The PBS was removed from each well and the slices permeabilised with 500 µl 0.5 % Triton X100 diluted in PBS overnight at 4 ℃. The permeabilisation solution was discarded and non-specific binding sites blocked with 500 µl 20 % BSA diluted in PBS for 4 hours at room temperature. The blocking solution was discarded and the slices incubated in 200 µl primary antibodies (see previously described concentrations) diluted in alternative immuno PBS overnight at

4 ℃. The slices were washed 3 times for 5 minutes with agitation in PBS then double-labelled with combinations of Alexa Fluor® IgG secondary antibodies (see previously described concentrations) diluted in alternative immuno PBS. The slices were washed 3 times for 5 minutes with agitation in PBS then mounted on glass slides using a drop of VectaShield mounting medium (Vector Laboratories), covered with glass coverslips, sealed and stored in the dark at 4 ℃.


## 2.1.6  Triple immunofluorescence

The protocol used was the same as for single and double immunofluorescence. Triple immunofluorescence was used for combinations of monoclonal mouse anti-calbindin D-28K (1:1000) and chicken anti-GFAP (1:300) with either rabbit anti-adenosine $A_1R$ (1:100), rabbit anti-adenosine $A_{2A}R$ (1:100) or rabbit anti-mGluR4 (1:100). The slices were double-labelled with combinations of Alexa Fluor® IgG secondary antibodies (1:500) diluted in immuno PBS. The secondary antibodies used were 405 nm against mouse for calbindin D-28K, 488 nm against rabbit for $A_1R$, $A_{2A}R$ and mGluR4 and 594 nm against chicken for GFAP.

In order to prevent secondary antibody cross-reaction, a sequential protocol was used to attempt triple immunofluorescence where 2 of the primary antibodies were generated in rabbit. The cerebellar block was fixed in PFA and the slices transferred to individual wells of a 24-well plate in the usual way. The PBS was removed from each well and non-specific binding sites were blocked with 500 µl 10 % normal goat serum diluted in immuno PBS for 1 hour at room temperature with agitation. The

slices were washed 5 times for 5 minutes with agitation in PBS then incubated in 200 µl rabbit anti-$A_1R$ antibody (1:100) diluted in immuno PBS for 1 hour at room temperature with agitation then overnight at 4 ℃.   Primary antibody dilutions were removed and stored at 4 ℃.  The slices were washed 5 times for 5 minutes with agitation in PBS then double-labelled with 300 µl Alexa Fluor® IgG 546 nm secondary antibody (1:500) diluted in immuno PBS for 4 hours at room temperature with agitation.  The secondary antibody was discarded and the slices washed 5 times for 5 minutes with agitation in PBS.  The non-specific binding sites were blocked again with 500 µl 10 % normal goat serum diluted in immuno PBS for 1 hour at room temperature with agitation.  The slices were washed 5 times for 5 minutes with agitation in PBS then incubated in 200 µl monoclonal mouse anti-calbindin (1:1000) and either rabbit anti-vGluT1 antibody (1:100) or rabbit anti-mGluR4 antibody (1:100) diluted in immuno PBS for 1 hour at room temperature with agitation then overnight at 4 ℃.   Primary antibody dilutions were removed and stored at 4 ℃.  The slices were washed 5 times for 5 minutes with agitation in PBS then double-labelled with 300 µl Alexa Fluor® IgG 405 nm and 488 nm secondary antibodies (1:500) diluted in immuno PBS for 4 hours at room temperature with agitation.   The secondary antibody was discarded and the slices washed 5 times for 5 minutes with agitation in PBS. The slices were mounted on glass slides using a drop of VectaShield mounting medium (Vector Laboratories), covered with glass coverslips, sealed and stored in the dark at 4 ℃.

## 2.1.7 Immunofluorescence for GFP-labelled CHO cells

Specificity of the anti-adenosine $A_1R$ primary antibody was tested using Chinese hamster ovary (CHO) cells transiently transfected with a construct containing $A_1R$ with GFP tagged to its intracellular C-terminal (Abigail Baines, Frenguelli lab). The CHO cells were transfected as required prior to experiments.

Monolayers of the cells on circular borosilicate glass slides were fixed for 30 minutes in separate wells of a 6-well plate each half-filled with 4 % PFA. The slides were dipped in PBS to rinse and transferred to a humidified chamber. All subsequent solutions were carefully applied to the slides using a pipette to create a bubble over the cells. Non-specific binding sites were blocked with 200 µl 10 % normal goat serum diluted in immuno PBS for 1 hour at room temperature with gentle agitation. The normal goat serum was discarded and slides dipped in PBS to rinse. The slides were incubated in 200 µl rabbit anti-adensoine $A_1R$ (1:100) diluted in immuno PBS for 1 hour at room temperature with gentle agitation then overnight at 4 ºC. The slides were washed 5 times for 5 minutes with gentle agitation in 200 µl PBS then double-labelled with 200 µl Alexa Fluor® IgG 633 nm secondary antibody (1:500) diluted in immuno PBS for 4 hours at room temperature with gentle agitation. The secondary antibody was discarded and the slides washed 5 times for 5 minutes with gentle agitation in 200 µl PBS. The slides were inverted onto glass microscope slides over a drop of VectaShield mounting medium, sealed and stored in the dark at 4 ºC.

### 2.1.8  Immunofluorescence controls

To ensure specificity of the secondary antibody labelling, negative controls were performed for single, double and triple immunofluorescence experiments. Following incubation with normal goat serum, slices were incubated in 200 µl immuno PBS with no primary antibodies added and then incubated with secondary antibodies in the usual way.

As a further control for double and triple immunofluorescence, to eliminate the possibility of cross-reaction between secondary antibodies, one of the secondary antibodies was omitted from the protocol.

### 2.1.9  Confocal microscopy

Immunofluorescence was analysed using a Leica SP2 confocal system linked to a Leica DM RE7 upright microscope with an argon laser emitting at 488 nm, helium/neon laser emitting at 543 nm and helium/neon laser emitting at 633 nm. Images were created using 6 averages of 2 sections taken from stacks of 10 µm thickness and analysed using Adobe Photoshop CS.

## 2.2 Electrophysiology

### 2.2.1 Solutions for electrophysiology

The solution (pH 7.4) for cerebellar dissection contained (mM) NaCl 127, $KH_2PO_4$ 1.2, KCl 1.9, $NaHCO_3$ 26, D-glucose 10, $CaCl_2$ 0.5 and $MgCl_2$ 7.

The aCSF (pH 7.4) for recording contained (mM) NaCl 127, $KH_2PO_4$ 1.2, KCl 1.9, $NaHCO_3$ 26, D-glucose 10, $CaCl_2$ 2.4 and $MgCl_2$ 1.3.

### 2.2.2 Drugs for electrophysiology

The drugs were made up as 10-100 mM stock solutions, frozen then thawed and diluted with normal aCSF as required.

Adenosine, inosine, 6-[(4-nitrobenzyl)thiol]-9-β-D-ribofuranosylpurine (NBTI), 8-cyclopentyl-theophylline (8-CPT), R(+)-baclofen hydrochloride, $N^6$-cyclopentyladenosine (CPA), cadmium and dipyridamole were purchased from Sigma. Iodotubericidin was purchased from Sigma and Molekula Ltd. Erythro-9-(2-hydroxy-3-nonyl) adenine (EHNA) was purchased from Tocris-Cookson. 6-cyano-7-nitroquinoxaline-2, 3-dione (CNQX), kynurenic acid, (-)-bicuculline methochloride, tetrodotoxin (TTX) and L-(+)-2-amino-4-phosphonobutyric acid (L-AP4) were purchased from Ascent Scientific. ATP was purchased from Roche.

### 2.2.3 Preparation of cerebellar slices for electrophysiology

In accordance with the Animals (Scientific Procedures) Act (1986) male Wistar rats at postnatal days 8-14 (P8-14) or 21-28 (P21-28) were killed by cervical dislocation and decapitated. The cerebellum was rapidly removed whilst washing with ice-cold dissection aCSF bubbled with 95 % $O_2$ and 5 % $CO_2$. Transverse slices of cerebellar vermis (400 µm) were cut on a Microm HM 650V microslicer in ice-cold dissection aCSF and stored at room temperature in aCSF bubbled with 95 % $O_2$ and 5 % $CO_2$ for 1 - 6 hours before recording.

### 2.2.4 Extracellular recording

Individual slices were held on a suspended grid in a recording chamber with a U-shaped stainless steel and nylon net. The chamber was continuously perfused at a rate of 6 ml/min with aCSF at a temperature of 30-32 ºC using a peristaltic pump. The suspended grid ensured that the slice was perfused from above and below, all solutions were bubbled with 95 % $O_2$ and 5 % $CO_2$ and the tubing had low gas permeability (Tygon) to inhibit induction of hypoxia. For experiments that required hypoxic conditions the solutions were bubbled with 95 % $N_2$ and 5 % $CO_2$.

Slices were visualised using a BMZ stereomicroscope (Brunel Microscopes Ltd). A concentric bipolar metal stimulating electrode (FHC) attached to an isolated pulse stimulator (model 2100 AM systems Everett WA) was placed on the molecular layer of the slice and set to apply a pair of stimuli (2-5 V, 200 µs duration) at 0.1 Hz with an interval of 50 ms. A glass recording microelectrode filled with aCSF was placed

"on beam" in the molecular layer so that it was on the same track along which the parallel fibres travel (Yuan and Atchison 1999) (figure 2.1). Extracellular recordings of pairs of field EPSPs were made using an ISO-DAM extracellular amplifier (WPI) filtered at 3 kHz and sampled at 10 kHz with a Micro CED (Mark 2) interface controlled by Spike software (Vs 6.1).

### 2.2.5 Confirmation and components of PF EPSPs

Application of pairs of stimuli at the PF-PC synapse resulted in paired pulse facilitation (PPF), where the amplitude of the second PF EPSP is larger than that of the first. This was used as a primary confirmation of PF EPSP identity (Atluri and Regehr 1996). The same stimulation of climbing fibres within the cerebellum would generate a smaller second EPSP indicating paired pulse depression (PPD) (Konnerth, Llano et al. 1990).

The amplitude of the first PF EPSP was used as a measure of $A_1R$ activation and the paired pulse ratio ($EPSP_2/EPSP_1$) was used to test for a presynaptic action on release probability. A significant increase in paired pulse ratio indicated an effect at presynaptic receptors.

Further confirmation of PF EPSP identity was obtained by examining the pharmacological profile. The PF EPSP amplitude was reduced by ~90 % with 25 μM baclofen due to its action as an agonist at presynaptic $GABA_B$ receptors (Dittman and Regehr 1996). In addition, 50 μM L-AP4 resulted in ~60 % inhibition

60

of PF EPSP amplitude due to its action as an agonist at presynaptic mGluR4 receptors present only on parallel fibres (Kinoshita, Ohishi et al. 1996).

The PF EPSPs consisted of two components, both of which could be completely blocked with 1 µM TTX. The initial parallel fibre volley component was unaffected by application of the glutamate receptor antagonists, 5 mM kynurenic acid or 10 µM CNQX. The amplitude of the second component could be greatly reduced with either 5 mM kynurenic acid or 10 µM CNQX (Clark and Barbour 1997). This kynurenic acid-sensitive potential was used as an estimate of PF EPSP amplitude when analysing data and was measured by deducting the potential remaining in kynurenic acid from the control potential.

## 2.2.6  Purine biosensors

Purine biosensors obtained from Sarissa Biomedical Ltd (Coventry, UK) were used to identify released substances in the cerebellar tissue. The biosensors contained entrapped enzymes within a matrix deposited around a 50 µm polarised platinum wire and had an exposed length of ~500 µm that was coated with enzymes to allow the detection of purines (Llaudet, Botting et al. 2003).

Null sensors, containing a matrix with no enzymes, were used to control for the release of non-specific electro-active interferents like 5-HT and noradrenaline. INO biosensors containing the enzymes purine nucleoside phosphorylase (PNP) and xanthine oxidase (XO) to detect inosine and hypoxanthine and ADO biosensors

containing adenosine deaminase (AD), PNP and XO to detect adenosine, inosine and hypoxanthine were used. The breakdown of hypoxanthine by XO in the biosensor matrix to uric acid and hydrogen peroxide ($H_2O_2$) resulted in the oxidation of $H_2O_2$ on the polarised platinum wire which produced a current proportional to the concentration of $H_2O_2$.

Biosensors were screened to reduce the response to non-specific electro-active interferents. This was checked via the response to application of 10 µM 5-HT. To account for reduction in sensitivity during experiments biosensors were calibrated with 10 μM of adenosine and inosine before the slice was added to the perfusion chamber and following its removal. Biosensors were inserted into (at an angle of ~70 deg), or bent parallel to the slice surface and placed above, the molecular cell layer (Wall and Dale 2007). The biosensor signals were acquired using a Micro C potentiostat (CED) with a Micro CED (Mark 2) interface at 1 kHz controlled by Spike software (6.1).

### 2.2.7 Calculation of the specific adenosine signal

The signal on the ADO biosensor can be used as a measure of purine tone (produced by adenosine and its metabolites inosine and hypoxanthine). The specific adenosine tone could, in theory, be calculated by deducting the INO biosensor signal (measuring adenosine metabolites) from the ADO biosensor signal (measuring adenosine and its metabolites). However, the calculation of a specific adenosine assumes that the concentration of purines within the slice is homogeneous and that

there are no purine 'hotspots'. This is unlikely to be the case, as often a negative concentration of adenosine was implied when the INO biosensor signal was deducted from that of the ADO biosensor. Thus, in most cases the purine tone was measured and assumed to be inosine and hypoxanthine (Wall, Atterbury et al. 2007).

## 2.2.8 Statistical analysis

Results were analysed using OriginPro (v8.1) and are recorded as averages $\pm$ SEM. The t-test, ANOVA and calculation of correlation coefficient were used for statistical analysis. The significance values calculated using the t-test and ANOVA were expressed as a p-value where significance was accepted at $p = 0.05$. All statistical analysis was performed for data with $n \geq 3$.
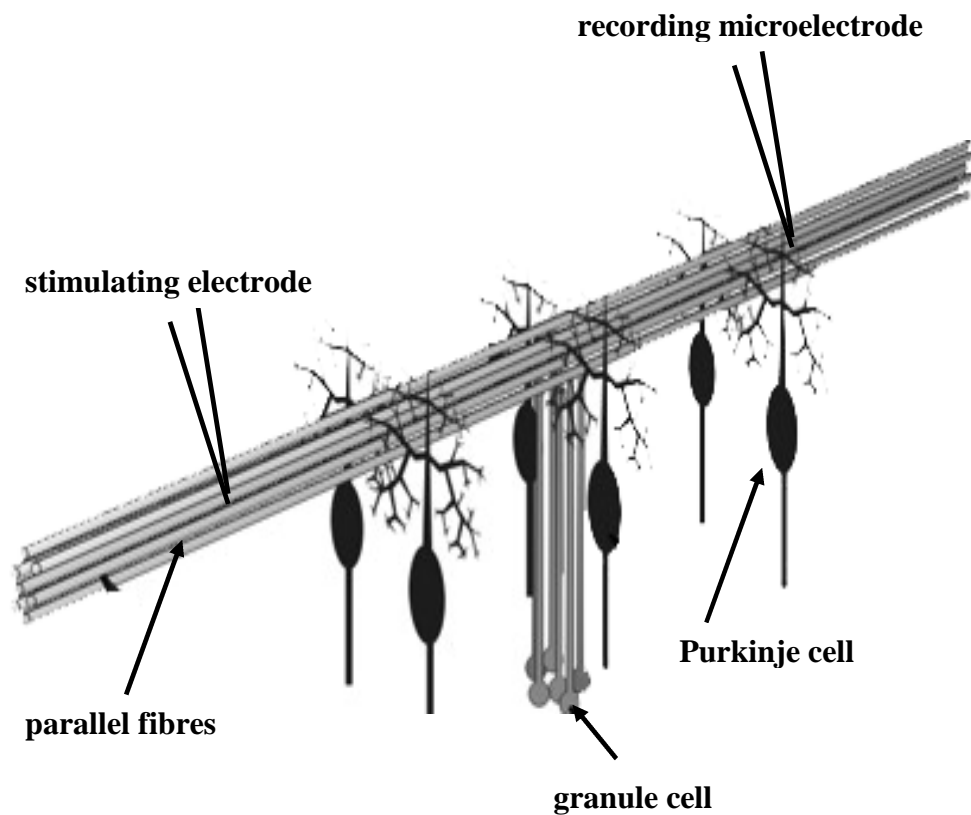
**Figure 2.1 Extracellular recordings at parallel fibre-Purkinje cell synapses in the rat cerebellum**

A concentric bipolar metal stimulating electrode attached to an isolated pulse stimulator is placed on the molecular layer of the transverse cerebellar slice and set to apply a pair of stimuli. A glass recording microelectrode filled with aCSF is placed "on beam" in the molecular layer so that it is on the same track along which the parallel fibres travel (Yuan and Atchison 1999).

# Chapter 3    The presence and distribution of $A_1R$

# and $A_{2A}R$ in the rat cerebellum at different stages of

# development

## 3.1    Introduction

The expression of $A_1R$ has been observed in mature rat cerebellar slices (Rivkees, Price et al. 1995; Yoshioka, Hosoda et al. 2002) however its distribution during cerebellar development or in relation to parallel fibre–Purkinje cell (PF-PC) synapses has not previously been described.

This study used primary antibodies against calbindin, $A_1R$ and mGluR4 to determine the distribution of $A_1R$ at PF-PC synapses in cerebellar slices at three developmental stages; postnatal day 3 prior to PF-PC synapse formation, postnatal days 8-14 and postnatal days 21-28. The distribution of $A_1R$ in relation to Bergmann glia has also been examined at each developmental stage using a primary antibody against GFAP.

## 3.2    Optimisation of the immunohistochemistry protocol

Transverse cerebellar slices (400 µm) were used for electrophysiological recordings to ensure that parallel fibres in contact with Purkinje cell dendrites remained intact and that climbing fibres were cut.  However, single immunofluorescence on thin transverse cerebellar slices (100 µm) using calbindin (1:1000) produced inconsistent staining and cells were frequently damaged.  Calbindin (1:1000) staining was only reliable if the cerebellar slices were cut parasaggitally so the immunohistochemistry protocol was optimised using calbindin primary antibody on cerebellar slices cut in this orientation.  Optimum confocal imaging was achieved using 6 averages of 2 sections taken from stacks of 10 µm thickness (10 µm optical stack).

The quality of calbindin staining was reduced in cerebellar slices cut thicker than 100 µm but was not optimised further in slices cut any thinner.  Cerebellar slices for immunohistochemistry were subsequently cut at 100 µm as they were less likely to be damaged during the immunofluorescence protocol than thinner slices.  In mature parasaggital cerebellar slices (100 µm) stained for calbindin (1:1000) Purkinje cell bodies, their axons in the granule layer and their dendrites in the molecular layer were clearly visible as were protrusions from Purkinje cell dendrites, in high magnification images, that were presumably dendritic spines (figure 3.1).

Single immunofluorescence was used on mature parasaggital cerebellar slices (100 µm) with various concentrations of each antibody prior to their use in experiments. Antibody concentrations of 1:100, 1:300, 1:500 and 1:1000 were tested for each

antibody so that future experiments allowed optimal staining whilst being cost-effective.
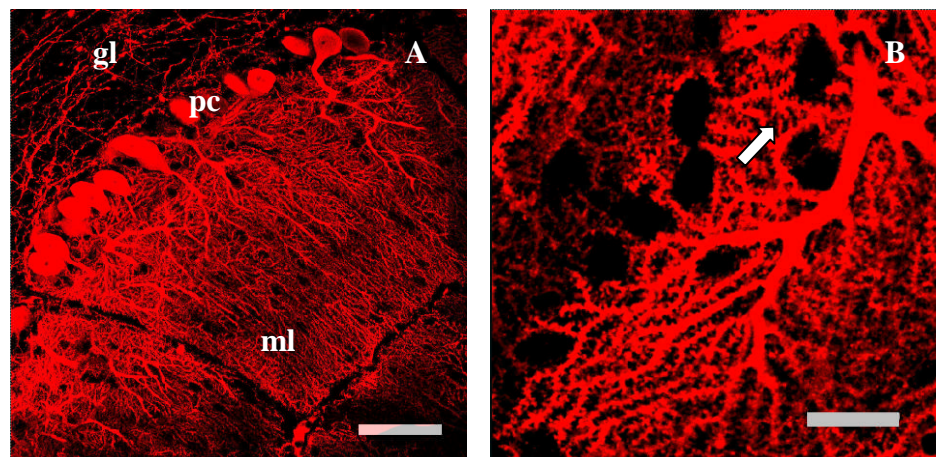


**Figure 3.1   Single staining for calbindin**

Parasaggital sections (100 µm) from adult rat cerebella (A P25, B P23) stained for calbindin (red, 1:1000).  A low magnification image shows staining of Purkinje cell (pc) bodies and their dendrites in the molecular layer (ml).  The small holes that are not stained within the molecular layer are presumably cell bodies of interneurones. Granule cells in the granule layer (gl) were not stained but Purkinje cell axons are visible (A).  A high magnification image within the molecular layer shows Purkinje cell dendrites with protrusions that are presumably dendritic spines (arrow).  The unstained holes around the dendrites are likely to be interneurone cell bodies (B). Optical stack 10 µm.  Scale bar A 45 µm, B 15 µm.

## 3.3 Confirmation that the $A_1R$ antibody is specific for $A_1R$

The specificity of the $A_1R$ antibody for the intracellular C-terminal of the $A_1R$ was tested using Chinese hamster ovary (CHO) cells transiently transfected with a construct containing $A_1R$ with GFP tagged to its intracellular C-terminal (Abigail Baines, Frenguelli lab) (Bevan, Palmer et al. 1999). Any cell that contains GFP should therefore contain the $A_1R$ so co-localisation of GFP and $A_1R$ would be expected.

Immunohistochemistry revealed punctate staining for $A_1R$ (1:100) only in CHO cells expressing GFP/$A_1R$ with no staining apparent in the CHO cell nucleus (as $A_1R$ is a transmembrane protein, figure 1.1) thus confirming specificity of the $A_1R$ antibody (figure 3.2, n = 2).

**GFP**    **$A_1R$**    **merge**
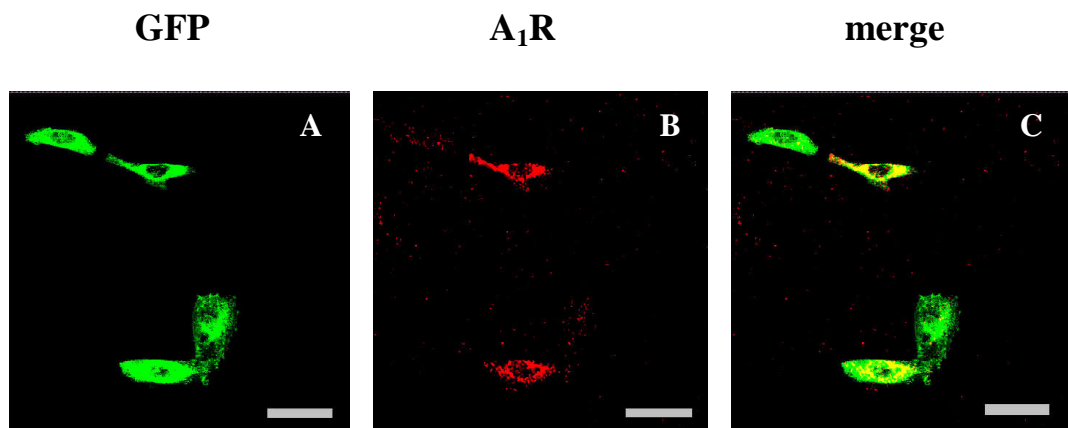


**Figure 3.2  Confirmation that the $A_1R$ antibody is specific for $A_1R$**
(A) The CHO cells were transfected with a construct containing $A_1R$ with GFP tagged at its intracellular C-terminal (green). (B) The CHO cells were stained for $A_1R$ (red, 1:100). (C) Co-localisation of GFP and $A_1R$ is yellow in the merged image where two of the four GFP-labelled CHO cells were successfully stained for $A_1R$. Scale bar 25 µm.

## 3.4 vGluT1 primary antibody as a potential marker for parallel fibres

It has previously been shown using double immunofluorescence in mature rat cerebellar slices that within the molecular layer parallel fibres only express vGluT1 for vesicular glutamate uptake and climbing fibres only express vGluT2 (Hioki, Fujiyama et al. 2003), allowing staining for vGluT1 to potentially be used in this study as a marker for parallel fibres in the cerebellum. However, an immunohistochemical study of the developing mouse cerebellum demonstrated that during the first 10 days of postnatal life vGluT2 predominates in parallel fibre terminals and that this is gradually replaced with expression of vGluT1 from the distal molecular layer upwards until postnatal day 30 (Miyazaki, Fukaya et al. 2003). As this study is looking at expression of $A_1R$ at PF-PC synapses during development, the use of vGluT1 as a marker for parallel fibres would only be possible in mature slices and an alternative would need to be used in immature slices.

Double immunofluorescence for calbindin (1:1000) and vGluT1 (1:50 and 1:100) in mature parasaggital cerebellar slices (100 µm, n = 3) was unsuccessful as the vGluT1 antibody did not stain slices consistently. Consequently, it was decided to use an alternative antibody to vGluT1 that could be used as a marker for parallel fibres in both immature and mature cerebellar sections.

## 3.5 mGluR4 primary antibody as a marker for parallel fibres

An alternative parallel fibre marker is mGluR4. Previous immunohistochemical studies have shown that this group III metabotropic glutamate receptor is located presynaptically in parallel fibres of the molecular layer in the cerebellum where it acts as an autoreceptor (Kinoshita, Ohishi et al. 1996; Mateos, Azkue et al. 1998). Although no immunohistochemical studies are available for mGluR4 expression in parallel fibres during development, it is known that mGluR4 mRNA expression increases rapidly from postnatal days 3-30 (Catania, Landwehrmeyer et al. 1994). Electrophysiological data obtained during this study also showed no significant difference between inhibition at the PF-PC synapse of rats at postnatal days 9-14 and 21-28 due to L-AP4 acting at mGluR4 ($p = 0.85$) suggesting no significant changes in mGluR4 expression during development. A primary antibody for mGluR4 was therefore purchased as an alternative parallel fibre marker to vGluT1 that could be used in both immature and mature cerebellar slices.

A parallel triple immunofluorescence technique, where all of the primary antibodies are applied and then labelled with secondary antibodies simultaneously, was not possible using primary antibodies for calbindin, mGluR4 and $A_1R$. The only primary antibodies available for mGluR4 and $A_1R$ were both generated in rabbit so a parallel immunofluorescence protocol would allow the secondary antibodies to cross-react with both the mGluR4 and $A_1R$ antibodies.

In order to determine the distribution of $A_1R$ relative to parallel fibres and Purkinje cells without antibody cross-reaction, triple immunofluorescence was attempted on immature and mature parasaggital slices (100 µm, n = 3) using a sequential protocol whereby double immunofluorescence with calbindin (1:1000) and $A_1R$ (1:100) was completed prior to staining for mGluR4 (1:100).

This method was unsuccessful as antibody cross-over staining between $A_1R$ and mGluR4 was observed in control slices. Staining for mGluR4 identical to that for $A_1R$ (1:100) was observed in control slices (100 µm, n = 3) where the triple immunofluorescence protocol was followed with the primary antibody for mGluR4 omitted.

## 3.6 Comparison of double immunofluorescence for calbindin/A$_1$R and calbindin/mGluR4 in mature and immature cerebellar slices

As an alternative to triple immunofluorescence with antibodies against calbindin, A$_1$R and mGluR4, the separate double staining of calbindin/A$_1$R and calbindin/mGluR4 was compared to analyse the distribution of A$_1$R at PF-PC synapses. Double immunofluorescence for calbindin (1:1000)/A$_1$R (1:100) and calbindin (1:1000)/mGluR4 (1:100) on mature parasaggital cerebellar slices (100 µm, n = 5) revealed similar patterns of co-localisation for A$_1$R and mGluR4 with calbindin (figure 3.3). Identical staining patterns (figure 3.4) were also observed in immature parasaggital cerebellar slices (100 µm, n = 5). Due to these similarities, the immature and mature slice staining patterns will be discussed together.

A large number of Purkinje cell bodies showed co-localisation for both A$_1$R and mGluR4 in immature and mature cerebellar slices. Previous immunoreactivity studies have not described mGluR4 staining at Purkinje cell bodies (Kinoshita, Ohishi et al. 1996; Mateos, Azkue et al. 1998), although dense staining for A$_1$R has previously been observed, but not discussed, at Purkinje cell bodies in mature cerebellar slices (Yoshioka, Hosoda et al. 2002). An earlier immunohistochemical study describing light A$_1$R staining at some Purkinje cell bodies suggested that this is likely to be the result of A$_1$R expression on basket cell processes that directly synapse with the Purkinje cell bodies (Rivkees, Price et al. 1995). There were three patterns of mGluR4 and A$_1$R co-localisation with Purkinje cell bodies; Purkinje cell bodies were densely stained with the exception of the nucleus (figure 3.5 C), lightly

stained across the cell body (figure 3.5 F) or only stained at the edges (figure 3.5 I), presumably where interneurones are in contact with the Purkinje cell body. A quantitative analysis was carried out using two slices double stained for calbindin (1:1000)/$A_1R$ (1:100) and calbindin (1:1000)/mGluR4 (1:100) from both immature and mature cerebella. The Purkinje cell staining patterns were observed in five random low magnification fields from each slice and only Purkinje cell bodies positively stained for calbindin were included in the analysis (table 3.1). Dense or light staining across the cell body was more frequently observed for the $A_1R$ in both mature and immature cerebellar slices and was more likely to be only at the edges of the cell body for mGluR4.

$A_1R$ and mGluR4 were densely distributed across Purkinje cell dendrites (figure 3.3 and 3.4) leaving small unstained holes within the molecular layer, presumably where the interneurones are located in immature and mature cerebellar slices. The same pattern of $A_1R$ staining within the molecular layer has previously been described in the mature rat cerebellum (Yoshioka, Hosoda et al. 2002) and an early autoradiographic study using [$^3$H]CHA to label $A_1R$ observed the highest density of $A_1R$ within the mature rat brain to be on parallel fibres within the molecular layer of the cerebellum (Goodman and Snyder 1982). As parallel fibres form synapses with the distal regions of the Purkinje cell dendritic tree (figure 1.7) the co-localisation of $A_1R$ at proximal dendrites is unlikely to be at PF-PC synapses. It is possible that these $A_1R$ are located on climbing fibres that wrap around the large proximal branches of Purkinje cells (figure 1.7) as inhibition of climbing fibre excitatory postsynaptic currents (CF EPSCs) is observed following application of adenosine to rat cerebellar slices (Takahashi, Kovalchuk et al. 1995; Hashimoto and Kano 1998).

Dense staining for mGluR4 within the molecular layer has been observed in immunoreactivity studies which have also used electron microscopy to specifically locate mGluR4 to the presynaptic sites made by parallel fibre axon terminals (Kinoshita, Ohishi et al. 1996; Mateos, Azkue et al. 1998). The dense staining for mGluR4 at proximal Purkinje cell dendrites is unusual as parallel fibres form synapses with distal Purkinje cell dendrites. There is no evidence for mGluR4 on climbing fibres that form synapses with the proximal Purkinje cell dendrites.

In high magnification images, different patterns of $A_1R$ and mGluR4 co-localisation with Purkinje cell dendrites were observed in both mature and immature cerebellar slices. The majority of dendrites showed dense co-localisation (figure 3.6 C, F) but occasionally small areas were found where there was no $A_1R$ or mGluR4 co-localisation with the Purkinje cell dendrites (figure 3.6 I) and in some instances there was also a border with no staining around the dendrite (figure 3.6L). Quantitative analysis was not possible due to the large numbers of Purkinje cell dendrites found within the molecular layer.

Staining for both $A_1R$ and mGluR4 was present around granule cells within the granule layer in both mature and immature cerebellar slices (figure 3.3 and 3.4). Previous immunoreactivity studies have not described mGluR4 staining in the granule layer (Kinoshita, Ohishi et al. 1996; Mateos, Azkue et al. 1998) and as parallel fibres are only present within the molecular layer of the cerebellum staining within the granule layer would not be expected. Light immunoreactivity for $A_1R$ around granule cells has previously been observed (Rivkees, Price et al. 1995; Yoshioka, Hosoda et al. 2002) and moderate labelling of $A_1R$ with [$^3$H]CHA has also

74

been described in the granule layer of the mature rat cerebellum (Goodman and Snyder 1982). A recent study using the patch-clamp technique on rat cerebella slices describes suppression of GABA input to granule cells via $A_1R$ activation although the exact site of $A_1R$ expression within the granule layer still remains unclear (Courjaret, Troger et al. 2009).

Identical staining patterns in the molecular layer, granule layer and Purkinje layer for $A_1R$ and mGluR4 were also observed when an alternative protocol was used (personal correspondence, Frenguelli lab) for double immunofluorescence of $A_1R$ (1:100)/calbindin (1:1000) and mGluR4 (1:100)/calbindin (1:1000) on immature cerebellar slices (n = 2).

**calbindin**  **A₁R**  **merge**

**calbindin**  **mGluR4**  **merge**
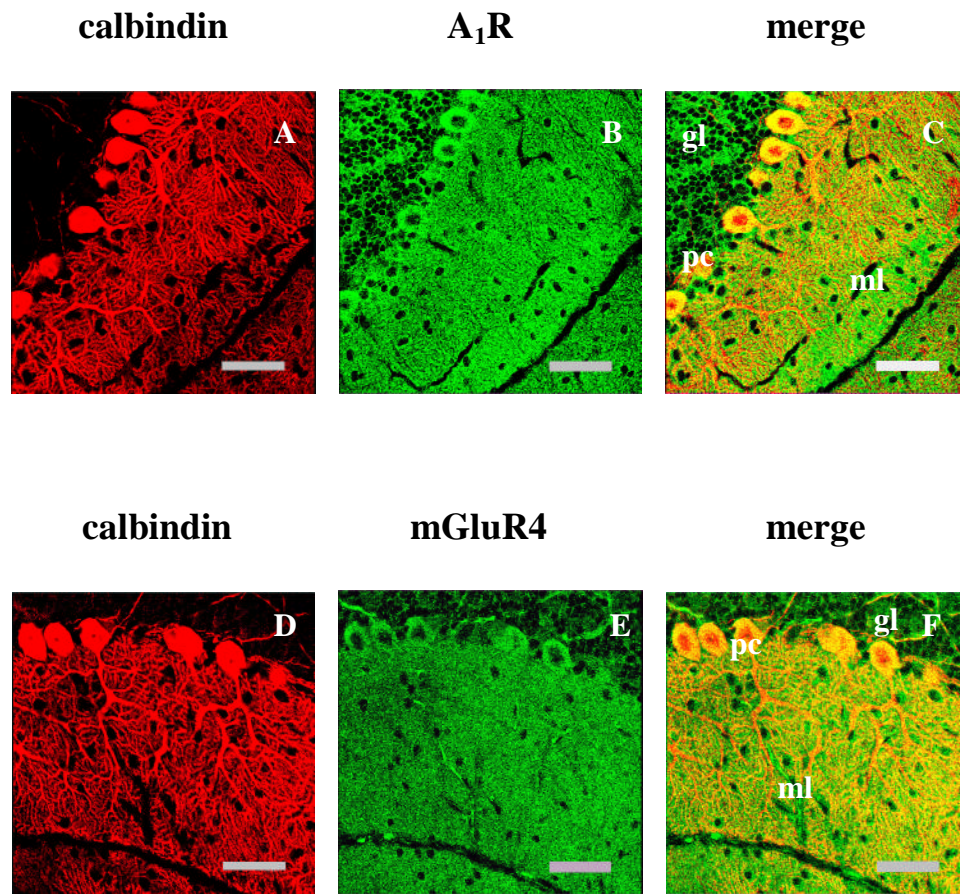
**Figure 3.3  Comparison of double staining for calbindin/A₁R and calbindin/mGluR4 in mature sections**

Parasaggital sections (100 µm) from adult rat cerebella (P23). Sections were stained for calbindin (red, 1:1000) (A, D) and A₁R (green, 1:100) (B) or mGluR4 (green 1:100) (E). Co-localisation of calbindin and A₁R (C) or calbindin and mGluR4 (F) is yellow in the merged images. A₁R and mGluR4 were densely distributed across dendrites throughout the molecular layer (ml). The small holes that are not stained are presumably cell bodies of interneurones. A₁R and mGluR4 were also densely co-localised with Purkinje cell (pc) bodies although not at the nucleus. A₁R and mGluR4 staining in the granule layer (gl) is presumably on interneurones or mossy fibres with the holes being unstained granule cells. Optical stack 10 µm. Scale bar 45 µm.

**calbindin**　　　**A₁R**　　　**merge**

**calbindin**　　　**mGluR4**　　　**merge**
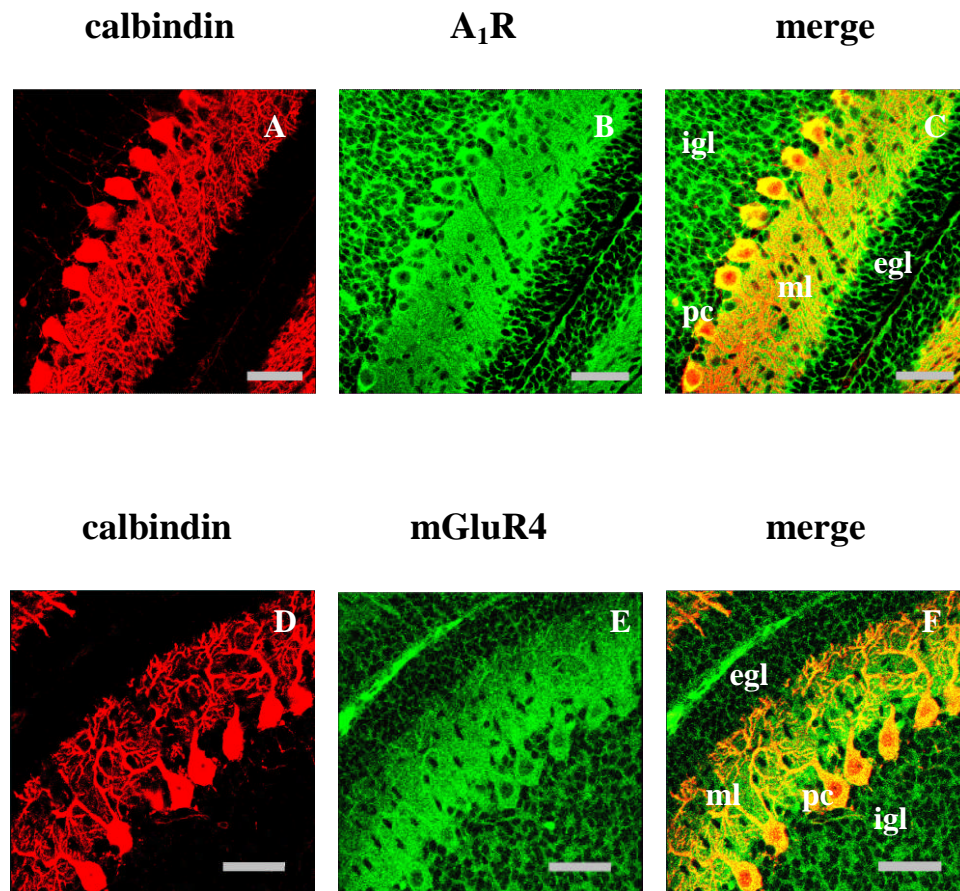
**Figure 3.4　Comparison of double staining for calbindin/A₁R and calbindin/mGluR4 in immature sections**

Parasaggital sections (100 µm) from immature rat cerebella (A-C P12, D-F P11). Sections were stained for calbindin (red, 1:1000) (A, D) and A₁R (green, 1:100) (B) or mGluR4 (green 1:100) (E). Co-localisation of calbindin and A₁R (C) or calbindin and mGluR4 (F) is yellow in the merged images. A₁R and mGluR4 were densely distributed across dendrites throughout the molecular layer (ml). The small holes that are not stained are presumably cell bodies of interneurones. A₁R and mGluR4 were also densely co-localised with Purkinje cell (pc) bodies although not at the nucleus. A₁R and mGluR4 staining in the internal granule layer (igl) is presumably on interneurones or mossy fibres. Migration of granule cells is not complete at this stage of development and the external granule layer (egl) is still visible. The staining patterns are identical to those in adult sections (figure 3.3). Optical stack 10 µm. Scale bar 45 µm.

| calbindin | A$_1$R | merge |
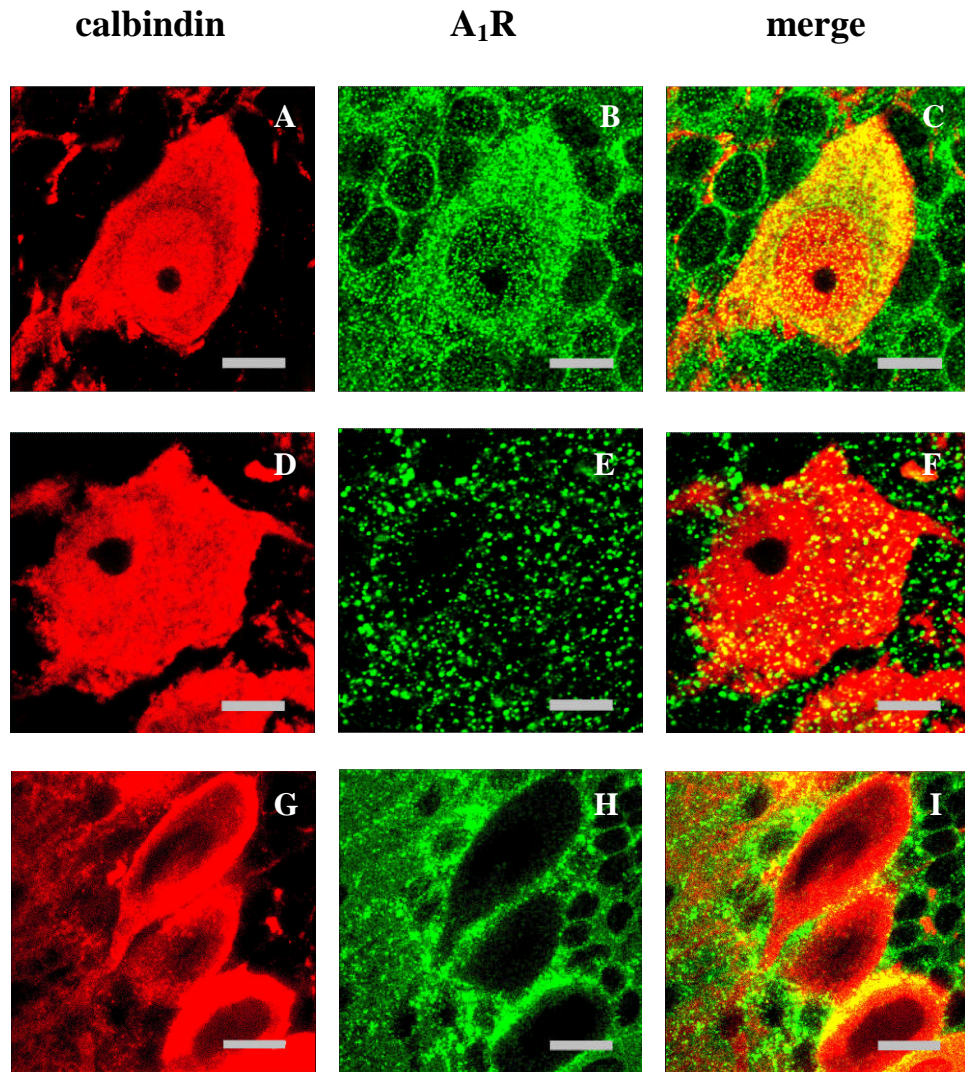
**Figure 3.5 Comparison of double staining for calbindin/A$_1$R on Purkinje cell bodies**

Parasaggital sections (100 µm) from rat cerebella (A-C P13, D-F P9, G-I P23). Sections were stained for calbindin (red, 1:1000) (A, D, G) and A$_1$R (green, 1:100) (B, E, H). Co-localisation of calbindin and A$_1$R is yellow in the merged images (C, F, I). It was expected that A$_1$R would only be present on distal Purkinje cell dendrites where parallel fibre-Purkinje cell (PF-PC) synapses are formed, however co-localisation was frequently seen at the Purkinje cell bodies. The majority of Purkinje cell bodies were densely stained for A$_1$R (C). A sparse co-localisation of A$_1$R was observed on a small number of Purkinje cell bodies (F). Occasionally there was only co-localisation of A$_1$R at the edges of the Purkinje cell bodies, presumably present on interneurones in contact with the cell bodies (I). The same staining patterns were observed for double staining with calbindin and mGluR4 (not shown). Optical stack 10 µm. Scale bar A-C 9µm, D-F 6µm, G-I 12 µm.

| calbindin | A$_1$R | merge |
|:---:|:---:|:---:|
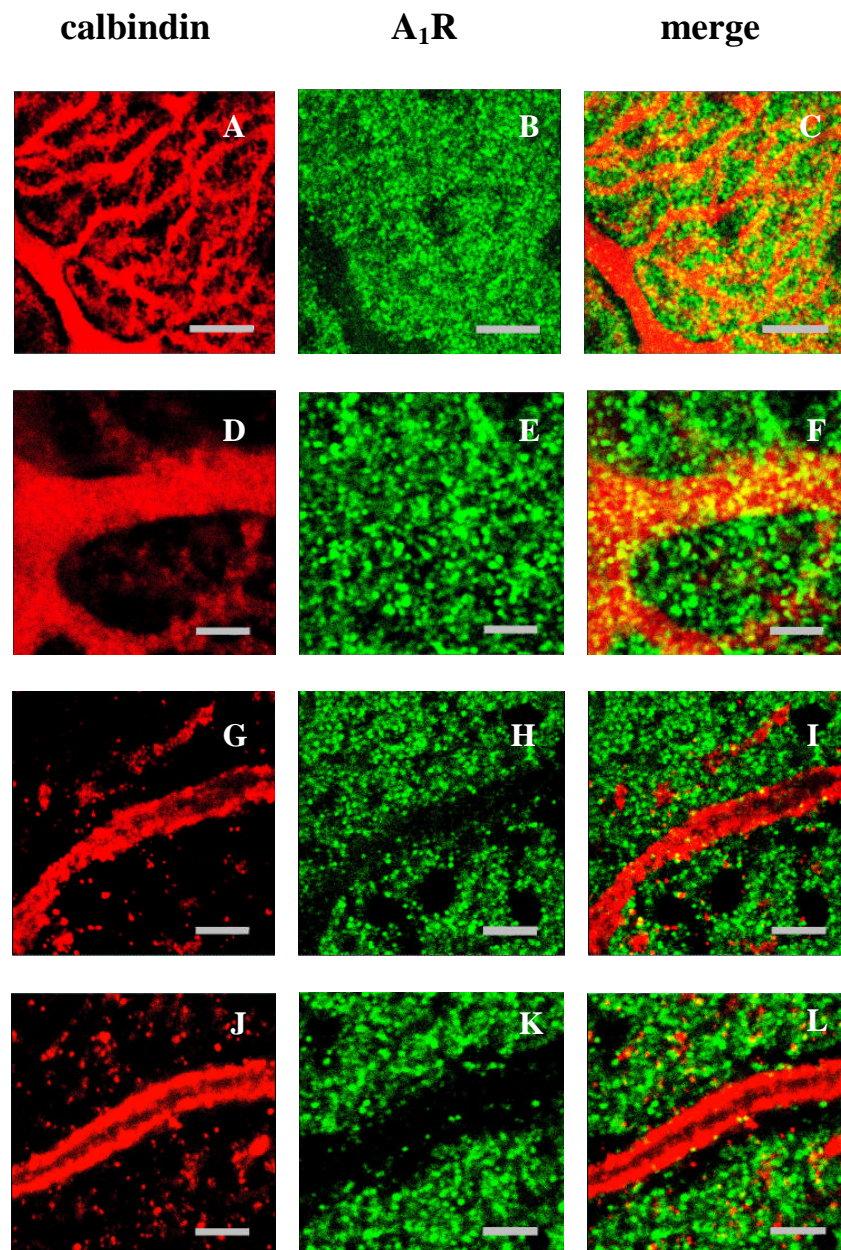


**Figure 3.6 Comparison of double staining for calbindin/A$_1$R on Purkinje cell dendrites**

Parasaggital sections (100 µm) from rat cerebella (A-C P22, D-F P13, G-I P23, J-L P23). Sections were stained for calbindin (red, 1:1000) (A, D, G, J) and A$_1$R (green, 1:100) (B, E, H, K). Co-localisation of calbindin and A$_1$R is yellow in the merged images (C, F, I, L). For immature and mature sections, the majority of Purkinje cell dendrites showed dense co-localisation with A$_1$R (C, F). Occasionally, dendrites did not stain for A$_1$R (I) and in some instances there was a border with no A$_1$R staining around these dendrites (L). Optical stack 10 µm. Scale bar A-C 8µm, D-F 3µm, G-I 4 µm, J-L 3 µm.

| | % immature Purkinje cell bodies stained (P12) | | % mature Purkinje cell bodies stained (P23) | |
| --- | --- | --- | --- | --- |
| | $A_1R$ | mGluR4 | $A_1R$ | mGluR4 |
| **Dense staining (figure 3.5 C)** | 40.2 | 0 | 71.4 | 19.4 |
| **Light staining (figure 3.5 F)** | 43.7 | 36.8 | 21.4 | 44.4 |
| **Staining at edges (Figure 3.5 I)** | 16.1 | 63.2 | 7.2 | 36.2 |

**Table 3.1    Quantitative analysis of Purkinje cell staining patterns in mature and immature cerebellar slices**

For each age (postnatal day 12 (P12) and P23), 2 parasaggital cerebellar slices were double stained for calbindin (1:1000)/$A_1R$ (1:100) and calbindin (1:1000)/mGluR4 (1:100).    The Purkinje cell staining patterns were observed in 5 random low magnification fields from each slice and only Purkinje cell bodies positively stained for calbindin were included.    Dense staining is described where there is staining across the entire cell body with the exception of the nucleus and light staining where there is only a scattering of $A_1R$/mGluR4 across the cell body.

## 3.7 Triple immunofluorescence with GFAP in combination with $A_1R$/calbindin and mGluR4/calbindin in mature and immature cerebellar slices

Immunonstaining with calbindin using cerebellar organotypic slices from transgenic GFAP-GFP mice that express GFP under the GFAP promoter in astrocytes shows interaction between the cell bodies of Purkinje cells and Bermann glial cells (Lordkipanidze and Dunaevsky 2005). It is therefore possible that the $A_1R$ staining observed on Purkinje cell bodies (figure 3.5) could be on glial cell bodies overlapping Purkinje cell bodies within the Purkinje cell layer of the cerebellar slices.

Triple immunofluorescence for calbindin (1:1000), GFAP (1:300) and $A_1R$ (1:100) showed minimal interaction between glial and Purkinje cell bodies in immature (n = 5) and mature (n = 2) cerebellar slices (figure 3.7 E) and although $A_1R$ staining was present on glial cell bodies it accounted for very little of the staining present on Purkinje cell bodies (figure 3.7 F, G). There is no evidence for the expression of $A_1R$ on Bergmann glia but their presence may contribute to the depression of glial extrasynaptic currents (ESC) observed with application of the $A_1R$ agonist CPA (Bellamy 2007).

**calbindin** **A₁R** **GFAP**

**calbindin/A₁R** **calbindin/GFAP** **A₁R/GFAP**

**triple merge**

**Figure 3.7 Triple staining for calbindin/A₁R/GFAP**

Parasaggital sections (100 µm) from immature rat cerebella (P11). Sections were stained for calbindin (red, 1:1000) (A), A₁R (green, 1:100) (B) and GFAP (blue, 1:300) (C). For merged images co-localisation of calbindin and A₁R is yellow (D), calbindin and GFAP is magenta (E), A₁R and GFAP is cyan (F) and calbindin, A₁R and GFAP is white (G). A₁R co-localisation was present on glial processes and cell bodies although this did not account for the staining present on Purkinje cell bodies (F, G). Optical stack 10 µm. Scale bar 45 µm.

## 3.8   The distribution of $A_1R$ in cerebellar slices prior to parallel fibre-Purkinje cell synapse formation

Postnatally, granule cells migrate parallel to the external granule layer for 1-2 days along bipolar axons before migrating radially through the molecular layer towards the internal granule layer for a further 2-3 days along a perpendicular axon (figure 1.8). The leading bipolar axons then create bundles of parallel fibres that form synapses with expanding Purkinje cell dendritic trees (Kawaji, Umeshima et al. 2004). The PF-PC synapse is formed around postnatal day 5 (Altman 1972) and a recent study using *in vitro* preparations of rat cerebellum-medulla-pons blocks describes postnatal day 5 as a critical developmental stage. Prior to this at postnatal days 0-3 PF EPSPs were usually absent and at postnatal day 4 were uncommon (Arata and Ito 2004).

The distribution of $A_1R$ in cerebellar slices prior to synapse formation has not previously been studied. Double immunofluorescence of calbindin (1:1000) and $A_1R$ (1:100) on parasaggital cerebellar slices (100 µm) at postnatal day 3 (n = 2) revealed dense co-localisation around the edges of Purkinje cell bodies with light $A_1R$ staining across some cell bodies (figure 3.8) similar to that described in mature cerebellar slices (figure 3.5). The $A_1R$ staining shows similarities with low magnification cocaine- and amphetamine-regulated transcript (CART) peptide immunofluorescence at postnatal day 4 that is associated with climbing fibres in the rat cerebellum (Press and Wall 2008). It is possible that the $A_1R$/calbindin co-localisation prior to parallel fibre synapse formation (figure 3.8) may be due to the presence of $A_1R$ on climbing fibres interacting with sprouting Purkinje cell dendrites. CF EPSCs are frequently

recorded at postnatal day 4 (Hashimoto and Kano 2003) so it is possible that climbing fibre-Purkinje cell (CF-PC) synapses are present in rats at postnatal day 3 used in this study. Dense $A_1R$ staining was also present around granule cells in the external and internal granule layers. Activation of $A_1R$ within the granule layer has recently been described in mature rats although the exact site of $A_1R$ remains unclear (Courjaret, Troger et al. 2009).

Identical staining patterns were observed for double immunofluorescence of calbindin (1:1000) and mGluR4 (1:100) on parasaggital cerebellar slices (100 µm) at P3 (n = 2, figure 3.9). Co-localisation was unexpected as PF-PC synapses are not functional at this stage of development (Arata and Ito 2004). The same staining was obtained using an alternative protocol (personal correspondence, Frenguelli lab) for double immunofluorescence of calbindin (1:1000) and mGluR4 (1:100) on parasaggital cerebellar slices at postnatal day 3 (n = 2).

Triple immunofluorescence of calbindin (1:1000), mGluR4 (1:100) and GFAP (1:300) on parasaggital cerebellar slices (100 µm) at postnatal day 3 (n = 2, figure 3.10) showed that glial cell bodies were positioned around Purkinje cell bodies and did not account for any of the mGluR4 staining observed although some light staining was apparent on glial processes (figure 3.10 F). Triple immunofluorescence of calbindin (1:1000), $A_1R$ (1:100) and GFAP (1:300) was unsuccessful (n = 2) despite being effective in mature cerebellar slices (figure 3.7).

**calbindin**      **A₁R**      **merge**
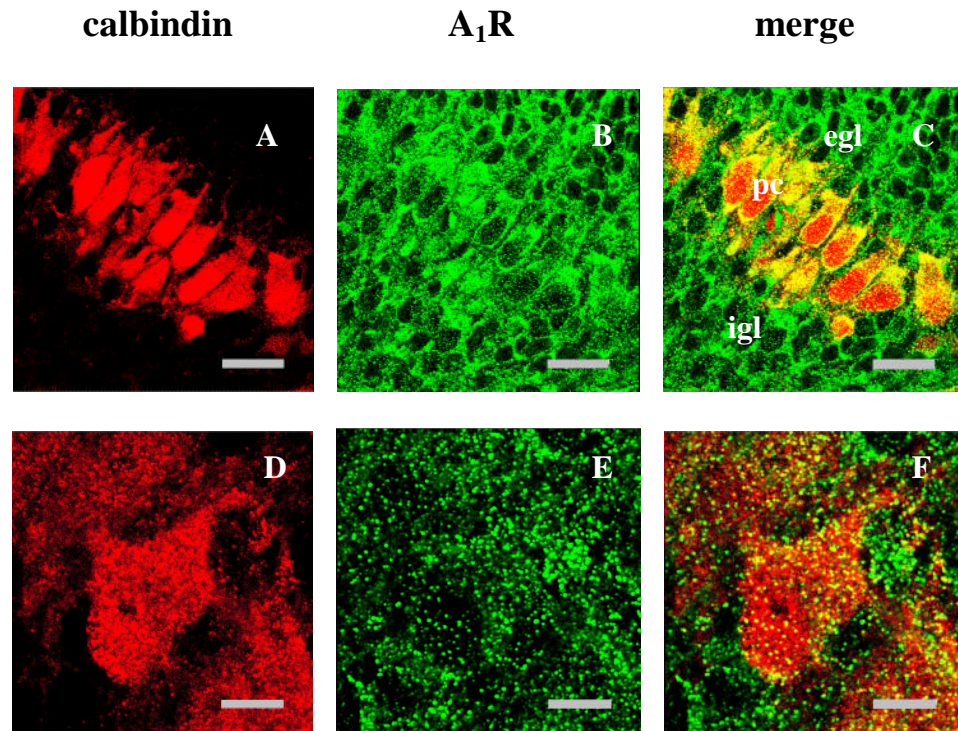
**Figure 3.8 Double staining for calbindin/A$_1$R prior to parallel fibre-Purkinje cell synapse formation**

Parasaggital sections (100 µm) from rat cerebella (P3). Sections were stained for calbindin (red, 1:1000) (A, D) and A$_1$R (green, 1:100) (B, E). Co-localisation of calbindin and A$_1$R is yellow in the merged images (C, F). There was dense A$_1$R co-localisation around the edges of Purkinje cell (pc) bodies. Dense A$_1$R staining was also present around granule cells in the external and internal granule layers (egl and igl) (C). There was sparse A$_1$R co-localisation across some Purkinje cell bodies (F) as previously described in older rats (figure 3.5). Optical stack 10 µm. Scale bar A-C 33 µm, D-F 8 µm.

|    calbindin    |    mGluR4    |    merge    |
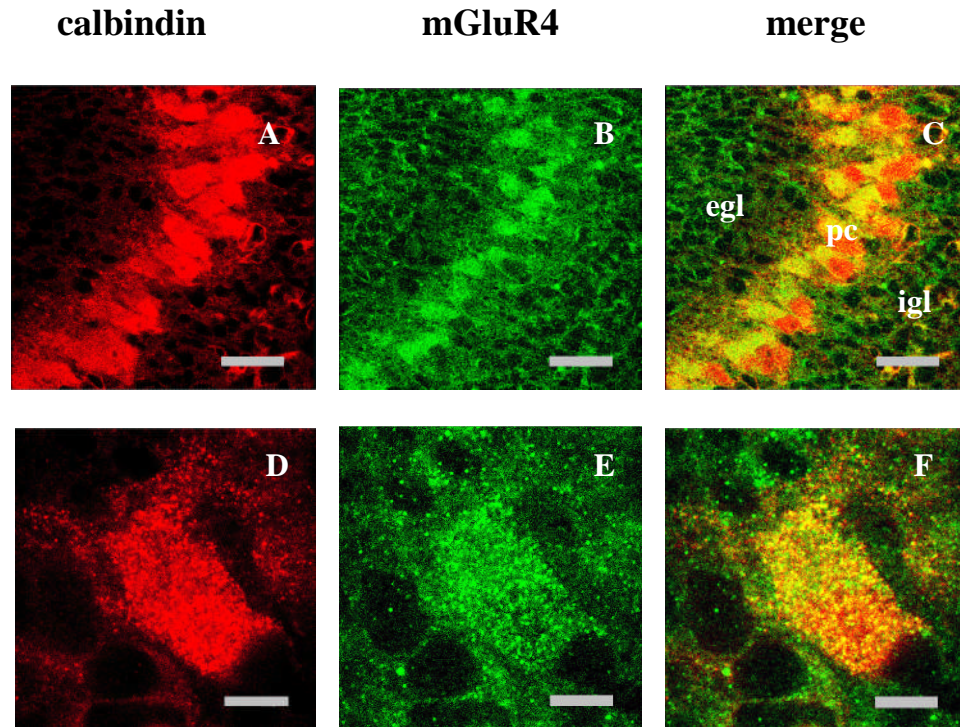
**Figure 3.9   Double staining for calbindin/mGluR4 prior to parallel fibre-Purkinje cell synapse formation**

Parasaggital sections (100 µm) from immature rat cerebella (P3). Sections were stained for calbindin (red, 1:1000) (A, D) and mGluR4 (green, 1:100) (B, E). Co-localisation of calbindin and $A_1R$ is yellow in the merged images (C, F). Although parallel fibre-Purkinje cell (PF-PC) synapses are not formed at this stage of development, mGluR4 co-localisation is present at Purkinje cell (pc) bodies and between cells in the external and internal granule layers (egl and igl) (C). In some cases, there was mGluR4 co-localisation across the Purkinje cell bodies, as previously described in older rats (figure 3.5). Optical stack 10 µm. Scale bar A-C 33 µm, D-F 7 µm.

**calbindin**      **mGluR4**      **GFAP**

**calbindin/mGluR4**    **calbindin/GFAP**    **mGluR4/GFAP**
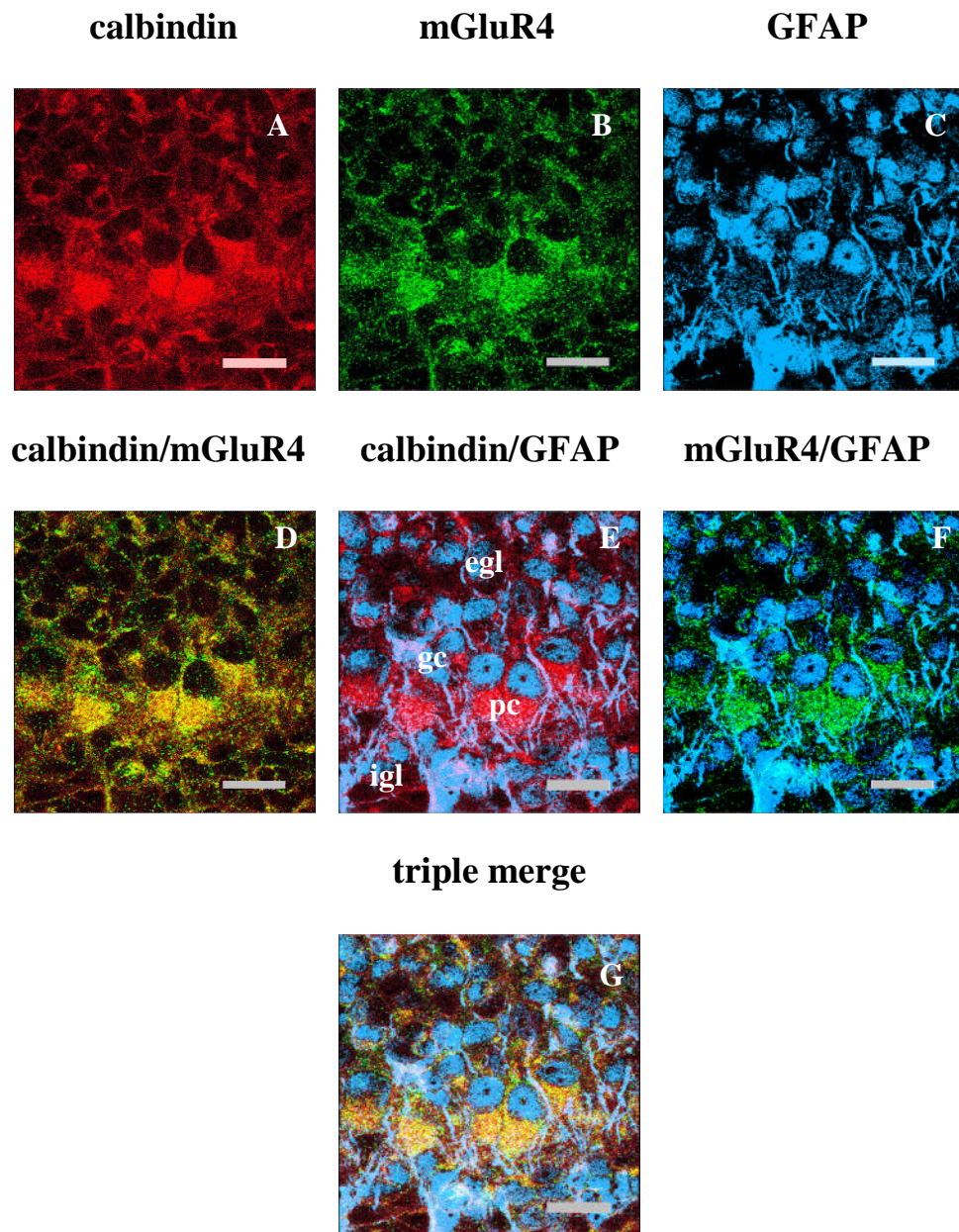
**triple merge**

**Figure 3.10**     **Triple staining prior to synapse formation for calbindin/mGluR4/GFAP**
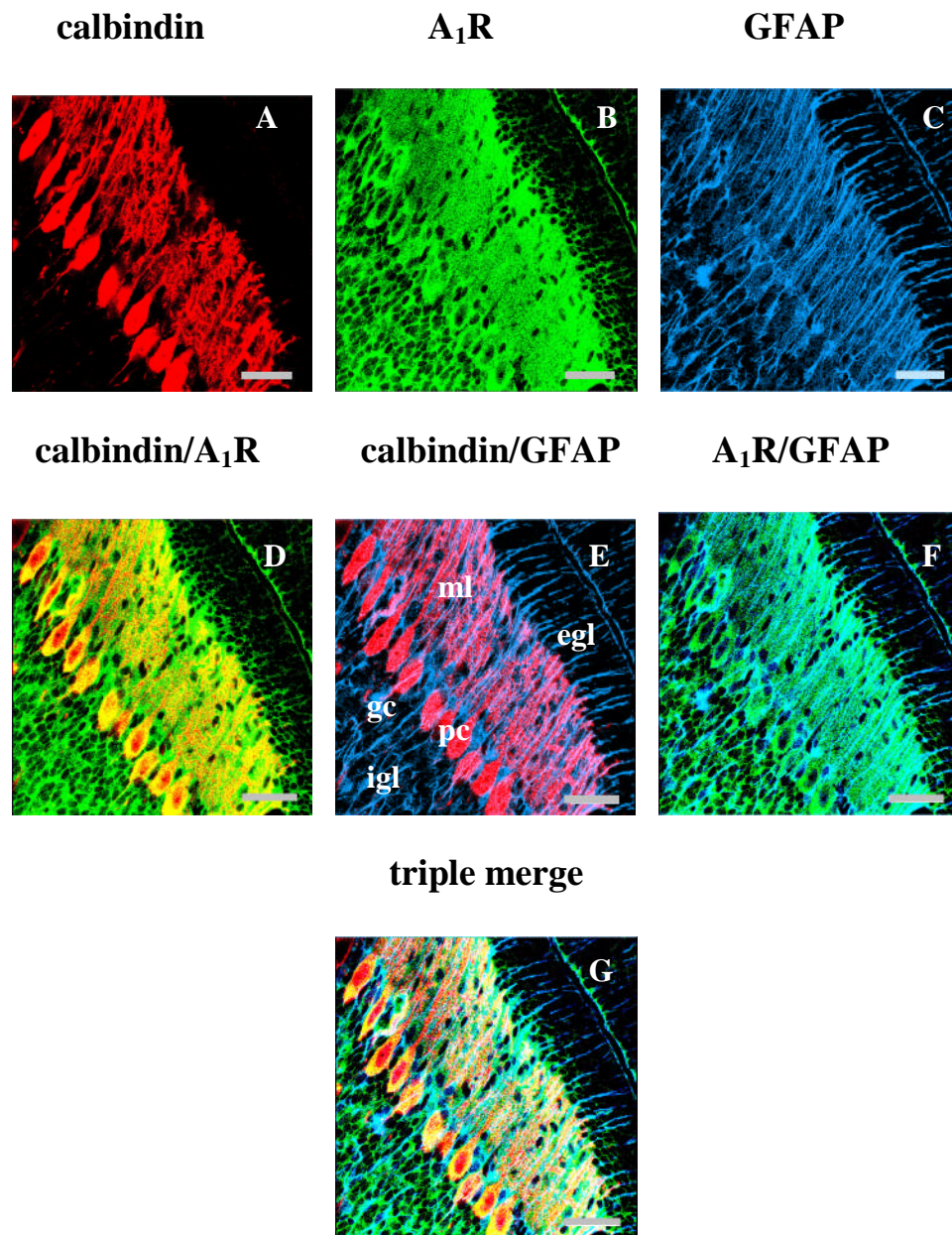
Parasaggital sections (100 μm) from immature rat cerebella (P3). Sections were stained for calbindin (red, 1:1000) (A), mGluR4 (green, 1:100) (B) and GFAP (blue, 1:300) (C). For merged images co-localisation of calbindin and mGluR4 is yellow (D), calbindin and GFAP is magenta (E), mGluR4 and GFAP is cyan (F) and calbindin, mGluR4 and GFAP is white (G). Glial cell bodies were positioned around Purkinje cell (pc) bodies (E). There was some co-localisation of mGluR4 with glial processes but none with glial cell bodies (F, G). Optical stack 10 μm. Scale bar 18 μm.

## 3.9 The distribution of $A_{2A}R$ in immature cerebellar slices

An immunohistochemical study using a high-affinity monoclonal antibody has suggested a discrete population of $A_{2A}R$ exist at Purkinje cells in the cerebellum (Rosin, Robeva et al. 1998). This correlates with a low $A_{2A}R$ mRNA expression observed in a subpopulation of Purkinje cells using in-situ hybridisation with a $^{35}S$-labelled cRNA probe for $A_{2A}R$ (Svenningsson, Le Moine et al. 1997).

Triple immunofluorescence using calbindin (1:1000), $A_{2A}R$ (1:100) and GFAP (1:300) on immature parasaggital cerebellar slices (100 µm, n = 2) showed a dense co-localisation of $A_{2A}R$ across Purkinje cell bodies and dendrites and further staining for $A_{2A}R$ around granule cells in the internal granule layer and on glial cell processes (figure 3.11). The staining is contradictory to the light staining of a small population of Purkinje cells observed in a previous study using mature cerebellar slices (Rosin, Robeva et al. 1998) and is unexpected as a role for $A_{2A}R$ within the cerebellum has not previously been described. Comparable staining patterns for $A_{2A}R$ were observed when immature cerebellar slices (250 µm, n = 1) were fixed separately instead of fixing the cerebellar block prior to slicing.

**calbindin**　　**A₂AR**　　**GFAP**

**calbindin/A₂A R**　　**calbindin/GFAP**　　**A₂AR/GFAP**
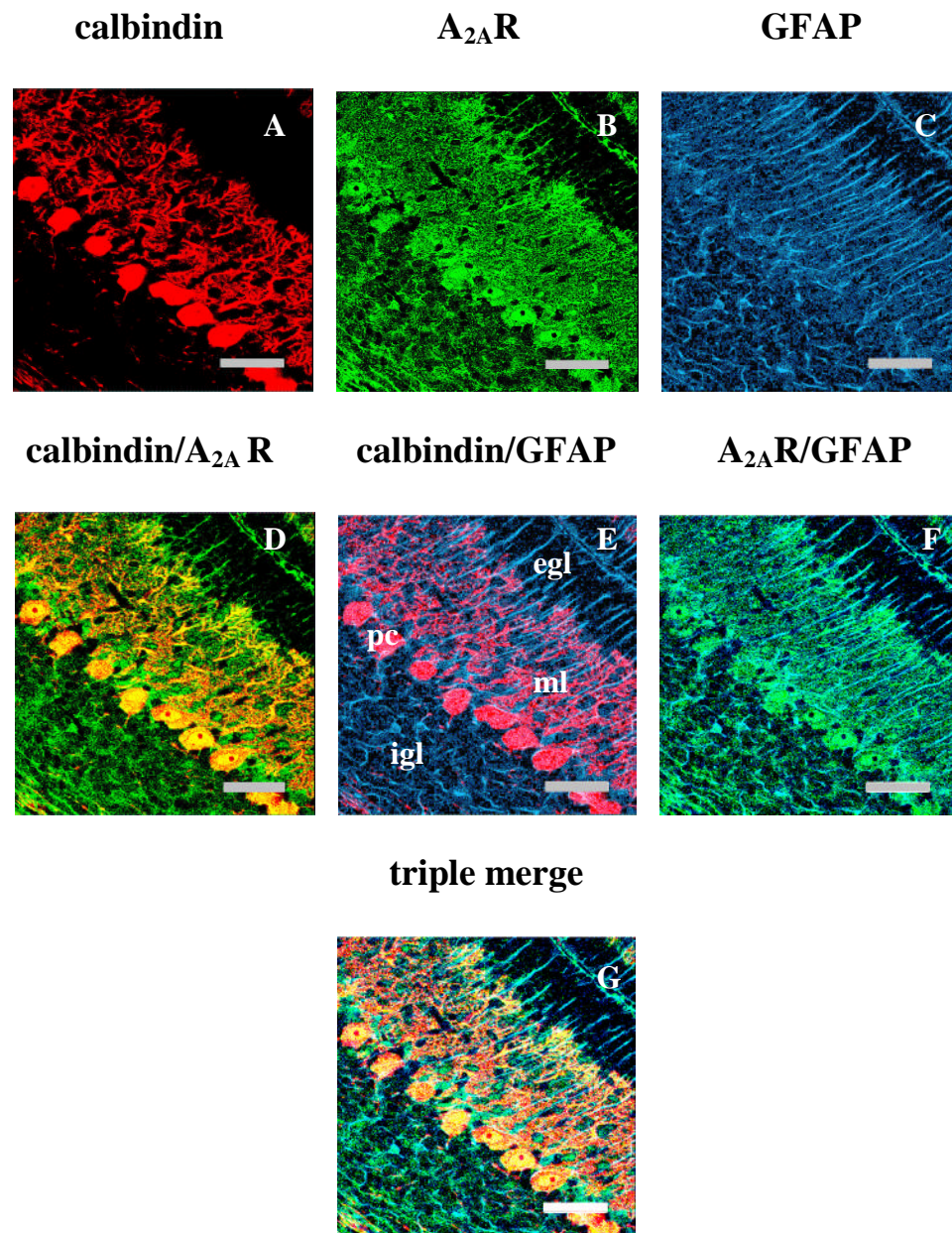
**triple merge**

**Figure 3.11 Triple staining for calbindin/A₂AR/GFAP**

Parasaggital sections (100 µm) from immature rat cerebella (P12). Sections were stained for calbinidin (red, 1:1000) (A), $A_{2A}R$ (green, 1:100) (B) and GFAP (blue, 1:300) (C). For merged images co-localisation of calbindin and $A_{2A}R$ is yellow (D), calbindin and GFAP is magenta (E), $A_{2A}R$ and GFAP is cyan (F) and calbindin, $A_{2A}R$ and GFAP is white (G). $A_{2A}R$ was densely distributed across Purkinje cell (pc) bodies and dendrites throughout the molecular layer (ml). Staining was also present around cells in the internal granule layer (igl) but not external granule layer (egl) (D). Some co-localisation of $A_{2A}R$ with glial cell processes was observed but glia do not account for the staining observed over Purkinje cell bodies (F, G). Optical stack 10 µm. Scale bar 45 µm.

## 3.10 Controls

To confirm that secondary antibodies bound specifically to their primary antibodies the immunofluorescence protocol was followed using parasaggital cerebellar sections (100 µm) with the primary antibody omitted (figure 3.12). Only minimal staining was observed, confirming that any unexpected staining patterns previously described were not due to a lack of secondary antibody specificity.

Further controls were carried out to eliminate the possibility that the unpredicted staining may have been a result of secondary antibody cross-over reactions. When parasaggital cerebellar sections (100 µm) were stained for calbindin (1:1000) and $A_1R$ (1:100) with the secondary antibody for $A_1R$ omitted no staining was observed for $A_1R$ (figure 3.13 A, B), confirming that the secondary antibody for calbindin does not cross-react with the $A_1R$ primary antibody. Cross-reaction of the secondary antibody for $A_1R$ with calbindin primary antibody was also eliminated in the same way by omitting the secondary antibody for calbindin (figure 3.13 C, D).

No staining for GFAP was observed using triple immunofluorescence with calbindin (1:1000), $A_1R$ (1:100) and GFAP (1:300) on parasaggital cerebellar sections (100 µm) with the secondary antibody for GFAP omitted (figure 3.13 E-G) confirming that the secondary antibodies for calbindin and $A_1R$ do not cross-react with the primary antibody for GFAP. The same control experiments were repeated using mGluR4 (1:100) and $A_{2A}R$ (1:100) in place of $A_1R$ primary antibody (not shown).

**calbindin**  **A₁R**  **mGluR4**



**A₂AR**  **GFAP**
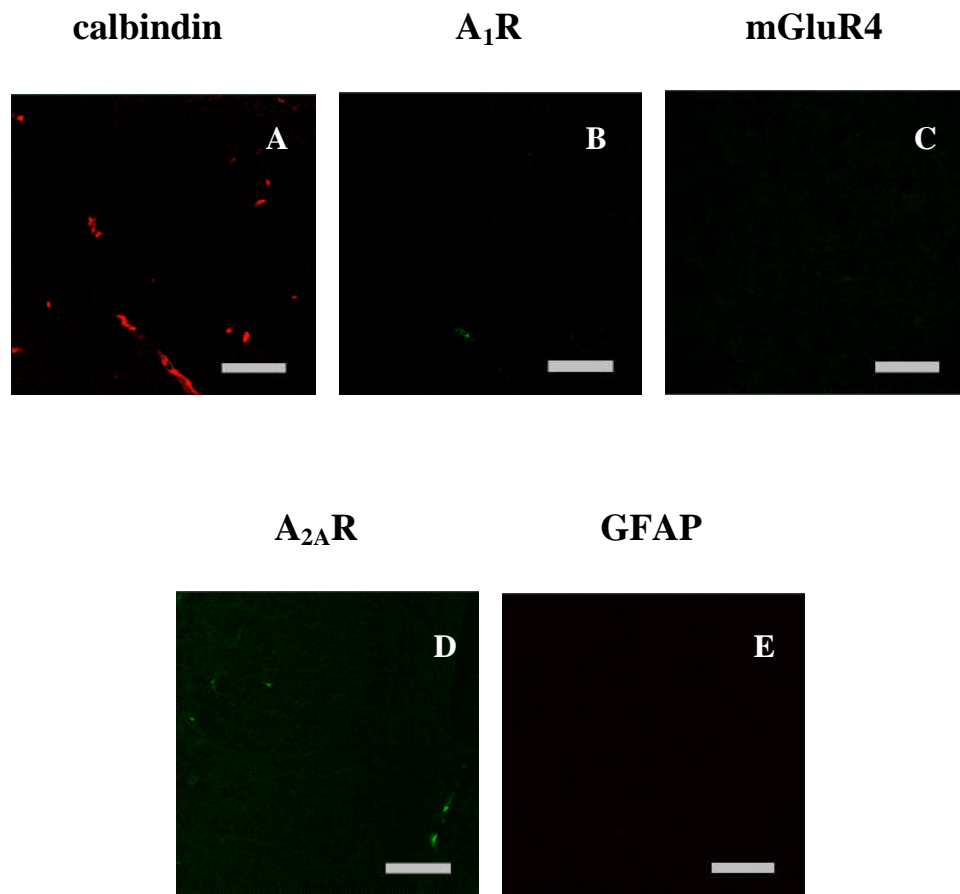


**Figure 3.12 Controls for secondary antibody specificity**

Parasaggital sections (100 µm) from rat cerebella (A, C-F P23, D P12). When the immunofluorescence protocol was followed with the primary antibody omitted no specific antibody staining was observed. Sections were stained with secondary antibodies for calbindin (red, 1:1000) (A), A₁R (green, 1:100) (B), mGluR4 (green, 1:100) (C), A₂AR (green, 1:100) (D) and GFAP (blue, 1:300) (E). Optical stack 10 µm. Scale bar 45 µm.
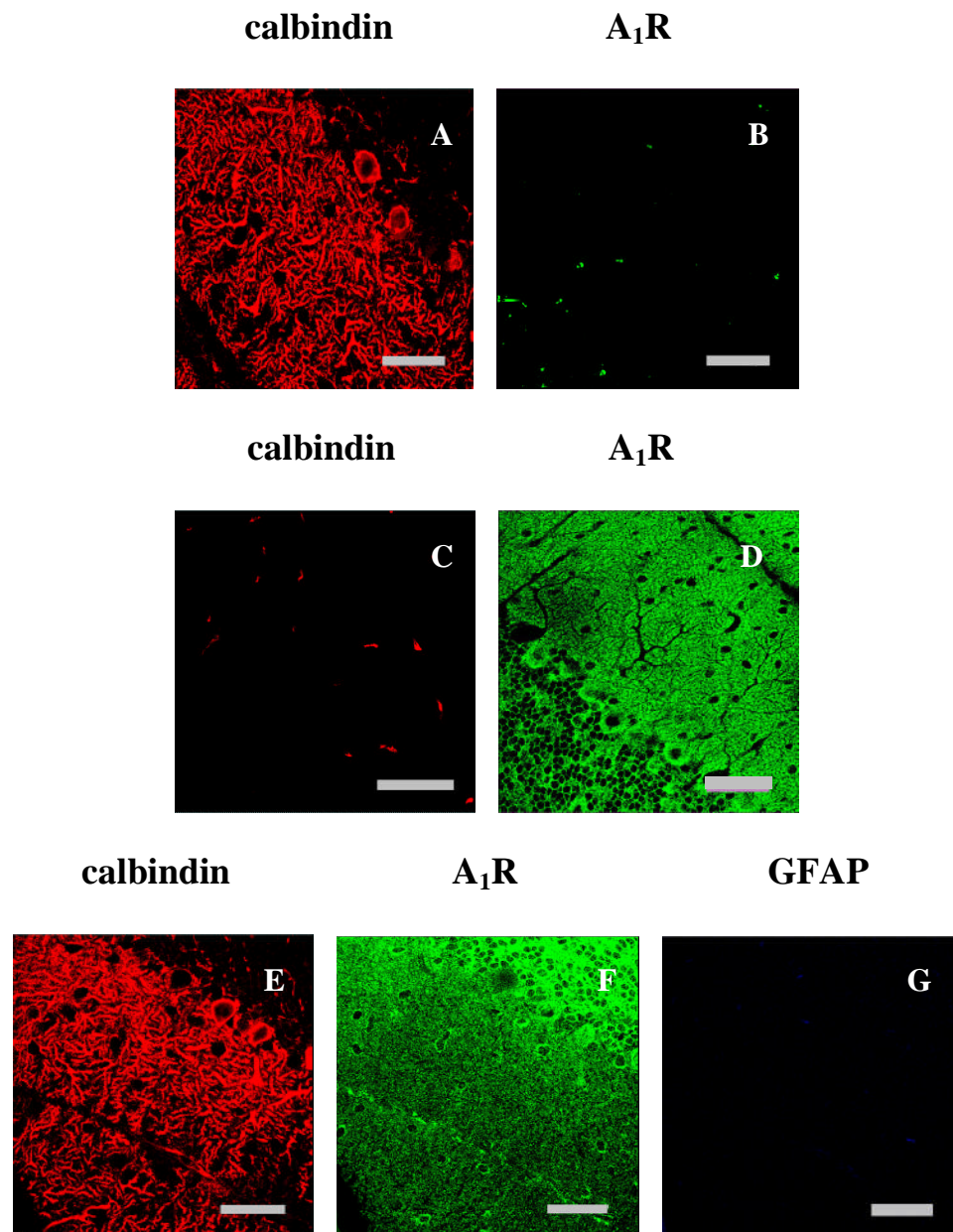
**Figure 3.13 Controls for secondary antibody cross-over**

Parasaggital sections (100 µm) from rat cerebella (A-B P21, C-D P23, E-G P12). When sections were stained for calbindin and $A_1R$ with the secondary antibody for $A_1R$ omitted no staining was observed for $A_1R$, confirming that the secondary antibody for calbindin does not cross-react with the $A_1R$ primary antibody (A, B). The same control was performed with the secondary antibody for calbindin omitted and no staining was observed for calbindin (C, D). For triple immunofluorescence with calbindin, $A_1R$ and GFAP the secondary antibody for GFAP was omitted. No staining was observed for GFAP confirming that the secondary antibodies for calbindin and $A_1R$ do not cross-react with the GFAP primary antibody (D, E, F). Optical stack 10 µm. Scale bar 45 µm.

## 3.11 Summary

The immunohistochemistry suggests that $A_1R$ and mGluR4 are widely distributed across Purkinje cell bodies, their dendrites and within the granule layer of the cerebellum throughout development. The same staining patterns were also observed in cerebellar slices prior to PF-PC synapse formation.

There is only minor co-localisation of $A_1R$ and mGluR4 with glial cell bodies or their processes, eliminating their involvement in the staining observed. Although these results were replicated using an alternative protocol, care should be taken in their interpretation as they are partly contradictory to the expression of $A_1R$ and mGluR4 described in previous studies and there is also no evidence for parallel fibre expression at Purkinje cell bodies or within the granule layer.

The widespread expression of $A_{2A}R$ within cerebellar slices which is identical to that of $A_1R$ is, in particular, contradictory to a number of previous immunohistochemical studies and a role for $A_{2A}R$ has not previously been described within the cerebellum.

# Chapter 4    Presynaptic pharmacology of immature parallel fibre-Purkinje cell synapses in the rat cerebellum

## 4.1    Introduction

The activation of presynaptic $A_1R$, mGluR4, $GABA_B$ and CB1 receptors at cerebellar parallel fibre terminals is known to decrease the probability of vesicle release and inhibit synaptic transmission (Bellamy 2007).

Separate studies have previously described the inhibitory effects of $GABA_B$ (Batchelor and Garthwaite 1992; Dittman and Regehr 1996), mGluR4 (Neale, Garthwaite et al. 2001) and $A_1R$ (Takahashi, Kovalchuk et al. 1995) activation on PF-PC synapse transmission at various stages of postnatal development prior to completion of the internal granule layer at around postnatal day 21.  This study used cerebellar slices from rats at postnatal days 9-14 to investigate the pharmacological profile of the immature rat PF-PC synapse.

Although it would have been ideal to examine the effect of presynaptic receptor activation from the initial formation of PF-PC synapses at around postnatal day 5 (Altman 1972), extracellular field recordings were frequently not possible to obtain below postnatal day 9 due to the low number of synapses present at this early stage of development.

## 4.2 Identification of parallel fibre excitatory postsynaptic potentials

Extracellular recordings of pairs of parallel fibre excitatory postsynaptic potentials (PF EPSPs) were recorded from the molecular layer of immature (postnatal day 9-14) and mature (postnatal day 21-28) rat cerebellar vermis. The cerebellar slices (400 µm) used for the measurements were cut transversely to ensure that the parallel fibres in contact with the Purkinje cell dendrites remained intact. This orientation also ensured that any climbing fibres forming synapses with proximal Purkinje cell dendrites were cut as climbing fibres run at a 90° angle to parallel fibres (figure 1.6).

Pairs of stimuli (2-5 V, 200 µs duration) at a frequency of 0.1 Hz resulted in paired pulse facilitation (PPF) where the amplitude of the second PF EPSP was larger than that of the first (figure 4.1A). The PPF, which provides a primary confirmation of PF EPSP identity (Atluri and Regehr 1996), occurs because the rapid arrival of a second action potential whilst $Ca^{2+}$ remains elevated in the parallel fibre terminal from the first depolarisation increases the probability of glutamate release from the readily-releasable pool of vesicles (Zucker and Regehr 2002). The paired pulse ratio (PPR, $1.4 \pm 0.01$, n = 220) was measured as $EPSP_2/EPSP_1$ and was used as a test of presynaptic action on release probability where an increase in PPR indicated an effect at presynaptic receptors. Application of the same pairs of stimuli at climbing fibre-Purkinje cell synapses in the molecular layer would have resulted in paired pulse depression (PPD) where the amplitude of the second EPSP is smaller than that of the first (Konnerth, Llano et al. 1990). This is thought to be due to a depletion of

the pool of readily-releasable glutamate vesicles in the climbing fibre terminal (Zucker and Regehr 2002).

The field potential consists of two components, both of which can be eliminated with application of the $Na^+$ channel inhibitor tetradotoxin (TTX, 1 µM) (figure 4.1C). The initial parallel fibre volley component was unaffected by application of the glutamate receptor antagonist kynurenic acid (5 mM) as it represents propagating action potentials that do not require the release of transmitter to be generated (Clark and Barbour 1997) but the amplitude of the second component was almost completely inhibited following its application (figure 4.1D). This verified that EPSP production was via postsynaptic glutamate receptor activation and further confirmed the identity of PF EPSPs (figure 4.1B) (Clark and Barbour 1997). The kynurenic acid-sensitive potential was deducted from the control potential and used as a measurement of PF EPSP amplitude in all electrophysiological experiments.

The residual potential persisting in kynurenic acid (5 mM) could be inhibited by 71.9 $\pm$ 7.7 % with cadmium (100 µM) which blocks voltage-dependent $Ca^{2+}$ channels and prevents the release of glutamate (n = 7, figure 4.1B, E). In whole cell patch clamp recordings from Bergmann glia in rat cerebellar slices the cadmium-sensitive component of the current generated by stimulation of parallel fibres was previously concluded to be a 'transporter current' produced by the uptake of synaptically released glutamate (Clark and Barbour 1997).

**A**

stimulating pulse

parallel fibre volley

kynurenic acid-
sensitive component

**B**

5 mM kynurenic acid

100 μM cadmium

EPSP amplitude (mV)

time (s)

**C**

1 μM TTX
control

**D**

5 mM kynurenic acid
control

**E**

100 μM cadmium
control
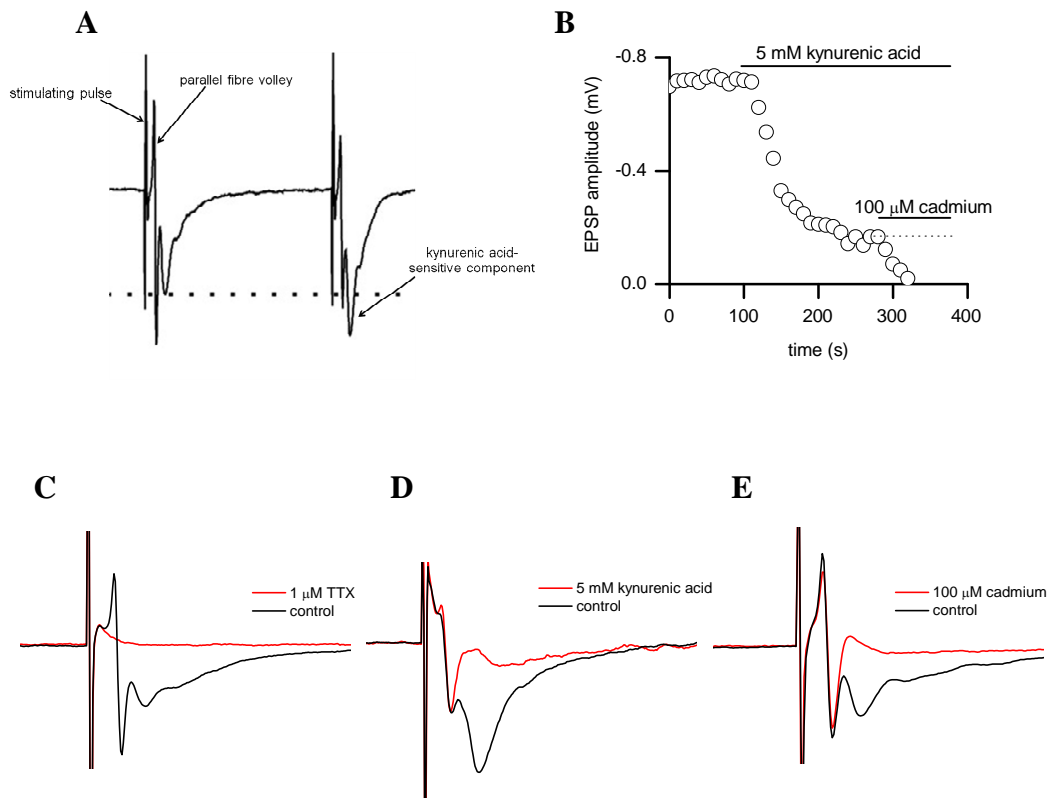
**Figure 4.1  Confirmation of parallel fibre excitatory postsynaptic potentials in extracellular recordings from the molecular layer of rat cerebellar slices**

(A)   Average of 50 pairs of parallel fibre excitatory postsynaptic potentials (PF EPSPs) obtained with pairs of stimuli (2-5 V, 200 μs duration) at a frequency of 0.1 Hz with an interval of 50 ms. Paired pulse facilitation (PPF) is illustrated by the greater amplitude of the second EPSP compared to the first (see dotted line).  The field potential consisted of two components that could be blocked with tetrodotoxin (TTX, 1 μM) (C).  The initial parallel fibre volley component was unaffected by application of kynurenic acid (5 mM) (D).  The kynurenic acid-sensitive component was used as an estimate of PF EPSP amplitude.  (B)  Graph plotting amplitude of individual EPSPs against time in an immature (P12) rat cerebellar slice.  Application of kynurenic acid (5 mM) resulted in almost complete inhibition.  Application of cadmium (100 μM) inhibited the residual potential persisting in kynurenic acid (5 mM) (E).

## 4.3   A variable GABA$_A$ response was present at immature parallel fibre-Purkinje cell synapses

Within the molecular layer, basket cell axons form GABAergic synapses with Purkinje cell bodies and stellate cell axons form GABAergic synapses with Purkinje cell dendrites to provide feed-forward inhibition (figure 1.7) (Hawkes 2005; Sillitoe and Joyner 2007).   In addition activation of presynaptic GABA$_A$ at parallel fibre terminals has also been shown to result in the release of glutamate onto Purkinje cells and interneurones (Stell, Rostaing et al. 2007).   It is possible that the pairs of stimuli in the molecular layer may have stimulated the release of GABA from the interneurones which could have affected the EPSP amplitudes recorded via activation of GABA$_A$ on Purkinje cells or at parallel fibre terminals.

Application of the GABA$_A$ antagonist bicuculline (10 µM) to immature cerebellar slices, where PF EPSP identity had been confirmed via PPF and inhibition with kynurenic acid (5mM), resulted in a net reduction in EPSP amplitude of 5.6 ± 4.6 % (n = 7) although the effect was variable.   An inhibition of 12.5 ± 5.6 % (figure 4.2A) was observed in 4 slices, no effect in 2 slices (figure 4.2B) and an increase of 11 % in 1 slice (figure 4.2C).   If GABA released from inhibitory interneurones was significantly affecting the EPSPs via activation of GABA$_A$ on Purkinje cells or at parallel fibre terminals a large change in amplitude would have been expected with bicuculline.   As the effect was variable with no large increases or decreases in EPSP amplitude observed it is unlikely that stimulation of inhibitory interneurones was affecting extracellular recordings in this study.
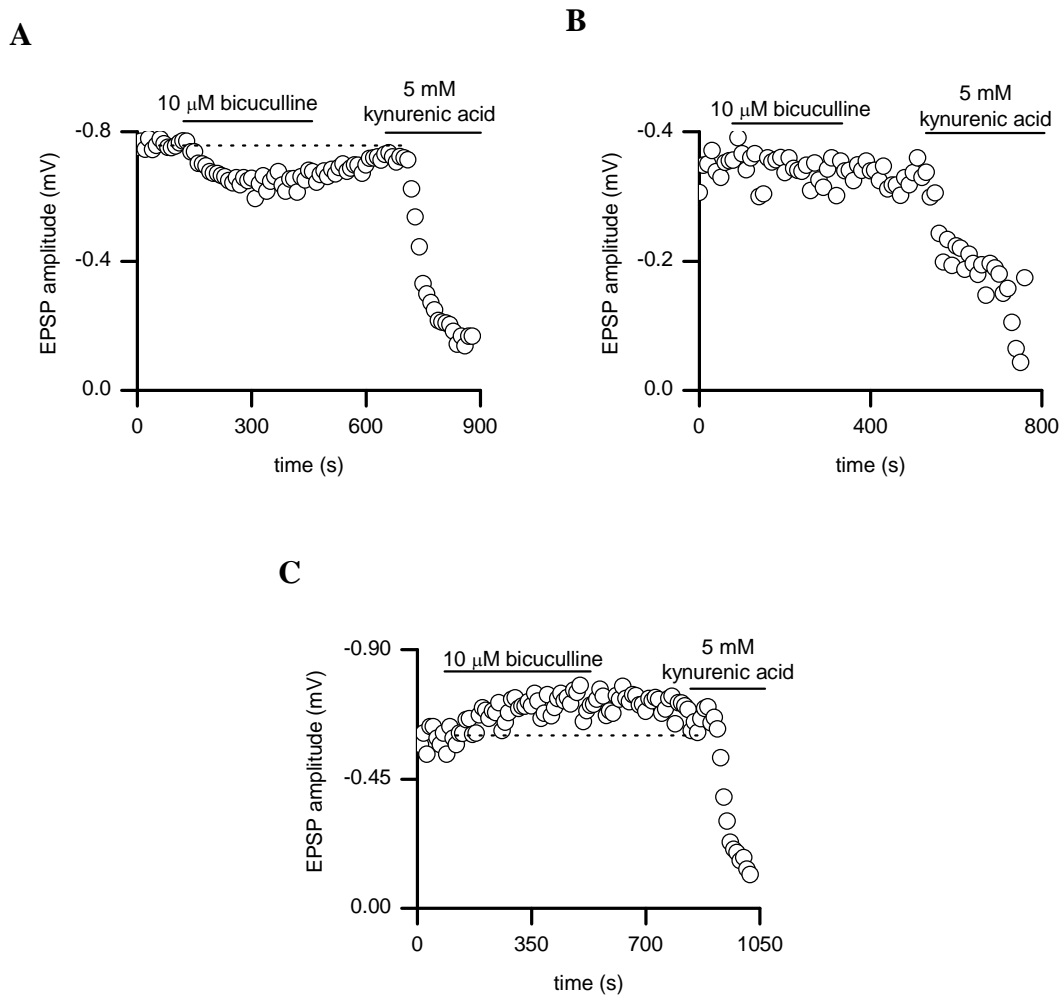
**Figure 4.2 A variable GABA_A response was present at immature parallel fibre-Purkinje cell synapses**

Graphs plotting amplitude of individual EPSPs against time in immature (P12-13) cerebellar slices. Application of bicuculline (10 µM) inhibited EPSP amplitude by 12.5 ± 5.6 % in 4 slices (A), had no effect in 2 slices (B) and increased EPSP amplitude by 11 % in 1 slice (C). PF EPSP identity was confirmed by inhibition with kynurenic acid (5 mM).

## 4.4 Confirmation of presynaptic GABA$_B$ and mGluR4 responses at parallel fibre-Purkinje cell synapses

It has previously been reported that GABA$_B$ receptors are expressed at high levels in the rat cerebellum both pre- and postsynaptically during postnatal development (Lujan and Shigemoto 2006) and that the GABA$_B$ agonist baclofen inhibits PF-PC synaptic transmission in mature (Batchelor and Garthwaite 1992) and immature (Batchelor and Garthwaite 1992; Dittman and Regehr 1996) rat cerebellar slices due to its action at presynaptic receptors. Confirming these previous observations in mature cerebellar slices baclofen (10 µM) reliably inhibited PF EPSP amplitude by $98.8 \pm 0.2$ % and significantly increased the PPR from $1.4 \pm 0.05$ to $2.9 \pm 0.4$ ($p < 0.001$, n = 5) indicating the presynaptic effect of baclofen. A similar inhibition of $97.3 \pm 1.3$ % and significant increase in PPR from $1.3 \pm 0.03$ to $2.6 \pm 0.2$ ($p < 0.001$, n = 16, figure 4.3A) was observed in immature slices suggesting little developmental difference in the activation of presynaptic GABA$_B$ receptors at PF-PC synapses (figure 4.4). However as the maximal effect of baclofen was obtained at the concentration used (10 µM) a developmental difference in presynaptic GABA$_B$ receptor activation may not have been observed.

Binding studies show a progressive increase in mGluR4 mRNA labelling in the rat cerebellum from very low levels at postnatal day 3 to very high levels at postnatal day 30 in line with the development of cerebellar circuitry (Catania, Landwehrmeyer et al. 1994) where mGluR4 are suggested to have a presynaptic autoreceptor function at the PF-PC synapse (Pekhletski, Gerlai et al. 1996). Previous electrophysiological studies have shown that application of the mGluR4 agonist L-(+)-2-amino-4-

phosphonobutyric acid (L-AP4) to rat cerebellar slices inhibits glutamatergic transmission at the PF-PC synapse at postnatal days 12-16 (Neale, Garthwaite et al. 2001) and in mature animals from postnatal day 21 onwards (Miniaci, Bonsi et al. 2001; Lorez, Humbel et al. 2003).

In mature cerebellar slices L-AP4 (50 µM) inhibited PF EPSP amplitude by $55.8 \pm 6.4$ % and increased PPR from $1.6 \pm 0.07$ to $1.9 \pm 0.2$ (n = 5). Similarly, application of L-AP4 (50 µM) to immature slices resulted in a $57.2 \pm 2.3$ % reduction in EPSP amplitude and significant increase in PPR from $1.4 \pm 0.03$ to $1.7 \pm 0.05$ ($p < 0.001$, n = 47, figure 4.3B) demonstrating an effect at presynaptic mGluR4 receptors and no significant developmental difference in inhibition of PF-PC synaptic transmission (figure 4.4).
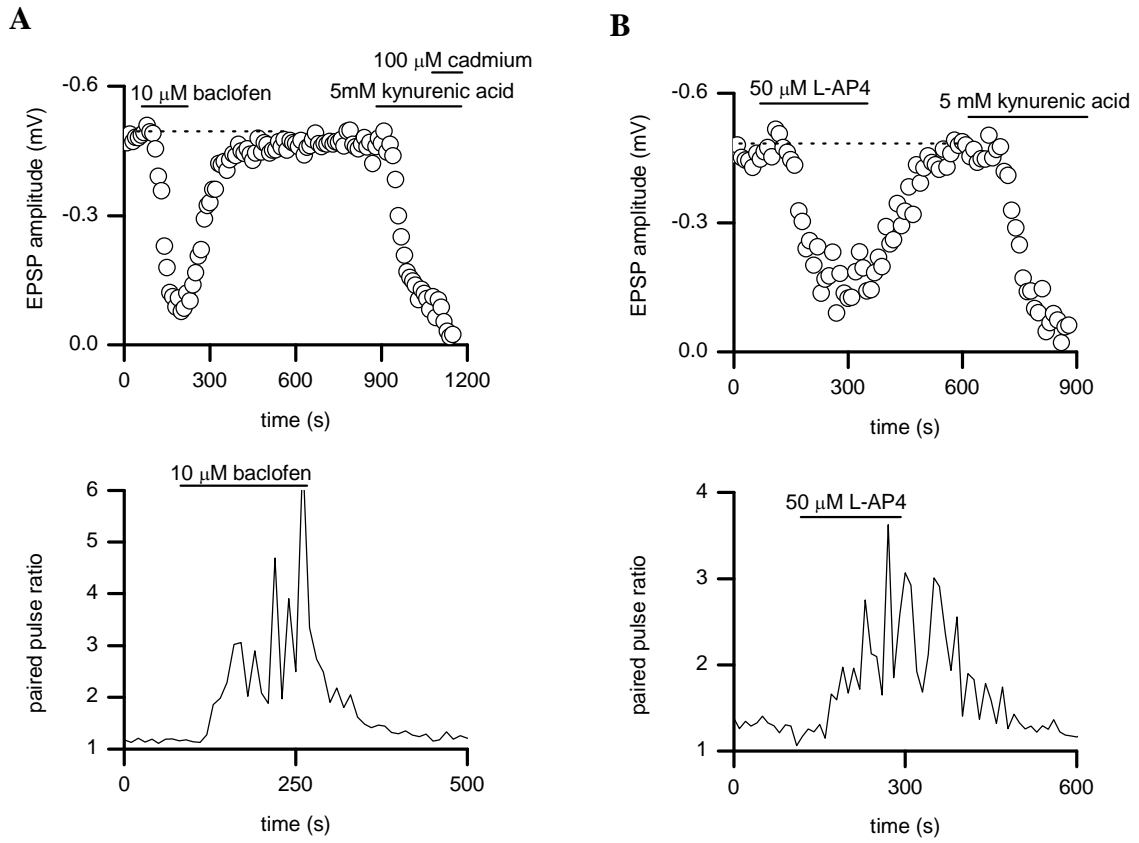
**Figure 4.3  Synaptic transmission at the immature parallel fibre-Purkinje cell synapse is inhibited by activation of presynaptic GABA$_B$ and mGluR4 receptors**

(A)  Graphs plotting amplitude of individual EPSPs against time and PPR against time for the same experiment in an immature (P11) cerebellar slice.  Application of baclofen (10 µM) inhibited PF EPSP amplitude and increased the PPR demonstrating an effect at presynaptic GABA$_B$ receptors.  (B)  Graphs plotting amplitude of individual EPSPs against time and PPR against time for the same experiment in an immature (P12) slice.  Application of L-AP4 (50 µM) blocked synaptic transmission and increased PPR due to action at presynaptic mGluR4 receptors.
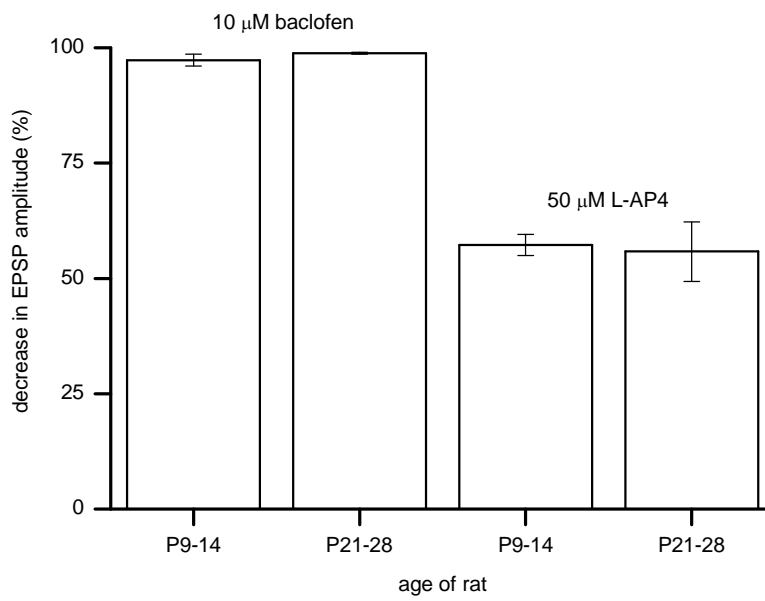
**Figure 4.4 There are no developmental differences in presynaptic inhibition via GABA$_B$ and mGluR4 receptors at parallel fibre-Purkinje cell synapses**

Graph comparing the inhibition resulting from application of baclofen (10 μM) to immature (P9-14, n = 16) and mature (P21-28, n = 5) cerebellar slices and L-AP4 (50 μM) to immature (n = 47) and mature (n = 5) slices. There were no significant developmental differences in inhibition at PF-PC synapses due to activation of presynaptic GABA$_B$ and mGluR4 receptors. However as the maximal effect of baclofen was obtained at the concentration used (10 μM) a developmental difference in presynaptic GABA$_B$ receptor activation may not have been observed.

## 4.5 The response to adenosine was variable at immature parallel fibre-Purkinje cell synapses

Previous studies have described inhibition following application of adenosine to mature (Kocsis, Eng et al. 1984) and immature (postnatal days 10-15) (Takahashi, Kovalchuk et al. 1995) rat cerebellar slices and stated that this inhibition occurs via the activation of $A_1R$ as it can be replicated with the $A_1R$ agonist CPA and blocked with the $A_1R$ antagonist 8-CPT (Takahashi, Kovalchuk et al. 1995). Application of adenosine (100 µM) to mature cerebellar slices resulted in a $59.9 \pm 2.1$ % decrease in EPSP amplitude (n = 53) and a significant increase in PPR from $1.5 \pm 0.03$ to $1.9 \pm 0.06$ ($p < 0.001$) due to the action of adenosine at presynaptic $A_1R$.

Application of adenosine (100 µM) to immature slices resulted in a variable PF EPSP amplitude reduction (figure 4.5). The expected inhibition of PF EPSPs was present at most synapses but little or no adenosine-mediated inhibition was also frequently observed despite clear PPF indicative of PF EPSP recordings. Further confirmation of PF EPSP identity with the mGluR4 agonist L-AP4 (50 µM) or $GABA_B$ agonist baclofen (10 µM) was obtained even when adenosine had little effect on synaptic transmission.

On average adenosine (100 µM) inhibited synaptic transmission by $47.7 \pm 2.3$ % (n = 167) and significantly increased PPR from $1.4 \pm 0.01$ to $1.7 \pm 0.03$ ($p < 0.001$) in immature slices indicating an action at presynaptic $A_1R$ (figure 4.6A). No inhibition or obvious changes in PPR were seen in 21 of the 167 (~12.5 %) slices (figure 4.6B) and confirmation of PF EPSP identity was obtained at these synapses with L-AP4

(50 μM, 57.3 ± 3.1 % inhibition, n = 19) or baclofen (10 μM, 96.5 ± 2.8 %, n = 6) in addition to almost complete inhibition with the glutamate receptor antagonist kynurenic acid (5 mM) (figure 4.6D).

In the slices where no adenosine-mediated inhibition was observed the reliable reduction in EPSP amplitude with L-AP4 (50 μM, figure 4.7A) provided the strongest evidence that the extracellular recordings were from PF-PC synapses as mGluR4 are unique to this synapse in the cerebellum (Pekhletski, Gerlai et al. 1996). In these slices the mean inhibition with L-AP4 (50 μM, 57.3 ± 3.1 %, n = 19) was almost identical to that observed with application of L-AP4 (50 μM, 57.1 ± 3.2 %, n = 28) to immature cerebellar slices where adenosine (100 μM) resulted in inhibition (figure 4.7B) suggesting no differences in the mGluR4 response between the two groups.

The PF-PC synapse properties in control were compared in immature slices where adenosine had little or no effect on PPF or synaptic transmission (inhibition < 15 %, n = 25) and slices where adenosine inhibited EPSP amplitude by more than 50 % and increased PPR (n = 98). There was no significant difference in either EPSP amplitude (-0.35 ± 0.02 mV and -0.3 ± 0.03 mV, p = 0.19) or the degree of PPF (1.38 ± 0.04 and 1.34 ± 0.03, p = 0.22). Thus other than the differential effect of adenosine on EPSP amplitude in immature slices, the synapses appeared identical in their properties and inhibition in response to baclofen, L-AP4 and kynurenic acid.

The variation in adenosine-mediated inhibition is unlikely to be due to developmental differences occurring within the immature age range tested (postnatal

105

days 9-14) as no inhibition with adenosine (100 µM) was observed in at least one animal at each postnatal day within this range. Similarly 100 % inhibition was observed in 4 animals at different ages within the range (postnatal days 9, 10, 12 and 13). A calculation of correlation coefficient confirms that there is no relationship between age and adenosine-mediated inhibition in rats between postnatal days 9 and 14 ($r = 0.04$).
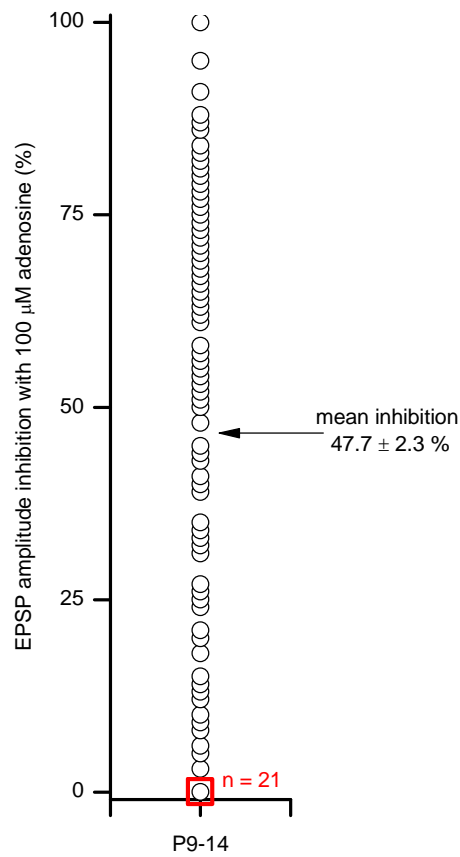
**Figure 4.5  Adenosine had a variable effect at presynaptic A₁R at immature parallel fibre-Purkinje cell synapses**

Graph summarising the % EPSP amplitude reduction observed with application of adenosine (100 µM) to immature (P9-14) cerebellar slices (n = 167).  Adenosine had a variable effect (47.7 ± 2.3 % mean inhibition) and had no effect at 21 of the 167 slices (~12.5 %) tested.
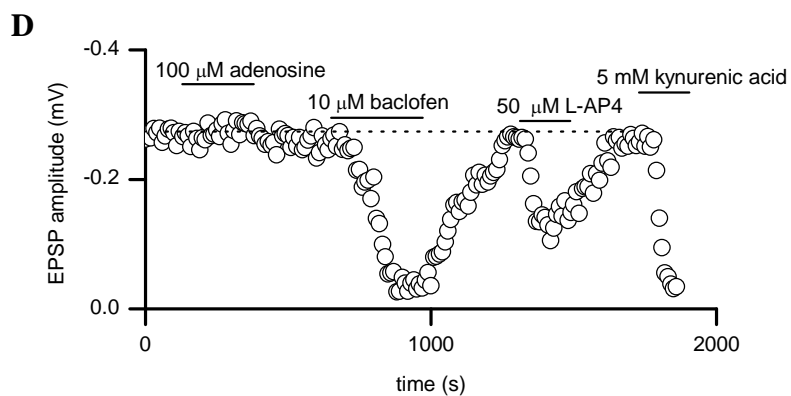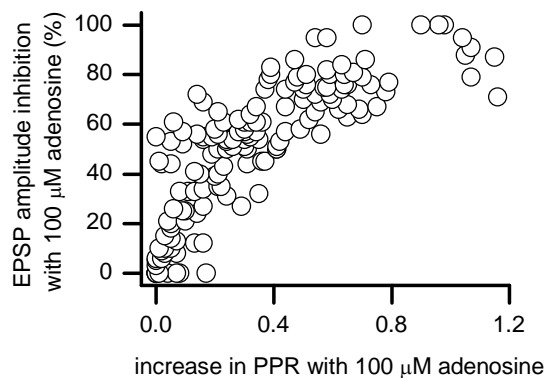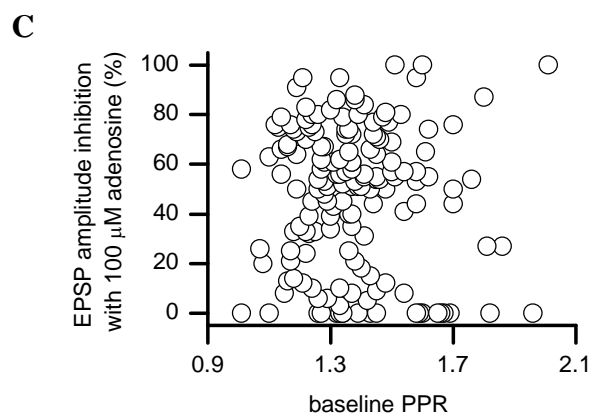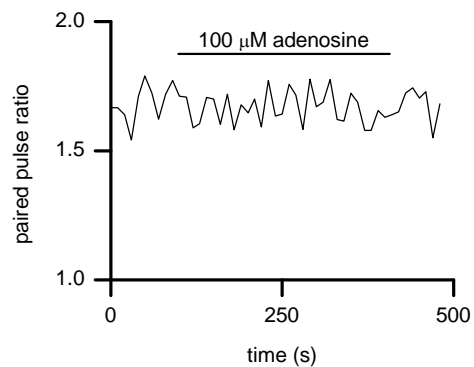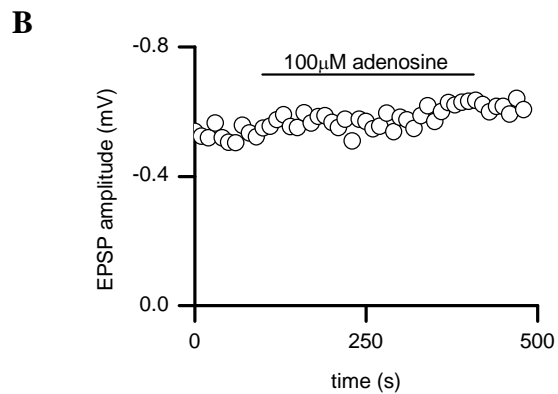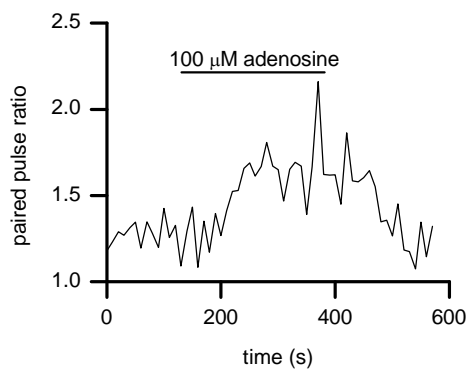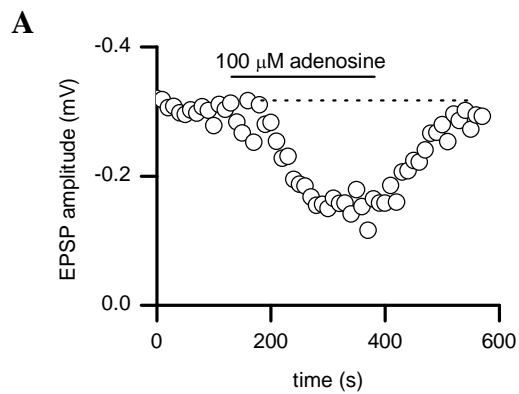
**Figure 4.6 Confirmation of parallel fibre excitatory postsynaptic potentials at synapses with no adenosine-mediated inhibition**

(A) Graphs plotting amplitude of individual EPSPs against time and PPR against time for the same experiment in an immature (P13) cerebellar slice. Application of adenosine (100 µM) inhibited PF EPSP amplitude and increased the PPR demonstrating an effect at presynaptic $A_1R$. (B) Graphs plotting amplitude of individual EPSPs against time and PPR against time for the same experiment in an immature (P9) slice. Adenosine had very little inhibitory effect on the EPSP amplitude and did not affect the PPR. (C) There is no relationship between baseline PPR and the magnitude of adenosine inhibition ($r = 0.03$) and a strong positive correlation between the increase in PPR and the magnitude of adenosine inhibition ($r = 0.70$) suggesting presynaptic inhibition. (D) Graph plotting amplitude of individual EPSPs against time in an immature (P12) slice. Application of adenosine (100 µM) resulted in little inhibition so confirmation of PF EPSPs was obtained by reduction in EPSP amplitude with L-AP4 (50 µM), baclofen (10 µM) and kynurenic acid (5 mM).
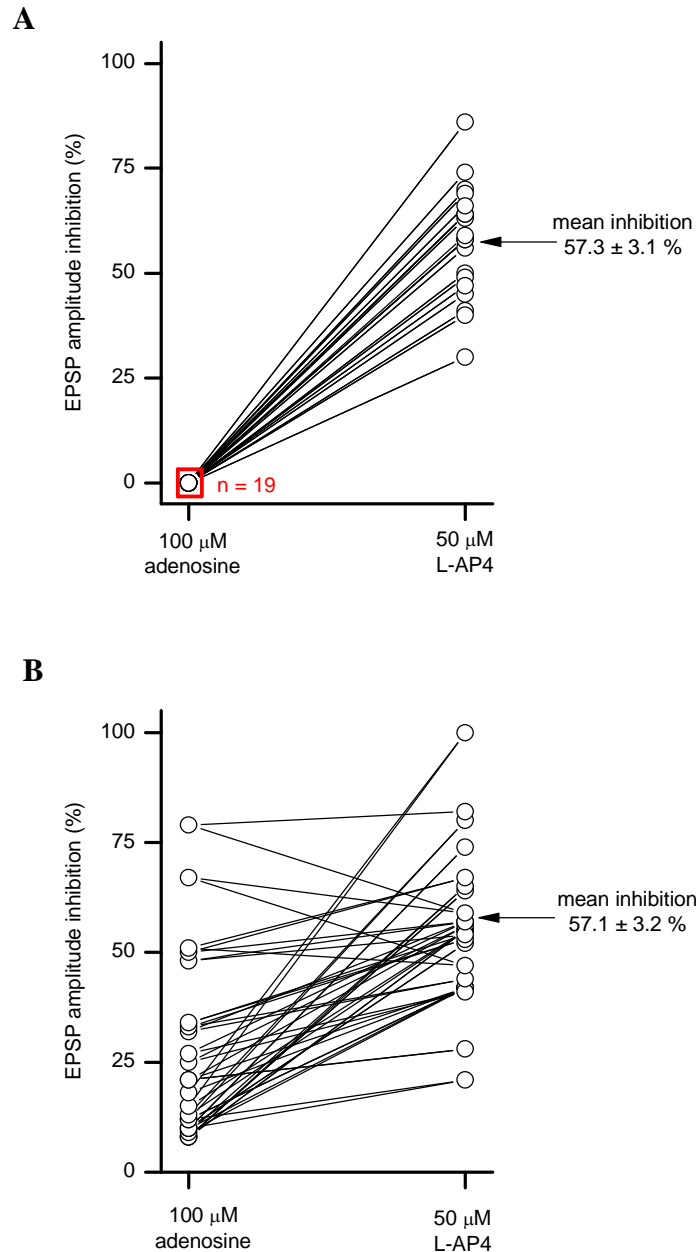
**Figure 4.7 Inhibition with L-AP4 at immature parallel fibre-Purkinje cell synapses**

(A) Graph demonstrating that application of L-AP4 (50 µM) reliably inhibited EPSP amplitude by $57.3 \pm 3.1$ % in immature (P9-14) cerebellar slices with no adenosine-mediated inhibition (100 µM, n = 19). (B) Graph showing the range of EPSP amplitude reduction with L-AP4 (50 µM, $57.1 \pm 3.2$ %, n = 28) in immature cerebellar slices with adenosine-mediated inhibition. The range of inhibition is similar to that of slices that do not respond to adenosine.

## 4.6 Parallel fibre excitatory postsynaptic potentials are unlikely to be a balance between $A_1R$ and $A_{2A}R$ activation

The earlier immunohistochemistry experiments in this study suggest a widespread distribution of both $A_1R$ and $A_{2A}R$ in the molecular layer which could indicate that adenosine is binding to both receptor subtypes at parallel fibre terminals and that the resultant EPSP amplitude is a balance of the inhibitory effect of $A_1R$ activation and the facilitatory effect of $A_{2A}R$ activation on glutamate release. At synapses where there are more $A_{2A}R$ this may have the net effect of adenosine having little or no effect on synaptic transmission.

To test this concept adenosine-mediated inhibition was measured in immature slices. The $A_1R$ antagonist 8-CPT (2 µM) was then applied followed by co-application of adenosine (100 µM) and 8-CPT. If both $A_1R$ and $A_{2A}R$ are functional at PF-PC synapses an increase in EPSP amplitude should be seen due to the action of adenosine at $A_{2A}R$ whilst $A_1R$ are blocked with 8-CPT. This increase should be greater in slices with little or no adenosine-mediated inhibition.

In 11 out of 12 slices tested adenosine (100 µM) inhibited EPSP amplitude between 45 and 91 %. In these slices simultaneous application of 8-CPT (2 µM) and adenosine had no effect on EPSP amplitude in 8 out of the 11 (~73 %) slices and increased EPSP amplitude by only $8.7 \pm 3.2$ % in the remaining 3 slices (figure 4.8). No effect on PPR was observed. This would be expected as adenosine-mediated inhibition via presynaptic $A_1R$ was apparent in these slices.

In the remaining slice adenosine (100 µM) inhibited EPSP amplitude by only 24 % and simultaneous application of 8-CPT (2 µM) and adenosine increased EPSP amplitude by 10 %. Identification of PF EPSPs was confirmed by inhibition with kynurenic acid (5 mM). This suggests the possibility that the presence of facilitatory $A_{2A}R$ may contribute to the reduced adenosine-mediated inhibition at some PF-PC synapses. However it is difficult to draw conclusions as in the 12 slices tested a low adenosine-mediated inhibition was only observed in one and it is in these slices where adenosine and 8-CPT co-application would be expected to have an effect.

These results suggest that if $A_{2A}R$ are present at PF-PC synapses they are unlikely to significantly influence EPSP amplitude. It may be that $A_{2A}R$ are functional or clustered at only a small number of PF-PC synapses and differences in $A_1R$ expression and affinity or adenosine metabolism has a greater effect on the variability in adenosine-mediated inhibition observed in immature slices.
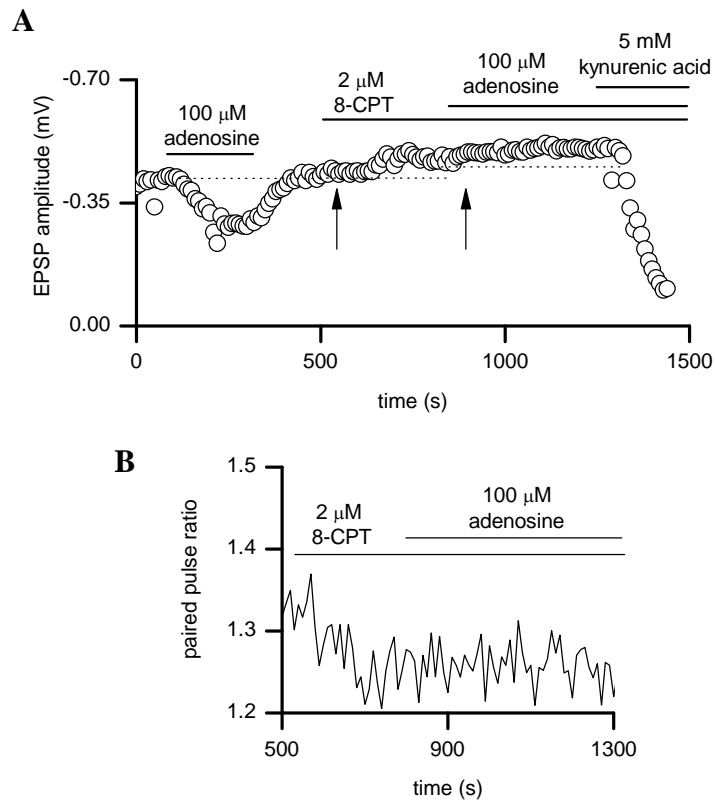
**Figure 4.8   Application of adenosine with 8-CPT had little effect at immature parallel fibre-Purkinje cell synapses**
(A) Graph plotting amplitude of individual EPSPs against time in an immature (P12) cerebellar slice. Adenosine (100 µM) inhibited EPSP amplitude by ~50 % and a small increase in PF EPSP amplitude was observed with 8-CPT (2 µM, arrow) indicating a low extracellular adenosine tone. Application of adenosine (100 µM) and 8-CPT (2 µM) resulted in a small increase in EPSP amplitude (arrow). (B) Graph plotting paired pulse ratio against time for the same experiment. The presynaptic action of 8-CPT was confirmed by a decrease in the paired pulse ratio as PF EPSP amplitude increased. Application of adenosine with 8-CPT had no further effect on PPR.

## 4.7 A low expression of $A_1R$ is unlikely to explain the variable adenosine-mediated inhibition in immature cerebellar slices

A concentration of 100 µM adenosine had been used to determine PF EPSP inhibition in immature cerebellar slices as this was the maximum concentration applied to slices in a previous electrophysiological study using rats of a similar age (Takahashi, Kovalchuk et al. 1995). In addition the extracellular concentration of adenosine in the brain is only estimated to vary between 25 nM and 250 nM (Dunwiddie and Masino 2001) so a response to adenosine should have been observed at 100 µM.

In immature slices where no inhibition was observed with application of adenosine (100 µM) a $42.3 \pm 6.1$ % decrease in EPSP amplitude and an increase in PPR from $1.5 \pm 0.2$ to $1.6 \pm 0.03$ was observed with a higher concentration of adenosine (300 µM) in 3 out of 4 slices indicating that functional $A_1R$ were present at these PF-PC synapses. In the other slice neither 100 nor 300 µM adenosine had any effect on EPSP amplitude. Confirmation of PF EPSP identity was obtained with application of L-AP4 (50 µM, $51.7 \pm 6.7$ % inhibition) and almost complete inhibition with kynurenic acid (5 mM) (figure 4.9).

The previously described immunohistochemistry experiments in this study suggested a dense co-localisation of $A_1R$ at all PF-PC synapses throughout development which also indicates that it is unlikely that the large variability in presynaptic inhibition

through activation of $A_1R$ would be due to a low expression of $A_1R$ at some immature PF-PC synapses.

To further confirm the presence of $A_1R$ the non-hydrolysable $A_1R$ agonist $N^6$-cyclopentyladenosine (CPA, 1 µM) was applied to immature cerebellar slices with no adenosine-mediated inhibition at PF-PC synapses where confirmation of PF EPSP identity had been obtained by inhibition with L-AP4 (50 µM, $59.6 \pm 3.7$ % inhibition, $n = 8$) or baclofen (10 µM, $100.0 \pm 0.0$ % inhibition, $n = 6$) and almost complete inhibition with kynurenic acid (5 mM, $n = 8$). The CPA reliably inhibited EPSP amplitude by $68.0 \pm 5.0$ % and significantly increased PPR from $1.4 \pm 0.1$ to $1.9 \pm 0.1$ ($p < 0.001$, $n = 8$) demonstrating its action at presynaptic $A_1R$ and confirming that the absence of adenosine-mediated inhibition at some immature PF-PC synapses is unlikely to be due to a low expression of $A_1R$ (figure 4.10).

The CPA is not metabolised and removed as adenosine would be in the extracellular space so its inhibitory effect at $A_1R$ that do not respond to adenosine (100 µM) may indicate a more rapid metabolism or uptake of adenosine by transporter proteins at some immature PF-PC synapses resulting in the removal of adenosine from the extracellular space before it can activate $A_1R$. Alternatively, the inhibition observed with CPA or a higher concentration of adenosine (300 µM) at PF-PC synapses that do not respond to adenosine (100 µM) may indicate that presynaptic $A_1R$ with a lower affinity for adenosine may be present at these synapses.

**A**
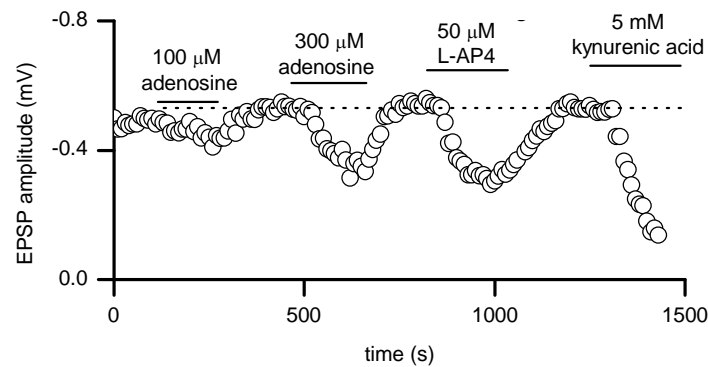


**B**
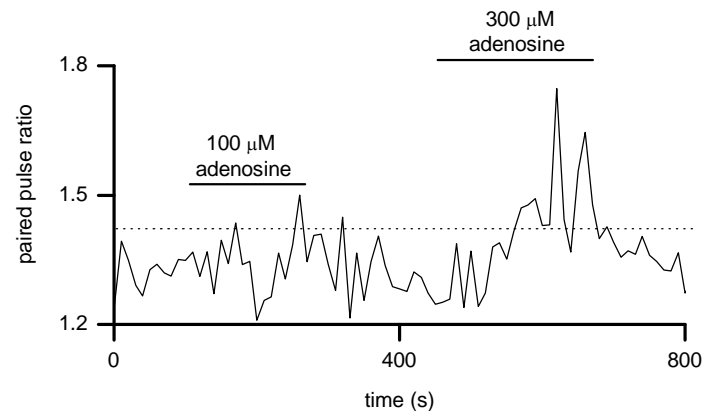


**Figure 4.9 A higher concentration of adenosine resulted in inhibition at some immature parallel fibre-Purkinje cell synapses where 100 µM adenosine had little inhibitory effect**

(A) Graph plotting amplitude of individual EPSPs against time in an immature (P12) cerebellar slice. Application of adenosine (100 µM) had little effect on PF EPSP amplitude although a higher concentration (300 µM) resulted in 54 % inhibition indicating the presence of functional $A_1R$. PF EPSP identity was confirmed with inhibition following application of L-AP4 (50 µM) and kynurenic acid (5 mM). (B) Graph plotting PPR against time for the same experiment showing that the response to the higher concentration of adenosine was due to an effect at presynaptic receptors.

116
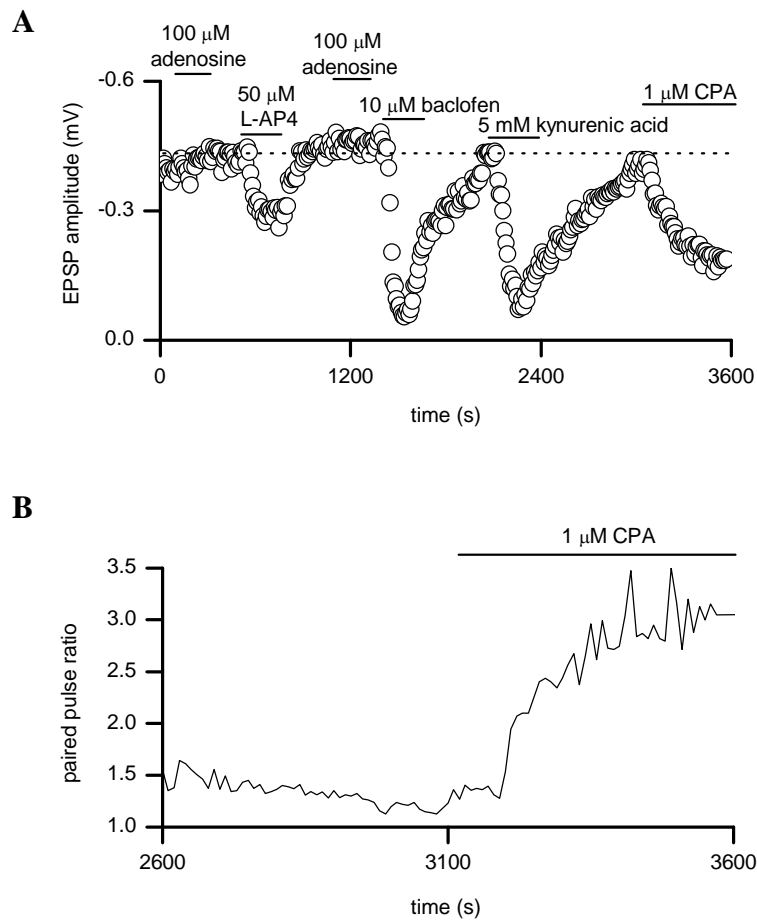
**Figure 4.10 The absence of adenosine-mediated inhibition at some immature parallel fibre-Purkinje cell synapses is unlikely to be due to a low expression of $A_1R$**

(A) Graph plotting amplitude of individual EPSPs against time in an immature (P12) cerebellar slice. PF EPSP identity was confirmed by inhibition via activation of presynaptic mGluR4 receptors with L-AP4 (50 µM), presynaptic $GABA_B$ receptors with baclofen (10 µM) and with the glutamate receptor antagonist kynurenic acid (5 mM). Application of the $A_1R$ agonist CPA (1 µM) decreased PF EPSP amplitude demonstrating that functional $A_1R$ were present at this PF-PC synapse even though no adenosine-mediated inhibition was observed with 2 applications of adenosine (100 µM). The slow wash-off of CPA has not been included. (B) Graph plotting paired pulse ratio against time for the same experiment. The presynaptic action of CPA was confirmed by an increase in the paired pulse ratio as PF EPSP amplitude decreased.

## 4.8 The variable inhibitory effect of adenosine acting at $A_1R$ at immature parallel fibre-Purkinje cell synapses may be due to differences in $A_1R$ efficacy

To further test the possibility that inconsistent adenosine-mediated inhibition at immature PF-PC synapses may be the result of a variability in $A_1R$ efficacy, two log concentration-response curves for EPSP amplitude reduction (figure 4.11) elicited by application of the $A_1R$ agonist CPA (0.001 µM – 100 µM) were generated. These were for slices where application of adenosine (100 µM) resulted in a greater than 50 % inhibition of PF EPSP amplitude (n = 4) and slices that showed little or no adenosine-mediated inhibition but where PF EPSP identity had been confirmed by inhibition with both L-AP4 (50 µM) and kynurenic acid (5 mM) (n = 6, figure 4.12).

The PF EPSP amplitude reduction resulting from application of CPA was greater at PF-PC synapses that were inhibited by application of adenosine (100 µM) than those where no adenosine-mediated inhibition was observed for each concentration of CPA tested (table 4.1). The lower $IC_{50}$ of 0.08 µM in slices that respond to adenosine compared to 2.10 µM in slices where there is no adenosine-mediated inhibition suggests that $A_1R$ efficacy may be lower at some immature PF-PC synapses and that this may account for the variability in response to adenosine. The log concentration-response curves (figure 4.12) also suggest that there may be differences in the efficacy of adenosine in immature slices.

| concentration | mean PF EPSP amplitude reduction (%) | |
|---|---|---|
| of CPA (μM) | adenosine-mediated inhibition | no adenosine-mediated inhibition |
| 0.001 | 0 | 0 |
| 0.003 | 7.5 | 1.4 |
| 0.01 | 15.8 | 6.0 |
| 0.3 | 32.0 | 10.2 |
| 0.1 | 58.2 | 10.2 |
| 0.3 | 76.3 | 18.5 |
| 1 | 91.3 | 26.2 |
| 3 | 100.0 | 32.5 |
| 10 | - | 39.3 |
| 30 | - | 51.5 |
| 100 | - | 59.0 |

**Table 4.1      Comparison of inhibition with CPA in immature cerebellar slices**

The mean % EPSP amplitude reduction resulting from application of CPA (0.001 μM - 100 μM) to immature cerebellar slices was greater at PF-PC synapses that were inhibited by application of adenosine (100 μM, n = 4) than those where no adenosine-mediated inhibition was observed (n = 6) for each concentration of CPA tested.

**A**
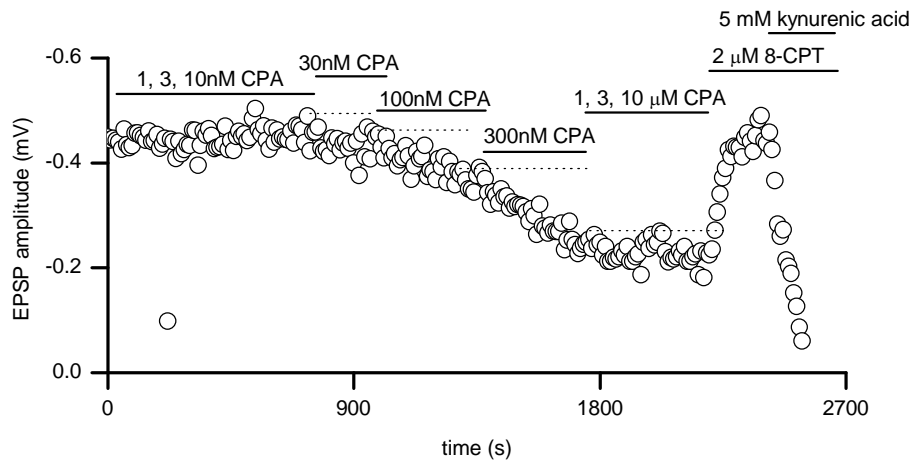


**B**
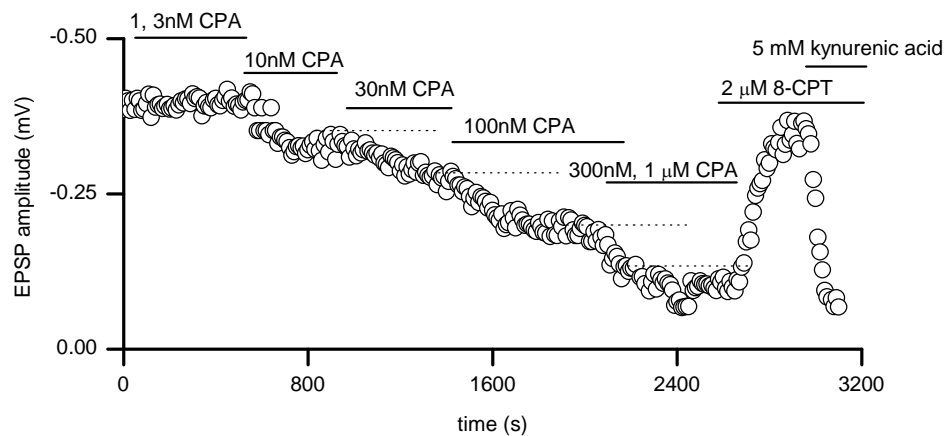


**Figure 4.11 Comparison of inhibition with CPA at immature parallel fibre-Purkinje cell synapses in the absence and presence of adenosine-mediated inhibition**

(A) Graph plotting amplitude of individual EPSPs against time in an immature (P10) cerebellar slice with no adenosine-mediated inhibition. Application of the $A_1R$ agonist CPA (1 nM – 10 µM) decreased PF EPSP by 58 % and was reversed with application of 8-CPT (2 µM). Identification of EPSPs was confirmed by inhibition with kynurenic acid (5 mM). (B) Graph plotting amplitude of individual EPSPs against time in an immature (P12) cerebellar slice with adenosine-mediated inhibition (75 %). Application of the $A_1R$ agonist CPA (1 nM – 1 µM) decreased PF EPSP by 97 % and was reversed with application of 8-CPT (2 µM). Identification of EPSPs was confirmed by inhibition with kynurenic acid (5 mM).
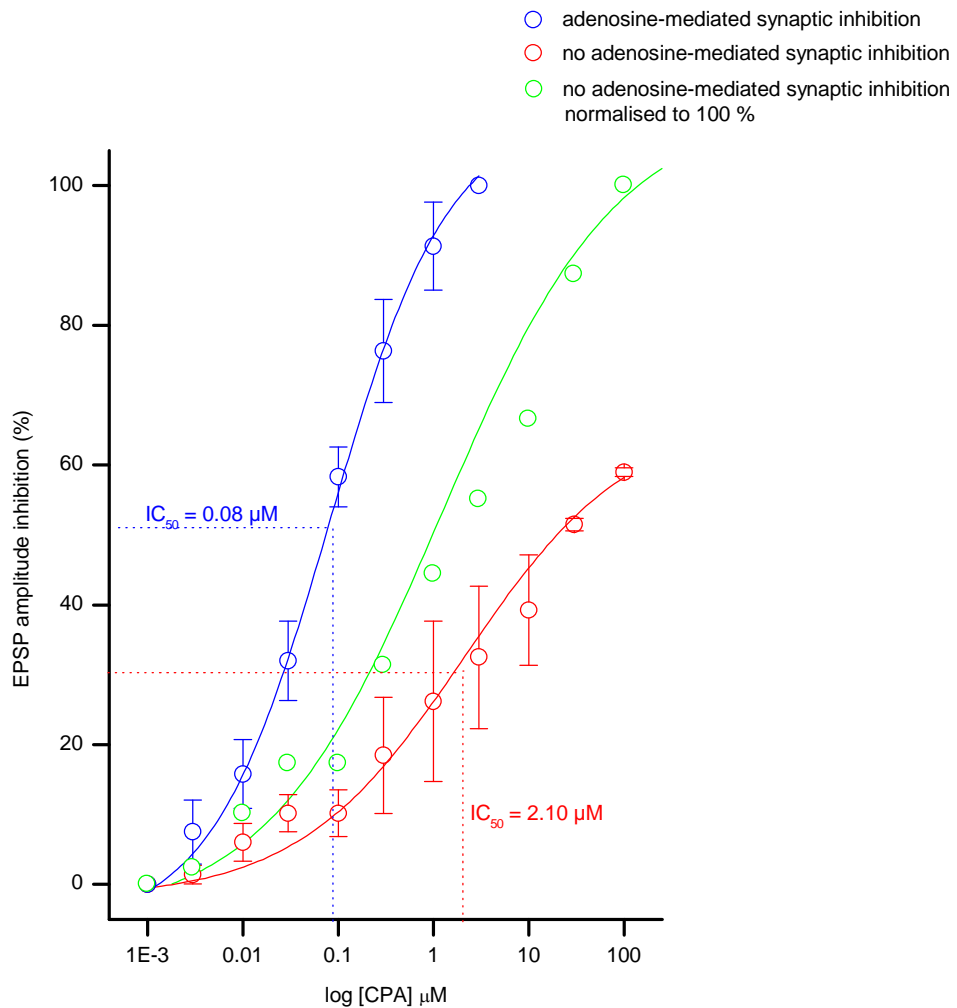
**Figure 4.12 The variable adenosine-mediated inhibition at immature parallel fibre-Purkinje cell synapses may be due to differences in $A_1R$ efficacy**

Log concentration-response curves for the reduction in PF EPSP amplitude by the $A_1R$ agonist CPA (0.001 µM – 100 µM) in immature (P9-14) cerebellar slices where EPSP amplitude was reduced by application of adenosine (100 µM, n = 4) and slices where there was no adenosine-mediated inhibition (n = 6). The $IC_{50}$ was higher in slices with no adenosine-mediated inhibition ($IC_{50} = 2.10$ µM) than in those where PF EPSP amplitude was reduced by adenosine ($IC_{50} = 0.08$ µM) suggesting variability in $A_1R$ efficacy at immature PF-PC synapses. At synapses where adenosine had little or no effect on EPSP amplitude, the concentration response curve was shifted to the right when normalised to 100 %. Thus synapses show variation in the efficacy of CPA suggesting that the variation stems from receptor properties (and possibly downstream signalling) rather than differences in adenosine uptake and metabolism.

## 4.9 The variability in adenosine-mediated inhibition in immature cerebellar slices is not gender-specific

In a study looking at the effects of neonatal caffeine exposure on epileptogenesis, rats exposed at postnatal days 2-6 to the $A_1R$ antagonist caffeine were infused intravenously with convulsants acting at various CNS receptors at postnatal days 70-90. The threshold for seizures induced by caffeine increases as a result of neonatal caffeine exposure and is significantly higher in females than males suggesting gender specificity in how developmental exposure to caffeine affects adult seizure susceptibility at the $A_1R$ (Guillet and Dunham 1995).

The $A_1R$-mediated inhibition at the PF-PC synapse in immature female cerebellar slices was compared to that of males to see whether the variability in inhibition was gender-specific. Application of adenosine (100 µM) to immature female cerebellar slices (400 µm) resulted in a similar range of inhibition of PF EPSP amplitude (figure 4.13A) to that of immature male cerebellar slices (figure 4.4) with an average adenosine-mediated inhibition of $34.6 \pm 7.5$ % (n = 16) and increase in PPR from $1.4 \pm 0.05$ to $1.6 \pm 0.1$. Although lower than the PF EPSP amplitude reduction seen with application of adenosine (100 µM) to male immature cerebellar slices ($47.7 \pm 2.3$ %, n = 167) the difference was not significant (p = 0.09) (figure 4.13B).

No adenosine-mediated inhibition or obvious changes in PPR were seen in 3 of the 16 (~18.8 %) female immature cerebellar slices compared with 12.5 % in male and confirmation of PF EPSP identity was obtained at these synapses with the mGluR4

agonist L-AP4 (50 µM, 68.3 ± 3.3 % inhibition) in addition to almost complete

inhibition with the glutamate receptor antagonist kynurenic acid (5 mM).

As a final observation, a lack of $A_1R$-mediated inhibition was often observed in

batches of slices taken from the same litter of rats. This may indicate a genetic

component for the response to adenosine.
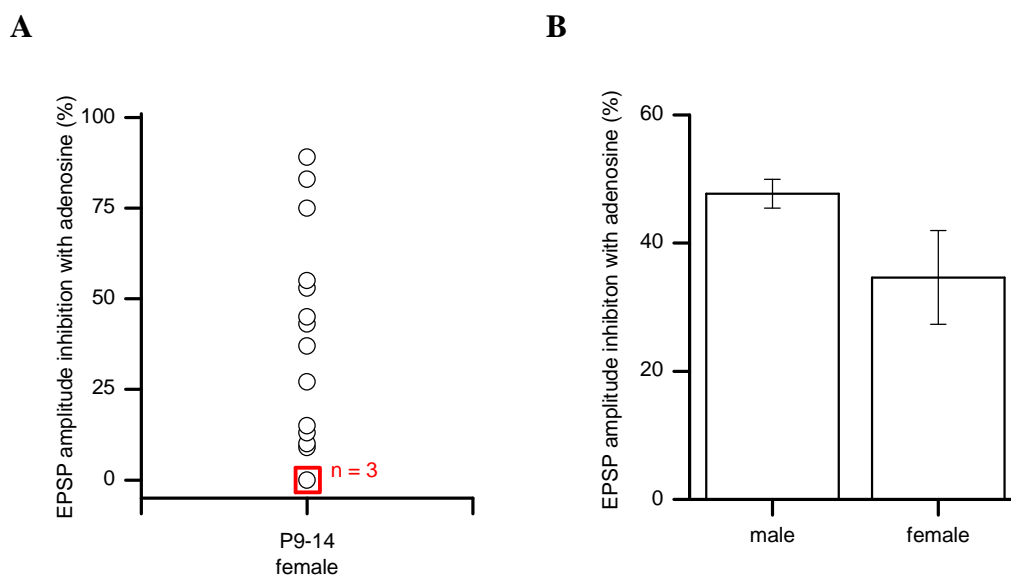


**Figure 4.13 Comparison of adenosine-mediated inhibition at immature parallel fibre-Purkinje cell synapses in male and female rats**

(A) Graph summarising the % EPSP amplitude reduction observed with application of adenosine (100 µM) to immature (P9-14) female cerebellar slices (n = 16). Adenosine had a variable effect (34.6 ± 7.5 % mean inhibition) and had no effect at 3 of the 16 slices (~18.8 %) tested. (B) Graph comparing the inhibition resulting from application of adenosine (100 µM) to immature male (n = 167) and female (n = 16) slices. Although the mean PF EPSP amplitude reduction is less at female (34.6 ± 7.5 %, n = 16) than male PF-PC synapses (47.7 ± 2.3 %, n = 167) the difference is not significant (p = 0.09).

## 4.10 Summary

The release of GABA from inhibitory interneurones in the molecular layer appeared to have little effect on EPSP amplitude at immature PF-PC synapses via activation of $GABA_A$ receptors. Reduction in EPSP amplitude due to activation of presynaptic mGluR4 and $GABA_B$ receptors was confirmed in slices at postnatal days 9-14 and found to be comparable to that obtained in slices at postnatal days 21-28.

The $A_1R$-mediated inhibition was found to be variable in immature slices with ~12.5 % of confirmed PF-PC synapses showing no response to adenosine. The variability in $A_1R$-mediated inhibition was not found to be gender-specific or correlated with age of rat (P9-14) and the synapses otherwise appeared identical in their properties and inhibition in response to baclofen, L-AP4 and kynurenic acid.

Previous immunohistochemistry experiments suggesting the widespread presence of $A_{2A}R$ in the molecular layer may indicate that adenosine could be acting at receptors other than $A_1R$ although co-application of adenosine and 8-CPT indicates that activation of $A_{2A}R$ is unlikely to contribute significantly to PF EPSP amplitude.

In immature slices with no $A_1R$-mediated inhibition the widespread distribution of $A_1R$ in the molecular was assumed from prior immunohistochemistry experiments and confirmed by inhibition of PF EPSP amplitude with a higher concentration of adenosine (300 µM) in 3 out of 4 slices and inhibition with the non-hydrolysable $A_1R$ agonist CPA.

A comparison of log concentration-response curves generated for the inhibition of PF EPSP amplitude at immature PF-PC synapses that respond to adenosine and those without $A_1R$-mediated inhibition suggest that some $A_1R$ may have a lower efficacy at this stage of development and that this may explain the variability in PF EPSP amplitude reduction observed with application of adenosine.

# Chapter 5     Adenosine signalling at immature

# parallel fibre-Purkinje cell synapses in the rat

# cerebellum

## 5.1   Introduction

The release (Wall and Dale 2008) and clearance (Baldwin, Beal et al. 2004; Noji, Karasawa et al. 2004; Boison 2007) of adenosine are reasonably well-documented in the mature CNS but relatively little is known about how adenosine signalling changes during postnatal development. In the mature cerebellum blockade of presynaptic $A_1R$ at PF-PC synapses enhances synaptic transmission suggesting the presence of an inhibitory adenosine tone (Wall, Atterbury et al. 2007).

The enzyme adenosine kinase is the major determinant of adenosine levels at PF-PC synapses and an extracellular purine tone is detectable with microelectrode biosensors under basal conditions (Wall, Atterbury et al. 2007). The active release of adenosine can also be stimulated with trains of activity in the molecular layer of mature cerebellar slices although this does not appear to be a source of the basal extracellular adenosine tone (Wall and Dale 2008).

Electrophysiology and microelectrode biosensors were used to examine immature adenosine signalling in cerebellar slices at postnatal days 9-12 shortly after the initial development of PF-PC synapses around postnatal day 5 in the rat (Altman 1972).

## 5.2 Tonic inhibition by endogenous adenosine is low or absent at immature parallel fibre-Purkinje cell synapses

Application of 8-CPT to block $A_1R$ in cerebellar slices potentiates synaptic transmission at the PF-PC synapse suggesting the tonic activation of $A_1R$ with an endogenous inhibitory tone of adenosine (Takahashi, Kovalchuk et al. 1995; Wall, Atterbury et al. 2007). To investigate whether this tonic $A_1R$-mediated inhibition is present at an early developmental stage soon after the formation of PF-PC synapses around postnatal day 5 (Altman 1972) the effect of 8-CPT on PF EPSP amplitude was observed in immature rat cerebellar slices (400 µm) at postnatal days 9-12.

Previously described electrophysiology experiments in this study suggested that some immature PF-PC synapses may express low efficacy $A_1R$ or adenosine receptors other than $A_1R$ (see Chapter 4). Presumably these synapses will have no $A_1R$ tone so were not included in this study. In all experiments, slices were only analysed where at least 50 % inhibition of PF EPSP amplitude was observed following application of adenosine (100 µM). Identification of PF EPSP was confirmed in all slices by the presence of PPF and an almost complete inhibition with kynurenic acid (5 mM).

Application of 8-CPT (2µM) increased PF EPSP amplitude by $7.4 \pm 5.6$ % (n = 20) with no effect on synaptic transmission or PPR observed in 9 of the 20 (45 %) slices (figure 5.1A). In these 9 slices the effect of 8-CPT was confirmed by applying adenosine (100 µM) in the presence of 8-CPT. This resulted in no reduction in EPSP amplitude (figure 5.1B). In the slices where 8-CPT had an effect, EPSP amplitude

was increased by $13.4 \pm 2.6$ % and the PPR was significantly decreased from $1.22 \pm 0.03$ to $1.16 \pm 0.03$ (n = 11, $p < 0.001$, figure 5.1C). The enhanced EPSP amplitude could be attributed to block of $A_1R$ as addition of adenosine (100 µM) in the presence of 8-CPT no longer blocked synaptic transmission. The overall increase in EPSP amplitude ($7.4 \pm 5.6$ %, n = 20) was significantly less ($p < 0.001$) than that observed at mature PF-PC synapses at postnatal days 21-28 where EPSP amplitude was increased by $45.6 \pm 7.0$ % in ~89 % slices (n = 8, figure 5.2) and see (Wall, Atterbury et al. 2007).

The lower inhibitory $A_1R$ tone at immature PF-PC synapses is unlikely to be due to developmental differences occurring within the age range tested (postnatal days 9-12) as no increase in PF EPSP amplitude was observed with 8-CPT (2 µM) in at least one animal at each postnatal day within this range.
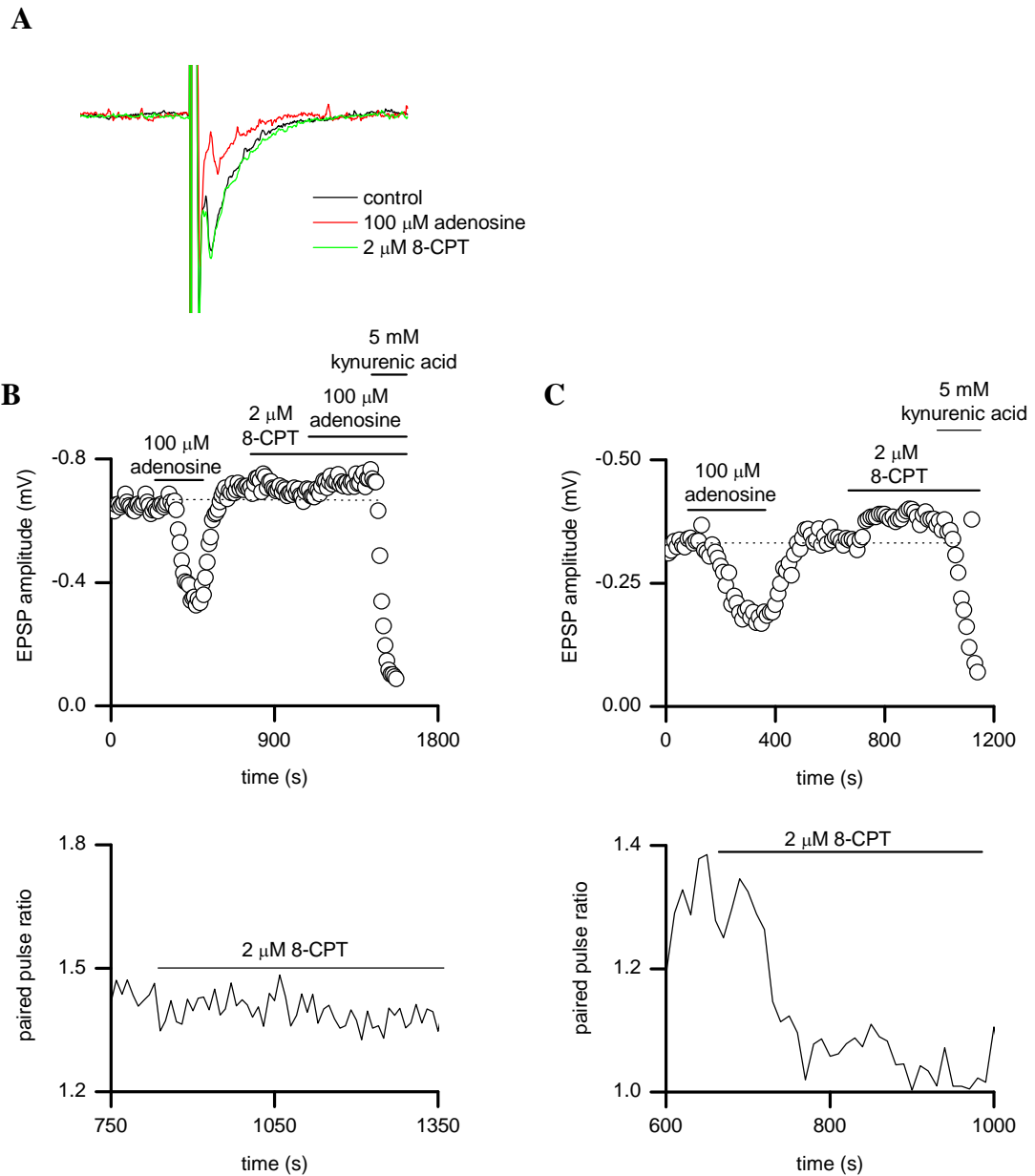
**Figure 5.1  Tonic activation of $A_1R$ is low or absent at immature parallel fibre-Purkinje cell synapses**

(A)  Superimposed averages of PF EPSPs from an immature cerebellar slice in control, adenosine (100 µM) and 8-CPT (2 µM).  (B)  Graphs plotting amplitude of individual EPSPs against time and PPR against time for the same experiment in an immature (P12) cerebellar slice.  Application of 8-CPT had little effect on EPSP amplitude or PPR.   Binding of 8-CPT to $A_1R$ was confirmed by no inhibition following application of adenosine in the presence of 8-CPT.  Identification of PF EPSPs was confirmed by inhibition with kynurenic acid (5 mM).  (C)  Graphs plotting amplitude of individual EPSPs against time and PPR against time for the same experiment in an immature slice (P12).  Application of 8-CPT enhanced EPSP amplitude slightly and decreased PPR indicating a small tonic activation of presynaptic inhibitory $A_1R$.
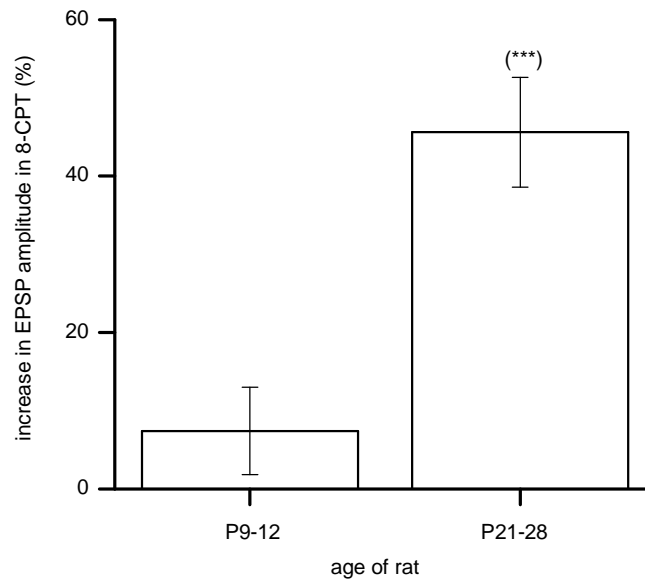
**Figure 5.2 Comparison of adenosine tone at immature and mature parallel fibre-Purkinje cell synapses**

Graph comparing the increase in PF EPSP amplitude resulting from application of 8-CPT (2 μM) to immature (P9-12, n = 20) and mature (P21-28, n = 8) cerebellar slices. The increase in EPSP amplitude at immature synapses (7.4 ± 5.6 %) was significantly less (p < 0.001) than that observed at mature synapses (45.6 ± 7.0 %).

## 5.3 The low adenosine tone in immature slices does not appear to result from changes in $A_1R$ expression or efficacy

The reduced adenosine tone at immature PF-PC synapses is unlikely to be the result of a low $A_1R$ expression as only slices where adenosine (100 µM) inhibited EPSP amplitude by at least 50 % were analysed. In addition the reduction in EPSP amplitude with adenosine (100 µM) was similar (70.5 ± 5.4 % and 68.5 ± 4.7 %) in the 9 immature slices where no inhibitory $A_1R$ tone was observed with 8-CPT and in the 11 immature slices where 8-CPT increased EPSP amplitude by 13.4 ± 2.6 % (figure 5.3A, B). Furthermore, the adenosine-mediated inhibition in immature slices with no $A_1R$ tone is also not significantly different to the inhibition seen with adenosine (61.5 ± 2.1 %) at mature synapses where EPSP amplitude was increased by 45.6 ± 7.0 % with 8-CPT (figure 5.3C).

It has previously been described how differences in $A_1R$-mediated inhibition in immature slices may be the result of a variable $A_1R$ efficacy (see Chapter 4). To confirm that the significantly reduced adenosine tone at immature PF-PC synapses in comparison to mature synapses is not due to a lower $A_1R$ efficacy, a log concentration-response curve for the non-hydrolysable $A_1R$ agonist $N^6$-cyclopentyladenosine (CPA) was generated at mature synapses and compared to the curve produced in earlier experiments for immature synapses with an adenosine-mediated inhibition greater than 50 % (figures 4.10, 5.4). The curves were almost identical suggesting that the lower inhibitory $A_1R$ tone at immature PF-PC synapses is unlikely to be the result of a lower $A_1R$ efficacy.

**no tone**

**A**

**tone**

**B**

**mature slices**

**C**
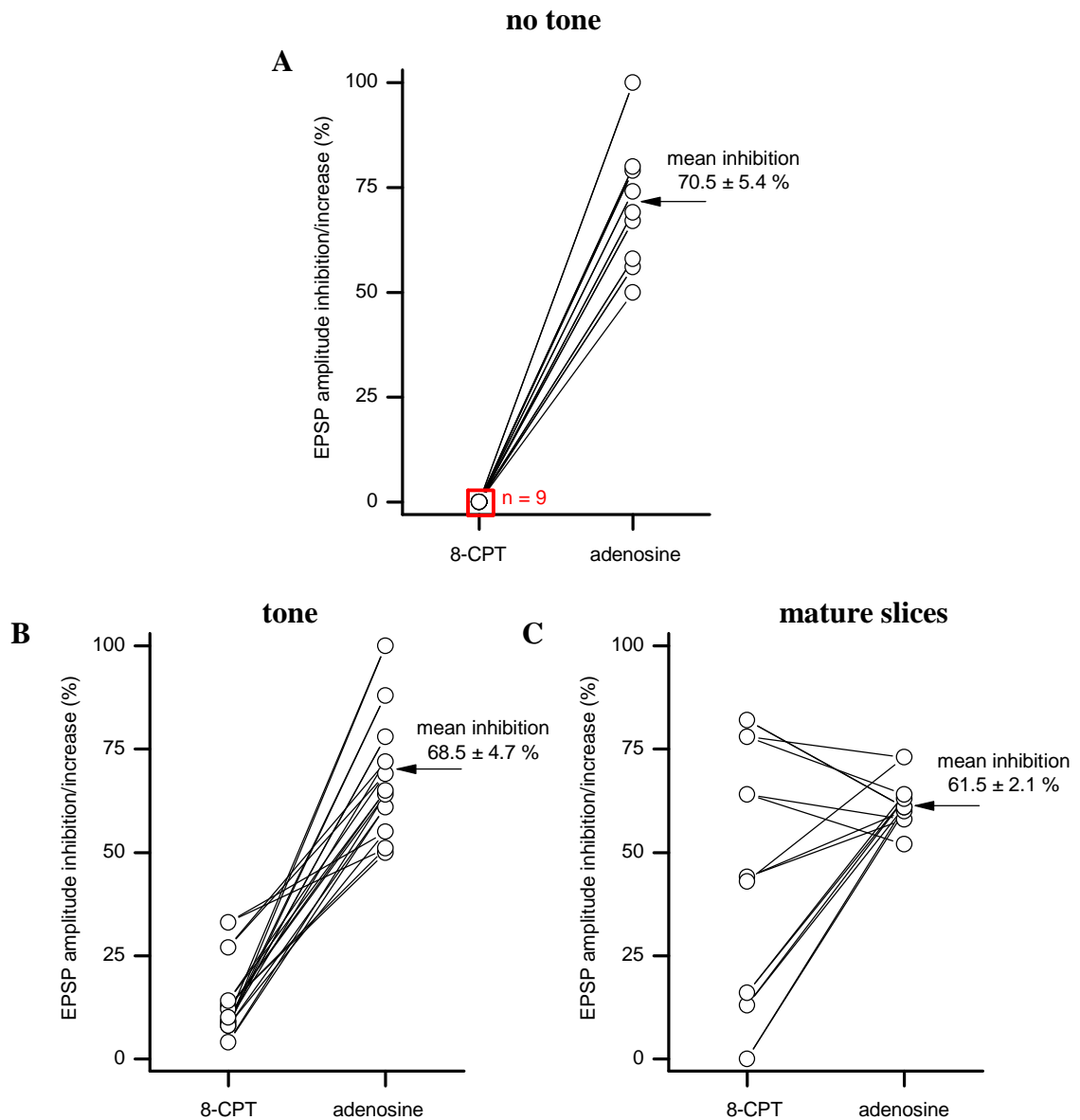
**Figure 5.3 A difference in A₁R expression does not appear to account for an absence in adenosine tone at immature synapses**

Graphs comparing EPSP amplitude reduction with adenosine (100 µM) and increase in EPSP amplitude following application of 8-CPT (2 µM) in cerebellar slices. There is no difference in the inhibition with adenosine (70.5 ± 5.4 %) in immature (P9-12) slices where no inhibitory A₁R tone was observed with 8-CPT (A) and the inhibition measured with adenosine (68.5 ± 4.7 %) in immature slices where 8-CPT increased EPSP amplitude by 13.4 ± 2.6 % (B). The adenosine-mediated inhibition in immature slices with no A₁R tone is also not significantly different to the inhibition seen with adenosine (61.5 ± 2.1 %) at mature synapses (P21-28) where EPSP amplitude was increased by 45.6 ± 7.0 % with 8-CPT (C).
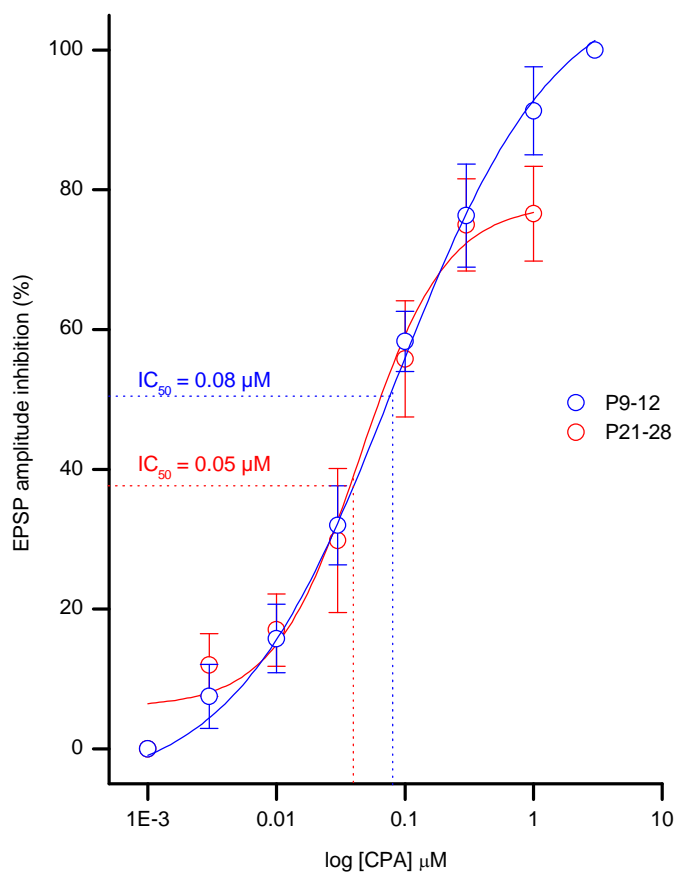
**Figure 5.4  A low adenosine tone at immature parallel fibre-Purkinje cell synapses does not appear to be due to a lower $A_1R$ efficacy**

Log concentration-response curves for the reduction in PF EPSP amplitude by the $A_1R$ agonist CPA (0.001 µM – 3 µM) in immature (P9-12, n = 6) and mature (P21-28, n = 5) cerebellar slices.  The curves and $IC_{50}$ values were similar for both age groups suggesting a minimal difference in $A_1R$ efficacy.

## 5.4 There is a low concentration of extracellular adenosine metabolites in immature slices

In the study using mature cerebellar slices (postnatal days 21-28) where an inhibitory $A_1R$ tone was indicated by an increase in EPSP amplitude with 8-CPT, microelectrode biosensors were placed into or above the slices to measure the extracellular concentration of adenosine and its metabolites (Wall, Atterbury et al. 2007). The biosensors measured a purine tone of inosine and hypoxanthine although the heterogeneous distribution of these metabolites resulted in the unreliable calculation of an adenosine concentration. The concentration of inosine and hypoxanthine could be lower in immature cerebellar slices if the low basal adenosine tone is due to a rapid uptake of adenosine or reduced adenosine release to the extracellular space. Alternatively, the concentration of inosine and hypoxanthine may be higher if the reduced $A_1R$ tone is the result of an enhanced metabolism of adenosine in the extracellular space.

The extracellular purine tone was measured using ADO biosensors containing the enzymes adenosine deaminase (ADA), purine nucleoside phosphorylase (PNP) and xanthine oxidase (XO) to detect adenosine, inosine and hypoxanthine and INO biosensors containing PNP and XO to detect inosine and hypoxanthine. In addition null sensors containing a matrix with no enzymes were used to control for non-specific electro-active interferents like 5-HT and noradrenaline.

For this study the biosensors were not inserted into the immature cerebellar slices thus eliminating the possibility that any signal detected was due to the release of

purines in response to tissue damage by the biosensors. Instead the extracellular purine tone was measured in a non-invasive way by moving the biosensors close to the surface of the slice over the molecular layer as done previously by Wall, Atterbury et al (2007). As in this previous study the biosensors were bent so that their longitudinal surface was parallel to the slice in order to increase the surface area close to the tissue thereby increasing the detection of an extracellular purine tone.

A small rapid increase of 43.4 ± 4.1 pA was detected when ADO biosensors were moved close to the surface of immature slices and a similar increase of 61.7 ± 18 pA was detected using INO biosensors (n = 15, figure 5.5). Following corrections for calibration (using 10 µM adenosine for ADO and 10 µM inosine for INO biosensors before and after each experiment) there was no significant difference between the current measured on either biosensor. As ADO biosensors detect adenosine, inosine and hypoxanthine and INO biosensors detect inosine and hypoxanthine it can be assumed that the small purine tone detected represents only inosine and hypoxanthine in the immature slices (Wall, Atterbury et al. 2007).

Using the assumption that all of the extracellular purine tone measured by the biosensors was inosine, the inosine concentration at the surface of immature slices was calculated using the calibration data (current measured at slice surface/current measured during calibration x concentration of inosine used in calibration).

The mean concentration of inosine at the immature slice surface was found to be 0.25 ± 0.03 µM compared to 1.6 ± 0.3 µM at the surface of mature cerebellar slices at postnatal days 21-28 (224.3 ± 35.9 pA increase in current, n = 8, figure 5.5). If the

135

low inhibitory $A_1R$ tone in immature slices was the result of an enhanced metabolism of extracellular adenosine in comparison to mature slices where an adenosine tone is present, a higher concentration of extracellular metabolites would have been expected (figure 5.6).
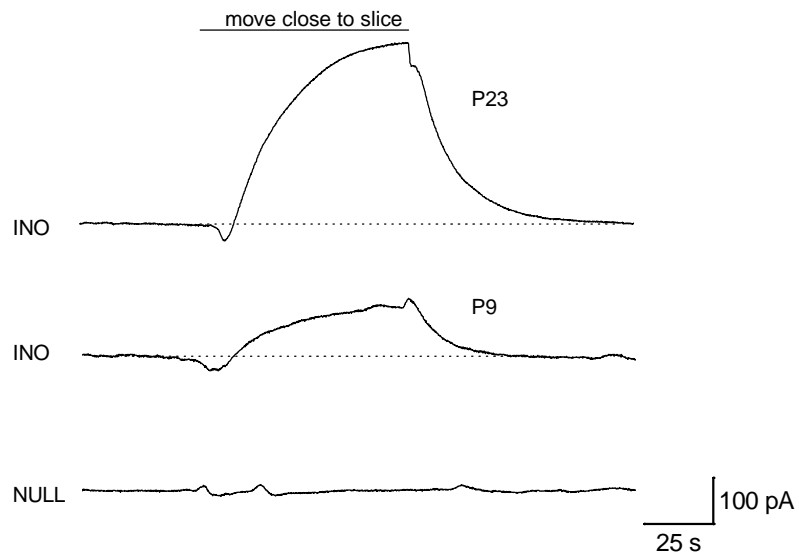
**Figure 5.5   There is a low concentration of extracellular adenosine metabolites in immature slices**

Example biosensor traces from experiments to measure the concentration of adenosine metabolites at the surface of immature (P9) and mature (P23) cerebellar slices.  The INO biosensor was moved close to the surface of the slices over the molecular layer.  A rapid increase in current of ~350 pA (P23) and ~100 pA (P9) was observed.  The null sensor showed no change in current when moved close to the surface of either slice (P23 illustrated).
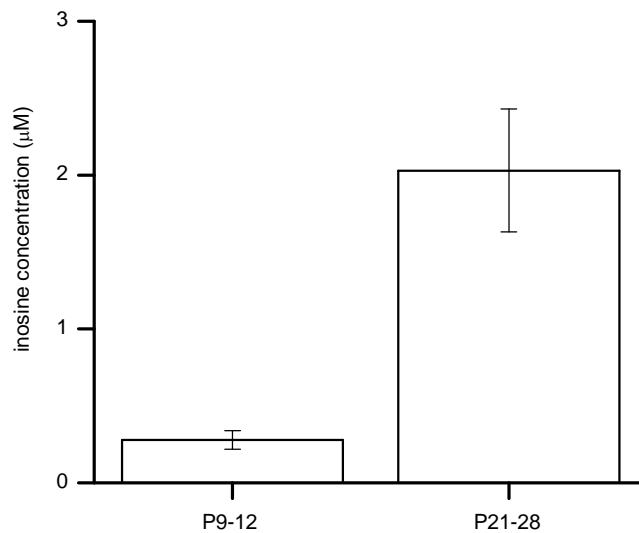
**Figure 5.6  The low inhibitory $A_1R$ tone in immature slices is unlikely to be the result of an enhanced metabolism of extracellular adenosine in comparison to mature slices**

The INO biosensor was moved close to the surface of immature (P9-12, n = 15) and mature (P21-28, n = 8) cerebellar slices over the molecular layer.  The mean concentration of inosine at the surface of immature slices was found to be 0.25 ± 0.03 µM compared to 1.6 ± 0.3 µM at the surface of mature slices.  The concentration assumes that all of the current arises from inosine and is determined following calibration of the biosensors.

## 5.5 Confirmation of a low extracellular adenosine metabolism in immature slices

The biosensor results suggest that the lack of an inhibitory $A_1R$ tone is unlikely to be the result of an enhanced metabolism of extracellular adenosine in immature cerebellar slices. To further investigate the role of the enzyme ectoADA that catalyses the deamination of adenosine to inosine, extracellular recordings of PF EPSPs were made in the presence of the ADA inhibitor erythro-9-(2-hydroxy-3-nonyl) adenine (EHNA) (Agarwal 1982). If ADA is active in immature slices its inhibition with EHNA should result in an increased extracellular concentration of adenosine and a reduction in EPSP amplitude via activation of presynaptic $A_1R$.

In immature slices application of EHNA (20 µM) inhibited synaptic transmission by only $1.2 \pm 1.6$ % (range 0 to 12 %, n = 5, figure 5.7) and did not significantly affect the PPR ($1.33 \pm 0.3$ to $1.34 \pm 0.3$). In the one slice where an EPSP amplitude reduction of 12 % was observed this could be reversed with application of 8-CPT (2 µM) in the presence of EHNA thus confirming an action of adenosine at presynaptic $A_1R$. Taken together with the INO biosensor data (figure 5.6), these results suggest that the action of ADA is unlikely to contribute to the low inhibitory $A_1R$ tone observed in immature slices. A small EPSP amplitude reduction of $1.2 \pm 0.7$ % was also observed in mature slices (n = 6, figure 5.14) and the activity of ADA was not found to be a major regulator of extracellular adenosine tone in a previous study using mature cerebellar slices (Wall, Atterbury et al. 2007).
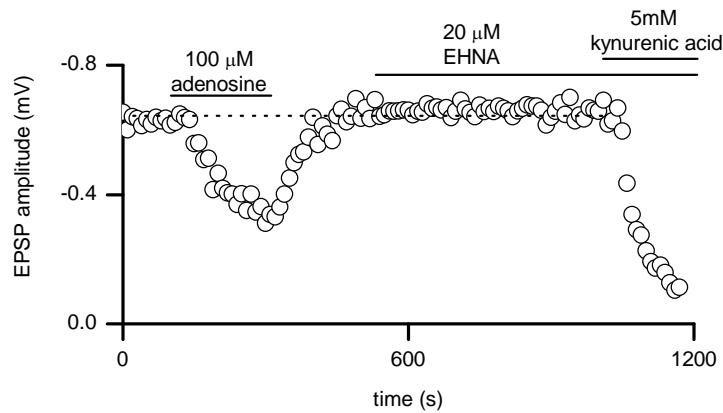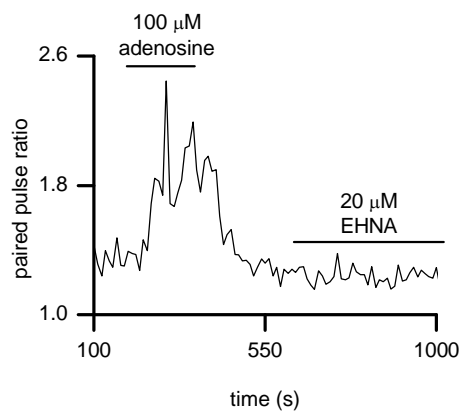
**Figure 5.7  Inhibition of adenosine deaminase has little effect on synaptic transmission in immature slices**

(A)  Graph plotting amplitude of individual EPSPs against time an immature (P12) cerebellar slice.  Although adenosine (100 µM) inhibited synaptic transmission by ~50 %, application of EHNA (20 µM) to block adenosine deaminase (ADA) activity had no effect on EPSP amplitude.  Identification of PF EPSPs was confirmed by inhibition with kynurenic acid (5mM).  (B)  Graph plotting PPR against time for the same experiment.  Application of adenosine increased PPR indicating activation of presynaptic inhibitory $A_1R$.  Inhibition of ADA with EHNA had no effect on PPR.

## 5.6 Inhibition of equilibrative transport has a variable effect on synaptic transmission in immature slices

If the reduced adenosine tone at immature PF-PC synapses is not the result of enhanced extracellular adenosine metabolism by ADA it may be due to the rapid transport of adenosine across neuronal or glial membranes by facilitated diffusion using the equilibrative transporters ENT1 or ENT2. The effect of these proteins has previously been found to be variable at mature rat PF-PC synapses (Wall, Atterbury et al. 2007) using 6-[(4-nitrobenzyl)thiol]-9-β-D-ribofuranosylpurine (NBTI) to inhibit ENT1 transporters and dipyridamole to inhibit both ENT1 and ENT2 proteins (Cass, Young et al. 1998). If the activity of ENT1 or ENT2 is enhanced in immature slices their inhibition with NBTI/dipyridamole should result in an increased extracellular concentration of adenosine and a reduction in EPSP amplitude via activation of presynaptic $A_1R$.

In immature slices application of NBTI (5 µM) and dipyridamole (10 µM) for 30 minutes inhibited EPSP amplitude by $16.9 \pm 3.5$ % (n = 31) although no effect on synaptic transmission was observed in 15 of these slices. In the 16 slices where inhibition was observed the mean reduction in EPSP amplitude was $32.7 \pm 4.0$ % with an increase in PPR from $1.4 \pm 0.05$ to $1.6 \pm 0.08$ (figure 5.8B) indicating the action of increased extracellular adenosine on presynaptic $A_1R$. To confirm activation of $A_1R$ the inhibition observed with NBTI/dipyridamole could be reversed with application of the $A_1R$ antagonist 8-CPT (2 µM, figure 5.8A). A similar reduction in EPSP amplitude of $37.5 \pm 6.9$ % was observed in 6 mature slices (figure 5.14) and the variability in response to application of NBTI/dipyridamole was similar

to that observed in a previous study using mature slices where EPSP amplitude was reduced by $47 \pm 8$ % in 9 out of 18 slices (Wall, Atterbury et al. 2007). There was no correlation between the reduction in EPSP amplitude with NBTI/dipyridamole and the absence of an inhibitory $A_1R$ tone in the immature slices.

Although previous experiments suggest that the activity of ADA is unlikely to be a major regulator of extracellular adenosine tone in immature slices, any increased extracellular adenosine resulting from the inhibition of equilibrative transporter proteins may be metabolised to inosine by ADA before activating presynaptic $A_1R$ at PF-PC synapses to inhibit synaptic transmission. If this is the case application of EHNA with NBTI/dipyridamole should result in a reduction in EPSP amplitude.

In immature slices NBTI (5 µM) and dipyridamole (10 µM) were applied for 30 minutes prior to the addition of EHNA (20 µM, n = 9). In 6 of the 9 slices neither application of NBTI/dipyridamole nor the addition of EHNA in the presence of NBTI/dipyridamole had an effect on synaptic transmission (figure 5.9A). In the remaining 3 slices NBTI/dipyridamole inhibited EPSP amplitude by $30.0 \pm 0.5$ % and application of EHNA in the presence of NBTI/dipyridamole produced a further inhibition of $27.0 \pm 3.0$ % (figure 5.9B) suggesting that some of the increased extracellular adenosine resulting from blockade of ENT1 and ENT2 was metabolised to inosine by ADA. To confirm activation of $A_1R$ the inhibition observed with NBTI/dipyridamole and EHNA could be reversed with application of the $A_1R$ antagonist 8-CPT (2 µM, figure 5.9B).

**Figure 5.8 Inhibition of equilibrative transport has little effect on synaptic transmission**

(A) Graph plotting amplitude of individual EPSPs against time in an immature (P12) cerebellar slice. Adenosine (100 µM) inhibited synaptic transmission by ~50 % and application of NBTI (5 µM) and dipyridamole (10 µM) to block equilibrative transport inhibited EPSP amplitude ~15 % and was reversed with application of 8-CPT (2 µM). Identification of PF EPSPs was confirmed by inhibition with kynurenic acid (5 mM). (B) Graph plotting PPR against time for the same experiment. Application of NBTI and dipyridamole increased PPR and application of 8-CPT at the same time decreased PPR indicating activation of presynaptic inhibitory $A_1R$.

**Figure 5.9 Some extracellular adenosine is metabolised when equilibrative transporter proteins are inhibited**

(A) Graph plotting amplitude of individual EPSPs against time in an immature (P12) cerebellar slice. Adenosine (100 µM) inhibited synaptic transmission by ~50 % but application of NBTI (5 µM) and dipyridamole (10 µM) to block equilibrative transport and EHNA (20 µM) in the presence of NBTI/dipyridamole had no effect on synaptic transmission. Identification of PF EPSPs was confirmed by inhibition with kynurenic acid (5mM) (B) Graph plotting amplitude of individual EPSPs against time an immature (P11) slice. Adenosine (100 µM) inhibited synaptic transmission by ~70 % and application of NBTI/dipyridamole inhibited EPSP amplitude by ~30%. EPSP amplitude was reduced further by ~15 % with EHNA in the presence of NBTI/dipyridamole. The block was reversed with application of 8-CPT (2 µM). Inset (red box area) illustrates that EPSP amplitude had stabilised prior to application of EHNA.

## 5.7 Inhibition of intracellular adenosine conversion has minor effects on the inhibitory adenosine tone in immature slices

It appears unlikely that the lack of an inhibitory $A_1R$ tone in immature slices is due to the rapid removal of adenosine from the extracellular space by metabolism to inosine with ADA or by facilitated transport via ENT1 or ENT2. It is possible that the low adenosine tone could be the result of enhanced intracellular phosphorylation of adenosine by adenosine kinase (AK) to form AMP thereby preventing adenosine efflux via equilibrative transporters (Boison 2006). If AK is active in immature slices its inhibition with iodotubericidin should increase the intracellular adenosine concentration resulting in the facilitative release of adenosine along its concentration gradient to the extracellular space via equilibrative transporter proteins and the subsequent reduction in EPSP amplitude via presynaptic $A_1R$ at PF-PC synapses (Latini and Pedata 2001).

In immature slices application of iodotubericidin (2 µM) inhibited EPSP amplitude by $25 \pm 3$ % and increased the PPR from $1.3 \pm 0.1$ to $1.5 \pm 0.1$ in 14 out of 21 (~67 %) slices indicating an action at presynaptic $A_1R$ at PF-PC synapses. Activation of $A_1R$ was confirmed by reversal of inhibition with the $A_1R$ antagonist 8-CPT (2 µM) (figure 5.10). In the remaining 7 slices iodotubericidin had no effect on synaptic transmission. The inhibition in synaptic transmission was significantly smaller and less reliable than that observed in mature slices ($51.0 \pm 2.0$ %, $p < 0.05$, n = 10, figure 5.14).

The increased extracellular adenosine resulting from the inhibition of AK may be metabolised to inosine by ADA before activating presynaptic $A_1R$ at PF-PC synapses to inhibit synaptic transmission. If this is the case application of EHNA with iodotubericidin should result in a greater reduction in EPSP amplitude than observed with iodotubericidin alone. In immature slices co-application of EHNA (20 µM) and iodotubericidin (2 µM) inhibited EPSP amplitude by $50.7 \pm 7.8$ % and increased PPR from $1.4 \pm 0.07$ to $1.6 \pm 0.1$ (n = 6, figure 5.11). The inhibition of synaptic transmission was significantly higher than that observed with iodotubericidin alone ($25 \pm 3$ %, $p < 0.05$) and could be reversed with application of 8-CPT (2 µM) to confirm activation of presynaptic $A_1R$. A similar reduction in EPSP amplitude of $54 \pm 3.5$ % following co-application of EHNA and iodotubericidin was also observed in mature slices (n = 3, figure 5.14).

To look at the effect of metabolism on the increased extracellular adenosine resulting from the inhibition of AK in more detail, iodotubericidin (2 µM) was applied to immature slices prior to co-application of iodotubercidin and EHNA (20 µM). Application of EHNA had little or no effect on synaptic transmission in 3 slices (figure 5.12A) but inhibited EPSP amplitude by $47.6 \pm 4.2$ % in another 4 slices (figure 5.12 B).

To investigate whether the equilibrative transporters facilitate any increase in extracellular adenosine during the inhibition of AK by iodotubericidin, the transporter proteins ENT1 and ENT2 were blocked with application of NBTI/dipyridamole prior to application of iodotubericidin in immature slices. In 4 out of 10 slices neither application of NBTI (5 µM) and dipyridamole (10 µM) nor

application of iodotubericidin (2 µM) in the presence of NBTI/dipyridamole had an effect on synaptic transmission suggesting that there was little or no transport of adenosine via equilibrative proteins in these slices (figure 5.13A). In the remaining 6 slices the inhibition resulting from AK block was not prevented by prior application of NBTI/dipyridamole and EPSP amplitude was still inhibited by $25.3 \pm 3.5$ % with iodotubericidin (figure 5.13B).

In mature cerebellar slices effective block of equilibrative transporters by NBTI/dipyridamole to prevent the efflux of an increased intracellular adenosine concentration due to inhibition of AK by iodotubericidin was only observed in 4 out of 8 slices suggesting a heterogeneous distribution of NBTI/dipyridamole-sensitive transporters at PF-PC synapses (Wall, Atterbury et al. 2007).

**A**



**B**
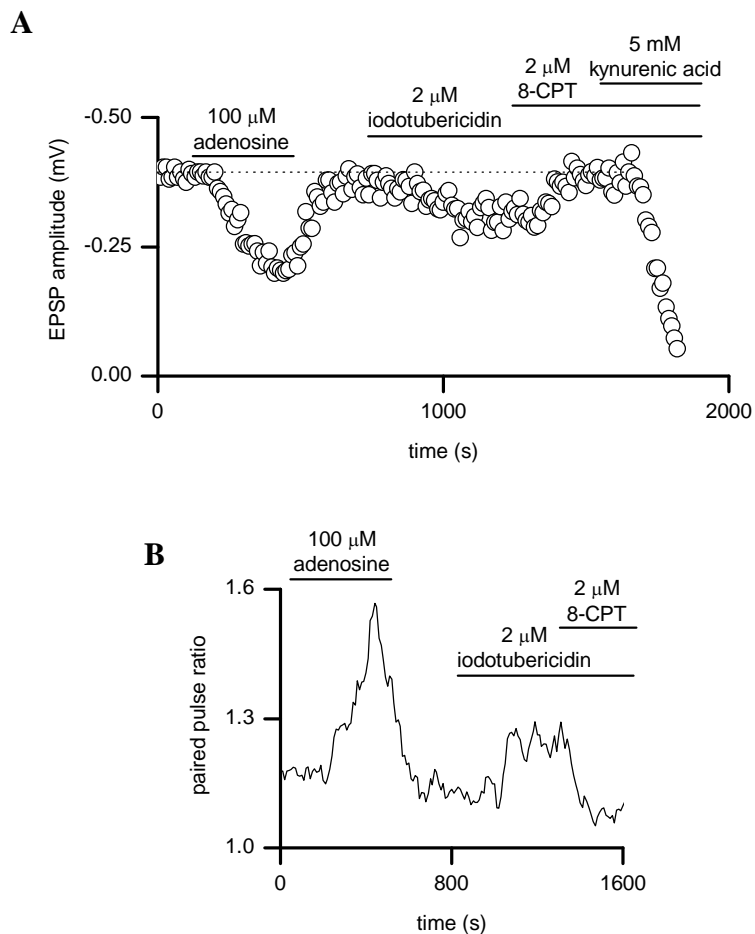
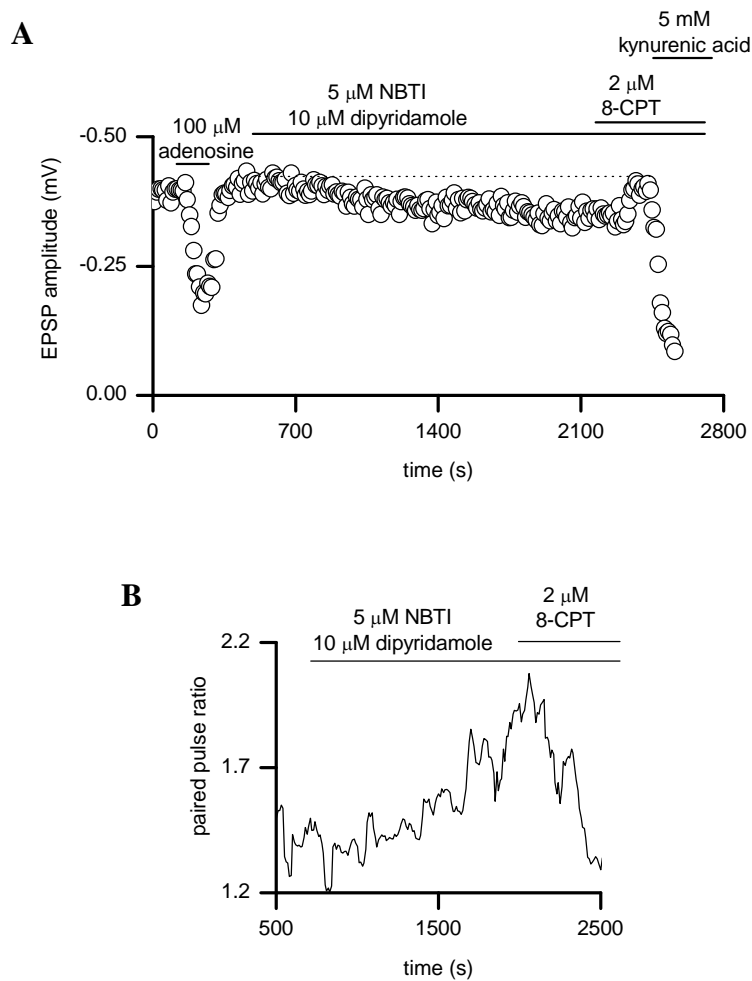**Figure 5.10 Inhibition of adenosine kinase has minor effects on synaptic transmission**

(A) Graph plotting amplitude of individual EPSPs against time in an immature (P10) cerebellar slice. Adenosine (100 µM) inhibited synaptic transmission by ~50 % and application of iodotubericidin (2 µM) to block adenosine kinase inhibited EPSP amplitude by ~30 % and was reversed with application of 8-CPT (2 µM). Identification of PF EPSPs was confirmed by inhibition with kynurenic acid (5 mM). (B) Graph plotting PPR against time for the same experiment. Application of iodotubericidin increased PPR and application of 8-CPT at the same time decreased PPR indicating activation of presynaptic inhibitory $A_1R$.
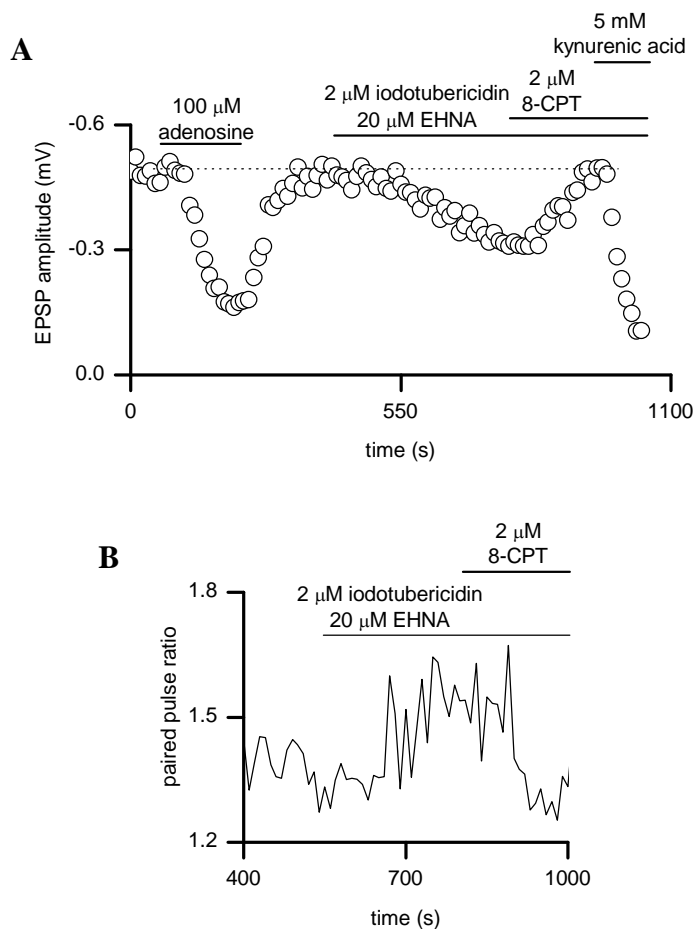
**Figure 5.11 Inhibition of adenosine kinase and adenosine deaminase inhibits synaptic transmission in some immature slices**

(A)  Graph plotting amplitude of individual EPSPs against time in an immature (P12) cerebellar slice.  Adenosine (100 µM) inhibited synaptic transmission by ~80 % and application of iodotubericidin (2 µM) with EHNA (20 µM) to block adenosine kinase and adenosine deaminase inhibited EPSP amplitude by ~50 % and was reversed with application of 8-CPT (2 µM).   Identification of PF EPSPs was confirmed by inhibition with kynurenic acid (5mM).   (B)   Graph plotting PPR against time for the same experiment.  Application of iodotubericidin and EHNA increased PPR and application of 8-CPT at the same time decreased PPR indicating activation of presynaptic inhibitory $A_1R$.
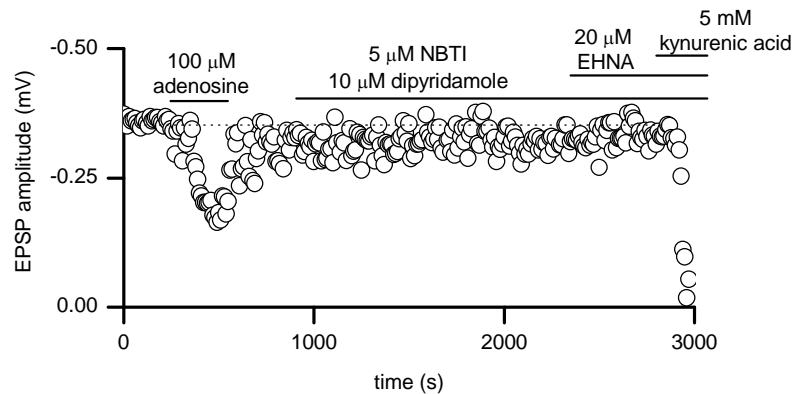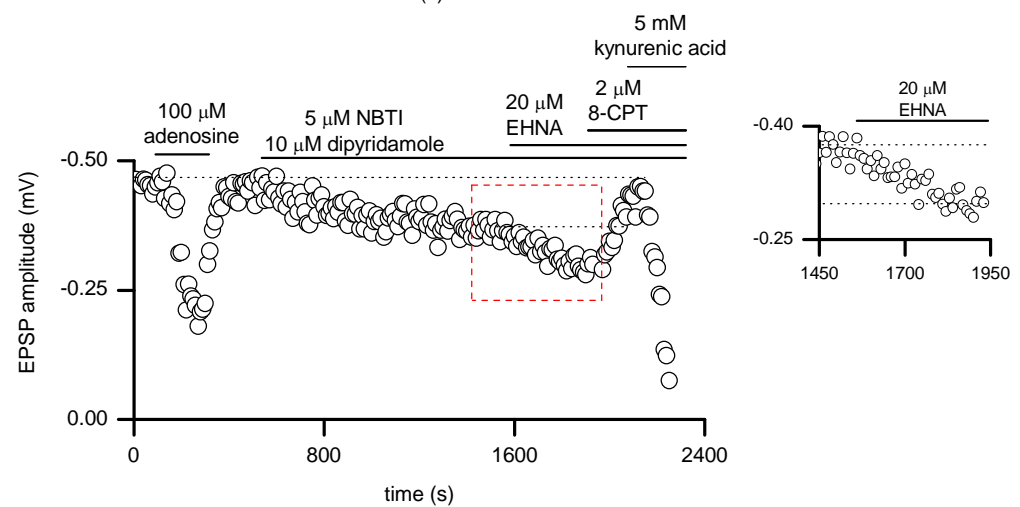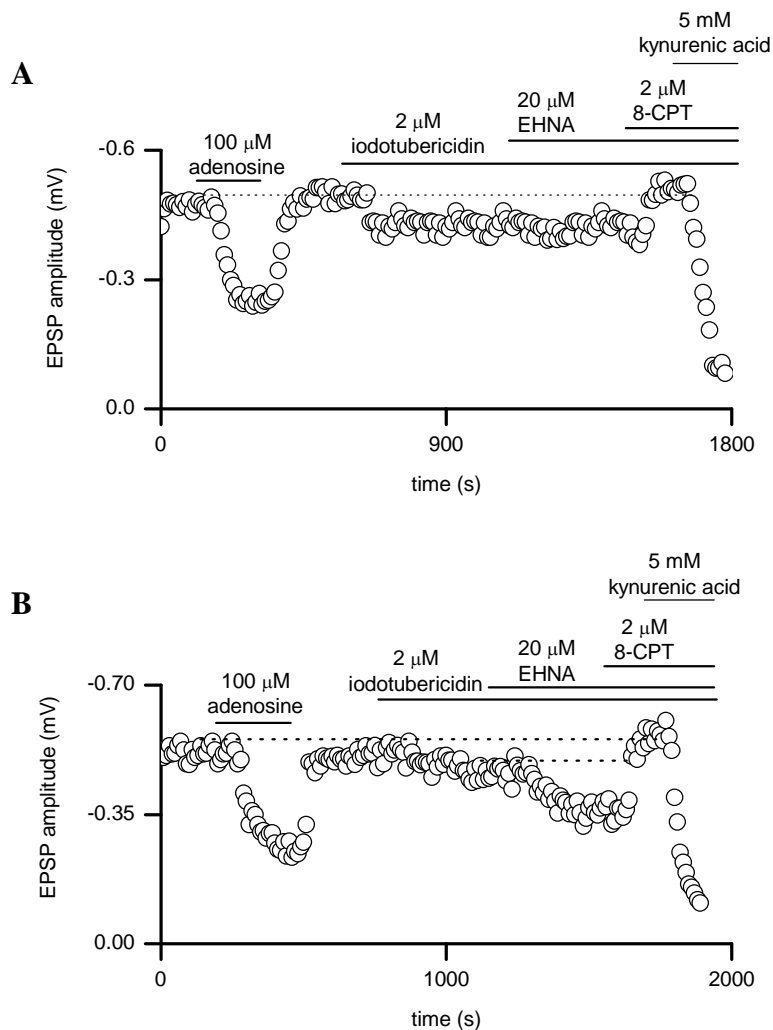
**Figure 5.12 Inhibition of adenosine kinase and adenosine deaminase in immature slices**

(A) Graph plotting amplitude of individual EPSPs against time in an immature (P12) cerebellar slice. Adenosine (100 μM) inhibited synaptic transmission by ~50 % and application of iodotubericidin (2 μM) to block adenosine kinase inhibited EPSP amplitude by ~20 %. Co-application of EHNA (20 μM) with iodotubericidin did not increase the block which was reversed with application of 8-CPT (2 μM). Identification of PF EPSPs was confirmed by inhibition with kynurenic acid (5mM). (B) Graph plotting amplitude of individual EPSPs against time an immature (P12) slice. Application of iodotubericidin inhibited EPSP amplitude by ~15 %. Co-application of EHNA with iodotubericidin produced a marked increase in EPSP amplitude reduction which was reversed with application of 8-CPT.
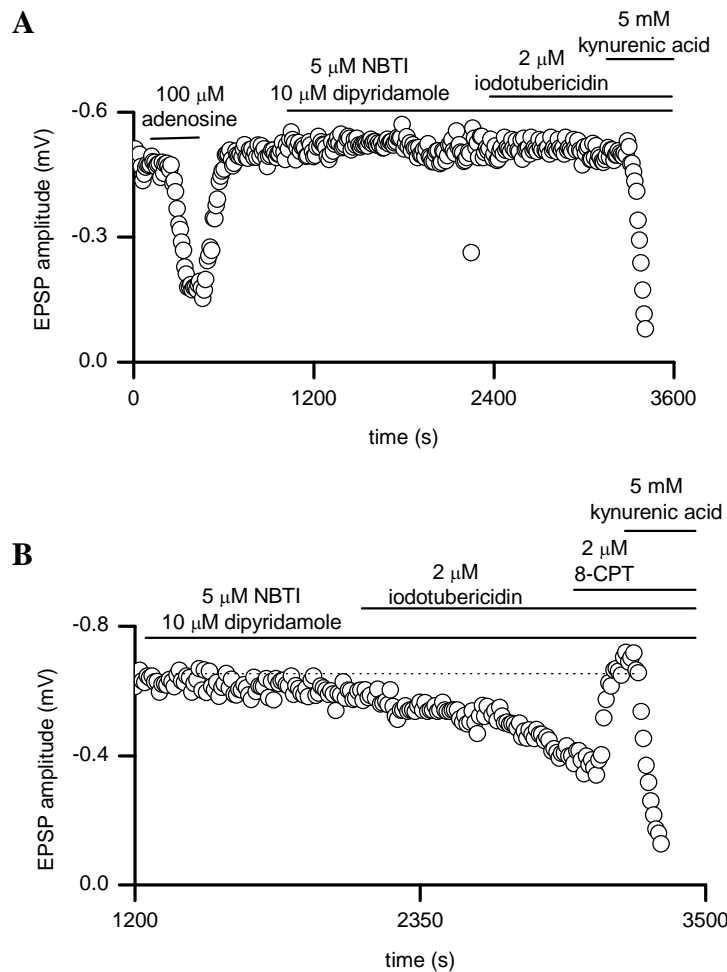
**Figure 5.13 Inhibition of equilibrative transporters had a variable effect on the effect of iodotubericidin in immature slices**

(A) Graph plotting amplitude of individual EPSPs against time in an immature (P9) cerebellar slice. Adenosine (100 µM) inhibited synaptic transmission by ~80 % and application of NBTI (5 µM) and dipyridamole (10 µM) to block equilibrative transporters had no effect. Co-application of iodotubericidin (2 µM) with NBTI/dipyridamole also had no effect on EPSP amplitude. Identification of PF EPSPs was confirmed by inhibition with kynurenic acid (5mM). (B) Graph plotting amplitude of individual EPSPs against time an immature (P12) slice. Pre-incubation with NBTI/dipyridamole (not illustrated) did not prevent inhibition with iodotubericidin. The block was reversed with application of 8-CPT (2 µM) demonstrating activation of presynaptic $A_1R$.
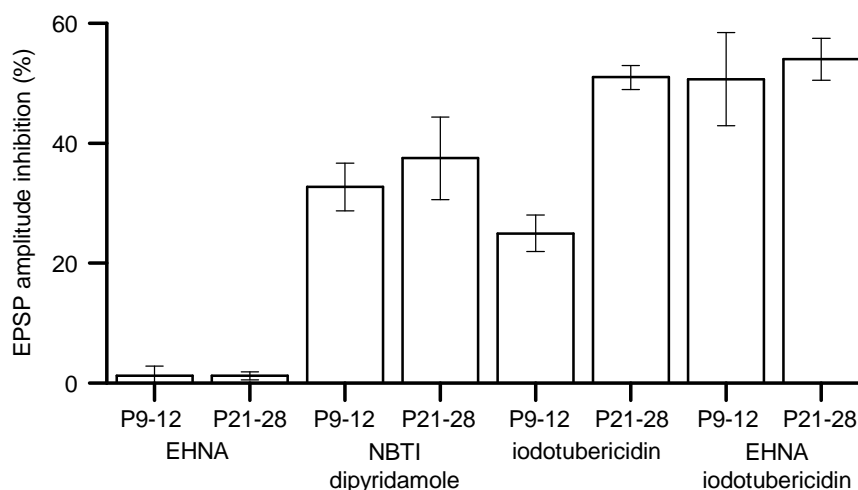
**Figure 5.14 Comparison of the effects of interrupting adenosine clearance at immature and mature parallel fibre-Purkinje cell synapses**

Graph comparing the inhibition of PF EPSP amplitude resulting from application of EHNA (20 µM) to immature (P9-12, n = 5) and mature (P21-28, n = 6) cerebellar slices, NBTI (5 µM) and dipyridamole (10 µM) to immature (n = 16) and mature (n = 6) slices, iodotubericidin (2 µM) to immature (n = 14) and mature (n = 10) slices and co-application of EHNA and iodotubericidin to immature (n = 6) and mature (n =3) slices where application of adenosine (100 µM) inhibited synaptic transmission by at least 50 %. ANOVA shows no significant difference between the groups (p = 0.89).

## 5.8 Adenosine release is delayed and slower at immature parallel fibre-Purkinje cell synapses during hypoxia

These results demonstrate that the tonic inhibition of PF-PC synapses by endogenous adenosine is greatly reduced or absent in immature cerebellar slices and that blocking the clearance of adenosine via metabolism or equilibrative transporters has little effect on the inhibitory tone. As this suggests that there is little release of adenosine under basal conditions, hypoxia and electrical stimulation were used to investigate the active release of adenosine in immature slices.

A 10 min period of hypoxia in immature slices reduced PF EPSP amplitude by $64 \pm 7$ % at steady state and increased PPR from $1.25 \pm 0.04$ to $1.8 \pm 0.1$ suggesting activation of $A_1R$ (n = 11). This was confirmed by reversal of inhibition with application of the $A_1R$ antagonist 8-CPT (2 µM, figure 5.15A). As an indication of the speed of increase in extracellular adenosine concentration during hypoxia the delay until the start of EPSP amplitude reduction was $3.7 \pm 0.6$ min with a steady state reached after $5.4 \pm 0.7$ min from the start of hypoxia. Re-oxygenation reversed the inhibition after $5.3 \pm 0.5$ min (n = 8).

A 10 min period of hypoxia in mature slices (P21-28) rapidly reduced PF EPSP amplitude by $81.3 \pm 6.6$ % at steady state although this could only be reversed with application of 8-CPT in 2 out of 5 slices. This is unlikely to indicate a mechanism of inhibition other than via presynaptic $A_1R$ as reversal of EPSP amplitude depression ($73.0 \pm 5.4$ %) was observed in 6 out of 8 slices following a shorter period of hypoxia (5 min, figure 5.15B). In slices where reversal of inhibition was observed

with 8-CPT, the speed of increase in extracellular adenosine to a steady state was double that measured in immature slices ($2.3 \pm 0.3$ min, n = 8) with a delay until the start of EPSP amplitude reduction of only $1.1 \pm 0.4$ min.

The purine release during hypoxia was measured with ADO, INO and null biosensors held over the molecular layer close to the slice surface. As previously described the biosensors were bent so that their longitudinal surface was parallel to the surface of the slice. A 10 min period of hypoxia produced a large current on ADO and INO biosensors in both immature and mature slices resulting from the release of purines as no current change was observed on the null biosensors (figure 5.16). Following corrections for calibration (using 10 µM adenosine for ADO and 10 µM inosine for INO biosensors before and after each experiment) there was no significant difference between the current measured on either biosensor in terms of rise or amplitude. As ADO biosensors detect adenosine, inosine and hypoxanthine and INO biosensors detect inosine and hypoxanthine it can be assumed that the biosensors detected the adenosine metabolites inosine and hypoxanthine.

Using the assumption that the all of the purine release measured by the biosensors was inosine, the maximum inosine concentration at the slice surface following hypoxia was calculated using the calibration data (current measured at slice surface/current measured during calibration x concentration of inosine used in calibration). The mean maximum concentration of inosine at the surface of mature slices was found to be significantly greater ($5.5 \pm 0.7$ µM, $p > 0.05$, n = 8) than at immature cerebellar slices ($3.5 \pm 0.4$ µM, n = 8). The bath inflow and outflow speeds were exactly the same for mature and immature slices so this difference is

154

most likely to be due to the greater delay in the start of purine release and slower rise in purine concentration resulting in the sensor current not reaching steady state after 10 mins of hypoxia in all 8 immature slices but reaching a plateau after $5.3 \pm 0.5$ min in the mature slices (figure 5.16). It is possible that adenosine release is delayed in immature slices due to better maintenance of ATP levels. The peak of ATP release during ischemia is smaller and delayed in hippocampal slices from younger rats (Frenguelli, Wigmore et al. 2007).
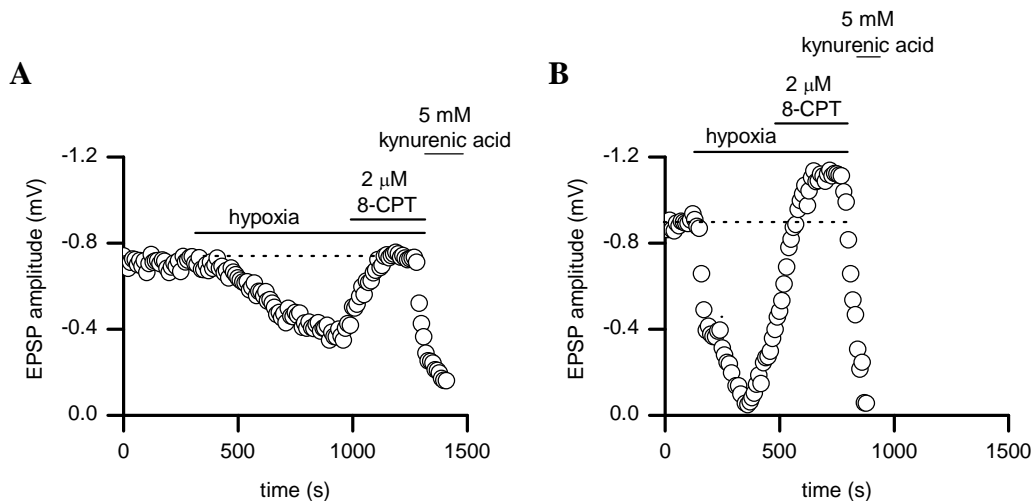
**Figure 5.15 Inhibition is delayed or reduced during hypoxia in immature slices**

(A) Graph plotting amplitude of individual EPSPs against time in an immature (P11) cerebellar slice during perfusion with aCSF bubbled with $N_2$ (95 %)-$CO_2$ (5 %) for 10 min. Hypoxia caused a slow reduction in EPSP amplitude of ~45 % which was reversed with the antagonist 8-CPT demonstrating activation of presynaptic $A_1R$. Identification of PF EPSPs was confirmed by inhibition with kynurenic acid (5 mM). (B) Graph plotting amplitude of individual EPSPs against time for the same experiment in a mature (P22) slice. The reduction in EPSP amplitude was larger and more rapid than in the immature slice. Inhibition was reversed with 8-CPT to an EPSP amplitude higher than in control due to the presence of an inhibitory $A_1R$ tone at PF-PC synapses.

**A**



**B**
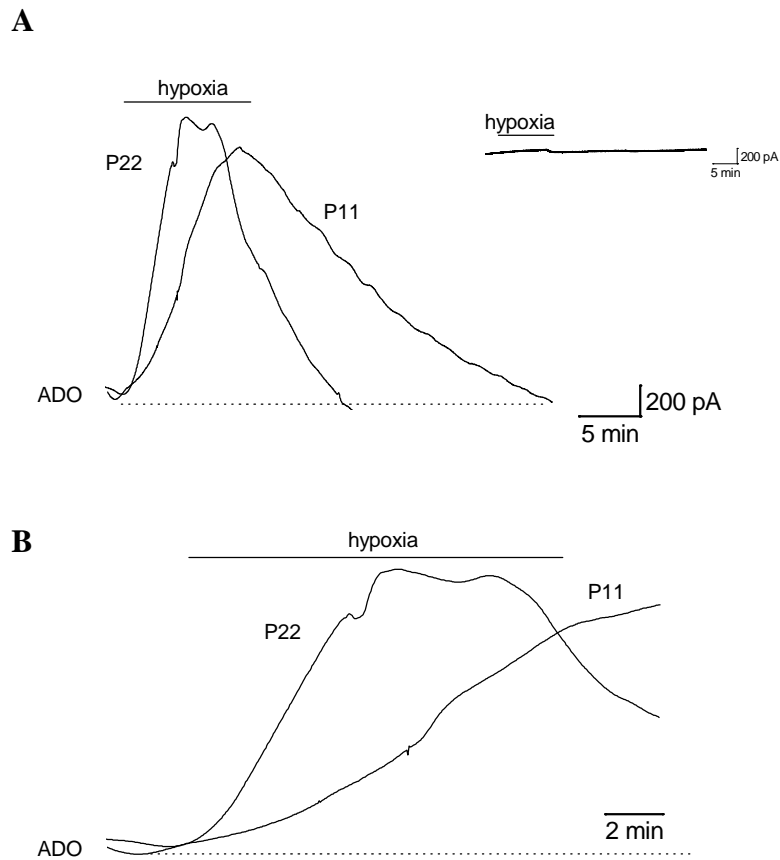


**Figure 5.16 Release of adenosine is delayed or reduced during hypoxia in immature slices**

Example ADO biosensor traces from experiments to measure the concentration of adenosine metabolites at the surface of immature (P11) and mature (P22) cerebellar slices during perfusion with aCSF bubbled with $N_2$ (95 %)-$CO_2$ (5 %) for 10 min. (A) Hypoxia caused an increase in extracellular purine concentration for both slices. The null sensor showed no change in current when moved close to the surface of either slice (P22 illustrated). (B) Traces from A expanded to show the greater delay in the start of purine release and slower rise in purine concentration during hypoxia in the immature slice.

## 5.9 Trains of activity do not release adenosine at immature parallel fibre-Purkinje cell synapses

During trains of stimuli (30 EPSPs, 20 Hz) transmission in slices from immature rats was facilitated and then depressed (n = 6, figure 5.17). The PF EPSP amplitude was increased to a maximum of 155 ± 8.0 % of the first EPSP amplitude at around the 14th EPSP and then decreased to approximately the same level as the first EPSP amplitude by the 30th EPSP. In subsequent experiments by Mark Wall measuring 100 EPSPs (20 Hz) rather than 30 in immature slices, the EPSP amplitude was facilitated in a similar way (maximum of 157 ± 10.9 % by the 10th EPSP) and was found to decrease to an amplitude less than the 1st EPSP amplitude by around the 70th EPSP (Atterbury and Wall 2009). An earlier study described a peak enhancement of EPSP amplitude relative to the first EPSP of up to 250 % in immature cerebellar slices during trains of activity at 50 Hz (Kreitzer and Regehr 2000).

Application of the $A_1R$ antagonist 8-CPT relieves the inhibition of EPSC amplitude at the Calyx of Held synapse observed during repetitive stimulation in rat brainstem slices. This suggests that endogenous adenosine inhibits EPSCs via activation of presynaptic $A_1R$ during high frequency activity to change the probability of release thus limiting transmitter depletion and allowing synaptic transmission to be maintained during trains of stimuli (Kimura, Saitoh et al. 2003). It has previously been described that adenosine that has been formed intracellularly may be released into the extracellular space of mature cerebellar slices in a neuronal activity-dependent manner (Wall and Dale 2007). As little or no adenosine tone is present at immature PF-PC synapses if the trains of stimuli applied to the immature slices had

resulted in an activation of presynaptic $A_1R$ due to a direct release of adenosine it would be expected that application of 8-CPT would have an effect on the facilitation and depression of EPSP amplitudes recorded.

Application of 8-CPT (2 µM) to block $A_1R$ during trains of stimuli (30 EPSPs, 20 Hz) had no significant effect on the amplitude of EPSPs. The PF EPSP amplitude was initially facilitated to a maximum of 157 ± 12.2 % of the first EPSP amplitude at around the 16th EPSP and then decreased to approximately the same level as the first EPSP amplitude by the 30th EPSP (figure 5.17). Subsequent experiments by Mark Wall measuring the effect of 8-CPT (2 µM) during trains of stimuli of 100 EPSPs (20 Hz) also demonstrated no significant effect of $A_1R$ blockade during EPSP facilitation and depression (Atterbury and Wall 2009). In addition to confirming an absence of adenosine tone these results also indicate that there is no significant adenosine release during trains of stimuli in immature slices.

ADO, INO and null biosensors placed over the molecular layer close to the slice surface were used to confirm that no adenosine was released during trains of electrical stimuli in immature slices. The response of the null sensor and ADO/INO sensors were indistinguishable even with prolonged high frequency stimulation in the molecular layer of immature slices (200 stimuli, 20-40 Hz, n = 15). In comparison, trains of stimuli (200 stimuli, 20 Hz) in mature slices produced a current on an ADO biosensor in 4 out of 4 slices (figure 5.18). This is comparable to the previously reported reliable activity-dependent release of adenosine at parallel fibre-Purkinje cell synapses in mature rats (Wall and Dale 2007).
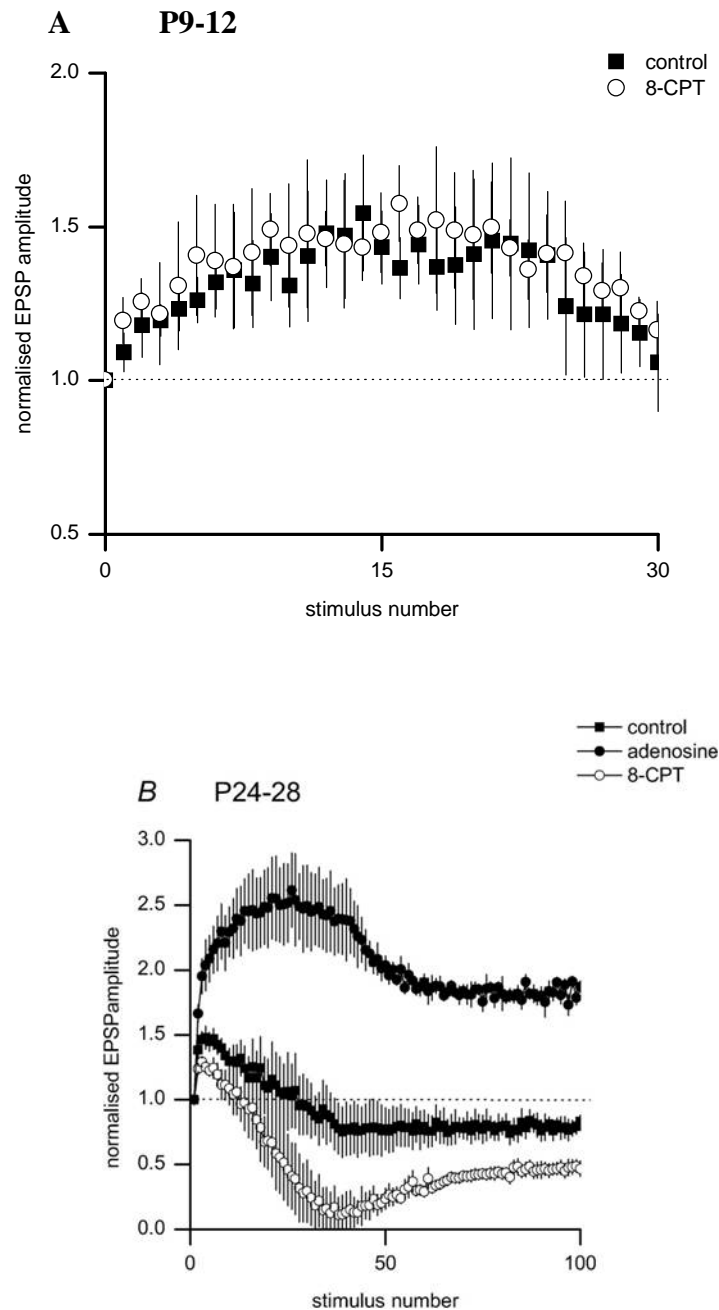
**Figure 5.17 Blocking A₁R has no significant effect on synaptic transmission during trains of activity in immature slices**

(A) A graph plotting normalised EPSP amplitude (relative to first EPSP amplitude) against stimulus number in control and 8-CPT (2 μM) during trains of activity (20 Hz) at immature (P9-12) PF-PC synapses (n = 6). (B) A graph using data from Mark Wall (Atterbury and Wall 2009) for comparison with (A) plotting normalised EPSP amplitude (relative to first EPSP amplitude) against stimulus number in control, adenosine (100 μM) and 8-CPT (2 μM) during trains of activity (20 Hz) at mature (P24-28) PF-PC synapses (n = 5). Addition of adenosine (100 μM) caused a marked increase in the degree of facilitation. Addition of 8-CPT (2 μM) caused a small reduction in facilitation followed by almost complete depression of transmission of EPSP amplitude and then recovery to ~50 % of the first EPSP.

160
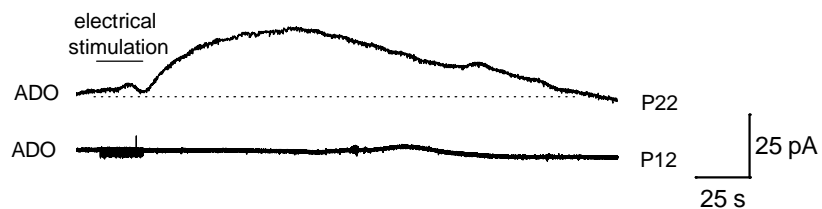
**Figure 5.18 Trains of activity do not release adenosine at immature parallel fibre-Purkinje cell synapses**

Example ADO biosensor traces from experiments to measure the release of adenosine metabolites at the surface of immature (P12) and mature (P22) cerebellar slices during trains of activity. Electrical stimulation (bar, 20 Hz) caused an increase in extracellular purine concentration in a mature slice but no detectable release in a P12 slice.

## 5.10 Summary

The effect of the $A_1R$ antagonist 8-CPT on PF EPSP amplitude was investigated in immature rat cerebellar slices at postnatal days 9-12. Application of 8-CPT had a significantly smaller effect on EPSP amplitude than in mature slices and suggested that an inhibitory adenosine tone is low or absent at this stage of development.

The reduced adenosine tone at immature synapses is unlikely to be the result of a low $A_1R$ expression as only slices where adenosine inhibited synaptic transmission were used. A log concentration-response curve generated for the $A_1R$ agonist CPA in immature slices was very similar to that generated in mature slices suggesting that the low adenosine tone is also not due to developmental differences in $A_1R$ efficacy.

Inhibition of adenosine clearance via adenosine deaminase, adenosine kinase and equilibrative transporters had little effect on synaptic transmission suggesting that little adenosine is moving between the intracellular and extracellular spaces under basal conditions. Active adenosine release measured by EPSP amplitude reduction and microelectrode biosensors could be stimulated with hypoxia in immature slices but this was delayed and slower in comparison to the release observed in mature slices. Adenosine could not be actively released at immature PF-PC synapses in response to electrical stimulation in the molecular layer.

# Chapter 6    Discussion

## 6.1    The presence and distribution of $A_1R$ and $A_{2A}R$ in the rat cerebellum at different stages of development

### 6.1.1  Summary of key findings

- $A_1R$ and mGluR4 are widely distributed across Purkinje cell bodies and their dendrites and within the granule layer of the cerebellum throughout postnatal development.

- There is only minor co-localisation of $A_1R$ and mGluR4 with glial cell bodies or their processes, eliminating their involvement in the staining observed.

- $A_{2A}R$ are widely distributed within cerebellar slices with co-localisation identical to that of $A_1R$.  A role for $A_{2A}R$ has not previously been described within the cerebellum.

### 6.1.2  Confirmation of antibody specificity

Immunohistochemistry revealed punctate staining for $A_1R$ (1:100) only in those CHO cells expressing GFP with no obvious background staining (figure 3.2). Although this result provides a control for specificity of the $A_1R$ primary antibody, it

only confirms that the $A_1R$ antibody does not bind non-specifically to any native CHO cell proteins in a well containing only CHO cells. It should therefore not be assumed that all staining observed with this antibody in cerebellar slices is specific, as cerebellar slices are densely packed with many cell types expressing different proteins that the $A_1R$ antibody may recognise.

In the CHO cell control experiments not all of the cells expressing GFP were stained for $A_1R$. This could be because the affinity of the $A_1R$ antibody may be low or the secondary antibody binding may not be optimal. Alternatively, the Triton X100 concentration may be too low for complete permeabilisation of the CHO cells, in order to access the intracellular C-terminal of the $A_1R$ for antibody binding although this seems unlikely as the concentration of Triton X100 was quite high (0.4 %).

No primary antibody specificity controls were conducted during this study for $A_{2A}R$ or mGluR4 primary antibodies in CHO cells although the manufacturer's information for each states that these antibodies have been tested for specificity in rat tissue using Western blot. Sufficient controls for secondary antibody specificity and cross-over reactions have been carried out in this study (figure 3.12, 3.13).

### 6.1.3 Interpretation of the immunofluorescence for $A_1R$, mGluR4 and $A_{2A}R$ in mature and immature cerebellar slices

Although immunofluorescence could be replicated using an alternative protocol, care should be taken in the interpretation of the immunohistochemistry in this study for the reasons outlined below.

Both immature (P8-14) and mature (P21-28) cerebellar slices showed co-localisation for $A_1R$ and mGluR4 across a large number of Purkinje cell bodies (figures 3.3, 3.4). Dense staining for $A_1R$ at Purkinje cell bodies is unusual as many electrophysiological studies describe the modulation of Purkinje cell activity via activation of presynaptic $A_1R$ (Burnstock 2006) but none suggest the presence of $A_1R$ on Purkinje cell bodies. There is also no reported electrophysiological evidence for the presence of mGluR4 at Purkinje cell bodies and previous immunoreactivity studies also indicate no such co-localisation (Kinoshita, Ohishi et al. 1996; Mateos, Azkue et al. 1998).

Triple immunohistochemistry with GFAP eliminated the possibility of the presence of these receptors on Bergmann glial cell bodies overlapping Purkinje cell bodies (figure 3.7). However, an earlier immunohistochemical study explained the very light $A_1R$ staining of Purkinje cell bodies as the result of $A_1R$ expression on basket cell processes that synapse with Purkinje cell bodies (Rivkees, Price et al. 1995). It is possible that $A_1R$ on basket cell processes enveloping Purkinje cell bodies would account for some but not all of the staining observed in this study as many cells are densely stained. There is also no evidence for the presence of mGluR4 on basket

cell processes so mGluR4 staining at Purkinje cell bodies is unlikely to be explained in the same way.

The difference in Purkinje cell body staining between studies may be the result of different fixation and staining methodologies. The Rivkees study fixed brain tissue in-situ by perfusion with 5 % paraformaldehyde (PFA) in contrast to this study which fixed isolated brain tissue with 4 % PFA. Similarly, the previous mGluR4 immunoreactivity studies fixed brain tissue in situ by perfusion with 4 % PFA (Kinoshita, Ohishi et al. 1996; Mateos, Azkue et al. 1998). Both PFA concentration and fixation via perfusion have been reported to impact on antibody affinity and selectivity (Fritschy 2008). The difference in the intensity of Purkinje cell body staining may alternatively be due to the sensitivity of alternative detection methods to immunofluorescence. The Rivkees $A_1R$ study used peroxidise anti-peroxidise (PAP)/3,3' diaminobenzidine (DAB) detection and the two mGluR4 studies used an alkaline phosphatase-labelled secondary antibody and an immunogold labelling method.

The dense $A_1R$ staining of rat Purkinje cell bodies is comparable with that of another immunofluorescence study using a different $A_1R$ antibody that is generated in mice (Yoshioka, Hosoda et al. 2002), suggesting that the staining observed in this study is not specific to the particular $A_1R$ antibody used. The possibility of yielding false-positive results within brain tissue when using concentrations of Triton X100 greater than 0.1 – 0.2 % (Weruaga, Alonso et al. 1998) may explain the dense Purkinje cell body staining observed in this study (0.4 % Triton X100) and the Yoshioka study (0.5 % Triton X100) but not in the earlier $A_1R$ study (Rivkees, Price et al. 1995)

166

(0.02 % Triton) or the mGluR4 immunoreactivity studies (Kinoshita, Ohishi et al. 1996; Mateos, Azkue et al. 1998) (no Triton). The alternative protocol (personal correspondence, Frenguelli lab) used in this study to confirm $A_1R$ antibody staining also used a higher concentration of Triton X100 (0.5 %). However, the specificity and possible low affinity of the $A_1R$ antibody was confirmed in CHO cells transfected with a GFP-tagged $A_1R$ construct when using 0.4 % Triton (figure 3.2).

The permeabilisation of cells with Triton X100 in order to allow the $A_1R$ and mGluR4 antibodies access to the intracellular C-terminals to which they bind may also result in contact with intracellular membrane compartments through which these molecules are shipped to the cell surface and binding to $A_1R$ or mGluR4 proteins that may be present internally but are not trafficked to the cell surface. This, in theory, could be overcome by using antibodies generated against the extracellular N-terminal of these receptors and no Triton X100. However, although available, no N-terminal-directed antibodies for these receptors have yet been reported as specific.

The use of Triton X100 may explain the differential staining patterns for $A_1R$ at Purkinje dendrites (figure 3.6). Areas of dendrites with no staining may be due to insufficient permeabilisation with Triton X100. However, cerebellar slices were agitated for one hour during incubation with primary antibody before being left overnight at 4°C which should minimise this risk.

The primary antibodies calbindin and GFAP are commonly used in immunohistochemical studies of brain tissue. The fact that their immunoreactivity observed in this study is comparable to that observed in other cerebellar sections, for

167

example (Nakamura and Uchihara 2004), provides an indicator of reliability for the methodology although does not take into consideration specificity issues or cross-over reactions that may be occurring with primary antibodies against $A_1R$ or mGluR4. It has also recently been reported that antibodies against G-protein coupled receptors (GPCR) such as $A_1R$ and mGluR4 are generally considered unreliable unless data is accompanied by rigorous controls such as the absence of staining in knockout mice. This particular review reports that in 49 antibodies against various GPCR tested none were found to be selective and that this may be due to the antibodies recognising structural similarities not just between members of the same family (for example, $A_1R$, $A_{2A}R$, $A_{2B}R$ and $A_3R$) but between the family of GPCR as a whole (Michel, Wieland et al. 2009). This may explain the identical mGluR4 and $A_1R$ staining in cerebellar slices and the unexpected widespread distribution of $A_{2A}R$ similar to that of $A_1R$. The primary antibodies used in this study for $A_1R$, $A_{2A}R$ and mGluR4 have, however, been generated against the less conserved C-terminal regions.

As a further consideration, the widespread immunoreactivity for $A_1R$, $A_{2A}R$ and mGluR4 in cerebellar slices may be the result of damage caused to cells in the cerebellar tissue during the sectioning process as mechanical lesions to histological sections are known to increase the risk of non-specific binding of IgGs (Fritschy 2008).

Given the factors that are potentially affecting the immunohistochemical results in this study, it is unwise to draw strong conclusions from any of the data without first performing more thorough controls for each primary antibody. This is of particular

importance given that staining for $A_{2A}R$ was contradictory to previous immunohistochemical and hybridisation studies (Svenningsson, Le Moine et al. 1997; Rosin, Robeva et al. 1998) and that there is no reported functional role for $A_{2A}R$ in the cerebellum. However, calcium signalling due to $A_{2A}R$ activation has recently been described in mouse olfactory bulb glial cells (Doengi, Deitmer et al. 2008) and staining for $A_{2A}R$ was present on glial cell processes (figure 3.11) in this study. The electrophysiological data in this study suggests that all the actions of adenosine on PF EPSPs are via the activation of $A_1R$ with no evidence for $A_{2A}R$ activation (figure 4.8). Thus if the widespread $A_{2A}R$ staining within the molecular layer is real perhaps it plays some other role perhaps in interneurone signalling.

Staining for the parallel fibre marker, mGluR4, around and over Purkinje cell bodies at an early developmental stage (figure 3.9) prior to the formation of functional PF-PC synapses (Altman 1972; Arata and Ito 2004), that is identical to the staining observed for $A_1R$ at this age (figure 3.8) provides a further indicator that the primary antibodies may be binding non-specifically. It is possible that the $A_1R$ staining is associated with climbing fibres shown to be present (Press and Wall 2008) and functional (Hashimoto and Kano 2003) at postnatal day 4 but there are no reports of mGluR4 expression by climbing fibres at any stage of cerebellar development.

### 6.1.4 Future work

The specificity of the $A_1R$ antibody for this study was confirmed in CHO cells transfected with $A_1R$ tagged with GFP (figure 3.2). The possibility of antibody

cross-reaction between subtypes of the adenosine receptor family could be eliminated by testing the $A_1R$ or $A_{2A}R$ antibody in CHO cells transfected with $A_1R$, $A_{2A}R$, $A_{2B}R$ and $A_3R$ (Rivkees, Price et al. 1995).

Accurate interpretation of the immunohistochemistry results in this study would require further experiments to establish the specificity of the $A_1R$, $A_{2A}R$ and mGluR4 primary antibodies. This could primarily be attempted by proving that each antibody stains only one band corresponding to the size of the relevant receptor on a Western blot. The process could then be applied to tissue preparations from cerebellar slices at different points from birth to postnatal day 21 to establish $A_1R$, $A_{2A}R$ and mGluR4 protein levels during development as the immunohistochemistry is difficult to quantify.

A complete absence of staining for the corresponding antibody in cerebellar sections obtained from an $A_1R$, $A_{2A}R$ or mGluR4 knockout mice would provide the most convincing control and give significant weight to the reliability of the confocal images obtained in this study. As a minor point, this study used cerebellar tissue from rats so even a comparison with mouse tissue would not be definitive. In addition, antibody staining may still be observed in a knockout animal if a truncated version of the protein is expressed or other homologous proteins that cross-react with the primary antibody are upregulated by the knockout (Lorincz and Nusser 2008). The reactivity of the primary antibodies used in this study with mouse tissue would also need to be considered.

A more cost-effective control would be to demonstrate a loss of staining when the primary antibody is pre-incubated with the synthetic peptide used to immunise the animal in which it was generated (possible for $A_1R$, $A_{2A}R$ and mGluR4 primary antibodies used in this study) thus indicating that the antibody is antigen-specific. Alternatively, in-situ hybridisation could be used as a control by comparing primary antibody immunoreactivity with the pattern of mRNA expression.

To address the possibility of $A_1R$ staining on Purkinje cell bodies being the result of $A_1R$ present on basket cell processes enveloping Purkinje cells, immunohistochemistry using primary antibodies against calbindin, $A_1R$ and a basket cell protein could be used. A possible antibody marker for basket cells would be the voltage-gated $K^+$ channel subunit Kv1.2 which is most densely localised to basket cells in the rat cerebellum (Chung, Shin et al. 2001). However, triple immunofluorescence would not be a possibility as this is only available as a primary antibody generated in the rabbit.

The potential for the staining of $A_1R$ at proximal Purkinje cell dendrites (figure 3.6) to be located on climbing fibres and not parallel fibres, especially prior to PF-PC synapse formation (figure 3.8), could be investigated with immunohistochemistry. The use of a vGluT2 primary antibody would not be an ideal marker to distinguish climbing fibres from parallel fibres as vGluT2 is also expressed at parallel fibre terminals and gradually replaced with vGluT1 until postnatal day 30 (Miyazaki, Fukaya et al. 2003). The CART peptide has been found to be localised to climbing fibres within the vestibular cerebellum (Press and Wall 2008) so a primary antibody against this peptide could be used as an alternative marker for these climbing fibres

during development. Immunohistochemistry using cerebellar slices from birth until postnatal day 2 could also be attempted.

The inhibition of CF EPSCs following application of adenosine has already been demonstrated in rat cerebellar slices at postnatal days 10-20 (Takahashi, Kovalchuk et al. 1995; Hashimoto and Kano 1998). As CF EPSCs are frequently recorded at postnatal day 4 (Hashimoto and Kano 2003) the effect of adenosine and therefore the presence of $A_1Rs$ can be studied during development using whole-cell patch clamping of Purkinje cells. This could also be attempted on rats at postnatal day 3, where the presence of $A_1R$ has been implicated by immunohistochemistry (figure 3.8), as the stage of cerebellar development may not be very different between a rat at postnatal day 3 born in the morning and a rat at postnatal day 4 born in the evening.

To investigate whether mechanical damage to cells in cerebellar sections caused by use of the vibratome affects staining patterns, an alternative preparation method could be attempted such as cryostat sectioning of cerebellar slices or using cardiac perfusion with PFA. The effect of using concentrations of Triton X100 lower than 0.1 % (Weruaga, Alonso et al. 1998) in the immuno PBS to permeabilise cells could also be examined. An alternative to Triton X100 would be an organic solvent, such as methanol, which would dissolve membrane lipids and allow the primary antibody access to intracellular components.

Following confirmation of primary antibody specificity with the controls outlined in this section, the immunohistochemistry could be extended to look at the presence of other cerebellar proteins during development. For example, primary antibodies

172

against the metabolic proteins adenosine deaminase and adenosine kinase could be used to compare their distribution in the molecular layer. In addition, co-localisation of mGluR4 and adenosine receptors could be examined at single Purkinje cells injected with a fluorescent dye via a patch pipette. This would allow the characterisation of receptor distribution on individual Purkinje cells which is currently very difficult because of the overlap of dendrites (particularly distal dendrites) from neighbouring cells.

If immunohistochemical controls failed to confirm antibody specificity, real-time PCR could be used as a tool to quantitatively determine levels of $A_1R$ gene expression in cerebellar tissue during development.

## 6.2 Presynaptic pharmacology of immature parallel fibre-Purkinje cell synapses in the rat cerebellum

### 6.2.1 Summary of key findings

- The release of GABA from inhibitory interneurones in the molecular layer appeared to have little effect on EPSP amplitude at immature PF-PC synapses via activation of $GABA_A$ receptors.

- Reduction in EPSP amplitude due to activation of presynaptic mGluR4 and $GABA_B$ was confirmed in slices at postnatal days 9-14 and found to be comparable to that obtained in slices at postnatal days 21-28.

- The $A_1R$-mediated inhibition was found to be variable in immature slices with ~12.5 % of confirmed PF-PC synapses showing no response to adenosine.

### 6.2.2 Possible explanations for the variable response to adenosine at immature parallel fibre-Purkinje cell synapses

The use of rats in the second postnatal week is ideal for studying the development of PF-PC synapse responses as this is a major period for the development of these synaptic connections in the rat cerebellum. The formation of glutamatergic synapses between parallel fibres and distal Purkinje cell dendrites commences from around

174

postnatal day 5 (Altman 1972) with the external granule cell layer ceasing to exist by the end of the third postnatal week (Komuro and Yacubova 2003).

Application of adenosine (100 µM) to immature slices (P9-14) resulted in a variable PF EPSP amplitude reduction (figure 4.5). A number of possible explanations for the variability in $A_1R$-mediated inhibition were tested:

### i.  *There may be variability in the expression of $A_1R$ at PF-PC synapses*

The previously described immunohistochemistry experiments in this study (chapter 3) showed dense $A_1R$ expression throughout development indicating that it is unlikely that the large variability in presynaptic inhibition through activation of $A_1R$ would be due to low expression of $A_1R$. However, it is not possible to exclude the lack of expression at individual synapses as it was not feasible to co-label synapses with a marker and with $A_1R$.

This was confirmed with application of the $A_1R$ agonist $N^6$-cyclopentyladenosine (CPA, at high concentrations up to 100 µM) which was found to reliably inhibit EPSP amplitude and increase PPF in immature cerebellar slices with no adenosine-mediated inhibition indicating the presence of $A_1R$ in these slices (figure 4.10). This result could have been made more reliable by blockade of inhibition with co-application of the $A_1R$ antagonist 8-CPT to confirm that the effect of CPA was via $A_1R$ activation and not an alternative mechanism. However, the adenosine analogue CPA has been used in previous studies of the rat PF-PC synapse as a specific agonist of $A_1R$ with an effect that is reversible with an $A_1R$ antagonist, for example (Kreitzer and Regehr 2000).

*ii. PF EPSP amplitude may be a balance between $A_1R$ and $A_{2A}R$ activation*

The earlier immunohistochemistry experiments in this study (chapter 3) suggested a widespread distribution of both $A_1R$ and $A_{2A}R$ in the molecular layer which could indicate that adenosine is binding to both receptor subtypes at parallel fibre terminals and that the resultant EPSP amplitude is a balance of the inhibitory effect of $A_1R$ activation and the facilitatory effect of $A_{2A}R$ activation on glutamate release. At synapses where there are more $A_{2A}R$ this may have the net effect of adenosine having little or no effect on synaptic transmission.

Co-application of adenosine and the specific $A_1R$ antagonist 8-CPT indicated that activation of $A_{2A}R$ is unlikely to significantly contribute to EPSP amplitude (figure 4.8) although only 1 slice out of 12 had no adenosine-mediated inhibition. It was difficult to test this effect as a lack of adenosine-mediated inhibition in control did not occur frequently; however similar experiments showed adenosine had no effect in 8-CPT whether or not adenosine produced a large inhibition in control (personal correspondence, Mark Wall).

*iii. A lack of $A_1R$-mediated inhibition may be due to rapid adenosine breakdown*

It is possible that the lack of adenosine-mediated inhibition in some slices could be the result of a rapid adenosine breakdown resulting in the metabolism of adenosine before it could activate presynaptic $A_1R$.

The non-hydrolysable $A_1R$ agonist CPA reliably inhibited EPSP amplitude and significantly increased PPR at immature PF-PC synapses (figure 4.10). The CPA is not metabolised as adenosine would be in the extracellular space so its inhibitory

effect at $A_1R$ that do not respond to adenosine (100 µM) may indicate a more rapid metabolism or uptake of adenosine by transporter proteins at some immature PF-PC synapses resulting in the removal of adenosine from the extracellular space before it can activate $A_1R$. However, the shifted log concentration-response curve generated for CPA (figure 4.12) in immature slices with no $A_1R$-mediated inhibition suggests that adenosine metabolism does not explain the variable response to adenosine – as CPA is not metabolised its effect would have been the same regardless of response to adenosine if adenosine metabolism was affecting $A_1R$-mediated inhibition.

Subsequent electrophysiology experiments (chapter 5) also suggested that adenosine clearance via adenosine deaminase, adenosine kinase and equilibrative transporters has only minor effects on synaptic transmission in immature slices.

### iv. There may be a variability in $A_1R$ efficacy

The log concentration-response curves for EPSP amplitude reduction elicited by application of the $A_1R$ agonist CPA (0.001 µM – 100 µM) suggest a variability in $A_1R$ efficacy (figure 4.12). The lower $IC_{50}$ in immature slices that respond to adenosine (0.08 µM) compared to slices where there is no adenosine-mediated inhibition (2.10 µM) suggests that $A_1R$ efficacy may be lower at some immature PF-PC synapses and that this may account for the variability in response to adenosine. Both of the $IC_{50}$ values are higher than that described for EPSP amplitude reduction with CPA in hippocampal slices (~0.019 µM) (Rebola, Coelho et al. 2003).

There may be a heterogeneous population of low affinity and high affinity presynaptic $A_1R$ at immature parallel fibre terminals resulting in the observed

177

variability in $A_1R$-mediated inhibition. This could be present within populations of PF-PC cell synapses or alternatively, as parallel fibre terminals also form excitatory synapses with basket cells and stellate cells in the molecular layer (Sillitoe and Joyner 2007), it may be that the low efficacy $A_1R$ are present only at these synapses. However, there was no significant difference in either EPSP amplitude (- $0.35 \pm 0.02$ mV and -$0.3 \pm 0.03$ mV, p = 0.19) or the degree of PPF ($1.38 \pm 0.04$ and $1.34 \pm 0.03$, p = 0.22) at synapses which were or weren't inhibited by adenosine. The synapses also appeared identical in their responses to baclofen, L-AP4 and kynurenic acid. Whole cell patch clamp recording from Purkinje cells or interneurones and stimulating parallel fibres could test the possibility of differential $A_1R$ expression.

*v. Other possible explanations for a variable $A_1R$-mediated inhibition*

The variability in $A_1R$-mediated inhibition was not found to be gender-specific (figure 4.12) - the lower PF EPSP amplitude reduction seen in female cerebellar slices was probably due to a much smaller sample size (16 female Vs 167 males). There was also no correlation with the age of rat (P9-14) and adenosine-mediated inhibition suggesting no developmental shift.

Other possibilities for the variability in adenosine response should also be considered. The functional association of presynaptic $A_1R$ with other receptor types may affect the response to adenosine. Interaction of $A_1R$ and $P2Y_1R$ as hetero-oligomers in the molecular layer of the rat cerebellum has previously been demonstrated (Yoshioka, Hosoda et al. 2002) as has an interaction between $A_1R$ and $mGlu_{1\alpha}R$ (Ciruela, Escriche et al. 2001). Such an interaction could reduce affinity and/or efficacy of signalling.

Alternatively, the variable response to adenosine may be due to differences in the expression or efficacy of G-proteins or other downstream signalling mechanisms at this stage in development. An immunocytochemical study of the expression of G-protein subunits in the developing murine cerebellum showed that $G_o$, which is coupled to $A_1R$ (figure 1.2), was only detectable in the molecular layer from postnatal day 8 with levels increasing until postnatal day 15. Similarly, $G_{i2}$ staining in the molecular layer was very weak at postnatal day 8 and increased in intensity until adulthood (Schuller, Lamp et al. 2001). It is possible that the variable expression of G-proteins that interact with presynaptic $A_1R$ may have influenced the ability of adenosine to inhibit synaptic transmission at PF-PC synapses at the age of rat used in this study (P9-14).

### 6.2.3 Future work

Activation of four presynaptic receptor types is known to decrease the probability of vesicle release at the PF-PC synapse (Bellamy 2007). This study discussed presynaptic $GABA_B$, mGluR4 and $A_1R$ responses at immature synapses but did not confirm the effect of endocannabinoid type 1 (CB1) receptor activation. A previous study has demonstrated that the presynaptic inhibition of rat parallel fibre-evoked EPSCs in Purkinje cells with the endocannabinoid receptor agonist WIN 55212-2 can be reversed with the CB1 receptor antagonist SR 141716 (Takahashi and Linden 2000).

Microelectrode biosensors could be used to compare the concentration of downstream adenosine metabolites in cerebellar slices with adenosine-mediated inhibition and in slices where EPSP amplitude is reduced by adenosine. The effect of inhibitors of adenosine clearance in immature slices with no adenosine-mediated inhibition could also be examined. To more accurately test the effect of $A_{2A}R$ at PF-PC synapses, an $A_{2A}R$ agonist could be used.

The age of rat used in this study (P9-14) is the earliest at which extracellular field PF EPSPs can be successfully recorded (Atterbury and Wall 2009). To examine whether the variability in adenosine-mediated inhibition is apparent at an earlier stage in development, patch clamp recordings from individual Purkinje cells (with parallel fibre stimulation) could be used.

The effect of adenosine on EPSP amplitude could also be examined in older rats at postnatal days 21-28 to establish whether variable adenosine-mediated inhibition is present throughout development or just at an early stage. Preliminary data suggests that $A_1R$-mediated inhibition may also be variable in this age group.

## 6.3 Adenosine signalling at immature parallel fibre-Purkinje cell synapses in the rat cerebellum

### 6.3.1 Summary of key findings

- Blockade of $A_1R$ suggested that an inhibitory adenosine tone is low or absent at postnatal days 9-12.

- Inhibition of adenosine clearance had little effect on synaptic transmission in immature slices suggesting that little adenosine is moving between the intracellular and extracellular spaces under basal conditions.

- Active adenosine release could be stimulated with hypoxia in immature slices but this was delayed and slow. Adenosine could not be actively released in response to electrical stimulation in the molecular layer in immature slices.

### 6.3.2 A low or absent tonic inhibition by endogenous adenosine at immature parallel fibre-Purkinje cell synapses

This study suggests that an inhibitory adenosine tone is often low or absent at postnatal days 9-12 but increases during development. Application of the $A_1R$ antagonist 8-CPT had a significantly smaller effect on PF EPSP amplitude in immature slices at postnatal days 9-12 than in mature slices at postnatal days 21-28 (figure 5.2).

There are no previous studies that have measured the basal adenosine tone or its regulation in the juvenile rat cerebellum. However at CA1 hippocampal neurones, the increase in presynaptic inhibition of EPSPs observed by blocking adenosine uptake with NBTI is less obvious in younger rats suggesting that a developmental increase in extracellular adenosine tone also occurs in this region (Psarropoulou, Kostopoulos et al. 1990). Conversely, a developmental decline in $A_1R$-mediated presynaptic inhibition and $A_1R$ immunoreactivity is observed at the glutamatergic synapse between the calyx of Held and principal cell in the MNTB of mice during the second postnatal week (Kimura, Saitoh et al. 2003).

### 6.3.3 Possible explanations for a low or absent basal adenosine tone in immature slices

A number of possible explanations for the reduced adenosine tone at immature PF-PC synapses were tested:

*i. There may be a low expression of $A_1R$ in immature slices*

A basal adenosine tone may be present in immature slices but undetectable due to a low expression of $A_1R$ at PF-PC synapses. This is unlikely as the previously described immunohistochemistry experiments in this study (chapter 3) suggested a dense co-localisation of $A_1R$ at all PF-PC synapses throughout development.

All experiments measuring tonic $A_1R$ activation only used slices where adenosine (100 µM) inhibited EPSP amplitude by at least 50 %. Thus the lack of tone is not the

result of low receptor expression or the expression of low affinity receptors. In addition, the $A_1R$-mediated inhibition was not affected by a low or absent basal adenosine tone (figure 5.3).

*ii. The $A_1R$ efficacy may differ between immature and mature slices*

It has previously been discussed how differences in $A_1R$-mediated inhibition in immature slices may be the result of a variable $A_1R$ efficacy (chapter 4). Log concentration-response curves for the $A_1R$ agonist $N^6$-cyclopentyladenosine (CPA) at mature synapses and immature synapses with an adenosine-mediated inhibition greater than 50 % (figures 4.10, 5.4) were almost identical suggesting that the lower inhibitory $A_1R$ tone at immature PF-PC synapses is unlikely to be the result of a difference in $A_1R$ efficacy.

*iii. There may be an enhanced adenosine clearance in immature slices*

The low concentration of extracellular adenosine metabolites measured by microelectrode biosensors (figure 5.5, 5.6) indicates that the lack of an inhibitory $A_1R$ tone at immature PF-PC synapses is unlikely to be the result of an enhanced extracellular adenosine metabolism. The low concentration could, however, indicate reduced adenosine release or rapid adenosine uptake from the extracellular space.

As expected from the microelectrode biosensor data, the inhibition of adenosine deaminase (ADA) with EHNA had little effect on EPSP amplitude at immature PF-PC synapses (figure 5.7). The activity of ADA is not considered to be a major regulator of extracellular adenosine tone in mature cerebellar slices (Wall, Atterbury et al. 2007). Similarly, in rat hippocampal slices the inhibition of neuronal activity

observed with application of adenosine is greatly reduced or not apparent with application of EHNA to inhibit ADA (Pak, Haas et al. 1994).

Inhibition of ENT1 and ENT2 with NBTI/dipyridamole was used to assess whether enhanced facilitated diffusion of adenosine from the extracellular space into the cytoplasm via equalibrative transporters contributes to the low inhibitory $A_1R$ tone in immature slices. Application of NBTI/dipyridamole had no effect on synaptic transmission at ~50 % of PF-PC synapses and resulted in ~ 32 % reduction in EPSP amplitude at the remaining synapses (figure 5.8). There was no correlation between the reduction in EPSP amplitude with NBTI/dipyridamole and the absence of an inhibitory $A_1R$ tone in the immature slices. A similar variability in response to NBTI/dipyridamole is reported in mature cerebellar slices where EPSP amplitude is reduced by ~ 47 % in 9 out of 18 slices (Wall, Atterbury et al. 2007).

To examine whether the low inhibitory $A_1R$ tone in immature slices is the result of enhanced intracellular phosphorylation of adenosine by AK, thus preventing adenosine efflux to the extracellular space (Boison 2006), iodotubericidin was applied to slices to inhibit AK. Iodotubericidin inhibited EPSP amplitude by ~25 % in 14 out of 21 slices which is a less reliable effect and significantly smaller than in mature slices (Wall, Atterbury et al. 2007) and suggests that AK is not particularly active under basal conditions.

The greater effect of intracellular AK activity in comparison to extracellular adenosine metabolism by ADA has also been reported in mature cerebellar slices (Wall, Atterbury et al. 2007) and hippocampal slices (Pak, Haas et al. 1994; Lloyd

184

and Fredholm 1995). An important role for AK in the control of extracellular adenosine is suggested in the rat prepiriform cortex where its inhibition potentiates the ability of adenosine to suppress bicuculline methiodide-induced seizures (Zhang, Franklin et al. 1993)

The inhibition resulting from block of the intracellular enzyme adenosine kinase (AK) with iodotubericidin was not prevented by prior application of NBTI/dipyridamole in 6 out of 10 immature slices (figure 5.13B) suggesting that block of ENT1 and ENT2 does not abolish all transport of adenosine. Similarly, in mature slices effective block of equilibrative transporters by NBTI/dipyridamole to prevent the efflux of an increased intracellular adenosine concentration due to inhibition of AK is only observed in 4 out of 8 slices (Wall, Atterbury et al. 2007). This may be due to expression of transporters not sensitive to NBTI/dipyridamole at PF-PC synapses which may be contributing to the low inhibitory $A_1R$ tone or a heterogeneous distribution of ENT1 and ENT2 transporters as ENT2 is only weakly blocked in rats (Baldwin, Beal et al. 2004). The lack of selective inhibitors prevents the involvement of the five known concentrative transporter subtypes in the regulation of adenosine levels from being determined.

During early postnatal development of the mouse hippocampus AK immunoreactivity is most prominent in neurones with a gradual transition of expression to newly-formed GFAP-positive astrocytes until around postnatal day 14 and neuronal expression being maintained in only a few areas (Studer, Fedele et al. 2006). If this also occurs in the cerebellum, the expression of AK in neurones may

reduce intracellular adenosine stores resulting in a decreased release of adenosine to the extracellular space and a low inhibitory $A_1R$ tone.

Overall, the effect of inhibition of ADA, AK and the equilibrative transporters ENT1 and ENT2 had minor and unreliable effects at immature PF-PC synapses and had less effect on EPSP amplitude reduction than in mature slices (figure 5.14) suggesting that the low basal inhibitory $A_1R$ tone in immature slices is not the result of an enhanced movement of adenosine between the intracellular and extracellular spaces under basal conditions.

   *iv.  Active adenosine release may be less efficient in immature slices*

Hypoxia and electrical stimulation were used to investigate whether there are developmental differences in the active release of adenosine in cerebellar slices.

A prolonged release of extracellular adenosine in response to the increased demand for energy from ATP during pathological events is a well-documented neuroprotective action of adenosine which is mediated primarily through cellular pathways triggered by $A_1R$ activation (Latini and Pedata 2001).  Hypoxia stimulated the release of adenosine in both immature and mature slices but the release was delayed and slower at immature PF-PC synapses (figure 5.15, 5.16) suggesting that the mechanism of adenosine release becomes more sensitive to hypoxia during development.   Synaptic depression during periods of hypoxia induced in rat hippocampal slices is blocked by an $A_1R$ antagonist (Fowler 1989; Gribkoff and Bauman 1992). These mechanisms inhibit some $Ca^{2+}$ channels to reduce glutamate and other neurotransmitter release and hyperpolarise neurones to limit excitotoxic

damage caused by the entry of $Ca^{2+}$ (Dunwiddie and Masino 2001). It is possible that the delayed and slower release of adenosine during hypoxia and low inhibitory $A_1R$ tone in immature slices may make them more sensitive to the effects of hypoxia. The immature rat brain was originally believed to be more resistant to the damaging effects of hypoxia compared to the more mature brain. However subsequent research suggests a non-linear relationship between hypoxic-ischemic brain damage and age. Brain damage following ischemia or hypoxia appears to be most severe in 1-3 week old rats followed by those aged 6 months and significantly less severe in 6-9 week old animals (Yager and Thornhill 1997). The increased vulnerability of the immature rat brain to the effects of hypoxia compared to the mature brain is consistent with the findings in this study.

It is unlikely that any inhibitory adenosine tone in the slices is the result of hypoxia as during experiments the recording chamber was continuously perfused at a rate of 6 ml/min with aCSF bubbled with 95 % $O_2$ and 5 % $CO_2$ using a peristaltic pump. A suspended grid also ensured that the slices were perfused from above and below and the tubing had low gas permeability to inhibit induction of hypoxia.

Blockade of $A_1R$ with 8-CPT had no effect on the facilitation and depression of EPSP amplitudes during trains of activity in immature slices suggesting that there is no adenosine release during trains of stimuli. The facilitation and depression of EPSP amplitude during trains of activity in immature slices is probably due to the exhaustion of glutamate stores rather than the active release of adenosine changing the probability of glutamate release to limit transmitter depletion and maintain synaptic transmission (Kimura, Saitoh et al. 2003).

Microelectrode biosensors were not able to measure the release of adenosine during trains of electrical stimuli in immature slices (figure 5.18) although it has previously been described that adenosine can be released into the extracellular space of mature slices in a neuronal activity-dependent manner that is likely to be from parallel fibre terminals (Wall and Dale 2007). Immature parallel fibre terminals may contain much smaller pools of releasable adenosine. Alternatively, as granule cell migration and PF-PC synapse formation is not complete in immature slices at postnatal days 9-12, the low number of parallel fibre terminals present may result in an undetectable level of adenosine release during molecular layer stimulation. A different mechanism of adenosine release may also exist that is not present at this stage in development.

Blocking action potential adenosine release with TTX has unreliable and small effects on basal adenosine levels in mature cerebellar slices suggesting that the activity-dependent release of adenosine is not a major contributor to the inhibitory $A_1R$ tone at postnatal days 21-28 (Wall, Atterbury et al. 2007). The absence of activity-dependent adenosine release in immature slices is therefore unlikely to be a major factor in the low or absent basal inhibitory $A_1R$ tone.

*v.* *An adenosine tone may be the result of ATP release in cerebellar slices*

Damage to cerebellar slices during preparation (and subsequent cell death) may result in the release of cytoplasmic ATP and conversion to adenosine. This is more likely to occur in mature slices which survive slicing less well than slices from young animals. The large population of granule cells could provide a source of ATP if they slowly die during recordings. ATP could also be released from neurones by

188

exocytosis (Edwards, Gibb et al. 1992; Dale 1998) or through the opening of gap junction hemichannels (Pearson, Dale et al. 2005) and then rapidly converted to adenosine by ectonucleotidases. Inhibition of PF EPSPs occurs following application of ATP to mature slices which can be prevented by blockade of $A_1R$ with 8-CPT suggesting that the exogenous ATP is rapidly metabolised to adenosine (Wall, Atterbury et al. 2007). Calcium signals in Bergmann glia triggered by bursts of parallel fibre activity in cerebellar slices can be blocked with application of the P2 receptor antagonist pyridoxal phosphate-6-azophenyl-2,4-disulfonic acid (PPADS) suggesting that the release of ATP from parallel fibres may provide a source of extracellular adenosine (Beierlein and Regehr 2006).

ATP increases the frequency of spontaneous postsynaptic currents (sPSCs) recorded in Purkinje neurones by activation of P2 receptors. Interestingly, application of the ecto-ATPase inhibitor ARL67156 from the second postnatal week onwards (Casel, Brockhaus et al. 2005) also increases sPSC frequency suggesting a tone of extracellular ATP. However, the direct measurement of ATP in mature cerebellar slices with microelectrode biosensors did not reveal an ATP signal although this may be due to rapid breakdown of ATP (Wall, Atterbury et al. 2007). Block of ATP metabolism had variable effects on the adenosine tone, suggesting that ATP is at least one of the sources of adenosine in mature slices (Wall, Atterbury et al. 2007).

### 6.3.4  Future work

The stimulation of bundles of parallel fibres during extracellular field recordings does not replicate a physiological situation.  It would be interesting to determine whether the results obtained in this study for the inhibitory $A_1R$ tone and adenosine clearance mechanisms are replicated with patch clamp recordings (from individual Purkinje cells) with the stimulation of a small number of parallel fibres (using a patch pipette rather than a bipolar electrode).

The use of microelectrode biosensors *in vivo* would also allow more physiologically-relevant recordings and would eliminate any incorrect measurement of adenosine metabolites due to cell death following slice preparation.

The simultaneous measurement of EPSP amplitude with microelectrode biosensor measurement has not been used in this study to confirm the effects of blockade of AK, ADA and equilibrative transporters as was used for mature cerebellar slices (Wall, Atterbury et al. 2007).  The effect of ADA block by EHNA cannot be directly measured with an ADA biosensor, which also uses the enzyme, but could be determined with IDO or HYPO biosensors.

Immunohistochemistry could be used to determine whether the expression of AK in neurones may reduce intracellular adenosine stores resulting in a decreased release of adenosine to the extracellular space and a low inhibitory $A_1R$ tone in immature slices.

Finally, this study has not determined the contribution of ATP metabolism to the low inhibitory $A_1R$ tone in immature slices. Although a lack of ATP metabolism to adenosine in the extracellular space is unlikely to contribute to the low or absent adenosine tone in immature slices this could be confirmed by applying ATP to slices and measuring the conversion to adenosine with microelectrode biosensors.

# Summary

The first aim of this study was to determine the distribution of $A_1R$ at PF-PC synapses in cerebellar slices at postnatal day 3 prior to PF-PC synapse formation, postnatal days 8-14 and postnatal days 21-28. Immunohistochemistry suggested that $A_1R$ are widely distributed across Purkinje cell bodies, their dendrites and within the granule layer of the cerebellum throughout development. The same staining patterns were also observed prior to PF-PC synapse formation. There was only minor co-localisation of $A_1R$ with glial cell bodies or their processes, eliminating their involvement in the staining observed. Although these results were replicated using an alternative protocol, care should be taken in their interpretation as they are partly contradictory to the expression of $A_1R$ described in previous studies.

The widespread expression of $A_{2A}R$ within cerebellar slices which was identical to that of $A_1R$ is contradictory to a number of previous immunohistochemical studies although a moderate distribution of $A_{2A}R$ has been described in the human cerebellum. A functional role for $A_{2A}R$ has not previously been described within the cerebellum.

A further aim of this study was to investigate the pharmacological profile of the immature rat PF-PC synapse with electrophysiology and microelectrode biosensors. Application of adenosine resulted in a variable $A_1R$-mediated inhibition at immature PF-PC synapses. This did not appear to be gender-specific or correlated with age of rat and the synapses otherwise appeared identical in their properties. This variability in adenosine-mediated inhibition contrasts with the actions of L-AP4 (mGluR4

agonist) and baclofen (GABA$_B$ receptor agonist) which consistently depress synaptic transmission. The comparison of log concentration-response curves generated for an A$_1$R agonist suggested that some A$_1$R may have a lower efficacy at this stage of development.

Blockade of presynaptic A$_1$R at immature PF-PC synapses suggested that an inhibitory adenosine tone is low or absent in immature slices and is not the result of a low A$_1$R expression or developmental differences in A$_1$R efficacy. Inhibition of adenosine clearance via adenosine deaminase, adenosine kinase and equilibrative transporters had little effect on synaptic transmission indicating that little adenosine is moving between the intracellular and extracellular spaces under basal conditions in immature slices. The control of extracellular adenosine concentration in the immature cerebellum appears comparable to that in the mature cerebellum and other brain regions where the activity of adenosine kinase is the major determining factor.

Although adenosine receptors and the mechanisms of adenosine clearance are present at this stage in development there is very little adenosine release. Active adenosine release measured by electrophysiology and microelectrode biosensors could be stimulated with hypoxia in immature slices but this was delayed and slower in comparison to the release observed in mature slices. In addition adenosine could not be actively released at immature PF-PC synapses in response to electrical stimulation in the molecular layer suggesting that the mechanisms of adenosine release become more efficient with development.

# References

Abbracchio, M. P., G. Burnstock, et al. (2009). "Purinergic signalling in the nervous system: an overview." <u>Trends Neurosci</u> **32**(1): 19-29.

Agarwal, R. P. (1982). "Inhibitors of adenosine deaminase." <u>Pharmacol Ther</u> **17**(3): 399-429.

Altman, J. (1972). "Postnatal development of the cerebellar cortex in the rat. II. Phases in the maturation of Purkinje cells and of the molecular layer." <u>J Comp Neurol</u> **145**(4): 399-463.

Anderson, C. M., S. A. Baldwin, et al. (1999). "Distribution of mRNA encoding a nitrobenzylthioinosine-insensitive nucleoside transporter (ENT2) in rat brain." <u>Brain Res Mol Brain Res</u> **70**(2): 293-297.

Anderson, C. M., W. Xiong, et al. (1999). "Distribution of equilibrative, nitrobenzylthioinosine-sensitive nucleoside transporters (ENT1) in brain." <u>J Neurochem</u> **73**(2): 867-873.

Arata, A. and M. Ito (2004). "Purkinje cell functions in the in vitro cerebellum isolated from neonatal rats in a block with the pons and medulla." <u>Neurosci Res</u> **50**(3): 361-367.

Atluri, P. P. and W. G. Regehr (1996). "Determinants of the time course of facilitation at the granule cell to Purkinje cell synapse." <u>J Neurosci</u> **16**(18): 5661-5671.

Atterbury, A. and M. J. Wall (2009). "Adenosine signalling at immature parallel fibre-Purkinje cell synapses in rat cerebellum." <u>J Physiol</u> **587**(Pt 18): 4497-4508.

Ault, B., M. A. Olney, et al. (1987). "Pro-convulsant actions of theophylline and caffeine in the hippocampus: implications for the management of temporal lobe epilepsy." Brain Res **426**(1): 93-102.

Baldwin, S. A., P. R. Beal, et al. (2004). "The equilibrative nucleoside transporter family, SLC29." Pflugers Arch **447**(5): 735-743.

Barbour, B. (1993). "Synaptic currents evoked in Purkinje cells by stimulating individual granule cells." Neuron **11**(4): 759-769.

Batchelor, A. M. and J. Garthwaite (1992). "GABAB Receptors in the Parallel Fibre Pathway of Rat Cerebellum." Eur J Neurosci **4**(11): 1059-1064.

Beierlein, M. and W. G. Regehr (2006). "Brief bursts of parallel fiber activity trigger calcium signals in bergmann glia." J Neurosci **26**(26): 6958-6967.

Bellamy, T. C. (2007). "Presynaptic modulation of parallel fibre signalling to Bergmann glia." Neuropharmacology **52**(2): 368-375.

Bevan, N., T. Palmer, et al. (1999). "Functional analysis of a human A(1) adenosine receptor/green fluorescent protein/G(i1)alpha fusion protein following stable expression in CHO cells." FEBS Lett **462**(1-2): 61-65.

Boison, D. (2006). "Adenosine kinase, epilepsy and stroke: mechanisms and therapies." Trends Pharmacol Sci **27**(12): 652-658.

Boison, D. (2007). "Adenosine as a modulator of brain activity." Drug News Perspect **20**(10): 607-611.

Boison, D. (2008). "Adenosine as a neuromodulator in neurological diseases." Curr Opin Pharmacol **8**(1): 2-7.

Braas, K. M., A. C. Newby, et al. (1986). "Adenosine-containing neurons in the brain localized by immunocytochemistry." J Neurosci **6**(7): 1952-1961.

Brager, D. H. and S. M. Thompson (2003). "Activity-dependent release of adenosine contributes to short-term depression at CA3-CA1 synapses in rat hippocampus." J Neurophysiol **89**(1): 22-26.

Bruns, R. F., G. H. Lu, et al. (1986). "Characterization of the A2 adenosine receptor labeled by [3H]NECA in rat striatal membranes." Mol Pharmacol **29**(4): 331-346.

Burnstock, G. (1972). "Purinergic nerves." Pharmacol Rev **24**(3): 509-581.

Burnstock, G. (1980). "Purinergic nerves and receptors." Prog Biochem Pharmacol **16**: 141-154.

Burnstock, G. (2006). "Purinergic signalling." Br J Pharmacol **147 Suppl 1**: S172-181.

Burnstock, G. (2007). "Purine and pyrimidine receptors." Cell Mol Life Sci **64**(12): 1471-1483.

Casel, D., J. Brockhaus, et al. (2005). "Enhancement of spontaneous synaptic activity in rat Purkinje neurones by ATP during development." J Physiol **568**(Pt 1): 111-122.

Cass, C. E., J. D. Young, et al. (1998). "Recent advances in the molecular biology of nucleoside transporters of mammalian cells." Biochem Cell Biol **76**(5): 761-770.

Catania, M. V., G. B. Landwehrmeyer, et al. (1994). "Metabotropic glutamate receptors are differentially regulated during development." Neuroscience **61**(3): 481-495.

Ceballos, G., J. B. Tuttle, et al. (1994). "Differential distribution of purine metabolizing enzymes between glia and neurons." J Neurochem **62**(3): 1144-1153.

Chung, Y. H., C. Shin, et al. (2001). "Immunohistochemical study on the distribution of six members of the Kv1 channel subunits in the rat cerebellum." Brain Res **895**(1-2): 173-177.

Ciruela, F., V. Casado, et al. (1995). "Immunological identification of A1 adenosine receptors in brain cortex." J Neurosci Res **42**(6): 818-828.

Ciruela, F., M. Escriche, et al. (2001). "Metabotropic glutamate 1alpha and adenosine A1 receptors assemble into functionally interacting complexes." J Biol Chem **276**(21): 18345-18351.

Clark, B. A. and B. Barbour (1997). "Currents evoked in Bergmann glial cells by parallel fibre stimulation in rat cerebellar slices." J Physiol **502 ( Pt 2)**: 335-350.

Courjaret, R., M. Troger, et al. (2009). "Suppression of GABA input by A1 adenosine receptor activation in rat cerebellar granule cells." Neuroscience **162**(4): 946-958.

Craig, C. G. and T. D. White (1993). "N-methyl-D-aspartate- and non-N-methyl-D-aspartate-evoked adenosine release from rat cortical slices: distinct purinergic sources and mechanisms of release." J Neurochem **60**(3): 1073-1080.

Dale, N. (1998). "Delayed production of adenosine underlies temporal modulation of swimming in frog embryo." J Physiol **511 ( Pt 1)**: 265-272.

De Lorenzo, S., M. Veggetti, et al. (2004). "Presynaptic inhibition of spontaneous acetylcholine release induced by adenosine at the mouse neuromuscular junction." Br J Pharmacol **142**(1): 113-124.

Descombes, S., M. Avoli, et al. (1998). "A comparison of the adenosine-mediated synaptic inhibition in the CA3 area of immature and adult rat hippocampus." Brain Res Dev Brain Res **110**(1): 51-59.

Dittman, J. S. and W. G. Regehr (1996). "Contributions of calcium-dependent and calcium-independent mechanisms to presynaptic inhibition at a cerebellar synapse." J Neurosci **16**(5): 1623-1633.

Doengi, M., J. W. Deitmer, et al. (2008). "New evidence for purinergic signaling in the olfactory bulb: A2A and P2Y1 receptors mediate intracellular calcium release in astrocytes." FASEB J **22**(7): 2368-2378.

Dumas, T. C. and T. C. Foster (1998). "Late developmental changes in the ability of adenosine A1 receptors to regulate synaptic transmission in the hippocampus." Brain Res Dev Brain Res **105**(1): 137-139.

Dunwiddie, T. V. and L. Diao (1994). "Extracellular adenosine concentrations in hippocampal brain slices and the tonic inhibitory modulation of evoked excitatory responses." J Pharmacol Exp Ther **268**(2): 537-545.

Dunwiddie, T. V., L. Diao, et al. (1997). "Adenine nucleotides undergo rapid, quantitative conversion to adenosine in the extracellular space in rat hippocampus." J Neurosci **17**(20): 7673-7682.

Dunwiddie, T. V. and S. A. Masino (2001). "The role and regulation of adenosine in the central nervous system." Annu Rev Neurosci **24**: 31-55.

Eccles, J. C., R. Llinas, et al. (1966). "The excitatory synaptic action of climbing fibres on the purinje cells of the cerebellum." J Physiol **182**(2): 268-296.

Edgley, S. A. and M. Lidierth (1988). "Step-related discharges of Purkinje cells in the paravermal cortex of the cerebellar anterior lobe in the cat." J Physiol **401**: 399-415.

Edwards, F. A., A. J. Gibb, et al. (1992). "ATP receptor-mediated synaptic currents in the central nervous system." Nature **359**(6391): 144-147.

FitzGerald, M. J. T. a. F.-C., J. (2002). Clinical Neuroanatomy and Related Neuroscience: Basic and Clinical, Saunders.

Fowler, J. C. (1989). "Adenosine antagonists delay hypoxia-induced depression of neuronal activity in hippocampal brain slice." Brain Res **490**(2): 378-384.

Franco, R., V. Casado, et al. (1997). "Cell surface adenosine deaminase: much more than an ectoenzyme." Prog Neurobiol **52**(4): 283-294.

Fredholm, B. B., M. P. Abbracchio, et al. (1994). "Nomenclature and classification of purinoceptors." Pharmacol Rev **46**(2): 143-156.

Fredholm, B. B., E. Irenius, et al. (2001). "Comparison of the potency of adenosine as an agonist at human adenosine receptors expressed in Chinese hamster ovary cells." Biochem Pharmacol **61**(4): 443-448.

Frenguelli, B. G., G. Wigmore, et al. (2007). "Temporal and mechanistic dissociation of ATP and adenosine release during ischaemia in the mammalian hippocampus." J Neurochem **101**(5): 1400-1413.

Fritschy, J. M. (2008). "Is my antibody-staining specific? How to deal with pitfalls of immunohistochemistry." Eur J Neurosci **28**(12): 2365-2370.

Fulga, I. and T. W. Stone (1998). "Comparison of an adenosine A1 receptor agonist and antagonist on the rat EEG." Neurosci Lett **244**(1): 55-59.

Geiger, J. D. and J. I. Nagy (1986). "Distribution of adenosine deaminase activity in rat brain and spinal cord." J Neurosci **6**(9): 2707-2714.

Gidday, J. M., Y. B. Kim, et al. (1996). "Adenosine transport inhibition ameliorates postischemic hypoperfusion in pigs." Brain Res **734**(1-2): 261-268.

Goldowitz, D. and K. Hamre (1998). "The cells and molecules that make a cerebellum." Trends Neurosci **21**(9): 375-382.

Goodman, R. R. and S. H. Snyder (1982). "Autoradiographic localization of kappa opiate receptors to deep layers of the cerebral cortex may explain unique sedative and analgesic effects." Life Sci **31**(12-13): 1291-1294.

Gribkoff, V. K. and L. A. Bauman (1992). "Endogenous adenosine contributes to hypoxic synaptic depression in hippocampus from young and aged rats." J Neurophysiol **68**(2): 620-628.

Gu, J. G., I. O. Foga, et al. (1995). "Involvement of bidirectional adenosine transporters in the release of L-[3H]adenosine from rat brain synaptosomal preparations." J Neurochem **64**(5): 2105-2110.

Guillet, R. and L. Dunham (1995). "Neonatal caffeine exposure and seizure susceptibility in adult rats." Epilepsia **36**(8): 743-749.

Gundappa-Sulur, G., E. De Schutter, et al. (1999). "Ascending granule cell axon: an important component of cerebellar cortical circuitry." J Comp Neurol **408**(4): 580-596.

Hashimoto, K. and M. Kano (1998). "Presynaptic origin of paired-pulse depression at climbing fibre-Purkinje cell synapses in the rat cerebellum." J Physiol **506 ( Pt 2)**: 391-405.

Hashimoto, K. and M. Kano (2003). "Functional differentiation of multiple climbing fiber inputs during synapse elimination in the developing cerebellum." Neuron **38**(5): 785-796.

Hashimoto, K., T. Yoshida, et al. (2009). "Influence of parallel fiber-Purkinje cell synapse formation on postnatal development of climbing fiber-Purkinje cell synapses in the cerebellum." Neuroscience **162**(3): 601-611.

Hawkes, R. (2005). Cerebellum: Anatomy and Organization. Encyclopedia of Life Sciences, John Wiley & Sons, Ltd: Chichester.

Hioki, H., F. Fujiyama, et al. (2003). "Differential distribution of vesicular glutamate transporters in the rat cerebellar cortex." Neuroscience **117**(1): 1-6.

Jacobson, K. A., O. Nikodijevic, et al. (1993). "A role for central A3-adenosine receptors. Mediation of behavioral depressant effects." FEBS Lett **336**(1): 57-60.

Jimenez, A. I., E. Castro, et al. (1999). "Potentiation of ATP calcium responses by A2B receptor stimulation and other signals coupled to Gs proteins in type-1 cerebellar astrocytes." Glia **26**(2): 119-128.

Kawaji, K., H. Umeshima, et al. (2004). "Dual phases of migration of cerebellar granule cells guided by axonal and dendritic leading processes." Mol Cell Neurosci **25**(2): 228-240.

Kimura, M., N. Saitoh, et al. (2003). "Adenosine A(1) receptor-mediated presynaptic inhibition at the calyx of Held of immature rats." J Physiol **553**(Pt 2): 415-426.

Kinoshita, A., H. Ohishi, et al. (1996). "Presynaptic localization of a metabotropic glutamate receptor, mGluR4a, in the cerebellar cortex: a light and electron microscope study in the rat." Neurosci Lett **207**(3): 199-202.

Kocsis, J. D., D. L. Eng, et al. (1984). "Adenosine selectively blocks parallel-fiber-mediated synaptic potentials in rat cerebellar cortex." Proc Natl Acad Sci U S A **81**(20): 6531-6534.

Komuro, H. and E. Yacubova (2003). "Recent advances in cerebellar granule cell migration." Cell Mol Life Sci **60**(6): 1084-1098.

Konnerth, A., I. Llano, et al. (1990). "Synaptic currents in cerebellar Purkinje cells." Proc Natl Acad Sci U S A **87**(7): 2662-2665.

Kreitzer, A. C. and W. G. Regehr (2000). "Modulation of transmission during trains at a cerebellar synapse." J Neurosci **20**(4): 1348-1357.

Kukulski, F., J. Sevigny, et al. (2004). "Comparative hydrolysis of extracellular adenine nucleotides and adenosine in synaptic membranes from porcine brain cortex, hippocampus, cerebellum and medulla oblongata." Brain Res **1030**(1): 49-56.

Lahiri, S., C. H. Mitchell, et al. (2007). "Purines, the carotid body and respiration." Respir Physiol Neurobiol **157**(1): 123-129.

Laine, J. and H. Axelrad (1994). "The candelabrum cell: a new interneuron in the cerebellar cortex." J Comp Neurol **339**(2): 159-173.

Latini, S., C. Corsi, et al. (1995). "The source of brain adenosine outflow during ischemia and electrical stimulation." Neurochem Int **27**(3): 239-244.

Latini, S. and F. Pedata (2001). "Adenosine in the central nervous system: release mechanisms and extracellular concentrations." J Neurochem **79**(3): 463-484.

Ledent, C., J. M. Vaugeois, et al. (1997). "Aggressiveness, hypoalgesia and high blood pressure in mice lacking the adenosine A2a receptor." Nature **388**(6643): 674-678.

Lin, A. S., T. W. Uhde, et al. (1997). "Effects of intravenous caffeine administered to healthy males during sleep." Depress Anxiety **5**(1): 21-28.

Llaudet, E., N. P. Botting, et al. (2003). "A three-enzyme microelectrode sensor for detecting purine release from central nervous system." Biosens Bioelectron **18**(1): 43-52.

Lloyd, H. G. and B. B. Fredholm (1995). "Involvement of adenosine deaminase and adenosine kinase in regulating extracellular adenosine concentration in rat hippocampal slices." Neurochem Int **26**(4): 387-395.

Londos, C., D. M. Cooper, et al. (1980). "Subclasses of external adenosine receptors." Proc Natl Acad Sci U S A **77**(5): 2551-2554.

Lordkipanidze, T. and A. Dunaevsky (2005). "Purkinje cell dendrites grow in alignment with Bergmann glia." Glia **51**(3): 229-234.

Lorez, M., U. Humbel, et al. (2003). "Group III metabotropic glutamate receptors as autoreceptors in the cerebellar cortex." Br J Pharmacol **138**(4): 614-625.

Lorincz, A. and Z. Nusser (2008). "Specificity of immunoreactions: the importance of testing specificity in each method." J Neurosci **28**(37): 9083-9086.

Lujan, R. and R. Shigemoto (2006). "Localization of metabotropic GABA receptor subunits GABAB1 and GABAB2 relative to synaptic sites in the rat developing cerebellum." Eur J Neurosci **23**(6): 1479-1490.

MacVicar, B. A. and F. E. Dudek (1980). "Local synaptic circuits in rat hippocampus: interactions between pyramidal cells." Brain Res **184**(1): 220-223.

Mateos, J. M., J. Azkue, et al. (1998). "Localization of the mGlu4a metabotropic glutamate receptor in rat cerebellar cortex." Histochem Cell Biol **109**(2): 135-139.

Mauritz, K. H., J. Dichgans, et al. (1979). "Quantitative analysis of stance in late cortical cerebellar atrophy of the anterior lobe and other forms of cerebellar ataxia." Brain **102**(3): 461-482.

Michel, M. C., T. Wieland, et al. (2009). "How reliable are G-protein-coupled receptor antibodies?" Naunyn Schmiedebergs Arch Pharmacol **379**(4): 385-388.

Middleton, F. A. and P. L. Strick (1994). "Anatomical evidence for cerebellar and basal ganglia involvement in higher cognitive function." Science **266**(5184): 458-461.

Miniaci, M. C., P. Bonsi, et al. (2001). "Presynaptic modulation by group III metabotropic glutamate receptors (mGluRs) of the excitatory postsynaptic potential mediated by mGluR1 in rat cerebellar Purkinje cells." Neurosci Lett **310**(1): 61-65.

Mishina, M., K. Ishiwata, et al. (2007). "Evaluation of distribution of adenosine A2A receptors in normal human brain measured with [11C]TMSX PET." Synapse **61**(9): 778-784.

Miyazaki, T., M. Fukaya, et al. (2003). "Subtype switching of vesicular glutamate transporters at parallel fibre-Purkinje cell synapses in developing mouse cerebellum." Eur J Neurosci **17**(12): 2563-2572.

Morton, S. M. and A. J. Bastian (2003). "Relative contributions of balance and voluntary leg-coordination deficits to cerebellar gait ataxia." J Neurophysiol **89**(4): 1844-1856.

Morton, S. M. and A. J. Bastian (2004). "Cerebellar control of balance and locomotion." Neuroscientist **10**(3): 247-259.

Mugnaini, E., M. R. Dino, et al. (1997). "The unipolar brush cells of the mammalian cerebellum and cochlear nucleus: cytology and microcircuitry." Prog Brain Res **114**: 131-150.

Nakamura, A. and T. Uchihara (2004). "Dual enhancement of triple immunofluorescence using two antibodies from the same species." J Neurosci Methods **135**(1-2): 67-70.

Neale, S. A., J. Garthwaite, et al. (2001). "Metabotropic glutamate receptor subtypes modulating neurotransmission at parallel fibre-Purkinje cell synapses in rat cerebellum." Neuropharmacology **41**(1): 42-49.

Noji, T., A. Karasawa, et al. (2004). "Adenosine uptake inhibitors." Eur J Pharmacol **495**(1): 1-16.

Otsuguro, K., Y. Yamaji, et al. (2006). "Involvement of adenosine in depression of synaptic transmission during hypercapnia in isolated spinal cord of neonatal rats." J Physiol **574**(Pt 3): 835-847.

Pak, M. A., H. L. Haas, et al. (1994). "Inhibition of adenosine kinase increases endogenous adenosine and depresses neuronal activity in hippocampal slices." Neuropharmacology **33**(9): 1049-1053.

Patel, B. T. and N. Tudball (1986). "Localization of S-adenosylhomocysteine hydrolase and adenosine deaminase immunoreactivities in rat brain." Brain Res **370**(2): 250-264.

Pearson, R. A., N. Dale, et al. (2005). "ATP released via gap junction hemichannels from the pigment epithelium regulates neural retinal progenitor proliferation." Neuron **46**(5): 731-744.

Pedata, F., S. Latini, et al. (1993). "Investigations into the adenosine outflow from hippocampal slices evoked by ischemia-like conditions." J Neurochem **61**(1): 284-289.

Pekhletski, R., R. Gerlai, et al. (1996). "Impaired cerebellar synaptic plasticity and motor performance in mice lacking the mGluR4 subtype of metabotropic glutamate receptor." J Neurosci **16**(20): 6364-6373.

Porkka-Heiskanen, T., R. E. Strecker, et al. (1997). "Adenosine: a mediator of the sleep-inducing effects of prolonged wakefulness." Science **276**(5316): 1265-1268.

Press, D. A. and M. J. Wall (2008). "Expression of cocaine- and amphetamine-regulated transcript (CART) peptides at climbing fibre-Purkinje cell synapses in the rat vestibular cerebellum." Neuropeptides **42**(1): 39-46.

Psarropoulou, C., G. Kostopoulos, et al. (1990). "An electrophysiological study of the ontogenesis of adenosine receptors in the CA1 area of rat hippocampus." Brain Res Dev Brain Res **55**(1): 147-150.

Ralevic, V. and G. Burnstock (1998). "Receptors for purines and pyrimidines." Pharmacol Rev **50**(3): 413-492.

Rand, M. K., D. A. Wunderlich, et al. (1998). "Adaptive changes in responses to repeated locomotor perturbations in cerebellar patients." Exp Brain Res **122**(1): 31-43.

Rathbone, M. P., P. J. Middlemiss, et al. (1999). "Trophic effects of purines in neurons and glial cells." Prog Neurobiol **59**(6): 663-690.

Rebola, N., J. E. Coelho, et al. (2003). "Decrease of adenosine A1 receptor density and of adenosine neuromodulation in the hippocampus of kindled rats." Eur J Neurosci **18**(4): 820-828.

Reddington, M. and R. Pusch (1983). "Adenosine metabolism in a rat hippocampal slice preparation: incorporation into S-adenosylhomocysteine." J Neurochem **40**(1): 285-290.

Rex, C. S., E. A. Kramar, et al. (2005). "Long-term potentiation is impaired in middle-aged rats: regional specificity and reversal by adenosine receptor antagonists." J Neurosci **25**(25): 5956-5966.

Rivkees, S. A., S. L. Price, et al. (1995). "Immunohistochemical detection of A1 adenosine receptors in rat brain with emphasis on localization in the hippocampal formation, cerebral cortex, cerebellum, and basal ganglia." Brain Res **677**(2): 193-203.

Rosin, D. L., A. Robeva, et al. (1998). "Immunohistochemical localization of adenosine A2A receptors in the rat central nervous system." J Comp Neurol **401**(2): 163-186.

Sala-Newby, G. B., A. C. Skladanowski, et al. (1999). "The mechanism of adenosine formation in cells. Cloning of cytosolic 5'-nucleotidase-I." J Biol Chem **274**(25): 17789-17793.

Schmahmann, J. D. and J. C. Sherman (1998). "The cerebellar cognitive affective syndrome." <u>Brain</u> **121 ( Pt 4)**: 561-579.

Schoen, S. W., M. B. Graeber, et al. (1987). "Light and electron microscopical immunocytochemistry of 5'-nucleotidase in rat cerebellum." <u>Histochemistry</u> **87**(2): 107-113.

Schuller, U., E. C. Lamp, et al. (2001). "Developmental expression of heterotrimeric G-proteins in the murine cerebellar cortex." <u>Histochem Cell Biol</u> **116**(2): 149-159.

Sillitoe, R. V. and A. L. Joyner (2007). "Morphology, molecular codes, and circuitry produce the three-dimensional complexity of the cerebellum." <u>Annu Rev Cell Dev Biol</u> **23**: 549-577.

Stell, B. M., P. Rostaing, et al. (2007). "Activation of presynaptic GABA(A) receptors induces glutamate release from parallel fiber synapses." <u>J Neurosci</u> **27**(34): 9022-9031.

Stenberg, D., E. Litonius, et al. (2003). "Sleep and its homeostatic regulation in mice lacking the adenosine A1 receptor." <u>J Sleep Res</u> **12**(4): 283-290.

Studer, F. E., D. E. Fedele, et al. (2006). "Shift of adenosine kinase expression from neurons to astrocytes during postnatal development suggests dual functionality of the enzyme." <u>Neuroscience</u> **142**(1): 125-137.

Svenningsson, P., C. Le Moine, et al. (1997). "Cellular expression of adenosine A2A receptor messenger RNA in the rat central nervous system with special reference to dopamine innervated areas." <u>Neuroscience</u> **80**(4): 1171-1185.

Sweeney, M. I. (1996). "Adenosine release and uptake in cerebellar granule neurons both occur via an equilibrative nucleoside carrier that is modulated by G proteins." J Neurochem **67**(1): 81-88.

Takahashi, K. A. and D. J. Linden (2000). "Cannabinoid receptor modulation of synapses received by cerebellar Purkinje cells." J Neurophysiol **83**(3): 1167-1180.

Takahashi, M., Y. Kovalchuk, et al. (1995). "Pre- and postsynaptic determinants of EPSC waveform at cerebellar climbing fiber and parallel fiber to Purkinje cell synapses." J Neurosci **15**(8): 5693-5702.

Timmann, D. and I. Daum (2007). "Cerebellar contributions to cognitive functions: a progress report after two decades of research." Cerebellum **6**(3): 159-162.

Vacas, J., M. Fernandez, et al. (2003). "Adenosine modulation of [Ca2+]i in cerebellar granular cells: multiple adenosine receptors involved." Brain Res **992**(2): 272-280.

van Calker, D., M. Muller, et al. (1979). "Adenosine regulates via two different types of receptors, the accumulation of cyclic AMP in cultured brain cells." J Neurochem **33**(5): 999-1005.

Wall, M. and N. Dale (2008). "Activity-dependent release of adenosine: a critical re-evaluation of mechanism." Curr Neuropharmacol **6**(4): 329-337.

Wall, M. J., A. Atterbury, et al. (2007). "Control of basal extracellular adenosine concentration in rat cerebellum." J Physiol **582**(Pt 1): 137-151.

Wall, M. J. and N. Dale (2007). "Auto-inhibition of rat parallel fibre-Purkinje cell synapses by activity-dependent adenosine release." J Physiol **581**(Pt 2): 553-565.

Wang, T. F. and G. Guidotti (1998). "Widespread expression of ecto-apyrase (CD39) in the central nervous system." Brain Res **790**(1-2): 318-322.

Weruaga, E., J. R. Alonso, et al. (1998). "Nonspecific labeling of myelin with secondary antisera and high concentrations of Triton X-100." J Histochem Cytochem **46**(1): 109-118.

Wink, M. R., E. Braganhol, et al. (2003). "Extracellular adenine nucleotides metabolism in astrocyte cultures from different brain regions." Neurochem Int **43**(7): 621-628.

Wong, A. Y., B. Billups, et al. (2006). "Endogenous activation of adenosine A1 receptors, but not P2X receptors, during high-frequency synaptic transmission at the calyx of Held." J Neurophysiol **95**(6): 3336-3342.

Xu, F., J. Xu, et al. (2006). "Adenosine stimulates depolarization and rise in cytoplasmic [Ca2+] in type I cells of rat carotid bodies." Am J Physiol Cell Physiol **290**(6): C1592-1598.

Yaar, R., E. D. Lamperti, et al. (2002). "Activity of the A3 adenosine receptor gene promoter in transgenic mice: characterization of previously unidentified sites of expression." FEBS Lett **532**(3): 267-272.

Yager, J. Y. and J. A. Thornhill (1997). "The effect of age on susceptibility to hypoxic-ischemic brain damage." Neurosci Biobehav Rev **21**(2): 167-174.

Yoshioka, K., R. Hosoda, et al. (2002). "Hetero-oligomerization of adenosine A1 receptors with P2Y1 receptors in rat brains." FEBS Lett **531**(2): 299-303.

Yu, J. and E. Eidelberg (1983). "Recovery of locomotor function in cats after localized cerebellar lesions." Brain Res **273**(1): 121-131.

Yuan, Y. and W. D. Atchison (1999). "Comparative effects of methylmercury on parallel-fiber and climbing-fiber responses of rat cerebellar slices." <u>J Pharmacol Exp Ther</u> **288**(3): 1015-1025.

Zhang, G., P. H. Franklin, et al. (1990). "Anticonvulsant effect of N-ethylcarboxamidoadenosine against kainic acid-induced behavioral seizures in the rat prepiriform cortex." <u>Neurosci Lett</u> **114**(3): 345-350.

Zhang, G., P. H. Franklin, et al. (1993). "Manipulation of endogenous adenosine in the rat prepiriform cortex modulates seizure susceptibility." <u>J Pharmacol Exp Ther</u> **264**(3): 1415-1424.

Zhou, Q. Y., C. Li, et al. (1992). "Molecular cloning and characterization of an adenosine receptor: the A3 adenosine receptor." <u>Proc Natl Acad Sci U S A</u> **89**(16): 7432-7436.

Zimmermann, H. (2000). "Extracellular metabolism of ATP and other nucleotides." <u>Naunyn Schmiedebergs Arch Pharmacol</u> **362**(4-5): 299-309.

Zucker, R. S. and W. G. Regehr (2002). "Short-term synaptic plasticity." <u>Annu Rev Physiol</u> **64**: 355-405.

# Control of basal extracellular adenosine concentration in rat cerebellum

Mark J. Wall, Alison Atterbury and Nicholas Dale

*Neuroscience Group, Department of Biological Sciences, University of Warwick, Coventry CV4 7AL, UK*

**To re-examine how the basal extracellular concentration of adenosine is regulated in acutely isolated cerebellar slices we have combined electrophysiological and microelectrode biosensor measurements. In almost all cases, synaptic transmission was tonically inhibited by adenosine acting via $A_1$ receptors. By contrast, in most slices, the biosensors did not measure an adenosine tone but did record a spatially non-uniform extracellular tone of the downstream metabolites (inosine and hypoxanthine). Most of the extracellular hypoxanthine arose from the metabolism of inosine by ecto-purine nucleoside phosphorylase (PNP). Adenosine kinase was the major determinant of adenosine levels, as its inhibition increased both adenosine concentration and $A_1$ receptor-mediated synaptic inhibition. Breakdown of adenosine by adenosine deaminase was the major source of the inosine/hypoxanthine tone. However adenosine deaminase played a minor role in determining the level of adenosine at synapses, suggesting a distal location. Blockade of adenosine transport (by NBTI/dipyridamole) had inconsistent effects on basal levels of adenosine and synaptic transmission. Unexpectedly, application of NBTI/dipyridamole prevented the efflux of adenosine resulting from block of adenosine kinase at only a subset of synapses. We conclude that there is spatial variation in the functional expression of NBTI/dipyridamole-sensitive transporters. The increased spatial and temporal resolution of the purine biosensor measurements has revealed the complexity of the control of adenosine and purine tone in the cerebellum.**

The purine adenosine is an important neuromodulator, with both excitatory and inhibitory actions within the CNS. This purine molecule is involved in diverse processes including locomotion, sleep and respiration, and provides neuroprotection during hypoxia/ischaemia. Although the basal extracellular levels of adenosine in the brain are low (Newman & McIlwain, 1977; Dunwiddie & Diao, 1994), there is still sufficient to tonically activate high-affinity $A_1$ receptors and produce synaptic inhibition (Dunwiddie & Diao, 1994; Takahashi *et al.* 1995; Dittman & Regehr, 1996). Regulation of the extracellular level of adenosine in the brain is crucial, since small changes in adenosine levels will affect the degree of synaptic inhibition, and thus modulate neural processing.

The extracellular concentration of adenosine will be determined by the balance of production and elimination. In many cases, the source and mechanism of adenosine release are unclear but could occur via ATP metabolism (released by exocytosis, Edwards *et al.* 1992; Jo & Schlichter, 1999, or released through gap junction hemi-channels, Arcuino *et al.* 2002; Stout *et al.* 2002; Pearson *et al.* 2005),

transport from the cell cytoplasm (Craig & White, 1993; Gu *et al.* 1995; Sweeney, 1996) or possibly by the exocytosis of adenosine itself (Wall & Dale, 2007). The actions of adenosine are terminated by a combination of metabolism to inosine (by the enzyme adenosine deaminase) and by translocation into neurons or glia by either equilibrative transporters such as ENT1 and ENT2 or concentrative transporters (for review see Noji *et al.* 2004; Baldwin *et al.* 2004).

Once internalised, adenosine can be phosphorylated (by adenosine kinase) to form AMP, thus maintaining low levels of intracellular adenosine (for review see Boison, 2006). Because the levels of adenosine are determined by a complex interplay of enzymes and transporters, several studies have investigated the components that contribute to determining extracellular adenosine concentration. In many studies blocking adenosine kinase has a major effect on adenosine concentration, whereas blockade of adenosine deaminase has a much smaller effect (Zhang *et al.* 1993; Pak *et al.* 1994; Lloyd & Fredholm, 1995).

The aim of this study is two-fold: firstly to investigate whether recently developed biosensors can be used to determine what controls the basal levels of adenosine in brain slices. Biosensors have inherently better spatial and temporal resolution than other methods such as HPLC or microdialysis, for measuring purine levels. Biosensors have been successfully used to investigate increases in adenosine during episodes of ischaemia, hypoxia and hypercapnia (Dale *et al.* 2000; Frenguelli *et al.* 2003, 2007; Dulla *et al.* 2005) and have been used to measure adenosine release following electrical stimulation (Wall & Dale, 2007). However, measurement of the basal tone of adenosine is more challenging as the concentration of adenosine will be low and may be more difficult to detect against a non-uniform background of downstream adenosine metabolites.

The second aim is to investigate adenosine levels in the cerebellum, since relatively little is known about how the extracellular concentration of adenosine is controlled in this part of the brain. There is growing evidence that adenosine plays an important role in the processing of information by cerebellar circuits. Adenosine is concentrated in the soma and dendrites of cerebellar Purkinje cells (Braas *et al.* 1986), and adenosine $A_1$ receptors are expressed within the cerebellum (Rivkees *et al.* 1995). The tonic activation of $A_1$ receptors, producing synaptic inhibition, provides indirect evidence that an extracellular tone of adenosine is present in cerebellar slices (Takahashi *et al.* 1995; Dittman & Regehr, 1996). The source of this extracellular adenosine is unclear, but in recent studies, Wall & Dale (2007) have directly measured adenosine release in the cerebellum and Beierlein & Regehr (2006) have reported the release of ATP from parallel fibres. The enzymes required for purine metabolism are present in the cerebellum: ecto-ATPase (CD39, Wang & Guidotti, 1998), $5'$nucleotidase (Schoen *et al.* 1987) and adenosine deaminase (Geiger & Nagy, 1986). Nucleoside transporters are also expressed in the cerebellum (Anderson *et al.* 1999*a,b*). However, the relative importance of adenosine transport, phosphorylation (by adenosine kinase) and metabolism (by adenosine deaminase) in the regulation of the adenosine tone remains uncertain. Studies of synaptic membranes, cultured glia and homogenised brain tissue suggest that adenosine deaminase activity in the cerebellum is comparable to or higher than in other brain regions (Yamada *et al.* 1998; Wink *et al.* 2003; Kukulski *et al.* 2004). However the physiological relevance of data from such studies is unclear.

## Methods

### Preparation of cerebellar slices

Parasagittal or transverse slices of cerebellar vermis (400 $\mu$m) were prepared from male Wistar rats, at post-natal days 21–28 (P21–28). As described previously (Wall & Usowicz, 1997) and in accordance with the UK Animals (Scientific Procedures) Act 1986, male rats were killed by cervical dislocation and decapitated. The cerebellum was rapidly removed and slices were cut on a Microm HM 650V microslicer in cold (2–4°C) high $Mg^{2+}$, low $Ca^{2+}$ aCSF, composed of (mM): 127 NaCl, 1.9 KCl, 7 $MgCl_2$, 0.5 $CaCl_2$, 1.2 $KH_2PO_4$, 26 $NaHCO_3$, 10 D-glucose (pH 7.4 when bubbled with 95% O2 and 5% CO2, 300 mosmol l$^{-1}$). Slices were stored in normal aCSF (1.3 mM $MgCl_2$, 2.4 mM $CaCl_2$) at room temperature for 1–6 h before recording.

### Extracellular recording

An individual slice was transferred to a recording chamber, submerged in aCSF and perfused at 6 ml min$^{-1}$ (30–35°C). Peristaltic pumps were used to pump aCSF in and out of the recording chamber, thus ensuring a constant flow rate. The slice was placed upon a suspended grid to allow perfusion of the slice from above and below and thus reduce the likelihood of hypoxia. Furthermore, all solutions were vigorously bubbled (95% O2/5% CO2) and all tubing had low gas permeability (Tygon). For the stimulation of parallel fibres, square voltage pulses (2–5 V, 200 $\mu$s duration) were delivered by an isolated pulse stimulator (model 2100 AM systems Everett WA, USA) via a concentric bipolar metal stimulating electrode (FHC) placed on the surface of the molecular layer in a transverse slice. The recording electrode (an aCSF-filled microelectrode) was placed on the same track along which the parallel fibres travel ('on-beam' Yuan & Atchison, 1999). A typical extracellular field potential consisted of an initial component which persisted in either 10 $\mu$M CNQX or 5 mM kynurenate but was blocked by 1 $\mu$M TTX (parallel fibre volley) followed by a component which could be blocked by 1 $\mu$M TTX and greatly reduced by either 10 $\mu$M CNQX or 5 mM kynurenate. This component is probably produced by parallel fibre-mediated glutamatergic excitatory synaptic currents and subsequent action potentials in Purkinje cells and interneurons (Clark & Barbour, 1997). Parallel fibre (PF) EPSP amplitude was estimated from the CNQX-/kynurenate-sensitive potential, which was measured by subtracting what remained in CNQX/kynurenate from control potentials. Confirmation of PF EPSP identity was achieved by evoking pairs of EPSPs (interval 50 ms) and observing facilitation (Atluri & Regehr, 1996) and by examining the pharmacological profile (inhibition by $A_1$, $GABA_B$ and mGlu4R receptor agonists). Pairs of PF EPSPs were evoked at 0.1 Hz, and the amplitude of the first EPSP was used as a measure of adenosine $A_1$ receptor activation. The paired pulse ratio (EPSP$_2$/EPSP$_1$) was used to test for a presynaptic action on release probability. Extracellular recordings were made using an ISO-DAM extracellular

amplifier (WPI), filtered at 1 kHz and digitised online (10 kHz) with a Digidata 1322A (Axon Instruments) controlled by 9.2 (Axon pCLAMP).

## Purine biosensors

Sensors were obtained from Sarissa Biomedical Ltd (Coventry UK). In brief, the adenosine sensor consisted of three entrapped enzymes (adenosine deaminase, AD, purine nucleoside phosphorylase, PNP and xanthine oxidase, XO), within a matrix that was deposited around a 25–50 $\mu$M platinum or platinum/iridium (90/10) wire (Llaudet *et al.* 2003). The biosensor had an exposed length of $\sim$500 $\mu$m that was screened with an inner permselectivity layer to greatly reduce responses to electro-active interferents (such as 5-HT, noradrenaline, dopamine and ascorbate). It was then coated with enzymes to make it capable of detecting purines. Five types of purine biosensor were used in this study to identify released substances. Firstly, a screened null sensor, possessing the deposition matrix but no enzymes, was used to control for the release of any non-specific electro-active interferents. Secondly, screened biosensors containing just XO (only responsive to hypoxanthine, HYPO), PNP and XO (responsive to inosine and hypoxanthine, INO) and PNP, XO and AD (responsive to inosine, hypoxanthine and adenosine, ADO) were used. The difference signal between these three types of biosensors gave the specific hypo-xanthine, inosine and adenosine signals. Matching the sizes and sensitivities of the biosensor types as well as careful positioning into or above the slice was vital to optimise the differential recordings. The screened ATP biosensor (Llaudet *et al.* 2005) consisted of the entrapped enzymes glycerol kinase (GK) and glycerol-3-phosphate oxidase (G3POx). Glycerol 2 mM was included in solutions, as glycerol is a co-substrate required for ATP detection. A full description of the properties of the biosensors has been published. They show a linear response to increasing concentration of analyte, are fast to respond and have a 10–90% rise time of less than 10 s (Llaudet *et al.* 2003, 2005).

The biosensors were either carefully inserted (at an angle of $\sim$70 deg) either into the molecular layer or positioned just above the surface of the slice (either at an angle of $\sim$70 deg or bent so their longitudinal surface was parallel to the slice surface). Biosensors were calibrated with known concentrations (10 $\mu$M) of adenosine, inosine, hypoxanthine and ATP. Calibration was performed before the slice was present in the perfusion chamber and after the slice had been removed; this allowed measurement of any reduction in sensitivity during the experiment.

To quantify the concentrations of adenosine, inosine and hypoxanthine, it was assumed that the concentrations of these purines were homogenous in the slice and thus the calibrated signals can be subtracted from

one another. The HYPO sensor will only detect hypoxanthine and thus this signal can be subtracted from the signal on the INO sensor to give the inosine signal. The signal from the INO sensor (comprising inosine and hypoxanthine) can be subtracted from the signal on the ADO sensor to give the specific adenosine signal. For example, assuming identical sensitivity for the ADO, INO and HYPO sensors and that 10 $\mu$M of each analyte (adenosine, inosine or hypoxanthine) produces 3000 pA. Clearly the ADO sensor will produce a current of 3000 pA in response to 10 $\mu$M adenosine, 10 $\mu$M inosine or 10 $\mu$M hypoxanthine, whereas the HYPO sensor will only respond to hypoxanthine. If upon exposure to tissue, the HYPO sensor produces a current of 300 pA, then the hypoxanthine concentration in the tissue is (300 pA/3000 pA $\times$ 10 $\mu$M) = 1 $\mu$M. If The INO sensor produces a current of 700 pA, then subtracting the current due to hypoxanthine (300 pA) leaves 400 pA which is the current due to inosine detection. Thus the inosine concentration in the tissue is (400 pA/3000 pA $\times$ 10 $\mu$M) = 1.3 $\mu$M. The signal from the INO sensor can then be subtracted (in a similar way) from the ADO sensor to give the specific adenosine signal. In reality, because the sensitivity of sensors to inosine and hypoxanthine will differ slightly, this has to be taken into account during subtraction by appropriate weighting. Note that this differential subtraction procedure only gives valid results if the metabolites are distributed in a uniform identical manner. If this is not the case, for example there are concentration 'hotspots', it will be virtually impossible to place the different sensors at identical relative locations with respect to the hotspots. Hence the signals will not be equivalent from the different sensors. Thus the detection of a purine tone will be accurate but its subdivision into concentrations of adenosine, inosine and hypoxanthine may be less so. Sensor signals were acquired at 1 kHz with a Digidata 1322A or a MiniDigi (Axon) using Pclamp 9.2 or Axoscope 9.2 (Axon). All values are mean $\pm$ SEM.

## Drugs

All drugs were made up as 10–100 mM stock solutions, stored frozen and then thawed and diluted with aCSF on the day of use. Iodotubercidin, pyridoxal phosphate-6-azo(benzene-2,4-disulfonic acid) tetrasodium salt (PPADs), suramin, Evans Blue, $\alpha$,$\beta$-methylene-ADP, adenosine, inosine, hypoxanthine, 6-[(4-nitrobenzyl)thiol]-9-$\beta$-D-ribofuranosylpurine (NBTI) 8-cyclopentyl-theophylline (8CPT) and dipyridamole were purchased from Sigma. Erythro-9-(2-hydroxy-3-nonyl) adenine (EHNA), 6-cyano-7-nitroquinoxaline-2,3-dione (CNQX), ARL67156 and D($-$)-2-amino-5-phosphonopentanoic acid (AP5) were purchased from Tocris-Cookson. ATP was purchased from Roche.
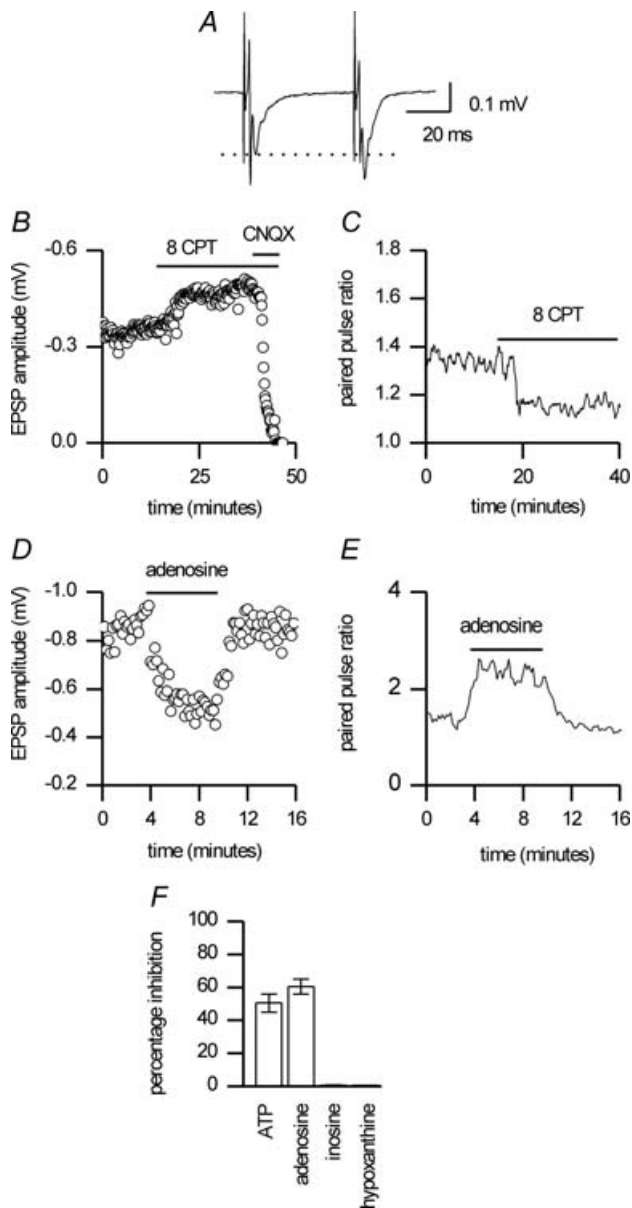
**Figure 1. Endogenous adenosine inhibits parallel fibre to Purkinje cell synaptic transmission**
*A*, average of 50 pairs (interval 50 ms) of parallel fibre–Purkinje cell (PF) EPSPs illustrating paired pulse facilitation (greater amplitude of second EPSP compared to first). PF EPSPs were averaged by aligning on the stimulus artefact. *B*, the $A_1$ receptor antagonist 8CPT (1 $\mu$M) increased PF EPSP amplitude (31%) demonstrating tonic activation of $A_1$ receptors. PF EPSPs were blocked by CNQX (10 $\mu$M), confirming their production through glutamate receptor activation. Graph plots the amplitude of individual PF EPSPs against time. *C*, The antagonist 8CPT (1 $\mu$M) decreased the paired pulse ratio, confirming a presynaptic site of action. Graph plots the paired pulse ratio against time for the PF EPSPs in *B*. The line is the mean paired pulse ratio for five EPSPs. *D*, adenosine (100 $\mu$M) reversibly decreased PF EPSP amplitude (48%). Graph plots the amplitude of individual PF EPSPs against time. *E*, adenosine produced a marked increase in the paired pulse ratio, indicating a presynaptic site of action. Graph plots the paired pulse ratio against time for the PF EPSPs in *D*. The line is the mean paired pulse ratio for three EPSPs. *F*, graph summarising the actions of purines on PF EPSP amplitude ($n = 5$–12).

# Results

## Parallel fibre EPSPs are tonically inhibited by adenosine in the majority of slices

Previous studies have shown that $A_1$ adenosine receptors on parallel fibre–Purkinje cell synapses tonically inhibit synaptic transmission, suggesting the presence of an extracellular adenosine tone (Kocsis *et al.* 1984; Takahashi *et al.* 1995; Dittman & Regehr, 1996). To confirm the presence of extracellular adenosine in our cerebellar slices, we have studied parallel fibre–Purkinje cell excitatory post-synaptic potentials (PF EPSPs). The identity of PF EPSPs was confirmed by the presence of paired pulse facilitation (PPF, with a 50 ms interval the paired pulse ratio was $1.3 \pm 0.01$, $n = 20$, Fig. 1*A*) and the sensitivity of PF EPSPs to the glutamate receptor antagonists CNQX (10 $\mu$M) or kynurenic acid (5 mM, Fig. 1*B*).

We confirmed previous reports (Takahashi *et al.* 1995; Dittman & Regehr, 1996) that inhibitory $A_1$ receptors on parallel fibre–Purkinje cell synapses are tonically activated in slices, as application of $A_1$ receptor antagonists enhanced PF EPSP amplitude (1 $\mu$M 8CPT or 200 $\mu$M theophylline $46.1 \pm 8.6\%$ increase) and significantly reduced the paired pulse ratio (from $1.3 \pm 0.04$ to $1.2 \pm 0.03$, Fig. 1*B* and *C*) in 17 out of 19 slices. In two slices, the antagonists had no effect on PF EPSP amplitude. The continual activation of $A_1$ receptors is probably a consequence of the presence of endogenous adenosine, since application of adenosine (100 $\mu$M) reduced PF EPSP amplitude by $60.5 \pm 4.8\%$ and increased the paired pulse ratio from $1.3 \pm 0.06$ to $1.6 \pm 0.08$, ($n = 12$, Fig. 1*D* and *E*). As the applied adenosine could be metabolised to inosine and hypoxanthine, the activity of these metabolites on synaptic transmission was assessed. As expected, neither inosine nor hypoxanthine (100 $\mu$M) had any significant effect on either the PF EPSP amplitude or the paired pulse ratio ($n = 5$, Fig. 1*F*). ATP (100 $\mu$M) also reduced EPSP amplitude ($50 \pm 6.5\%$). Since this inhibition was blocked by $A_1$ receptor antagonists ($n = 6$), ATP must be metabolised to adenosine. Our results confirm previous reports that there is a tone of extracellular adenosine in the cerebellum which inhibits synaptic transmission and is present in the majority ($\sim$90%) of slices.

## Biosensors detect adenosine metabolites but not adenosine in most cerebellar slices

We have used microelectrode biosensors to directly measure the concentration of extracellular adenosine present in cerebellar slices. The use of different sensors allows the detection of ATP (a possible source of adenosine), adenosine and the adenosine metabolites (inosine and hypoxanthine). A null sensor was also

present to control for any non-specific electro-active interferents. To verify our findings we used two different methods. Firstly, we measured the current produced when purine biosensors were moved close to the slice surface (Fig. 2A). This method has the advantage that it is non-invasive and thus any purines detected do not result from biosensor-mediated tissue damage. Movement of null sensors (with no enzyme cascade, $n = 10$) close to the slice surface produced either no current or a small negative current; thus any electro-interferents released from the slice are not detected by the biosensors. The signal on ATP biosensors ($n = 10$) was no different from that on null sensors (Fig. 2A), and thus the level of ATP at the slice surface is below the limits of detection by the biosensors (~60 nM). In contrast, large currents were measured when ADO, INO and HYPO biosensors were moved close to the

slice surface (Fig. 2A). After calibration and subtraction (Fig. 2B), to determine the specific analyte concentration (see Methods), adenosine was only detected in a single slice (1 out of 12 slices at 1.5 $\mu$M), whereas hypoxanthine was detected in all slices (0.8 ± 0.2 $\mu$M, 12 of 12 slices) and inosine was detected in 50% of slices (0.5 ± 0.1 $\mu$M, in 6 slices, Fig. 2B).

The second method measured the extracellular concentration of purines within the cerebellum, by carefully inserting purine biosensors into the slice. After 30 min biosensors were removed from the tissue and the resultant deflection in baseline current was used as a measure of purine concentration within the slice. If extracellular purines are present, removal of the biosensor from the slice should result in a rapid fall in baseline, as the purines will no longer be measured. This method avoids



**Figure 2. Adenosine metabolites, but not adenosine, can be measured in the extracellular space of cerebellar slices**
A, example of biosensor traces from an experiment to measure the concentration of purines at the slice surface. Superimposed traces from ADO, INO, HYPO and ATP sensors. After the biosensors were moved close to the slice surface there was a rapid increase in the baseline current of ~300–500 pA on the ADO, INO and HYPO sensors. Moving the ATP biosensor close to the slice produced a small drop in the baseline current. B, the traces from A were normalised by calibration and subtracted to give the amounts of adenosine, inosine and hypoxanthine detected at the slice surface (see Methods). C, graph plots the mean concentration of purines measured at the surface of 12 cerebellar slices. Currents were scaled by sensor calibration and then subtracted (as in B). D, examples of experiments where biosensors were used to measure the purine concentration within slices. Biosensors were carefully pushed into slices, left in position for ~30 min and then withdrawn. The top panel shows the response following removal of an ATP sensor from a slice. There is a small sustained increase in current (similar to that observed on null sensors) and thus no ATP was detected. In contrast when an inosine (INO) sensor was removed there was a sustained fall in current as a result of terminating purine detection (bottom panel). The transient upward deflections (arrows) are presumably due to cell damage and the release and resultant metabolism of ATP. E, graph plotting the mean concentration of purines measured in the extracellular space of 16 cerebellar slices. Currents were scaled by sensor calibration and then subtracted (see Methods).
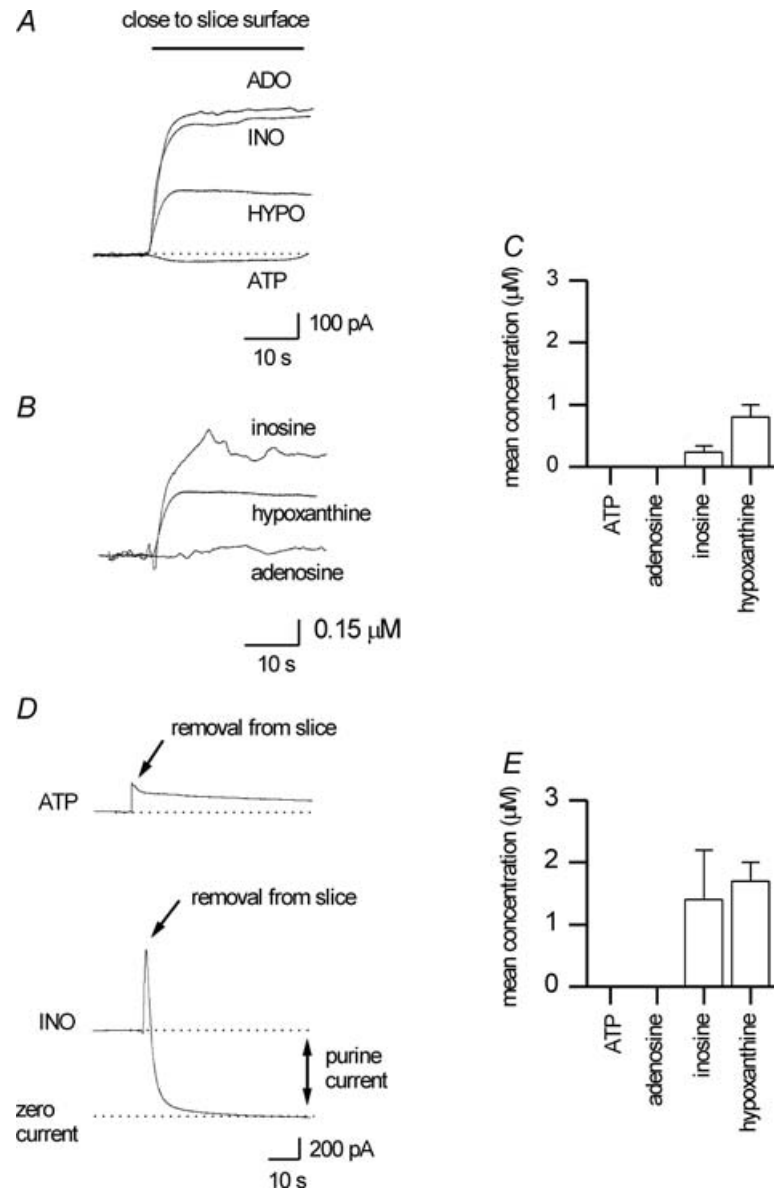
the detection of purine release due to tissue damage during sensor insertion. Removal of null sensors produced either no current deflection or a small positive current deflection. The response of ATP biosensors was no different from null sensors (32–34°C $n = 20$ slices, room temperature $n = 10$ slices, Fig. 2*D*), and thus no ATP tone could be detected within the tissue. However clear falls in baseline current were observed following the removal of ADO, INO and HYPO biosensors from slices ($n = 6$ slices, Fig. 2*D*). After calibration and subtraction, hypoxanthine was detected in 81% of the slices ($1.8 \pm 0.3 \mu$M, $n = 13$ slices), inosine was detected in 50% of the slices ($2.5 \pm 1.1 \mu$M, $n = 8$ slices) and adenosine was detected in only 12.5% of the slices ($1.2 \pm 0.5 \mu$M, $n = 2$ slices Fig. 2*E*). Thus both methods of purine measurement gave similar results: no ATP was detected, an adenosine tone was occasionally

present and most slices exhibited a tone for inosine and or hypoxanthine.

The inability to reliably detect adenosine with the biosensors contrasts with electrophysiological studies on synaptic transmission that demonstrate an extracellular adenosine tone in 90% of cases. Adenosine could be metabolised to inosine and hypoxanthine before it reaches the sensors, and may thus be present only in the restricted space around parallel fibre synapses. However it is very unlikely that the sensors will not sample from this compartment, as the synapses are present at a high density in the molecular layer.

A more likely explanation for this discrepancy is that the subtraction procedure used to measure adenosine is inaccurate. This could arise from a non-uniform distribution of the analytes adenosine, inosine and hypoxanthine, which would reduce the accuracy of the subtraction procedure (see Methods) In many cases, subtraction of the calibrated INO sensor signals implied a negative concentration of adenosine (clearly impossible), strongly indicating non-uniform concentrations of inosine and hypoxanthine. Our data suggest considerable variation in the levels of inosine ($0$–$0.6 \mu$M) and hypoxanthine (range $0.1$–$3 \mu$M) between slices. If this reflects hotspots of release/production, depending on enzyme location relative to sensor position, then the differential measurement procedure will not give accurate concentrations of adenosine and inosine.
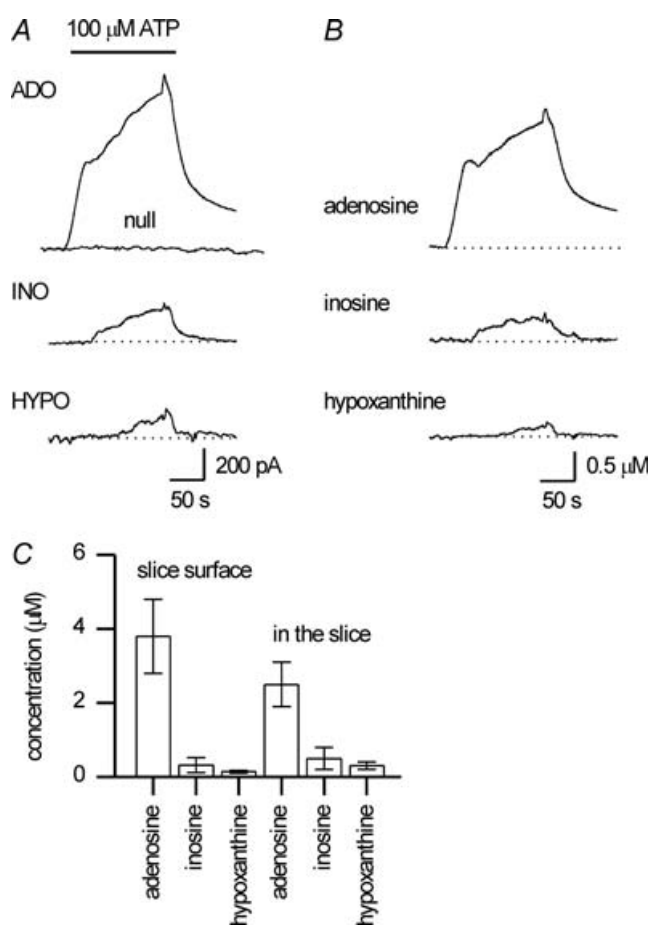


**Figure 3. Exogenous ATP is metabolised by cerebellar slices**
*A*, example traces from adenosine (ADO), null, inosine (INO) and hypoxanthine (HYPO) biosensors placed on the surface of a cerebellar slice. Following application of 100 $\mu$M ATP, currents were produced on all the sensors except the null. *B*, the traces from *A*, calibrated and subtracted illustrating the metabolism of ATP to adenosine, inosine, and hypoxanthine. *C*, graph plots the mean concentration of ATP metabolites measured at the surface of slices ($n = 6$) and within slices ($n = 7$) following application of 100 $\mu$M ATP.

### Exogenous ATP and adenosine are metabolised through to hypoxanthine

To test whether: (1) adenosine can be metabolised to inosine and hypoxanthine (to give the observed purine tone), (2) adenosine can be detected in cerebellar slices, and (3) there are hotspots of extracellular purine metabolism, exogenous ATP was applied to slices and the real-time production of metabolites was measured using ADO, INO and HYPO biosensors. As before, this experiment was carried out in two ways: firstly non-invasively with sensors placed close to the slice surface, and secondly with the biosensors placed within the slice. The inflow was changed from control saline to 100 $\mu$M ATP for 5 min. The exact duration of the ATP application is not known (as the 5 min includes the time taken for the ATP to reach the bath and exchange with the bath solution). However, because the flow rate is constant, the applications will be reproducible. Application of ATP rapidly resulted in the detection of $3.8 \pm 1 \mu$M adenosine, $0.3 \pm 0.2 \mu$M inosine and $0.14 \pm 0.03 \mu$M hypoxanthine at the slice surface ($n = 6$, Fig. 3). Similar results were found when the biosensors were placed within the slice ($2.5 \pm 0.6 \mu$M adenosine, $0.5 \pm 0.3 \mu$M inosine and $0.3 \pm 0.1 \mu$M hypo-xanthine, $n = 7$, Fig. 3*C*). In all slices, after subtraction,

there was a positive amount of adenosine demonstrating that the subtraction procedure was successful. This confirms that biosensors can be used to measure adenosine in cerebellar slices.

To test that the inosine arose from the metabolism of adenosine and that hypoxanthine arose from inosine breakdown, adenosine and inosine were applied to slices. Following a 1 min application of 100 $\mu$M adenosine, $3.2 \pm 0.7$ $\mu$M inosine and $0.3 \pm 0.06$ $\mu$M hypoxanthine were detected ($n = 5$) and 100 $\mu$M inosine produced $0.7 \pm 0.1$ $\mu$M hypoxanthine ($n = 5$). These results demonstrate that cerebellar slices contain the enzymes that rapidly break down adenosine to hypoxanthine (adenosine deaminase and purine nucleoside phosphorylase). Thus it is feasible for the inosine/hypoxanthine tone to arise from the breakdown of endogenous adenosine. The breakdown of ATP to adenosine suggests that the extracellular metabolism of ATP could be a potential source of adenosine.

There was considerable variation in the relative quantities of the metabolites detected following ATP application. At the surface of the slice, the proportion of ATP metabolites (relative proportions of adenosine, inosine and hypoxanthine) ranged from 25% to 91% for adenosine, (mean $84 \pm 7\%$), inosine accounted for 0–60% (mean $11 \pm 6\%$) and hypoxanthine accounted for 0–14% (mean $5 \pm 1\%$). Similar results were observed with biosensors placed within slices. This suggests that the distribution of metabolising enzymes within slices is not uniform and that the positioning of the biosensors relative to the enzymes may dictate the proportions of metabolites detected. This strengthens the argument that the inability to detect basal levels of adenosine using biosensors results from a non-homogenous distribution of inosine/hypoxanthine in the cerebellum.

### Extracellular purine nucleoside phosphorylase (PNP) is present in the cerebellum

The conversion of inosine to hypoxanthine is catalysed by purine nucleoside phosphorylase (PNP) which is an important enzyme in the salvage of nucleotide bases (Bzowska *et al.* 2000). Although PNP is considered an intracellular enzyme it has been described in rat CSF (Silva *et al.* 2004). The production of hypoxanthine following ATP, adenosine or inosine application suggests that an extracellular form of PNP is expressed in the cerebellum. To confirm the extracellular expression of PNP, we used a specific inhibitor of PNP, immucillin H (Horenstein & Schramm, 1993). Immucillin H (200 nM) caused a $66 \pm 3\%$ reduction in the production of hypoxanthine (following changing the inflow from control saline to 100 $\mu$M inosine for 2.5 min) as measured by a HYPO biosensor laid on the surface of the slice ($n = 3$, Fig. 4A).

Immucullin H had no effect on the responsiveness of the HYPO sensor to hypoxanthine, and HYPO sensors could not detect inosine (Fig. 4B)

### What determines the extracellular concentration of adenosine in the cerebellum?

**Adenosine kinase.** Adenosine kinase is a key intra-cellular enzyme that phosphorylates adenosine to form AMP and thus maintains low levels of intracellular adenosine helping to prevent efflux via equilibrative transporters (for review see Boison, 2006). To assess whether adenosine kinase is important in the cerebellum, we blocked the enzyme adenosine kinase with iodotubercidin and measured the effects on synaptic transmission and the extracellular concentration of adenosine. Application of iodotubercidin (1–2 $\mu$M) reliably inhibited PF EPSPs (9 out of 10 slices, $51 \pm 2\%$, Fig. 5A) and increased the paired pulse ratio (from $1.58 \pm 0.06$ to $1.86 \pm 0.02$) indicating a presynaptic action. The effects of iodotubercidin were reversed by 8CPT (1 $\mu$M) and the mean increase in PF EPSP amplitude was much larger ($168 \pm 21\%$) than in control (46.1%) indicating increased $A_1$ receptor
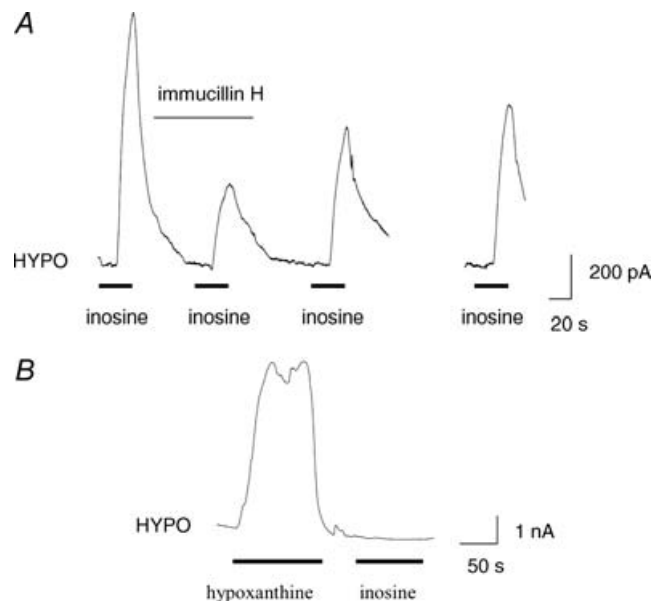


**Figure 4. Extracellular purine nucleoside phosphorylase (PNP) metabolises inosine to hypoxanthine in cerebellar slices**
*A*, record from a HYPO biosensor placed on the surface of a cerebellar slice (the sensor was bent so that it was laid parallel to the slice surface, increasing the sensitivity of purine detection). Application of 100 $\mu$M inosine (bar) produced a large current on the sensor due to rapid conversion of inosine to hypoxanthine. Application of the PNP inhibitor, immucillin H (200 nM), markedly reduced the conversion of inosine to hypoxanthine. Following wash there was recovery in the conversion of inosine to hypoxanthine. *B*, the same sensor as *A*, with no slice present. The sensor responds to hypoxanthine but does not respond to inosine.

activation. Iodotubercidin was without effect in only one slice (although EPSP amplitude was increased by 8CPT, suggesting the presence of an adenosine tone). Simultaneous biosensor measurements reliably detected an increased level of purines following iodotubercidin application (8 out of 10 slices, Fig. 5*B*). After subtraction, the concentration of adenosine was increased by $0.68 \pm 0.1 \ \mu$M and inosine was increased by $0.37 \pm 0.2 \ \mu$M. The consistent increase in adenosine suggests that adenosine kinase is an important and global mechanism for determining the extracellular concentration of purines in cerebellar slices. This also demonstrates that our method of measuring adenosine is reliable and that the variable results obtained with other manipulations of adenosine concentration must be due to biological not technical mechanisms.

To investigate whether the equilibrative transporters mediate the increase in adenosine tone following block of adenosine kinase, we applied NBTI/dipyridamole (to block ENT1/ENT2) prior to application of iodotubercidin (to inhibit adenosine kinase). NBTI and dipyridamole have been used to block ENT1 and ENT2 in a number of studies (Dunwiddie & Diao, 1994; Frenguelli *et al.* 2007). In four out of eight slices, the inhibitory actions of iodotubercidin were almost completely occluded by the prior application of NBTI/dipyridamole (Fig. 5*C*). At these synapses the equilibrative transport of adenosine was abolished and thus the increase in intracellular adenosine concentration (as a result of adenosine kinase inhibition) did not result in adenosine efflux. In the remaining four slices, NBTI/dipyridamole did not occlude the actions of iodotubercidin (Fig. 5*D*). Presumably in these slices, the equilibrative transport of adenosine was not effectively blocked and thus the increase in intracellular adenosine concentration (as a result of adenosine kinase inhibition) still resulted in an efflux of adenosine. These results suggest heterogeneous expression of synaptic adenosine transporters with different proportions of NBTI-/dipyridamole-sensitive transporters expressed at different synapses.
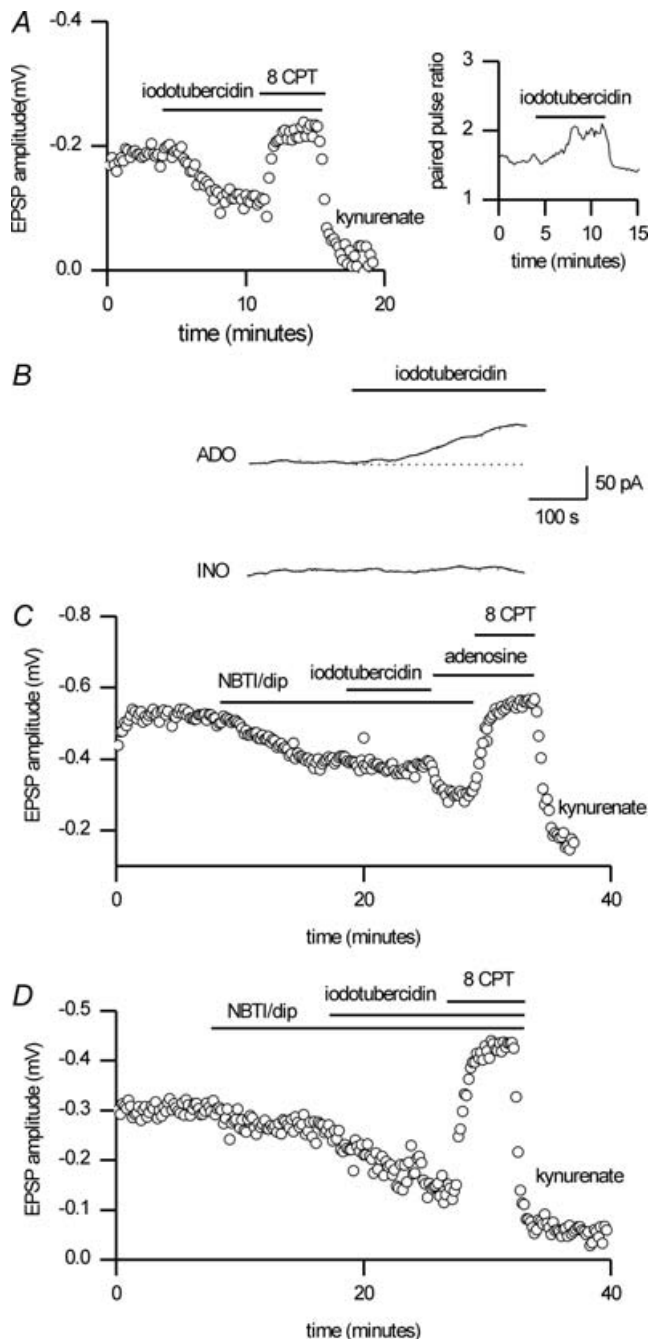
**Figure 5. Inhibition of adenosine kinase increases the extracellular concentration of adenosine**

*A*, the adenosine kinase inhibitor iodotubercidin (1 $\mu$M) caused a reduction in PF EPSP amplitude ($\sim$50%) which was reversed by the A$_1$ receptor antagonist 8CPT (1 $\mu$M). At the end of the experiment, PF EPSPs were blocked by kynurenate (5 mM). Graph plots the amplitude of individual PF EPSPs against time. Inset, iodotubercidin (1 $\mu$M) caused an increase in the paired pulse ratio, confirming presynaptic inhibition due to adenosine efflux. Graph plots the paired pulse ratio against time for the PF EPSPs in *A*. The average paired pulse ratio for five EPSPs is plotted. *B*, trace from an ADO and INO sensor placed within the same slice as *A*. Application of iodotubercidin (1 $\mu$M) produced a current on the ADO sensor with little effect on the INO sensor. After calibration there was a net increase in the extracellular adenosine

concentration of $\sim$0.5 $\mu$M. *C*, the equilibrative transport inhibitors NBTI (5 $\mu$M) and dipyridamole (10 $\mu$M) inhibited PF EPSP amplitude and occluded the effects of iodotubercidin. Although iodotubericidin (2 $\mu$M) had no effect on PF EPSP amplitude (in the presence of NBTI/dipyridamole), the adenosine receptors were not saturated as application of adenosine (100 $\mu$M) produced increased inhibition. The modulation of PF EPSPs was reversed by block of A$_1$ receptors (1 $\mu$M 8CPT), and EPSPs were blocked by kynurenate (5 mM) at the end of the experiment. *D*, NBTI (5 $\mu$M) and dipyridamole (10 $\mu$M) caused a small inhibition of PF EPSP amplitude but did not occlude the effects of iodotubercidin. Application of 2 $\mu$M iodotubericidin (in the presence of NBTI/dipyridamole) markedly inhibited EPSP amplitude. The modulation of PF EPSPs was reversed by block of A$_1$ receptors (1 $\mu$M 8CPT), and EPSPs were blocked by 5 mM kynurenate at the end of the experiment.

**Equilibrative transporters.** We further tested the role of equilibrative transporters (ENT1 and ENT2) in the control of the adenosine tone. Adenosine can be removed from the extracellular space by transport into neurons and glia. Long applications (30 min) of NBTI (5 $\mu$M) and dipyridamole (10 $\mu$M) had variable effects on PF EPSP amplitude and biosensor measurements ($n = 18$ slices). Results could be divided into three categories: in nine slices, PF EPSP amplitude was decreased (47 ± 8%) with an increase in PPF (from 1.6 ± 0.1 to 1.9 ± 0.1) and a large increase in EPSP amplitude following 8CPT (1 $\mu$M) application (180 ± 20% *vs.* 46.1 ± 8.6%, Fig. 6*A*), indicating increased $A_1$ receptor activation. However there was no shift in the baseline current measured by purine biosensors, suggesting no change in the bulk concentration of purines within the slice (Fig. 6*B*). In one additional slice, as well as reducing PF EPSP amplitude, the block of adenosine uptake also increased the purine (inosine/hypoxanthine) concentration measured by the biosensor (Fig. 6*C*). In the final eight slices, blocking adenosine transport had little or no effect on either PF EPSP amplitude (decrease 3 ± 6%, PPF 1.56 ± 0.1 *vs.* 1.5 ± 0.1) or biosensor baseline current. However application of 8CPT (1 $\mu$M) still increased EPSP amplitude by 55 ± 17% (*vs.* 46.1 ± 8.6% in control) suggesting that a baseline level of adenosine was present in these synapses (Fig. 6*D*). These highly variable data do not reflect technical deficiencies of measurement, as iodotubercidin reliably evokes changes in adenosine tone. Rather they probably reflect that NBTI-/dipyridamole-sensitive transporters determine the concentration of purines at only a subset of parallel fibre to Purkinje cell synapses.

**Adenosine deaminase.** As well as being an intracellular enzyme, adenosine deaminase can convert extracellular adenosine to inosine. As our biosensor measurements routinely detect an extracellular inosine and hypoxanthine tone, we have investigated the contribution of adenosine deaminase to this tone by means of simultaneous biosensor and PF EPSP recordings in the presence of EHNA, a selective blocker of adenosine deaminase (Agarwal, 1982).

Although the increase in adenosine concentration cannot be measured directly (biosensor detection of adenosine uses adenosine deaminase), the effects of EHNA can be monitored via changes in PF EPSP amplitude and by changes in inosine/hypoxanthine concentration. EHNA (20 $\mu$M) is effective at inhibiting adenosine deaminase as it blocks the adenosine deaminase present on the adenosine biosensor, with no effect on the detection of inosine and hypoxanthine (Wall & Dale, 2007). Application of EHNA had only minor effects on PF EPSPs: the mean PF EPSP amplitude was slightly reduced (11 ± 5%) and the paired pulse ratio was increased (from 1.4 ± 0.07 to 1.6 ± 0.07, $n = 7$, Fig. 7*A* and *B*). Furthermore, application of 1 $\mu$M 8CPT (in the presence of EHNA) produced a significantly
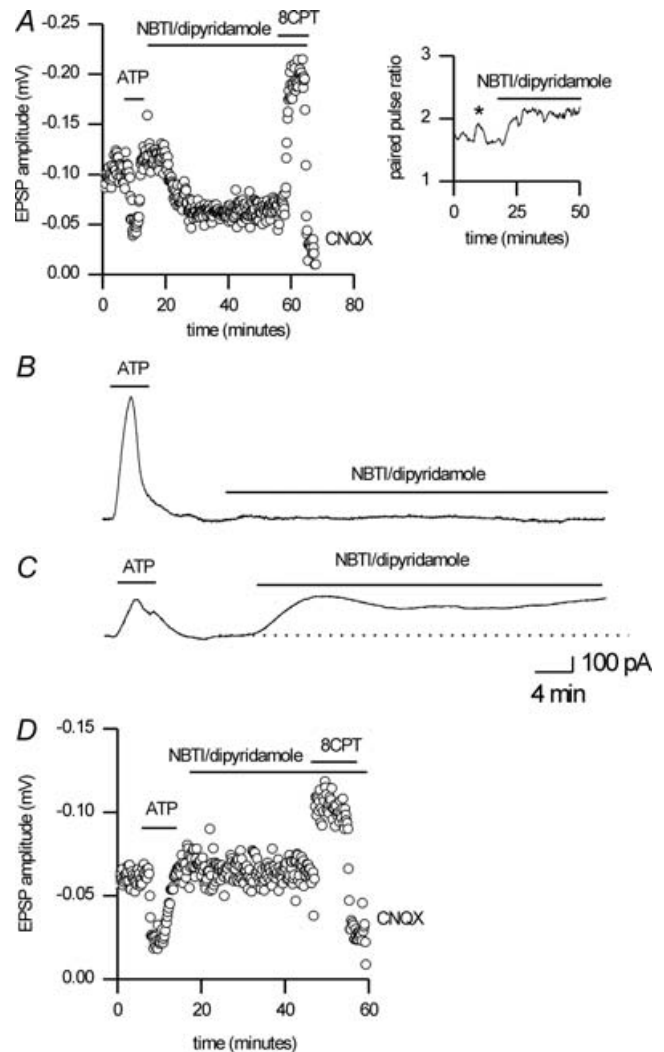


**Figure 6. Blocking equilibrative transport has heterogeneous effects**

*A*, application of ATP (100 $\mu$M) caused a reversible inhibition of PF EPSP amplitude. Block of equilibrative transport with 5 $\mu$M NBTI and 10 $\mu$M dipyridamole caused a reduction in PF EPSP amplitude, which was reversed by block of $A_1$ receptors with 8CPT (1 $\mu$M). PF EPSPs were blocked by CNQX at the end of the experiment. Graph plots the amplitude of individual PF EPSPs against time. Inset, application of ATP (*) and NBTI/dipyridamole caused an increase in the paired pulse ratio, confirming a presynaptic site of action. Graph plots the paired pulse ratio against time for the PF EPSPs in *A*. The average paired pulse ratio for five EPSPs is plotted. *B*, trace from an ADO biosensor present in the same slice as *A*. Application of 100 $\mu$M ATP caused an increase in adenosine concentration (as a result of metabolism), but 5 $\mu$M NBTI/10 $\mu$M dipyridamole had no effect. *C*, trace from an ADO biosensor in a different slice. Application of 5 $\mu$M NBTI/10 $\mu$M dipyridamole produced a current on the sensor, suggesting an increase in the concentration of purines in the bulk of the slice. *D*, application of ATP (100 $\mu$M) caused a reduction in PF EPSP amplitude, but 5 $\mu$M NBTI/10 $\mu$M dipyridamole had no effect. There was also no effect on the paired pulse ratio (not illustrated). There is an adenosine tone, as block of $A_1$ receptors with 8CPT (1 $\mu$M) increased PF EPSP amplitude. PF EPSPs were blocked by CNQX (10 $\mu$M) at the end of the experiment.

larger increase in PF EPSP amplitude than in control ($84 \pm 19\%$ *vs.* $46.1 \pm 8.6\%$), demonstrating greater $A_1$ receptor activation. Simultaneous biosensor recordings revealed a fall in the extracellular levels of inosine



*A*, the adenosine deaminase inhibitor EHNA (20 $\mu$M) caused a reduction in EPSP amplitude ($\sim$17%), which was reversed by block of $A_1$ receptors with 8CPT (1 $\mu$M). EPSPs were blocked at the end of the experiment with 5 mM kynurenate. Graph plots the amplitude of individual PF EPSPs against time. *B*, EHNA caused an increase in the paired pulse ratio whereas 8CPT reduced the ratio, confirming a presynaptic site of action. Graph plots the paired pulse ratio against time for the PF EPSPs in *A*. The average paired pulse ratio for five EPSPs is plotted. *C*, trace from an INO sensor placed within the same slice as *A*. Application of EHNA caused a fall in the concentration of the adenosine metabolites inosine/hypoxanthine.

and hypoxanthine, which was coincident with the effect on PF EPSP amplitude (Fig. 7*C*) There was a fall in hypoxanthine concentration of $1.2 \pm 0.7$ $\mu$M (7 out of 7 slices) and a fall in inosine concentration of $0.3 \pm 0.2$ $\mu$M (4 out of 7 slices). As the basal concentration of hypoxanthine in the slices is 1.8 $\mu$M, then at least 66% of the hypoxanthine arises from the metabolism of adenosine. The remaining hypoxanthine could arise from other sources such as inosine monophosphate. Although ecto-adenosine deaminase does contribute to the inosine/hypoxanthine tone, it does not appear to be the major regulator of the adenosine tone.
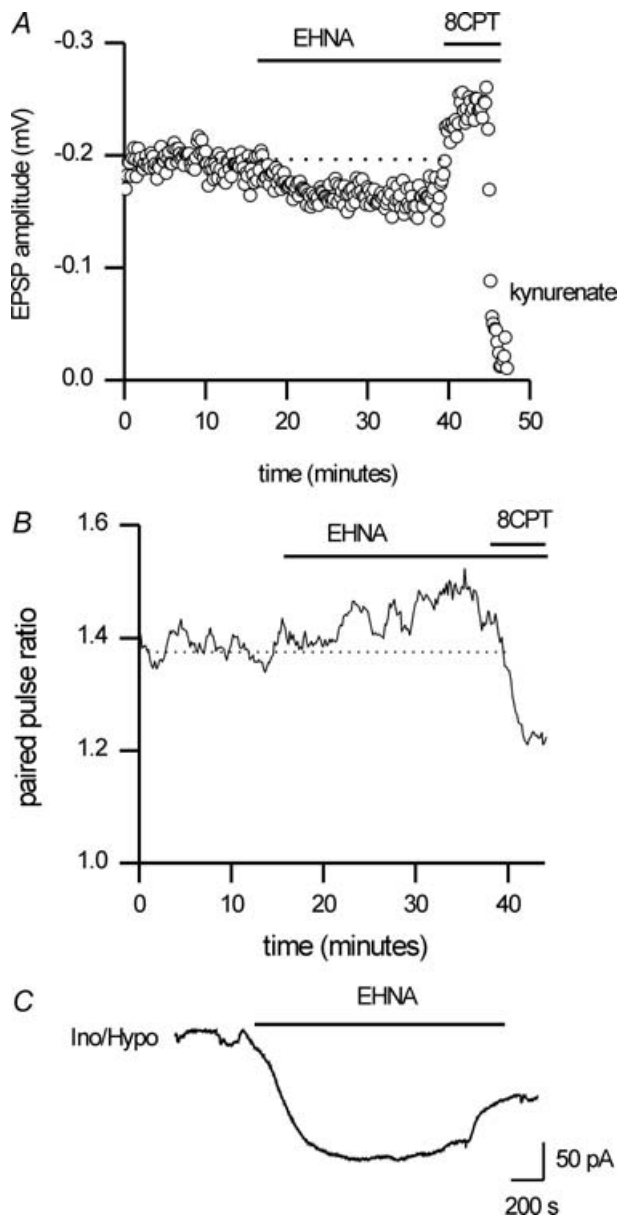
## Endogenous sources of extracellular adenosine

We have recently demonstrated that action potential-dependent adenosine release occurs in response to short trains of electrical stimuli in the molecular layer (Wall & Dale, 2007). If this adenosine were to be metabolised to inosine/hypoxanthine then it could contribute to the extracellular purine tone. We therefore stimulated in the molecular layer and recorded the release of adenosine (with an ADO sensor) and measured any breakdown of the released adenosine to hypoxanthine (with a HYPO sensor). Following stimulation there was a rapid release of adenosine (as previously described, Wall & Dale, 2007) measured on the ADO sensor, followed by a much slower build-up of hypoxanthine detected by the HYPO sensor ($n = 6$, Fig. 8*A*). If the entire ADO sensor signal was due to adenosine, then $360 \pm 100$ nM adenosine was released, which was metabolised to $45 \pm 58$ nM hypoxanthine. Both the adenosine and hypoxanthine signals were blocked following addition of TTX to block action potentials (1 $\mu$M, $n = 3$). If the action potential-dependent release of adenosine occurs spontaneously, then it could contribute to the inosine/hypoxanthine tone measured in slices. Blocking action potential adenosine release with TTX (1 $\mu$M) produced a small fall ($\sim$15 pA) in the baseline current of the ADO biosensor in three out of ten slices, suggesting that activity-dependent adenosine is only a minor contributor to the purine tone in the slice. However *in vivo* this source of adenosine may be more important, as there is much greater parallel fibre activity.

We next tested whether release of ATP is the source of endogenous adenosine (and the inosine/hypoxanthine tone). Under control conditions we could not measure any extracellular ATP (in or above the slice), suggesting either that little ATP is released or that it is rapidly metabolised. We thus inhibited the metabolism of ATP with ARL67156 (100 $\mu$M), an inhibitor of ecto-ATPase (Crack *et al.* 1995). Following ARL67156 application, there was still no difference between ATP and null sensors at either room temperature ($n = 15$) or 33–35°C ($n = 20$). Similar results

**Figure 7. The metabolism of adenosine contributes to the extracellular inosine/hypoxanthine tone but has little effect on synaptic transmission**

were found with other ecto-ATPase inhibitors: PPADS (10–100 $\mu$M), suramin (100 $\mu$M), dipyridamole (10 $\mu$M, Connolly & Duley, 2000) and Evans Blue (100 $\mu$M). We have previously shown that the agents ARL67156 and Evans Blue are effective inhibitors of ATP breakdown by cerebellar slices (Wall & Dale, 2007).

An alternative approach to directly observing the release of ATP is to inhibit the conversion of ATP to adenosine and thus measure a fall in adenosine concentration (measured as an increase in PF EPSP amplitude and by a fall in inosine/hypoxanthine levels). The ecto-5′-nucelotidase inhibitor $\alpha,\beta$-methylene-ADP was used to reduce the conversion of AMP to adenosine (effective in the cerebellum, Wall & Dale, 2007). To increase the likelihood of reducing the conversion of ATP to adenosine, $\alpha,\beta$-methylene-ADP (100 $\mu$M) was applied in combination with ARL67156 (100 $\mu$M). In the majority of slices ($n = 8$) there was no effect on either PF EPSP amplitude or biosensor current (Fig. 8$B$ and $C$). In four slices there was a small reversible decrease in inosine/hypoxanthine levels, as detected by a fall in the baseline current measured by biosensors (mean fall in current $49 \pm 35$ pA, Fig. 8$E$). In three out of the four slices this was accompanied by a small increase in PF EPSP amplitude (mean increase $8.6 \pm 5.8\%$, Fig. 8$D$). Upon wash there was a transient increase in adenosine concentration, presumably as accumulated ADP and AMP are rapidly broken down to adenosine by the now uninhibited enzymes. This was measured by biosensors as a current increase of $56 \pm 23$ pA and by a transient reduction in PF EPSP amplitude of $36.6 \pm 11\%$ (Fig. 8$D$ and $E$). We therefore find that metabolism of ATP may contribute to the production of adenosine in some slices, but that in many slices this does not appear to be the source of the purine tone.
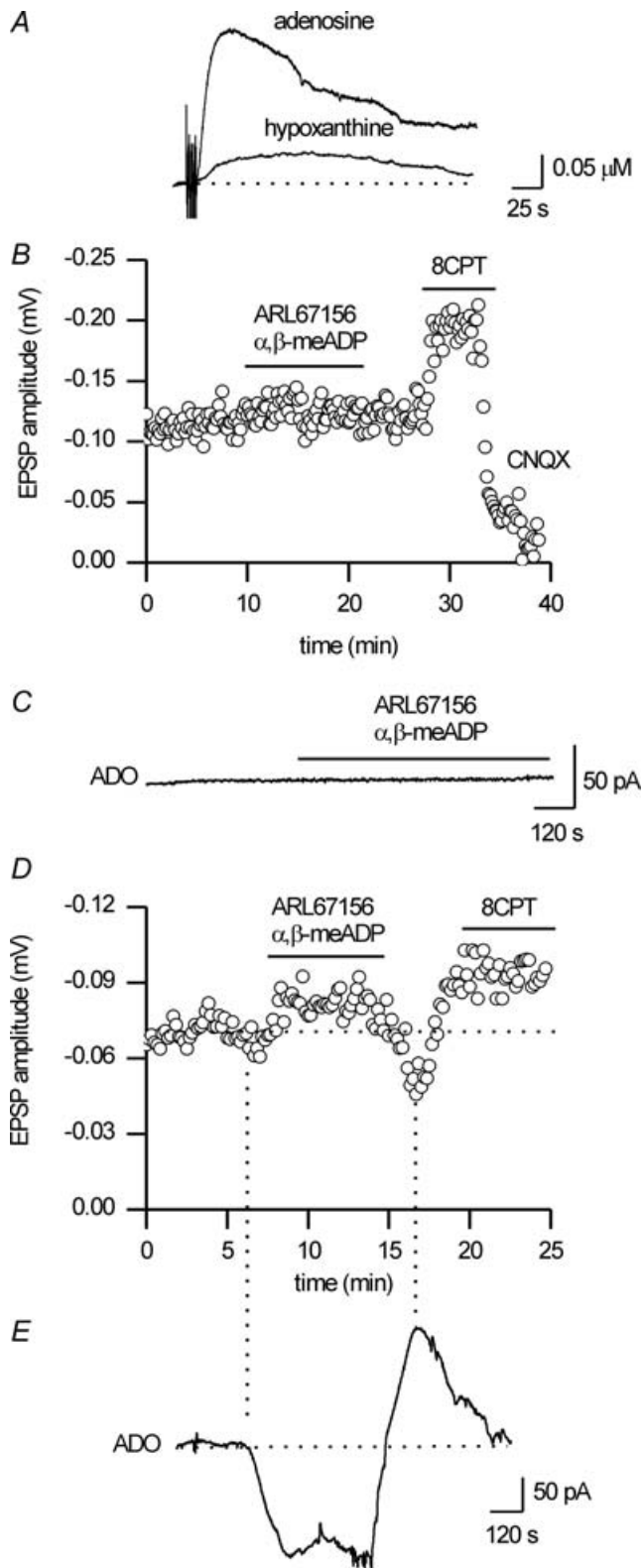


**Figure 8. What is the source of endogenous adenosine?**
$A$, superimposed traces from ADO and HYPO biosensors placed parallel to the molecular layer surface. Following stimulation (5 V, 20 Hz, 10 s) in the molecular layer, adenosine is released and a proportion is metabolised to hypoxanthine. The traces are normalised by the biosensor calibration, assuming that all ADO biosensor signal results from adenosine detection. $B$, application of $\alpha,\beta$-methylene-ADP (100 $\mu$M) and ARL67156 (100 $\mu$M), to reduce conversion of ATP to adenosine, had no effect on PF EPSP amplitude. However, application of 8CPT (1 $\mu$M) increased PF EPSP amplitude, demonstrating that synaptic $A_1$ receptors were activated by endogenous adenosine. Graph plots the amplitude of individual PF EPSPs against time. $C$, trace from ADO biosensor positioned in the same slice as $A$. Application of 100 $\mu$M $\alpha,\beta$-methylene-ADP and ARL67156 had no effect on the baseline current. $D$, application of $\alpha,\beta$-methylene-ADP (100 $\mu$M) and ARL67156 (100 $\mu$M) increased PF EPSP amplitude. Upon wash there was a transient reduction in PF EPSP amplitude below control levels. $E$, trace from ADO biosensor positioned in the same slice as $D$. Addition of $\alpha,\beta$-methylene-ADP and ARL67156 caused a reduction in the baseline current (reduction in conversion of ATP to adenosine, coincident with increase in PF EPSP amplitude). Upon wash there was a transient increase in the level of adenosine, which coincided with the inhibition of PF EPSP amplitude.

## Discussion

Many studies have demonstrated the presence of an adenosine tone in the CNS (including the cerebellum, Takahashi *et al.* 1995; Dittman & Regehr, 1996). We have confirmed this by examining synaptic transmission. Nevertheless, direct measurements with biosensors failed to reliably detect an extracellular adenosine tone in the cerebellum. Instead we demonstrated the presence of an extracellular inosine and hypoxanthine tone that arises (at least in part) from the breakdown of adenosine. The conversion of adenosine to hypoxanthine requires the extracellular expression of adenosine deaminase and purine nucleoside phosphorylase (PNP). The inhibition of the conversion of inosine to hypoxanthine by the specific PNP inhibitior immucullin-H confirms the extracellular expression of PNP. This is unexpected since PNP is usually considered an intracellular enzyme (Bzowska *et al.* 2000). Interestingly, astrocytes cultured from neonatal cerebellum also metabolise exogenous ATP to hypoxanthine (Wink *et al.* 2003), suggesting that the adenosine metabolising enzymes could be expressed by glia. The rationale for the conversion of adenosine to inosine seems obvious: the conversion of active (adenosine) to inactive (inosine) molecules. Although inosine is often considered inert, its metabolism to hypoxanthine suggests that it may be functionally active and plays some role in the cerebellum. There is growing support for inosine being active as it appears to play a role in the immune system and may be neuroprotective (Hasko *et al.* 2004).

### Inability to directly detect endogenous adenosine with biosensors

In common with findings in other studies (Takahashi *et al.* 1995; Dittman & Regehr, 1996), parallel fibre–Purkinje cell synaptic transmission is tonically inhibited by endogenous adenosine in cerebellar slices. However we have been unable to directly measure this extracellular adenosine using biosensors. A similar finding has been reported in the hippocampus where an adenosine tone was not detectable in three out of four slices, although tonic adenosine-mediated synaptic inhibition was present (Frenguelli *et al.* 2007). It is unlikely that the levels of adenosine are below the levels of detection, as pharmacological experiments have estimated that 200–400 nM adenosine is present in the extracellular space of the brain (Dunwiddie & Diao, 1994). This concentration of adenosine would give a current on an ADO biosensor of 60–120 pA, which in normal conditions would easily be detected. There are two possibilities which would explain this inability to detect adenosine: firstly, adenosine is metabolised to inosine/hypoxanthine before it reaches the sensor. It could be argued that the sensor is further from the adenosine release sites than the $A_1$ receptors and thus

breakdown in or around the synapses occurs before any purines reach the biosensor. However the large density of parallel fibre synapses in the molecular layer makes it unlikely that the sensor does not sample from the synaptic compartment. Furthermore, blockade of extracellular breakdown (with EHNA) had little effect on synaptic inhibition, suggesting that it is not the major mechanism of removing adenosine. Dilution of adenosine before detection was also unlikely, as biosensors were inserted through the slice and the sensing area of the biosensors was in intimate contact with the tissue. Secondly, it is more likely that a non-homogenous distribution of inosine and hypoxanthine in the extracellular space prevented reliable measurement of adenosine for technical reasons. If the levels of inosine/hypoxanthine are not equivalent for each sensor (ADO, INO and HYPO), then upon subtraction an inaccurate adenosine concentration will be measured. A failure of subtraction will result in either an over-estimate or underestimate of the adenosine concentration. Subtraction of the calibrated inosine and hypoxanthine signals gave either a negative adenosine signal or a large adenosine signal (1–2 $\mu$M). The presence of a non-uniform distribution of inosine and hypoxanthine is supported by the observations that (1) there is a large variation in the amount of inosine and hypoxanthine measured in different slices, and (2) movement of sensors to different parts of the slice detected differing amounts of inosine and hypoxanthine following ATP application (M.J. Wall and N. Dale, unpublished observations). A heterogeneous distribution of inosine/hypoxanthine could stem from the distribution of adenosine-metabolising enzymes. If the enzymes are clustered (rather than spread uniformly), then the positioning of the sensors relative to the enzymes will determine the amounts of inosine and hypoxanthine detected. Future work is required to test directly for the clustering of enzymes. Despite these limitations we reliably observed a purine tone. Furthermore, when we used iodotubercidin (to block adenosine kinase) there was a global increase in the adenosine tone, which was reliably detected by the biosensors.

### Control of purine levels in cerebellum compared to other brain regions

The levels of adenosine in the cerebellum are controlled by the balance between the rates of production and elimination. The tone of inosine and hypoxanthine arises (at least in part) from adenosine metabolism. What is the source of this adenosine? The two major possibilities are production via extracellular ATP breakdown (for review see Zimmermann, 2000) or direct release (either by transport or by exocytosis). Although we have used several different methods to distinguish between these possibilities, the major source of adenosine remains uncertain. It has not been possible to directly measure

ATP in cerebellar slices with biosensors (limit of detection $\sim$60 nM), and reducing ATP breakdown (with ecto-ATPase inhibitors) did not reveal an ATP signal. Thus either the ATP tone described by Brockhaus *et al*. (2004) (detected indirectly by its effect on the spontaneous activity of inhibitory interneurons) must be too small to detect by our methods, or the breakdown of ATP is very rapid and not prevented by the inhibitors. However, slowing the conversion of ATP to adenosine did reduce the concentration of adenosine metabolites in some slices. However, the reduction was small (15%) and the effect on EPSP amplitude was minor (10% increase *vs*. 46% inhibition). Thus the contribution of ATP metabolism to the purine tone appears minor. This contrasts with the hippocampus, where metabolism of ATP is a major contributor to the purine tone (Frenguelli *et al.* 2007; Pascual *et al.* 2005).

We have recently described the release of adenosine in response to focal electrical stimulation of the molecular layer, a process which is both $Ca^{2+}$ and TTX sensitive (Wall & Dale, 2007). Blocking any spontaneous release of action potential-dependent adenosine release with TTX had only a small effect on the inosine/hypoxanthine tone. However, *in vivo*, the activity of parallel fibres is much greater and thus this source of adenosine may be much more important.

Elimination of adenosine occurs by a combination of two processes: metabolism (by adenosine deaminase) to inactive metabolites and transport into neurons and glia followed by phosphorylation to AMP (by adenosine kinase). Using pharmacological agents, we have investigated which of these components is more important in determining extracellular adenosine levels in the cerebellum. Changes in adenosine levels were assessed by comparing synaptic inhibition with direct measurement of purines via biosensors. Blocking adenosine deaminase had minor effects on parallel fibre–Purkinje cell synaptic transmission ($\sim$10% reduction), but did reduce the levels of extracellular inosine and hypoxanthine ($\sim$50%) measured by biosensors. The small effect of EHNA on synaptic transmission suggests that extracellular metabolism is not the major mechanism controlling synaptic adenosine concentration, and adenosine deaminase maybe located outside the synapses. Similar small effects of EHNA on synaptic transmission in the hippocampus have also been observed (Dunwiddie & Diao, 1994; Pak *et al.* 1994). The effect of EHNA on the inosine/hypoxanthine tone demonstrates that around half of the tone arises from adenosine metabolism (the rest may arise from other sources such as inosine monophosphate). As the tone of inosine/hypoxanthine is $\sim$1–2 $\mu$M, the adenosine concentration would be expected to increase by 0.5–1 $\mu$M, which should markedly increase synaptic inhibition. The small effect of EHNA on synaptic transmission suggests that any increase in adenosine is presumably diminished by greater equilibrative transport into neurons and glia around synapses.

In contrast to the minor effects of blocking metabolism, inhibition of adenosine kinase produced a marked decrease ($\sim$50%) in PF EPSP amplitude in the majority of slices, accompanied by a simultaneous increase in adenosine concentration detected by biosensors. The agreement of biosensor measurements with the increase in synaptic inhibition suggests that blocking adenosine kinase produces a global increase in adenosine concentration. Presumably blockade of adenosine kinase causes an increase in the intracellular concentration of adenosine and a resultant efflux of adenosine via equilibrative transporters (see Boison, 2006). The greater importance of adenosine kinase activity compared to extracellular adenosine metabolism has been observed in other brain regions (Zhang *et al.* 1993; Pak *et al.* 1994; Lloyd & Fredholm, 1995).

The role of equilibrative transport in determining adenosine concentration was assessed by blocking ENT1 and ENT2. In $\sim$50% of parallel fibre–Purkinje cell synapses, synaptic transmission was markedly inhibited ($\sim$45%) as a result of the build-up of adenosine following the inhibition of adenosine transport. However (apart from one slice), no increase in adenosine concentration could be measured by biosensors. The effects of blocking equilibrative transport were very inconsistent (compared to blocking adenosine kinase). We can exclude any technical difficulties in measuring an adenosine increase, as adenosine was reliably detected following adenosine kinase inhibition. Also, after removing the biosensors from the tissue there was very little reduction in sensitivity. Thus the biosensors retain their ability to detect adenosine throughout the experiment. Furthermore, similar biosensors could reliably detect an increase in adenosine in hippocampal slices following application of NBTI/dipyridamole (Frenguelli *et al.* 2007). The most likely explanation is that equilibrative transport in the cerebellum is not always effectively blocked by application of NBTI/dipyridamole. This is supported by the observation that we cannot always occlude the effects of iodotubercidin by prior application of NBTI/dipyridamole. Heterogeneous expression of ENT1 and ENT2 could lead to variation in the actions of NBTI/dipyridamole. Although rat ENT1 is effectively blocked by NBTI, rat ENT2 is only weakly blocked by NBTI and dipyridamole (Baldwin *et al.* 2004).Thus variable expression of ENT2 at parallel fibre synapses, could plausibly account for the observed effects of NBTI/dipyridamole. Alternatively, differential phosphorylation of ENT1 and or ENT2 at different synapses could change the proportion of transport via ENT1 or ENT2 (Stolk *et al.* 2005). It is also possible that there is heterogeneous expression of another transporter (other than ENT1 and ENT2) that is

insensitive to NBTI/dipyridamole. The variation in effect of NBTI/dipyridamole between different slices suggests that any rise in adenosine concentration is localised and does not spread between all synapses. This is supported by the observation that an increase in purine concentration (following block of equilibrative transport) could only be measured by biosensors in one slice. Although antibody staining has revealed diffuse expression of the transporters in the molecular layer, granule cell layer and Purkinje cell bodies (Anderson *et al.* 1999*a*,*b*), the density of ENT1 and ENT2 relative to each other and to individual synapses is currently unclear.

In conclusion, we have demonstrated that a combination of biosensor measurements and electro-physiology can be used to determine how the basal extracellular levels of adenosine are regulated. Using these methods, we have documented an inosine/hypoxanthine tone (undetectable by electrophysiology alone) that has a heterogeneous distribution (which would not be observed with either HPLC or microdialysis). The control of extracellular adenosine concentration in the cerebellum appears comparable to that in other brain regions where the activity of adenosine kinase is the major determining factor. However the variable effects of blocking adenosine transport (on both synaptic inhibition and biosensor measurements) suggest that the transporters display an unexpected non-uniform distribution relative to synapses.

# References

Agarwal RP (1982). Inhibitors of adenosine deaminase. *Pharmacol Ther* **17**, 399–429.

Anderson CM, Baldwin SA, Young JD, Cass CE & Parkinson FE (1999*a*). Distribution of mRNA encoding a nitrobenzylthioinosine-insensitive nucleoside transporter (ENT2) in rat brain. *Brain Res Mol Brain Res* **70**, 293–297.

Anderson CM, Xiong W, Geiger JD, Young JD, Cass CE, Baldwin SA & Parkinson FE (1999*b*). Distribution of equilibrative, nitrobenzylthioinosine-sensitive nucleoside transporters (ENT1) in brain. *J Neurochem* **73**, 867–873.

Arcuino G, Lin JH, Takano T, Liu C, Jiang L, Gao Q, Kang J & Nedergaard M (2002). Intercellular calcium signaling mediated by point-source burst release of ATP. *Proc Natl Acad Sci U S A* **99**, 9840–9845.

Atluri PP & Regehr WG (1996). Determinants of the time course of facilitation at the granule cell to Purkinje cell synapse. *J Neurosci* **16**, 5661–5671.

Baldwin SA, Beal PR, Yao SYM, King AE, Cass CE & Young JD (2004). The equilibrative nucleoside transporter family, SLC29. *Pflugers Arch* **447**, 735–743.

Beierlein M & Regehr WG (2006). Brief bursts of parallel fiber activity trigger calcium signals in Bergmann glia. *J Neurosci* **26**, 6958–6967.

Boison D (2006). Adenosine kinase, epilepsy and stroke: mechanisms and therapies. *Trends Pharmacol Sci* **27**, 652–658.

Braas KM, Newby AC, Wilson VS & Snyder SH (1986). Adenosine-containing neurons in the brain localised by immunocytochemistry. *J Neurosci* **6**, 1952–1961.

Brockhaus J, Dressel D, Herold S & Deimer JW (2004). Purinergic modulation of synaptic input to Purkinje neuons in rat cerebellar slices. *Eur J Neurosci* **19**, 2221–2230.

Bzowska A, Kulikowska E & Shugar D (2000). Purine nucleoside phosphorylase: properties, functions and clinical aspects. *Pharmacol Ther* **88**, 349–425.

Clark BA & Barbour B (1997). Currents evoked in Bergmann glial cells by parallel fibre stimulation in rat cerebellar slices. *J Physiol* **502**, 335–350.

Connolly GP & Duley JA (2000). Ecto-nucleotidase of cultured rat superior cervical ganglia: dipyridamole is a novel inhibitor. *Eur J Pharmacol* **397**, 271–277.

Crack BE, Pollard CE, Beukers MW, Roberts SM, Hunt SF, Ingall AH, McKechnie KCW, Ijzerman AP & Leff P (1995). Pharmacological and biochemical analysis of FPL 67156, a novel, selective inhibitor of ecto-ATPase. *Br J Pharmacol* **114**, 475–481.

Craig CG & White TD (1993). N-methyl-D-aspartate and non-*N*-methyl-D-aspartate-evoked adenosine release from rat cortical slices: distinct purinergic sources and mechanisms of release. *J Neurochem* **60**, 1073–1080.

Dale N, Pearson T & Frenguelli BG (2000). Direct measurement of adenosine release during hypoxia in the CA1 region of the rat hippocampal slice. *J Physiol* **526**, 143–155.

Dittman JS & Regehr WG (1996). Contributions of calcium-dependent and calcium-independent mechanisms to presynaptic inhibition at a cerebellar synapse. *J Neurosci* **16**, 1623–1633.

Dulla CG, Dobelis P, Pearson T, Frenguelli BG, Staley KJ & Masino SA (2005). Adenosine and ATP link $P_{CO_2}$ to cortical excitability via pH. *Neuron* **48**, 1011–1023.

Dunwiddie TV & Diao L (1994). Extracellular adenosine concentration in hippocampal brain slices and the tonic inhibitory modulation of evoked excitatory responses. *J Pharmacol Exp Ther* **268**, 537–545.

Edwards FA, Gibb AJ & Colquhoun D (1992). ATP receptor-mediated synaptic currents in the central nervous system. *Nature* **359**, 144–147.

Frenguelli BG, Llaudet E & Dale N (2003). High-resolution real-time recording with microelectrode biosensors reveals novel aspects of adenosine release during hypoxia in rat hippocampal slices. *J Neurochem* **86**, 1506–1515.

Frenguelli BG, Wigmore G, Llaudet E & Dale N (2007). Temporal and mechanistic dissociation of ATP and adenosine release during ischemia in the mammalian hippocampus. *J Neurochem* (in the press).

Geiger JD & Nagy JI (1986). Distribution of adenosine deaminase activity in rat brain and spinal cord. *J Neurosci* **6**, 2707–2714.

Gu JG, Foga IO, Parkinson FE & Geiger JD (1995). Involvement of bidirectional adenosine transporters in the release of L-[$^3$H]adenosine from rat brain synaptosomal preparations. *J Neurochem* **64**, 2105–2110.

Hasko G, Sitkovsky MV & Szabo C (2004). Immunomodulatory and neuroprotective effects of inosine. *Trends Pharmacol Sci* **25**, 152–157.

Horenstein BA & Schramm VL (1993). Correlation of the molecular eletrostatic potential surface of an enzymatic transition state with novel transition-state inhibitors. *Biochemistry* **32**, 9917–9925.

Jo YH & Schlichter R (1999). Synaptic corelease of ATP and GABA in cultured spinal neurons. *Nat Neurosci* **2**, 241–245.

Kocsis JD, Eng DL & Bhisitkul RB (1984). Adenosine selectively blocks parallel-fiber-mediated synaptic potentials in rat cerebellar cortex. *Proc Natl Acad Sci U S A* **81**, 6531–6534.

Kukulski F, Sévigny J & Komoszyński M (2004). Comparative hydrolysis of extracellular adenine nucleotides and adenosine in synaptic membranes from porcine brain cortex, hippocampus, cerebellum and medulla oblongata. *Brain Res* **1030**, 49–56.

Llaudet E, Botting N, Crayston J & Dale N (2003). A three enzyme microelectrode sensor for detecting purine release from central nervous system. *Biosens Bioelectron* **18**, 43–52.

Llaudet E, Hatz S, Droniou M & Dale N (2005). Microelectrode biosensor for real-time measurement of ATP in biological tissue. *Anal Chem* **77**, 3267–3273.

Lloyd HG & Fredholm BB (1995). Involvement of adenosine deaminase and adenosine kinase in regulating extracellular adenosine concentration in rat hippocampal slices. *Neurochem Int* **26**, 387–395.

Newman ME & McIlwain H (1977). Adenosine as a constituent of the brain and of isolated cerebral tissues and its relationship to the generation of cyclic AMP. *Biochem J* **164**, 131–137.

Noji T, Karaswa A & Kusaka H (2004). Adenosine uptake inhibitors. *Eur J Pharmacol* **495**, 1–16.

Pak MA, Haas HL & Decking UK & Schrader J (1994). Inhibition of adenosine kinase increases endogenous adenosine and depresses neuronal activity in hippocampal slices. *Neuropharmacology* **33**, 1049–1053.

Pascual O, Casper KB, Kubera C, Zhang J, Revilla-Sanchez R, Sul JY, Takano H, Moss SJ, McCarthy K & Haydon PG (2005). Astrocytic purinergic signaling coordinates synaptic networks. *Science* **310**, 113–116.

Pearson RA, Dale N, Llaudet E & Mobbs P (2005). ATP released via gap junction hemichannels from the pigment epithelium regulates neural retinal progenitor proliferation. *Neuron* **46**, 731–744.

Rivkees SA, Price SL & Zhou FC (1995). Immunohistochemical detection of A1 adenosine receptors in rat brain with emphasis on localization in the hippocampal formation, cerebral cortex, cerebellum and basal ganglia. *Brain Res* **677**, 193–203.

Schoen SW, Graeber MB, Reddington M & Kreutzberg GW (1987). Light and electron microscopical immunocytochemistry of 5′-nucleotidase in rat cerebellum. *Histochemistry* **87**, 107–113.

Silva RG, Santos DS, Basso LA, Oses JP, Wofchuk S, Portela LV & Souza DO (2004). Purine nucleoside phosphorylase activity in rat cerebrospinal fluid. *Neurochem Res* **10**, 1831–1835.

Stolk M, Cooper E, Vilk G, Litchfield DW & Hammond JR (2005). Subtype-specific regulation of equilibrative nucleoside transporters by protein kinase CK2. *Biochem J* **386**, 281–289.

Stout CE, Costantin JL, Naus CC & Charles AC (2002). Intercellular calcium signaling in astrocytes via ATP release through connexin hemichannels. *J Biol Chem* **277**, 10482–10488.

Sweeney MI (1996). Adenosine release and uptake in cerebellar granule neurons both occur via an equilibrative nucleoside carrier that is modulated by G proteins. *J Neurochem* **67**, 81–88.

Takahashi M, Kovalchuk Y & Atwell D (1995). Pre- and postsynaptic determinants of EPSC waveform at cerebellar fiber and parallel fiber to Purkinje cell synapses. *J Neurosci* **15**, 5693–5702.

Wall MJ & Dale N (2007). Auto-inhibition of parallel fibre-Purkinje cell synapses by activity dependent adenosine release. *J Physiol* (in the press).

Wall MJ & Usowicz MM (1997). Development of action potential-dependent and independent spontaneous $GABA_A$ receptor-mediated currents in granule cells of postnatal rat cerebellum. *Eur J Neurosci* **9**, 533–548.

Wang TF & Guidotti G (1998). Widespread expression of ecto-apyrase (CD39) in the central nervous system. *Brain Res* **790**, 318–321.

Wink MR, Braganhol E, Tamajusuku ASK, Casali EA, Karl J, Barreto-Chaves ML, Sarkis JJF & Battastini AMO (2003). Extracellular adenine nucleotides metabolism in astrocyte cultures from different brain regions. *Neurochem Int* **43**, 621–628.

Yamada T, Kobayashi T & Okada Y (1998). The effects of simulated ischemia on the levels of adenosine and its metabolites in slices of cerebellum, superior colliculus and hippocampus in the guinea pig – *in vitro* study. *Brain Res* **787**, 220–225.

Yuan Y & Atchison WD (1999). Comparative effects of methylmercury on parallel-fiber and climbing fiber responses of rat cerebellar slices. *J Pharmacol Exp Ther* **288**, 1015–1025.

Zhang G, Franklin PH & Murray TF (1993). Manipulation of endogenous adenosine in the rat prepiriform cortex modulates seizure susceptibility. *J Pharmacol Exp Ther* **264**, 1415–1424.

Zimmermann H (2000). Extracellular metabolism of ATP and other nucleotides. *Naunyn-Schmiedebergs Arch Pharmacol* **362**, 299–309.

## Acknowledgements

# Adenosine signalling at immature parallel fibre–Purkinje cell synapses in rat cerebellum

Alison Atterbury and Mark J. Wall

*Neuroscience Group, Department of Biological Sciences, University of Warwick, Coventry CV4 7AL, UK*

The purine adenosine is an extracellular signalling molecule involved in a large number of physiological and pathological conditions throughout the mammalian brain. However little is known about how adenosine release and its subsequent clearance change during brain development. We have combined electrophysiology and microelectrode biosensor measurements to investigate the properties of adenosine signalling at early stages of cerebellar development, when parallel fibre–Purkinje cell synapses have recently been formed (postnatal days 9–12). At this stage of development, we could detect little or no inhibitory $A_1$ receptor tone in basal conditions and during trains of stimuli. Addition of pharmacological agents, to inhibit adenosine clearance, had only minor effects on synaptic transmission suggesting that under basal conditions, the concentration of adenosine moving in and out of the extracellular space is small. Active adenosine release was stimulated with hypoxia and trains of electrical stimuli. Although hypoxia released significant concentrations of adenosine, the release was delayed and slow. No adenosine release could be detected following electrical stimulation in the molecular layer. In conclusion, at this stage of development, although adenosine receptors and the mechanisms of adenosine clearance are present there is very little adenosine release.

**Abbreviations** AD, adenosine deaminase; ADO biosensor, adenosine biosensor/INO inosine biosensor; CPA, $N^6$-cyclopentyladenosine; 8-CPT, 8-cyclopentyltheophylline; EHNA, erythro-9-(2-hydroxy-3-nonyl)adenine; NBTI, $S$-(4-nitrobenzyl)-6-thioinosine; PF, parallel fibre; PNP, purine nucleoside phosphorylase; XO, xanthine oxidase.

The purine adenosine is involved in many diverse CNS processes including sleep, locomotion and respiration and provides neuroprotection during hypoxia and ischaemia. (for review see Boison, 2007). The mechanism of how adenosine is released into the extracellular space is still, in many cases, unclear (for review see Wall & Dale, 2008) but could occur by extracellular ATP metabolism (ATP released by exocytosis, Edwards *et al.* 1992; Dale, 1998; or through gap junction hemi channels, Pearson *et al.* 2005), adenosine transport from the cell cytoplasm (Craig & White, 1993; Sweeney, 1996) or possibly by the exocytosis of adenosine itself (Wall & Dale, 2007). Once released, the actions of adenosine are terminated by a combination of extracellular metabolism to inosine (by the enzyme adenosine deaminase) and transport into neuronal or glial cytoplasm by equilibrative transporters such as ENT1 and ENT2 or concentrative transporters (for review see Noji *et al.* 2004; Baldwin *et al.* 2004). Once internalised adenosine is phosphorylated (by adenosine kinase) to form AMP, maintaining low levels

of intracellular adenosine (for review see Boison, 2007). Because the levels of adenosine are determined by the interplay of enzymes and transporters, a number of studies have investigated which components play a major role in determining extracellular adenosine concentration. In many studies blocking adenosine kinase has a major effect on adenosine concentration where extracellular metabolism (via adenosine deaminase) appears less important (Pak *et al.* 1994; Lloyd & Fredholm, 1995; Wall *et al.* 2007).

Although adenosine release probably occurs in most brain areas, relatively little is known about how adenosine release, receptor signalling and clearance change during brain development. At the calyx of Held in mice, $A_1$ receptor expression declines during the second postnatal week (Kimura *et al.* 2003). In the hippocampus, there is a developmental increase in the $A_1$ receptor tone at CA1 synapses, with no change in receptor properties (Psarropoulou *et al.* 1990). There is also a shift of adenosine kinase expression from neurones to astrocytes (Studer *et al.*

2006). Adenosine appears a more potent anticonvulsant in hippocampal slices from adult rats compared to immature rats (Descombes *et al.* 1998). This is supported by the observation that pair pulse facilitation shows greater enhancement in young adult slices (P28–35) compared to juvenile slices (P15–21) even though the amount of synaptic depression was similar (Dumas & Foster, 1998).

Thus the aim of this study is to combine biosensor measurements and electrophysiology to investigate the properties of adenosine signalling at a period early in cerebellar development, soon after synapse formation. The glutamatergic parallel fibre–Purkinje cell synapse is formed around postnatal day 5 in the rat (Altman, 1972) and we have investigated the properties of adenosine signalling between postnatal days 9 and 12 (the earliest period when extracellular field parallel fibre–Purkinje cell EPSPs can reliably be measured). Previous studies have shown that adenosine $A_1$ receptors are present at the synapses at postnatal days 10–15 (Takahashi *et al.* 1995), with $A_1$ receptors expressed in the cerebellum before birth (Weaver, 1996). In previous studies (from P21–28) rats we have shown that there is a tone of extracellular adenosine which tonically inhibits parallel fibre–Purkinje cell synapses. The concentration of this adenosine is controlled, in the main, by the level of adenosine kinase activity (Wall *et al.* 2007). The source of this extracellular adenosine is currently unclear but it does not appear to arise from action potential-dependent release (Wall & Dale, 2007).

## Methods

### Preparation of cerebellar slices

Transverse slices of cerebellar vermis (400 $\mu$m) were prepared from male Wistar rats, at postnatal days 9–28 (P9–28). As described previously (Wall *et al.* 2007) and in accordance with the UK Animals (Scientific Procedures) Act 1986, male rats were killed by cervical dislocation and decapitated. The cerebellum was rapidly removed and slices were cut on a Microm HM 650V microslicer in cold (2–4°C) high $Mg^{2+}$, low $Ca^{2+}$ artificial cerebrospinal fluid (aCSF; composed of, mM: 127 NaCl, 1.9 KCl, 7–8 $MgCl_2$, 0.5 $CaCl_2$, 1.2 $KH_2PO_4$, 26 $NaHCO_3$, 10 D-glucose (pH 7.4 when bubbled with 95% $O_2$–5% $CO_2$, 300 mosmol l$^{-1}$). Slices were stored in normal aCSF (1.3 mM $MgCl_2$, 2.4 mM $CaCl_2$) at room temperature for 1–6 h before recording.

### Extracellular recording

An individual slice was transferred to a recording chamber, submerged in aCSF and perfused at 6 ml min$^{-1}$ (30–32°C). The slice was placed upon a suspended grid to allow perfusion from above and below, and this reduce the likelihood of hypoxia. Furthermore, all solutions were vigorously bubbled (95% $O_2$–5% $CO_2$) and all tubing had low gas permeability (Tygon). For the stimulation of parallel fibres, square voltage pulses (2–5 V, 200 $\mu$s duration) were delivered by an isolated pulse stimulator (model 2100, AM systems, Everett, WA, USA) via a concentric bipolar metal stimulating electrode (FHC Inc., Bowdoin, ME, USA) placed on the surface of the molecular layer. The recording electrode (an aCSF filled microelectrode) was placed on the same track along which the parallel fibres travel ('on-beam', Yuan & Atchison, 1999). A typical extracellular field potential consisted of a presynaptic fibre volley followed by a component which could be blocked by 1 $\mu$M TTX and greatly reduced by 5 mM kynurenate. This component is probably produced by parallel fibre mediated glutamatergic excitatory synaptic currents in Purkinje cells and interneurones (Clark & Barbour, 1997). Parallel fibre EPSP amplitude was estimated from the kynurenate sensitive potential, which was measured by subtracting what remained in kynurenate from control potentials. Confirmation of PF EPSP identity was achieved by evoking pairs of EPSPs (interval 50 ms) and observing facilitation (20–30%), and by examining the pharmacological profile (inhibition by $A_1$, $GABA_B$ or mGlu4R receptor agonists). Extracellular recordings were made using an ISO-DAM extracellular amplifier (WPI, Sarasota, FL, USA), filtered at 1 kHz and digitised on-line (10 kHz) with a Micro 1401-2 (Mark 2) interface controlled by Spike software (v. 6.1) (Cambridge Electronic Design, Cambridge, UK).

### Purine biosensors

Biosensors were obtained from Sarissa Biomedical Ltd (Coventry, UK). In brief the biosensors consisted of entrapped enzymes (adenosine deaminase, AD; purine nucleoside phosphorylase, PNP; and xanthine oxidase, XO) within a matrix that was deposited around a Pt or Pt/Ir (90/10) wire etched to ~50 $\mu$m (Llaudet *et al.* 2003). The biosensor had an exposed length of ~500 $\mu$m that was coated with enzymes and thus capable of detecting purines. Biosensors were screened, which greatly reduced the responses to electro-active interferents (such as 5-HT, noradrenaline, dopamine and ascorbate). Three types of purine biosensor were used in this study to identify the released substances. Firstly, a screened null sensor, possessing the matrix but no enzymes, was used to control for the release of any non-specific electro-active interferents. Secondly, screened biosensors containing PNP and XO (responsive to inosine and hypoxanthine) and NP, XO and AD ((INO) responsive to inosine, hypoxanthine and adenosine (ADO)) were used. The difference signal between these two types of biosensors gave the specific adenosine and adenosine metabolite (inosine and

hypoxanthine) signals. A full description of the properties of the biosensors has already been published but they show a linear response to increasing concentration of analyte, are fast to respond, and have a rise time of less than 10 s (Llaudet *et al.* 2003).

The biosensors were positioned just above the surface of the molecular layer. Biosensors were bent so their longitudinal surface was parallel to the slice surface, thus increasing the detection area (Wall & Dale, 2007). Biosensors were calibrated with known concentrations (10 $\mu$M) of adenosine and inosine. The screening of biosensors was checked by applying 10 $\mu$M of 5-HT. Calibration was performed before the slice was present in the perfusion chamber and after the slice had been removed; this allowed measurement of any reduction in sensitivity during the experiment. Biosensor signals were acquired at 1 kHz with a Micro 1401-2 (Mark 2) interface using Spike (v. 6.1) software.

### Drugs and substances

All drugs were made up as 10–100 mM stock solutions, stored frozen and then thawed and diluted with aCSF on the day of use. Adenosine, inosine, *S*-(4-nitrobenzyl)-6-thioinosine (NBTI), 8-cyclopentyltheophylline (8-CPT), and dipyridamole were purchased from Sigma. Iodotubercidin was purchased from Sigma and Molekula (Fine Chemicals, Gillingham, Dorset, UK). Erythro-9-(2-hydroxy-3-nonyl) adenine (EHNA) was purchased from Tocris-Cookson (Bristol, UK). Kynurenic acid and CNQX were purchased from Ascent Scientific (Bristol, UK). Hypoxia was induced by changing the inflow from oxygenated aCSF to aCSF bubbled with $N_2$ (95%)–$CO_2$ (5%).

## Results

### The tonic inhibition of parallel fibre–Purkinje cell synapse by endogenous adenosine is greatly reduced or absent in slices from P9–12 rats

Previous studies have shown that $A_1$ adenosine receptors at parallel fibre–Purkinje cell synapses tonically inhibit synaptic transmission, suggesting the continual presence of extracellular adenosine (Takahashi *et al.* 1995; Wall *et al.* 2007). We have investigated whether such tonic $A_1$ receptor-mediated inhibition is present at a developmental period soon after the formation of parallel fibre–Purkinje cell synapses (postnatal days 9–12). Application of the $A_1$ receptor antagonist 8-CPT (1–2 $\mu$M) had no effect on the amplitude of PF EPSPs or the paired pulse ratio in 9 out of 20 slices (45%, Fig. 1*A* and *B*). In the remaining 11 slices, 8-CPT increased PF EPSP amplitude by 13.4 ± 2.6%. Overall the block of $A_1$ receptors only increased EPSP amplitude by 7.4 ± 5.6% ($n = 20$), which

is significantly less ($P < 0.001$) than that observed in interleaved experiments on slices from P21–28 rats (45.6 ± 7% increase, 8 slices Fig. 1*B* and see Wall *et al.* 2007). There was no correlation between the age of rat (between P9 and 12) and the presence or absence of an adenosine receptor tone.

A reduced adenosine $A_1$ receptor tone, early in development, could result from low receptor expression or the expression of low affinity $A_1$ receptors. This was tested by applying adenosine (100 $\mu$M) to inhibit PF EPSPs ($n = 54$ slices) and then following wash, applying 8-CPT (1–2 $\mu$M) to measure the $A_1$ receptor tone. There were some synapses where adenosine (100 $\mu$M) had little or no effect on synaptic transmission. These synapses were not investigated further as presumably they would have no $A_1$ receptor tone. In the remaining synapses (where 100 $\mu$M adenosine produced at least a 50% reduction in PF EPSP amplitude), adenosine produced the same reduction in PF EPSP amplitude whether or not an inhibitory adenosine receptor tone was present (no tone, 70.5 ± 5.4% *vs.* 68.5 ± 4.7% with mean tone of 14.3 ± 2.8%; Fig. 1*A* and *C*). The inhibition produced by adenosine (100 $\mu$M) was not different from that observed in slices from P21–28 rats (61.5 ± 2.1%, $n = 47$ slices; and see Wall *et al.* 2007). There was also no significant change in the adenosine-mediated increase in paired pulse facilitation between young (increased from 1.38 ± 0.02 to 1.85 ± 0.04, $n = 54$) and adult slices (increased from 1.45 ± 0.02 to 1.92 ± 0.06, $n = 47$). To check the properties of the $A_1$ receptors more carefully, dose–response curves were constructed for the non-hydrolysable $A_1$ receptor agonist $N^6$-cyclopentyladenosine (CPA). The curves constructed from P9–12 and P21–28 could be superimposed (Fig. 1*D*). Thus the lack of adenosine tone at immature synapses does not appear to result from changes in $A_1$ receptor properties or expression. In all experiments, the sensitivity of synapses was first tested (with 100 $\mu$M adenosine) and synapses were rejected if adenosine did not produce at least a 50% reduction in EPSP amplitude.

### The presence or absence of tonic $A_1$ receptor activation has marked effects on trains of activity

Numerous studies have demonstrated that presynaptic inhibition has important effects on trains of activity, with a reduction in initial transmitter release allowing synaptic transmission to persist for longer during a train of stimuli (for example see Kreitzer & Regehr, 2000; Kimura *et al.* 2003; Wong *et al.* 2006). We have investigated what effect the adenosine tone has on trains of EPSPs (100 EPSPs, 20 Hz) in young and mature slices. During trains of stimuli, transmission in slices from P9–12 rats was first facilitated and then depressed (Fig. 2*A*). PF EPSP amplitude was increased to a maximum of 157 ± 10.9% of

the first EPSP amplitude ($n = 6$) at around the 10th EPSP and then decreased to an amplitude less than the first EPSP by around the 70th EPSP. Blocking of $A_1$ receptors (with 2 $\mu$M 8-CPT) had no significant effect on the amplitude of PF EPSPs during the train (Fig. 2*A*). This was expected since there is little or no tonic activation of $A_1$ receptors, but it also suggests that there is little or no adenosine release during the train (see Wall & Dale, 2007). Addition of (100 $\mu$M) adenosine produced a marked change in the trains of PF EPSPs, with significantly ($P < 0.01$) greater facilitation (maximum 215 $\pm$ 27%) and the EPSP

amplitude remaining elevated above the amplitude of the first EPSP for the duration of the train (Fig. 2*A*).

Trains of EPSPs were also evoked at parallel fibre–Purkinje cell synapses in slices from P21–28 rats where there is a much larger inhibitory $A_1$ receptor tone (Fig. 2*B*). Like immature synapses, PF EPSP amplitude was facilitated (146 $\pm$ 8.1%) and then depressed, although this depression happened much earlier in the train (EPSP amplitude less than first EPSP amplitude by around the 30th EPSP, Fig. 2*B*). Addition of adenosine (100 $\mu$M) caused a marked increase in the degree
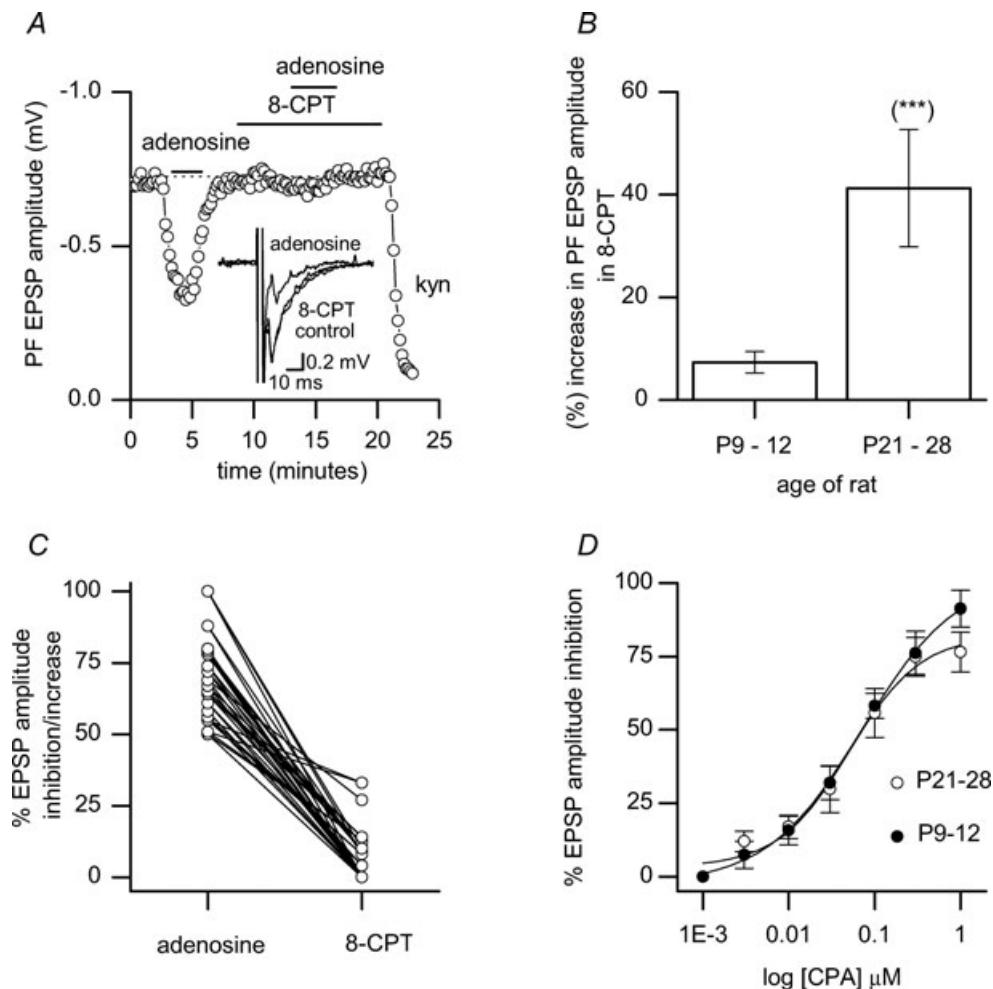


**Figure 1. Little or no tonic activation of presynaptic $A_1$ receptors at immature parallel fibre to Purkinje cell synapses**
*A*, plot of the amplitude of individual parallel fibre (PF) EPSPs (field) against time in a slice from a P10 rat. Although application of adenosine (100 $\mu$M) produced a decrease in EPSP amplitude of ~55%, block of $A_1$ receptors with 8-CPT (2 $\mu$M) had no effect on EPSP amplitude. Addition of adenosine (100 $\mu$M) in the presence of 8-CPT had no effect on EPSP amplitude showing $A_1$ receptors were blocked. Synaptic transmission was blocked at the end of the experiment with 5 mM kynurenate (Kyn). Inset, superimposed average EPSPs from *A* in control, adenosine (100 $\mu$M) and 8-CPT (2 $\mu$M). *B*, summary of the effects of 8-CPT on the amplitude of PF EPSPs recorded from 20 slices from P9–12 rats and 8 slices from P21–28 rats. *C*, plot of the reduction in PF EPSP amplitude following application of adenosine (100 $\mu$M) against the increase in PF EPSP amplitude following block of $A_1$ receptors with 8-CPT (2 $\mu$M). Adenosine was applied first, then washed and then 8-CPT was applied (as in *A*). *D*, concentration–response curves constructed for the reduction in PF EPSP amplitude by the $A_1$ receptor agonist CPA in P9–12 ($n = 5$) and P21–28 ($n = 4$) slices.

of facilitation ($255 \pm 32\%$), which was maintained at $\sim200\%$ throughout the train (Fig. 2$B$). Addition of 8-CPT (1–2 $\mu$M) caused a small but significant ($P < 0.05$) reduction in the degree of facilitation (from $146 \pm 8.1\%$ to $129 \pm 32\%$) followed by almost complete depression of transmission (11% of first EPSP amplitude) of EPSP amplitude and then recovery (to $\sim50\%$ of the first EPSP, Fig. 2$B$). The actions of 8-CPT appeared larger later in the train suggesting that adenosine release occurred during the train (see Wall & Dale, 2007).

## There is a low concentration of extracellular adenosine metabolites in immature slices

In a previous study (Wall *et al.* 2007), although $A_1$ receptors were tonically activated in cerebellar slices from P21–28 rats, biosensors placed in or above the slices could not detect adenosine but instead detected the adenosine metabolites inosine and hypoxanthine. It can be predicted that the concentration of these metabolites would be reduced in immature slices since there is little or no $A_1$ receptor tone. The extracellular purine tone was measured by moving purine (ADO and INO) and null sensors close to the slice surface. Sensors were bent so they were parallel to the slice surface, thus increasing the amount of sensing surface in close proximity to the slice (this will increase the measured purine tone compared to Wall *et al.* (2007), where the sensors were not bent). The advantage of this experiment is that the slice is not damaged by sensor insertion and no resultant purine release occurs (see Wall *et al.* 2007). As predicted, there was only a small increase in baseline current when ADO or INO sensors were moved close to the slice surface (mean change in current: $43.4 \pm 4.1$ pA, ADO sensors; $61.7 \pm 18$ pA, INO sensors; $n = 15$ slices; Fig. 3$A$). There was little or no change in baseline current when a null sensor was moved close to or away from the slice surface (Fig. 3$A$). After correcting for calibration, there was no significant difference between the current measured on the ADO and INO sensors, and thus the current is not produced by adenosine but is produced by the metabolites (inosine and hypoxanthine, see Wall *et al.* 2007). If we assume that all of the purine detected is inosine then the net concentration of inosine measured on the surface of the slice was $0.25 \pm 0.03$ $\mu$M ($n = 15$ slices, Fig. 3$B$). Interleaved experiments with slices from P21–28 rats showed an almost 5-fold larger increase in current when purine sensors were moved close to the slice surface ($224.3 \pm 35.9$ pA, Fig. 3$A$, $n = 8$ slices, equivalent to $1.6 \pm 0.3$ $\mu$M inosine also see Wall *et al.* 2007). The low extracellular concentration of adenosine metabolites suggests that the lack of adenosine $A_1$ receptor activation does not result from the metabolism of significant concentrations of extracellular adenosine (Fig. 3$B$).

## Interrupting adenosine clearance has only small effects on the inhibitory $A_1$ receptor tone

The lack of adenosine tone could stem from either the rapid removal of adenosine or reduced extracellular production. Adenosine is removed from the extracellular space by a combination of extracellular metabolism (adenosine deaminase) and uptake (equilibrative and
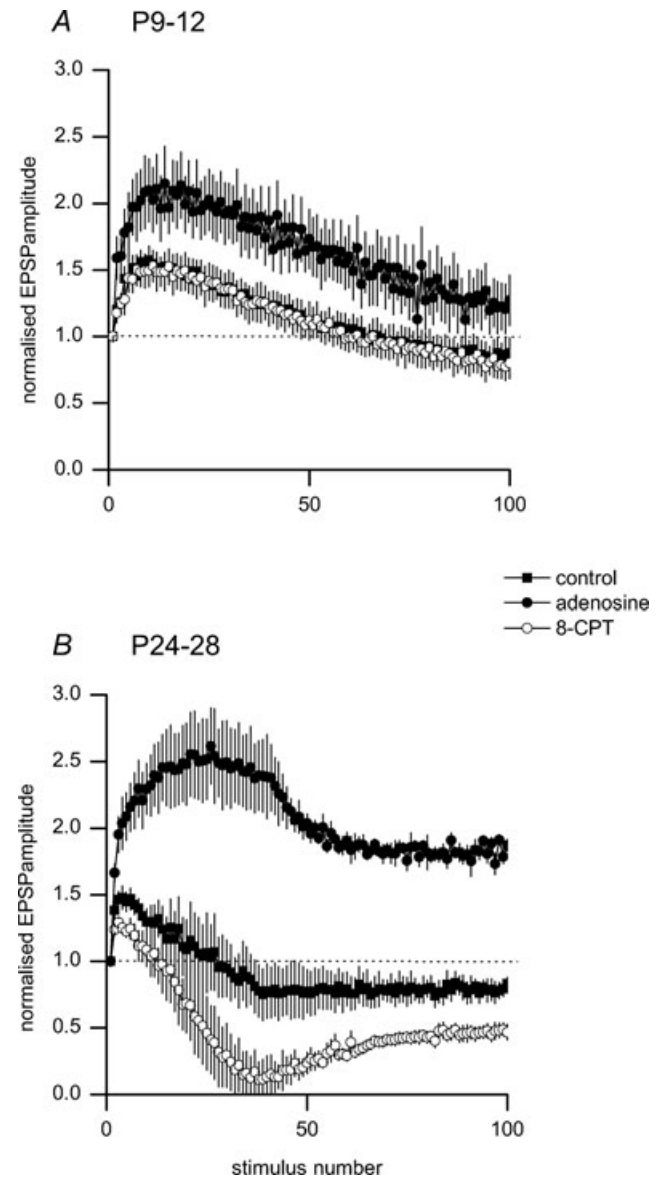


**Figure 2. An $A_1$ receptor tone has marked effects on trains of activity**

*A*, plot of normalised EPSP amplitude (relative to the first EPSP amplitude) against stimulus number in control, 100 $\mu$M adenosine and 2 $\mu$M 8-CPT for 6 parallel fibre–Purkinje cell synapses in slices from P9–12 rats. *B*, plot of normalised EPSP amplitude (relative to the first EPSP amplitude) against stimulus number in control, 100 $\mu$M adenosine and 2 $\mu$M 8-CPT for 5 parallel fibre–Purkinje cell synapses in slices from P24–28 rats. Stimulus frequency was 20 Hz.

concentrative transporters) followed by intracellular conversion to adenosine monophosphate by adenosine kinase. We have used pharmacological agents to reduce adenosine clearance and thus investigated the rate of basal adenosine production.

**Adenosine metabolism.** To investigate the role of metabolism, PF EPSPs recordings were made in the presence of EHNA. EHNA blocks the enzyme adenosine deaminase (Agarwal, 1982) and thus should produce extracellular adenosine accumulation and inhibition of PF EPSPs. Application of EHNA (20 $\mu$M) had little effect on PF EPSPS; the amplitude (1.2 ± 1.6% reduction, 5 slices, range 0 to 12%, Fig. 4*A*) and the paired pulse ratio (1.33 ± 0.3 *vs.* 1.34 ± 0.3) were not significantly changed.

Thus as suggested by the biosensor results, there appears to be little ongoing adenosine metabolism.

**Equilibrative transporters.** We have investigated the roles of the equilibrative transporters (ENT1 and ENT2) using the inhibiters NBTI and dipyridamole (Dunwiddie & Diao, 1994; Frenguelli *et al.* 2007). Application of 10 $\mu$M dipyridamole and 5 $\mu$M NBTI for prolonged periods (30 min) produced a mean reduction in EPSP amplitude of 16.9 ± 3.5% (31 slices). In 15 out of the 31 slices NBTI/dipyridamole had no effect on EPSP amplitude (Fig. 5*C*). In the remaining 16 slices, EPSP amplitude was
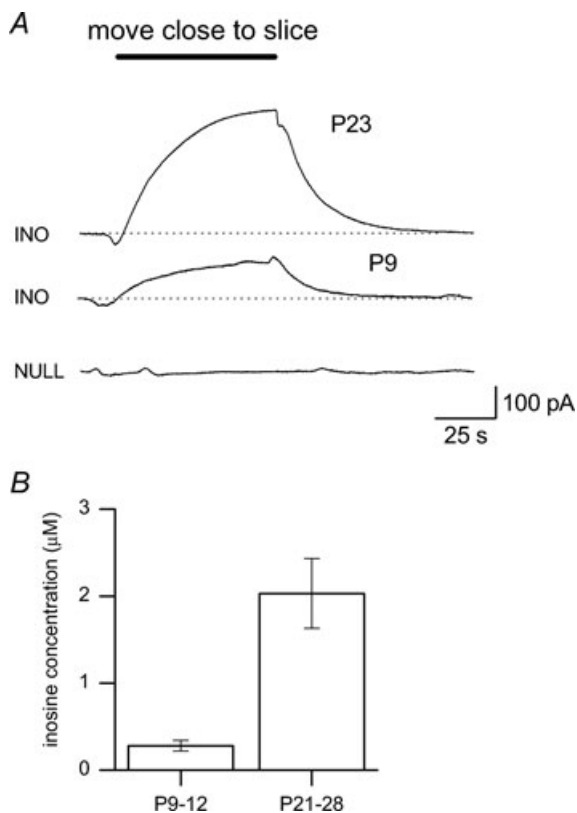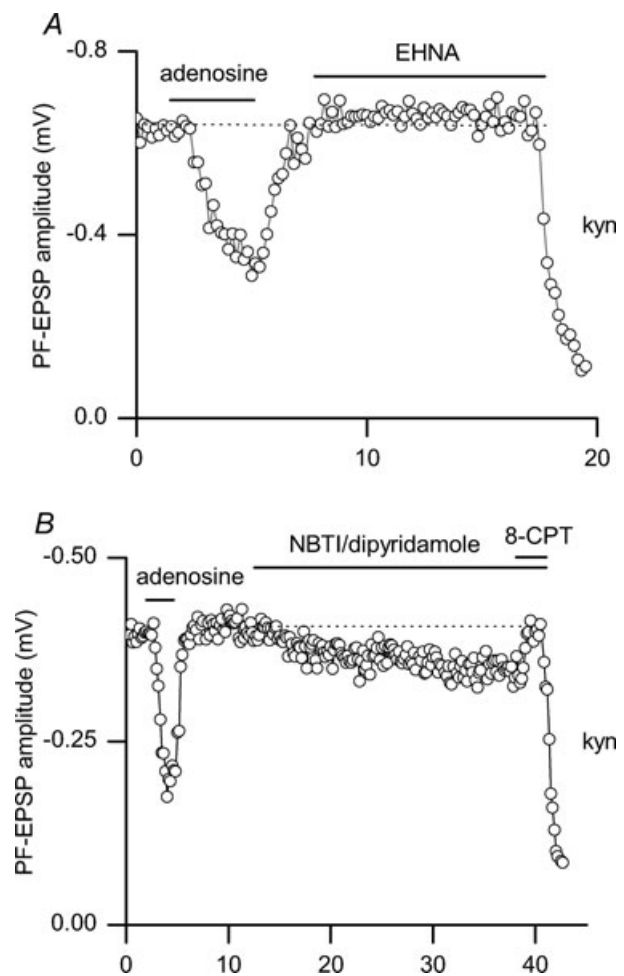


**Figure 3. The concentration of extracellular adenosine metabolites is reduced in immature slices**
*A*, example biosensor traces from experiments to measure the concentration of purines at the surface of slices from P23 and P9 rats (interleaved experiments). After the inosine (INO) biosensor was moved close to the slice surface there was a rapid increase in the baseline current of ∼350 pA (P23) and ∼100 pA (P9). Movement of the null sensor to the surface of the slice had no effect in P23 or P9 slices (P23 illustrated). *B*, plot of the mean concentration of inosine measured close to the slice surface (from 15 slices from P9–12 rats and 8 slices from P21–28 rats). The concentration of inosine was determined following calibration of the biosensor and assumes all the current arises from inosine.



**Figure 4. Inhibition of extracellular adenosine metabolism and equilibrative transport has little effect on synaptic transmission**
*A*, although PF EPSPs were markedly reduced by adenosine (100 $\mu$M, ∼50%), the adenosine deaminase inhibitor EHNA (20 $\mu$M) had no effect on PF EPSP amplitude. *B*, block of equilibrative transport with 5 $\mu$M NBTI and 10 $\mu$M dipyridamole caused a small reduction (∼15%) in PF EPSP amplitude, which was reversed by blocking A$_1$ receptors with 8-CPT (1.5 $\mu$M). Addition of adenosine (100 $\mu$M) at the beginning of the experiment reduced EPSP amplitude by ∼55%. The graphs in *A* and *B* plot the amplitude of individual PF EPSPs against time. PF EPSPs were blocked at the end of the experiment with 5 mM kynurenate (kyn).
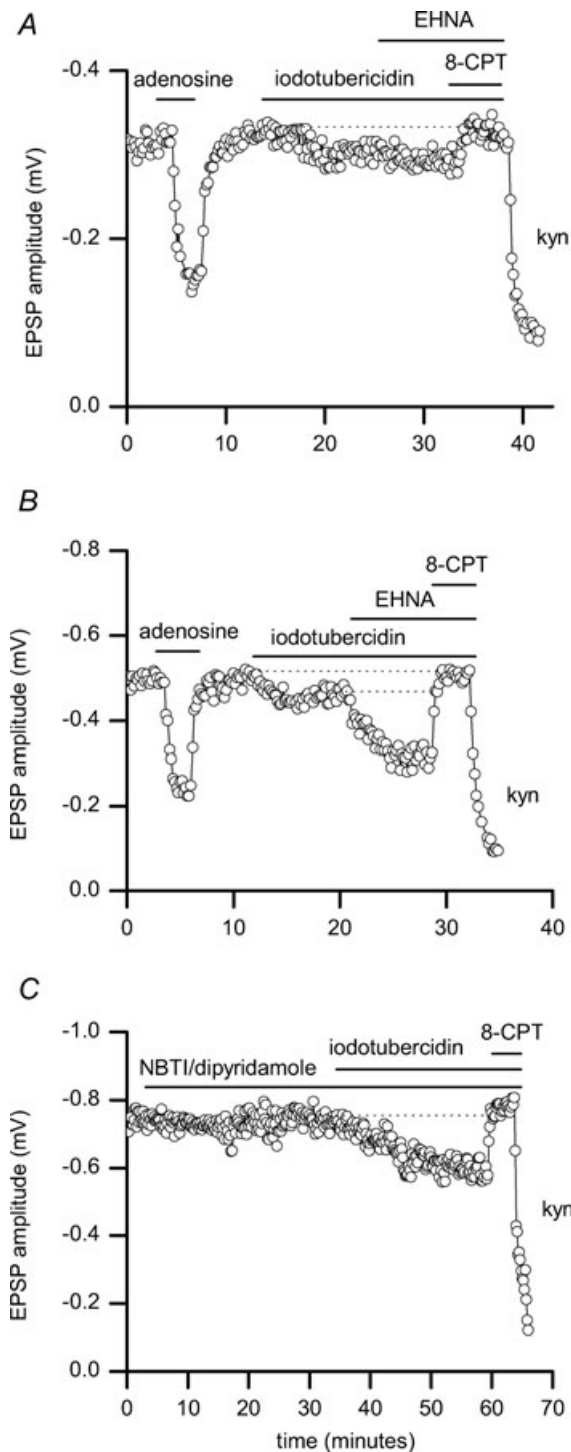
**Figure 5. Inhibition of adenosine kinase has minor effects on synaptic transmission**

*A*, the block of adenosine kinase with iodotubercidin (2 $\mu$M) produced a small reduction in PF EPSP amplitude ($\sim$20%). Block of adenosine deaminase (EHNA 20 $\mu$M) did not increase the block, which was reversed by blocking $A_1$ receptors with 8-CPT (1.5 $\mu$M). *B*, following addition of iodotubercidin (2 $\mu$M), block of extracellular adenosine metabolism (EHNA 20 $\mu$M) produced a marked increase in the inhibition of PF EPSP amplitude. The block was reversed by addition of 8-CPT (2 $\mu$M). *C*, pre-incubation with 5 $\mu$M NBTI and 10 $\mu$M

reduced by $32.7 \pm 4\%$ (Fig. 4*B*) with an increase in paired pulse ratio from $1.4 \pm 0.05$ to $1.6 \pm 0.08$. This inhibition was reversed by blocking $A_1$ receptors with 8-CPT (2 $\mu$M). There was no correlation between the reduction in EPSP amplitude produced by NBTI/dipyridamole and the presence or absence of an $A_1$ receptor tone. These results are similar to those observed at mature slices, where the actions of NBTI/dipyridamole were heterogeneous, although the mean inhibition was higher ($\sim$50%; Wall *et al.* 2007).

It is possible that any increase in extracellular adenosine concentration, following the block of equilibrative transport, is rapidly reduced by metabolism. Thus the adenosine deaminase inhibitor EHNA (20 $\mu$M) was applied in the presence of NBTI/dipyridamole (after 20–30 min pre-incubation). In six cells, pre-incubation with NBTI/dipyridamole had no effect on EPSP amplitude and nor did the addition of EHNA. In three cells, NBTI/dipyridamole decreased EPSP amplitude by $30 \pm 0.5\%$, and addition of EHNA produced a further decrease in EPSP amplitude of $27 \pm 3\%$. Thus some of the adenosine is metabolised by adenosine deaminase.

**Adenosine kinase.** Once transported into cells, adenosine is phosphorylated to form AMP by the enzyme adenosine kinase, thus maintaining low levels of intracellular adenosine and preventing efflux via equilibrative transporters (for review see Boison, 2006). To assess the importance of adenosine kinase activity, the adenosine kinase blocker iodotubercidin was applied. Iodotubercidin (2 $\mu$M) reduced PF EPSP amplitude ($25 \pm 3\%$) and increased the paired pulse ratio ($1.3 \pm 0.1$ to $1.47 \pm 0.1$) in 14 out of 21 slices (Fig. 5*A*). The effects of iodotubercidin were completely reversed by blocking $A_1$ receptors with 8-CPT (1 $\mu$M). In the remaining seven slices, iodotubercidin had no effect on PF EPSP amplitude. The effects of iodotubercidin were significantly smaller than those observed in interleaved adult slices (68% inhibition, $n = 3$) and in published data (Wall *et al.* 2007).

To check if the elevated concentration of extracellular adenosine, produced by blocking adenosine kinase, is metabolised, we co-applied EHNA with iodotubercidin. The co-application of EHNA and iodotubercidin reduced PF EPSP amplitude by $50.7 \pm 7.8\%$ ($n = 6$), which was significantly ($P < 0.05$) higher than that observed with the block of adenosine kinase alone. This increased reduction in PF EPSP amplitude was reversed by addition

dipyridamole did not occlude the effects of blocking adenosine kinase (2 $\mu$M iodotubercidin). The plots in *A*, *B* and *C* are of individual PF EPSPs against time with synaptic transmission blocked at the end of the experiment with kynurenate (kyn, 5 mM).

of 8-CPT (1 $\mu$M). To examine this in more detail we applied EHNA (20 $\mu$M), after first blocking adenosine kinase with iodotubercidin (2 $\mu$M). We found the effects of EHNA mixed, producing little or no effect in three slices (Fig. 5*A*) and producing a large block in another four slices (Fig. 5*B*).

We have tried to occlude the increase in adenosine tone produced by iodotubercidin by blocking equilibrative transport. Iodotubercidin would be expected to have no effect if adenosine translocation is blocked. In six slices, following application of NBTI/dipyridamole, block of adenosine kinase with iodotubercidin still reduced EPSP amplitude by $25.3 \pm 3.5\%$ (Fig. 5*C*). Thus, as observed with mature slices (Wall *et al.* 2007), NBTI/dipyridamole does not occlude the actions of iodotubercidin. In four slices, there was little or no adenosine transport as neither iodotubercidin nor NBTI/dipyridamole had any effect on synaptic transmission.

## Adenosine release is delayed or reduced at immature parallel fibre–Purkinje cell synapses

Our results demonstrate that there is a low concentration of extracellular adenosine at parallel fibre–Purkinje cell synapses in slices from P9–12 rats. Since blocking clearance had little effect, there is little release of adenosine under basal conditions. To investigate the active release of adenosine we have used hypoxia and local electrical stimulation as release stimuli.

A 10 min period of hypoxia reversibly reduced PF EPSP amplitude, an effect which was reversed by blocking $A_1$ receptors with 8-CPT (1–2 $\mu$M). At steady state, PF EPSP amplitude was reduced by $64 \pm 7\%$ and the paired pulse ratio was increased from $1.25 \pm 0.04$ to $1.8 \pm 0.1$ ($n =$ 11 slices, Fig. 6*A*). The reduction in PF EPSP amplitude can be used to measure the speed of rise in extracellular adenosine concentration. The inhibition reached steady state after $5.4 \pm 0.7$ min (delay until start of depression $3.7 \pm 0.6$ min). The decrease in PF EPSP amplitude was fully reversed by reoxygenation after $5.3 \pm 0.5$ min ($n =$ 8 slices).

As a comparison, hypoxia (10 min) was also induced in P21–28 slices where it induced a marked depression in PF EPSP amplitude ($81.3 \pm 6.6\%$, $n = 5$ slices). However, following 10 min of hypoxia, the inhibition was often not completely reversed by blocking $A_1$ receptors with 8-CPT (complete reversal was only observed in 2 out of 5 slices). However, with shorter periods of hypoxia (5 min), reversal of block was observed in 6 out of 8 slices (mean inhibition $73 \pm 5.4\%$, $n = 6$ slices). The speed of depression was very rapid; the time to reach a steady state depression was $2.3 \pm 0.3$ min ($n = 8$ slices), which is double the rate of inhibition observed in young animals. The delay until the start of PF EPSP amplitude depression was $1.1 \pm 0.4$ min.

To investigate the kinetics of purine release in more detail we have used purine biosensors. ADO, INO and null sensors were placed on the surface of the molecular layer (sensors were bent to be parallel with the slice surface, see Wall & Dale 2007). A short period of hypoxia (10 min) produced a large current on ADO and INO sensors in both P9–12 and P21–28 rats (Fig. 6*C* and *D*). As no increase in baseline current was observed on null sensors, the current was produced by the release of purines (Fig. 6*C* inset). Since the currents on ADO and INO sensors were not different in rise or amplitude (after correction for calibration), the sensors detected adenosine metabolites (inosine and hypoxanthine). Assuming that all the metabolite is inosine, then the maximum concentration of inosine detected at the surface of the slice (following hypoxia) was $3.5 \pm 0.4$ $\mu$M for P9–12 slices ($n = 8$) and $5.5 \pm 0.7$ $\mu$M for P21–28 slices ($n = 8$). Although hypoxia appeared to release significantly ($P > 0.05$) more purines from older slices, this difference probably stems from the slower rate of purine release in P9–12 slices. In all P9–12 slices ($n = 8$), the sensor current had not reached steady state after 10 min of hypoxia and was still rising during reoxygenation (Fig. 6*C* and *D*). In contrast, the sensor current reached a plateau after $5.3 \pm 0.5$ min in P21–28 slices (Fig. 6*D*). The slow release in P9–12 slices resulted from a greater delay in the start of purine release combined with a much slower rise in purine concentration (experiments were interleaved so the bath inflow and outflow speed were exactly the same in mature and immature slices). The rising phase of the sensor current could be fitted with a single exponential to give a time constant of $9.1 \pm 0.4$ min for P9–12 slices and $1.5 \pm 0.3$ min for P21–28 slices. In some slices (both adult and young), following reoxygenation, the rate of purine release appeared enhanced before it began to fall. Such a phenomenon has been observed following ischemia in the hippocampus (termed post-hypoxic purine efflux, PPE, Frenguelli *et al.* 2003) and was more apparent if the biosensor was pushed into the slice ($n = 2$). After reoxygenation, the decay of the biosensor current could be fitted with a single exponential with a time constant of ~15 min for both P9–12 and P21–28 slices.

In P21–28 rats, adenosine can be reliably released by trains of electrical stimulation in the molecular layer, a process which is both action potential and $Ca^{2+}$ dependent (Fig. 6*E*; observed in 4 out of 4 slices in interleaved experiments, and see Wall & Dale (2007)). However it was not possible to observe such adenosine release (the response of the ADO sensor was the same as the null sensor) at immature synapses, even with prolonged high frequency stimulation (200 stimuli, 20–40 Hz, $n = 15$ slices, Fig. 6*E*). To check that it was possible to detect adenosine release in these slices, the stimulus strength was increased (above 25 V) to electroporate the cells under the stimulating electrode (Hamann & Attwell, 1996; Wall &

Dale, 2007). A large signal was then observed on the ADO sensor but not on the null sensor ($n = 3$, not illustrated).

## Discussion

There is little or no tonic $A_1$ receptor activation at parallel fibre–Purkinje cell synapses in slices from P9–12 rats compared to synapses in slices from P21–28 rats (Wall *et al.* 2007). This low level of receptor activation does not result from either a lack of $A_1$ receptors or the presence of low affinity receptors. Thus during cerebellar development there is an increase in the level of tonic $A_1$ receptor activation with no obvious change in receptor properties. A similar developmental increase in $A_1$ receptor tone has been reported in the hippocampus (Psarropoulou *et al.* 1990) also with no change in receptor properties. In contrast, at the calyx of Held (in mice) there is a developmental reduction in both adenosine tone and receptor number (Kimura *et al.* 2003). Takahashi *et al.* (1995) have report a larger $A_1$ receptor activation in the cerebellum of postnatal day 10–15 rats ($\sim$24%). However
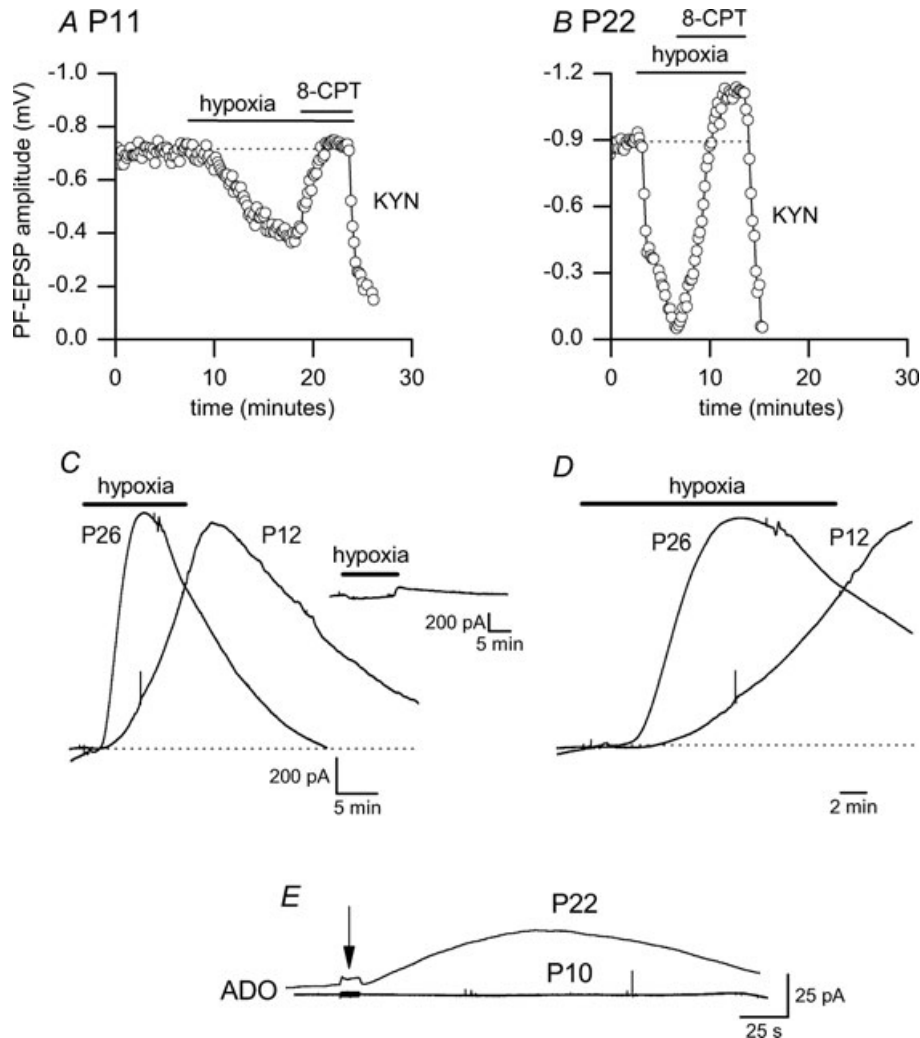


**Figure 6. Hypoxia but not electrical stimulation releases adenosine in immature slices**
*A*, the perfusion of a slice from a P11 rat with aCSF bubbled with $N_2$ (95%)–$CO_2$ (5%) for 10 min (hypoxia) caused a slow reduction in PF EPSP amplitude ($\sim$45%), which was reversed by block of $A_1$ receptors with 8-CPT (2 $\mu$M). *B*, in an interleaved experiment (recording from a slice from a P22 rat), the application of aCSF bubbled with $N_2$–$CO_2$ caused a much more rapid and larger inhibition of PF EPSP amplitude, which again could be reversed with block of $A_1$ receptors (8-CPT, 2 $\mu$M). Note the clear presence of an $A_1$ receptor tone in the slice from the P22 rat (*B*). *C*, example traces from ADO biosensors placed on the surface of slices (molecular layer) from P12 and P26 rats (interleaved experiments). Perfusion with aCSF bubbled with $N_2$–$CO_2$ for 10 min caused an increase in extracellular purine concentration for both slices but the rise was much more rapid in the slice from the P26 rat. Inset, hypoxia causes a small drop in current on the null sensor. *D*, traces from *C* expanded to show the difference in rise-time of biosensor current. *E*, electrical stimulation (at arrow, 10 s, 20 Hz, 5 V) caused the release of purines in a slice from a P22 rat but no detectable release in a P10 slice.

these experiments were carried out at room temperature, where the clearance of adenosine may be reduced.

Clearly, the presence or absence of an $A_1$ receptor tone will have marked effects on synaptic transmission. Addition of exogenous adenosine enhanced facilitation at both immature and mature synapses during trains of stimuli. Removal of the $A_1$ receptor tone, at mature synapses resulted in almost complete synaptic depression. Developmental changes in other modulators (such as cannabinoids, Crepel, 2007) will also alter the properties of parallel fibre–Purkinje cell synaptic transmission during trains of activity.

## Control of basal adenosine concentration at immature parallel fibre–Purkinje cell synapses

We have reduced the clearance of extracellular adenosine at immature parallel fibre–Purkinje cell synapses to investigate basal adenosine production. The small effect of blocking adenosine deaminase (with EHNA) suggests little ongoing extracellular metabolism. Similar small effects of EHNA have been observed in the hippocampus (Pak *et al.* 1994; Dunwiddie & Diao, 1994) and in mature cerebellar slices (Wall *et al.* 2007).

Adenosine kinase inhibition had minor effects on synaptic transmission (∼25% inhibition). Blockade of adenosine kinase causes an increase in the intracellular concentration of free adenosine and thus a resultant efflux of adenosine via equilibrative transporters (see Boison, 2006 for review). This is supported by the observation that blocking extracellular metabolism (with EHNA) can produce a reduction in PF EPSP amplitude following adenosine kinase inhibition. This also demonstrates that EHNA can reduce extracellular adenosine metabolism. The greater importance of adenosine kinase activity compared to extracellular metabolism has been observed in other brain regions (Pak *et al.* 1994; Lloyd & Fredholm, 1995) and in mature cerebellar slices (Wall *et al.* 2007).

The role of equilibrative transport was assessed by blocking ENT1 and ENT2. The effects on synaptic transmission were mixed with ∼50% of synapses inhibited (∼30%). Surprisingly, there was no correlation between the presence of an adenosine tone in control and the actions of NBTI/dipyridamole. As with mature slices, the application of NBTI/dipyridamole was unable to occlude the effects of adenosine kinase inhibition. Thus NBTI/dipyridamole was unable to block all adenosine transport. Such effects have also been observed at mature synapses (Wall *et al.* 2007) and may result from either expression of a transporter which is not blocked by NBTI/dipyridamole or high expression of ENT2, which is only weakly blocked in rat (Baldwin *et al.* 2004).

The blockade of adenosine breakdown, uptake and intracellular conversion to AMP all had relatively minor effects at immature synapses. The effects were also heterogeneous with synaptic transmission not effected at a large proportion of synapses. Thus the extracellular production of adenosine, under basal conditions, is low at immature synapses.

## The active release of adenosine

We used hypoxia and electrical stimulation to actively release adenosine and investigate whether there are pools of releasable adenosine. Hypoxia produced robust adenosine release and marked PF EPSP inhibition at both immature and mature synapses. Biosensor recordings suggest that similar concentrations of adenosine are released but release is slower and delayed at immature synapses. At mature slices, adenosine release is very sensitive to hypoxia as the synaptic depression (and therefore adenosine release) starts almost as soon as the hypoxic aCSF reaches the bath. It seems unlikely that the increased extracellular concentration of adenosine present in mature synapses stems from the slices being continually hypoxic as the slices were perfused (from above and below) by highly oxygenated aCSF at a fast perfusion rate (6 ml min$^{-1}$) via gas tight tubing. Thus this mechanism of adenosine release appears to become sensitive to hypoxia during development.

It was not possible to measure adenosine release in response to electrical stimuli in P9–12 slices, which contrasts with the reliable release in slices from older rats (Wall & Dale, 2007). It is possible that this mechanism of adenosine release is not present at this developmental stage or perhaps the number of adenosine release sites is so small that the concentration of adenosine released is below the levels of detection (∼30 nM). As parallel fibre activity is required for adenosine release (Wall & Dale, 2007), the smaller number of parallel fibre synapses present in the immature molecular layer may produce undetectable adenosine release. However the contribution of action potential-dependent adenosine release to the basal extracellular adenosine tone is small at mature synapses, as TTX had only a very minor effect on the tone (Wall *et al.* 2007). Thus the lack of this form of adenosine release cannot explain the developmental difference in basal adenosine receptor activation.

In conclusion, the extracellular concentration of adenosine is low at immature parallel fibre–Purkinje cell synapses and interference with adenosine clearance suggests that little adenosine is being cycled between intra- and extracellular compartments under basal conditions. Reduced release in response to electrical stimulation and slowed release in response to hypoxia suggest that the mechanisms of adenosine release become more efficient with development. It is possible that changes in adenosine kinase expression could account for the change

in the amount of releasable adenosine (and thus lack of adenosine tone). Studer *et al.* (2006) showed that early in development, hippocampal adenosine kinase expression is mainly in neurones and shifts to glia during the second postnatal week. Adenosine kinase expression in neurones could account for the lack of intracellular adenosine stores and the reduced extracellular release. It would be interesting to use immunohistochemistry to confirm cerebellar adenosine kinase expression.

# References

Altman J (1972). Postnatal development of the cerebellar cortex in the rat II. Phases in the maturation of Purkinje cells and of the molecular layer. *J Comp Neurol* **145**, 399–463.

Agarwal RP (1982). Inhibitors of adenosine deaminase. *Pharmacol Ther* **17**, 399–429.

Baldwin SA, Beal PR, Yao SYM, King AE, Cass CE & Young JD (2004). The equilibrative nucleoside transporter family, SLC29. *Pflugers Arch* **447**, 735–743.

Boison D (2006). Adenosine kinase, epilepsy and stroke: mechanisms and therapies. *Trends Pharmacol Sci* **27**, 652–658

Boison D (2007). Adenosine as a modulator of brain activity. *Drug News Perspect* **20**, 607–611

Clark BA & Barbour B (1997). Currents evoked in Bergmann glial cells by parallel fibre stimulation in rat cerebellar slices. *J Physiol* **502**, 335–350.

Craig CG & White TD (1993). N-methyl-D-aspartate and non-N-methyl-D-aspartate-evoked adenosine release from rat cortical slices: distinct purinergic sources and mechanisms of release. *J Neurochem* **60**, 1073–1080.

Crepel F (2007). Developmental changes in retrograde messengers involved in depolarization-induced suppression of excitation at parallel fibre-Purkinje cell synapses in rodents. *J Neurophysiol* **97**, 824–836.

Dale N (1998). Delayed production of adenosine underlies temporal modulation of swimming in frog embryo. *J Physiol* **511**, 265–272.

Descombes S, Avoli M & Psarropoulou C (1998). A comparison of the adenosine-mediated synaptic inhibition in the CA3 area of immature and adult rat hippocampus. *Brain Res Dev Brain Res* **110**, 51–59.

Dumas TC & Foster TC (1998). Late developmental changes in the ability of adenosine A1 receptors to regulate synaptic transmission in the hippocampus. *Brain Res Dev Brain Res* **105**, 137–9.

Dunwiddie TV & Diao L (1994). Extracellular adenosine concentration in hippocampal brain slices and the tonic inhibitory modulation of evoked excitatory responses. *J Pharmacol Exp Ther* **268**, 537–545.

Edwards, FA, Gibb AJ & Colquhoun D (1992). ATP receptor-mediated synaptic currents in the central nervous system. *Nature* **359**, 144–147.

Frenguelli BG, Llaudet E & Dale N (2003). High-resolution real-time recording with microelectrode biosensors reveals novel aspects of adenosine release during hypoxia in rat hippocampal slices. *J Neurochem* **86**, 1506–15.

Frenguelli BG, Wigmore G, Llaudet E & Dale N (2007). Temporal and mechanistic dissociation of ATP and adenosine release during ischaemia in the mammalian hippocampus. *J Neurochem* **101**(5), 1400–1413.

Hamann M & Attwell D (1996). Non-synaptic release of ATP by electrical stimulation in slices of rat hippocampus, cerebellum and habenula. *Eur J Neurosci* **8**, 1500–1515.

Kimura M, Saitoh N & Takahashi T (2003). Adenosine A1 receptor-mediated presynaptic inhibition at the calyx of Held of immature rats. *J Physiol* **553**, 415–426.

Kreitzer AC & Regehr WG (2000). Modulation of transmission during trains at a cerebellar synapse. *J Neurosci* **20**, 1348–1357.

Llaudet E, Botting N, Crayston J & Dale N (2003). A three enzyme microelectrode sensor for detecting purine release from central nervous system. *Biosens Bioelectron* **18**, 43–52.

Lloyd HG & Fredholm BB (1995). Involvement of adenosine deaminase and adenosine kinase in regulating extracellular adenosine concentration in rat hippocampal slices. *Neurochem Int* **26**, 387–395.

Noji T, Karaswa A & Kusaka H (2004). Adenosine uptake inhibitors. *Eur J Pharmacol* **495**, 1–16.

Pak MA, Haas HL, Decking UK & Schrader J (1994). Inhibition of adenosine kinase increases endogenous adenosine and depresses neuronal activity in hippocampal slices. *Neuropharmacology* **33**, 1049–1053.

Pearson RA, Dale N, Llaudet E & Mobbs P (2005). ATP released via gap junction hemichannels from the pigment epithelium regulates neural retinal progenitor proliferation. *Neuron* **46**, 731–744.

Psarropoulou C, Kostopoulos G & Haas HL (1990). An electrophysiological study of the ontogenesis of adenosine receptors in the CA1 area of rat hippocampus. *Dev Brain Res* **55**, 147–150.

Studer FE, Fedele DE, Marowsky A, Schwerdel C, Wernli K, Vogt K, Fritschy JM & Boison D (2006). Shift of adenosine kinase expression from neurons to astrocytes during postnatal development suggests dual functionality of the enzyme. *Neuroscience* **142**, 125–137.

Sweeney MI (1996). Adenosine release and uptake in cerebellar granule neurons both occur via an equilibrative nucleoside carrier that is modulated by G proteins. *J Neurochem* **67**, 81–88.

Takahashi M, Kovalchuk Y & Attwell D (1995). Pre- and postsynaptic determinants of EPSC waveform at cerebellar fibre and parallel fibre to Purkinje cell synapses. *J Neurosci* **15**, 5693–5702.

Wall MJ & Dale N (2007). Auto-inhibition of parallel fibre-Purkinje cell synapses by activity dependent adenosine release. *J Physiol* **581**, 553–567.

Wall MJ, Atterbury A & Dale N (2007). Control of basal extracellular adenosine concentration in rat cerebellum. *J Physiol* **582**, 137–151.

Wall MJ & Dale N (2008). Activity-dependent release of adenosine: A critical re-evaluation of mechanism. *Curr Neuropharmacol* **6**, 329–337.

Weaver DR (1996). A1-adenosine receptor gene expression in fetal rat brain. *Brain Res Dev Brain Res* **94**, 205–223.

Wong AYC, Billups B, Johnston BJ, Evans RJ & Forsythe ID (2006). Endogenous activation of adenosine A1 receptors but not P2X receptors during high-frequency synaptic transmission at the calyx of Held. *J Neurophysiol* **95**, 3336–3342.

Yuan Y & Atchison WD (1999). Comparative effects of methylmercury on parallel-fibre and climbing fibre responses of rat cerebellar slices. *J Pharmacol Exp Ther* **288**, 1015–1025.

## Author contributions

M.J.W. designed research. A.A. and M.J.W. performed research & analysed data. M.J.W. wrote paper.

## Acknowledgements